



**HAL**  
open science

# Contribution à l'étude des mouvements forts en Iran : du catalogue aux lois d'atténuation

Mehdi Zare

► **To cite this version:**

Mehdi Zare. Contribution à l'étude des mouvements forts en Iran : du catalogue aux lois d'atténuation. Géophysique [physics.geo-ph]. Université Joseph-Fourier - Grenoble I, 1999. Français. NNT : . tel-00708207

**HAL Id: tel-00708207**

**<https://theses.hal.science/tel-00708207v1>**

Submitted on 14 Jun 2012

**HAL** is a multi-disciplinary open access archive for the deposit and dissemination of scientific research documents, whether they are published or not. The documents may come from teaching and research institutions in France or abroad, or from public or private research centers.

L'archive ouverte pluridisciplinaire **HAL**, est destinée au dépôt et à la diffusion de documents scientifiques de niveau recherche, publiés ou non, émanant des établissements d'enseignement et de recherche français ou étrangers, des laboratoires publics ou privés.



OBSERVATOIRE DE GRENOBLE

et

LABORATOIRE DE GÉOPHYSIQUE INTERNE ET TECTONOPHYSIQUE

## THÈSE

présentée par

Mehdi ZARÉ

pour obtenir le titre de DOCTEUR de

L'UNIVERSITÉ JOSEPH FOURIER - GRENOBLE I

(Arrêtés ministériels du 5 juillet 1984 et du 30 mars 1992)

Specialité: Géophysique - Géochimie - Géomécanique

Contribution à l'étude des mouvements forts en Iran; du catalogue  
aux lois d'atténuation

20 AOUT 2003

Date de soutenance: 9 Mars 1999

Composition du jury:

Composition du jury:

P.-Y. Bard	Directeur de Thèse	Ingénieur au LCPC, Paris
M. M. Campillo	Président	Professeur à l'Université Joseph Fourier, Grenoble
Y. Fukushima	Rapporteur	Shimizu Corporation, Tokyo, Japon
M. Ghafory-Ashtiany	Invité	Président de IIEES, Téhéran, Iran
D. Hatzfeld	Examineur	Directeur de Recherche CNRS au LGIT, Grenoble
B. Mohammadioun	Rapporteur	Conseiller auprès de l'IPSN, Paris
P. Mouroux	Examineur	Directeur de Recherche au BRGM, Marseille

Univ. J. Fourier - O.S.U.G.  
 MAISON DES GEOSCIENCES  
 DOCUMENTATION  
 B.P. 53  
 F. 38041 GRENOBLE CEDEX  
 Tél. 04 76 83 58 27 - Fax 04 76 51 40 58  
 Mail: ptaloue@ujf-grenoble.fr

OBSERVATOIRE DE GRENOBLE  
et  
LABORATOIRE DE GÉOPHYSIQUE INTERNE ET TECTONOPHYSIQUE

**THÈSE**

présentée par

**Mehdi ZARÉ**

pour obtenir le titre de DOCTEUR de

**L'UNIVERSITÉ JOSEPH FOURIER - GRENOBLE I**

(Arrêtés ministériels du 5 juillet 1984 et du 30 mars 1992)

Specialité: Géophysique - Géochimie - Géomécanique

**Contribution à l'étude des mouvements forts en Iran; du catalogue  
aux lois d'atténuation**

Date de soutenance: 9 Mars 1999

Composition du jury:

P.-Y. Bard	Directeur de Thèse	Ingénieur au LCPC, Paris
M. M. Campillo	Président	Professeur à l'Université Joseph Fourier, Grenoble
Y. Fukushima	Rapporteur	Shimizu Corporation, Tokyo, Japon
M. Ghafory-Ashtiany	Invité	Président de IIEES, Téhéran, Iran
D. Hatzfeld	Examineur	Directeur de Recherche CNRS au LGIT, Grenoble
B. Mohammadioun	Rapporteur	Conseiller auprès de l'IPSN, Paris
P. Mouroux	Examineur	Directeur de Recherche au BRGM, Marseille

10204083

Quand la terre tremblera d'un violent tremblement,  
et que la terre fera sortir ses fardeaux,  
et que l'homme dira: Qu'a-t-elle?!

Le Saint Coran; Zelzaal (1 à 3)

A mon père; Mohammad

A ma mère; Fatemeh

A mon frère; Mehrdad

A l'esprit de mon oncle qui

est mort pour sa patrie; Radjab Nasiri (1965-1986)

et à l'esprit de son ami; Amir-Reza Keshmiri (1964-1987)

A la prospérité de l'Iran dans

21ème siècle... inshaallah!

CONTRIBUTION À L'ÉTUDE DE MOUVEMENTS FORTS EN IRAN; DU CATALOGUE  
AUX LOIS D'ATTÉNUATION

Les études de risque sismique en Iran sont dans leur phase initiale. Ainsi, il n'existait jusqu'à présent aucun catalogue d'enregistrements accélérométriques en Iran, et aucune étude sur l'ensemble des données iraniennes n'avait été réalisée. Ce mémoire présente donc la première étude d'ensemble sur les mouvements forts en Iran. Un premier objectif a été d'établir un catalogue des mouvements forts d'Iran en faisant correspondre à chaque enregistrement de qualité suffisante, un événement sismique de localisation et magnitude connues, pour 279 enregistrements accélérométriques, analogues et digitaux. Cette correspondance a pu se faire sur la base des catalogues sismologiques internationaux (ISC, NEIC,... etc.) ou nationaux. Pour 189 autres enregistrements numériques, pour lesquelles aucune information télésismique ou locale n'était disponible, les distance hypocentrales et les moments sismiques ont été estimés sur la base des enregistrements eux-mêmes. Une attention particulière a été accordée aux effets de sites, en choisissant notamment 50 stations accélérométriques du réseau national où les enregistrements ont été nombreux. Une nouvelle classification pour les effets de sites est proposée -basée sur les rapports H/V - qui s'avère relativement simple dans son principe, et plus fiable que les classifications déjà utilisées. Finalement, les lois d'atténuation pour différents paramètres de mouvement fort (dont Arms, Intensité Arias, PGA, PGV, et PGD, énergie, durée et valeurs spectrales) sont obtenues et discutées sur la base d'un total de 468 enregistrements accélérométriques en 3 composantes.

## CONTRIBUTION TO THE STRONG MOTION STUDIES IN IRAN; FROM THE CATALOG TO THE ATTENUATION LAWS

The seismic risk studies in Iran are in the first stages. Till now, no catalog of strong motion accelerograms was existing in Iran, and no study has been conducted on the entire of the strong motion data. This thesis presents therefore the first study on the whole strong motion data-set in Iran. A first objective in this work was to establish a catalog of strong motion to assign to each record - of a satisfactory quality - a seismic event with known location and magnitude. Such correspondance was possible based on the international (NEIC, ISC, ...etc) or national seismologic catalogs, for 279 analog and digital accelerograms. For 189 other digital data, for which no teleseismic or local information was available, the hypocentral distance and the moment magnitude are estimated based on each record. A special attention was paid to site effects, choosing 50 strong motion stations of the national network, where there were a lot of records. A new classification for site effects is proposed - based on the H/V ratio - which is relatively simple, and more reliable than the previously proposed methods. Finally, the attenuation laws for different parameters of strong motion (such as Arms, Arias intensity, PGA, PGV, and PGD, energy, duration and the spectral ordinates) are obtained and discussed, based on the whole set of 468 three-component accelerometric records.

پژوهش و بررسی

جنبش شدید زمین در ایران : از کاتالوگ تا قانونهای کاهندگی

پژوهشهای خطر زمینلرزه در ایران هنوز در گامهای نخستین می باشد. پیش از مطالعات ارائه شده در این رساله هیچ کاتالوگی از جنبش شدید زمین در ایران وجود نداشته است. از سوی دیگر تاکنون مطالعه ای جامع بر روی داده های شتابنگاری ایران صورت نگرفته است. بنابراین رساله حاضر اولین مطالعه بر روی تمام داده های شتابنگاری ایران می باشد. یک هدف اولیه این مطالعات تهیه کاتالوگ جنبش زمین ایران بود که در آن برای ۲۷۹ نگاشت ۳ مولفه ای آنالوگ و دیجیتال - که کیفیتی مناسب داشتند - اطلاعات جنبش زمین و سرچشمه ارائه شد. داده های سرچشمه بر اساس گزارش مرکز های جهانی و کشوری گردآوری شد. برای ۱۸۹ نگاشت دیجیتال که که گزارشی از سرچشمه آنها در دسترس نبود فاصله کانونی و بزرگای گشتاوری آنها بر اساس خود نگاشتها محاسبه گردید. اثرهای ساختگاه با انتخاب ۵۰ ایستگاه شتابنگاری - جایی که بیشترین نگاشتها بدست آمده بود - مطالعه گردید. یک روش جدید برای طبقه بندی ساختگاه پیشنهاد شد که اساسی ساده و کارایی بیشتری از روشهای پیشین دارد. در نهایت قانون های کاهندگی برای پارامترهای مختلف جنبش زمین (بیشینه شتاب، سرعت و تغییرمکان، انرژی، دوام و مقدار های طیفی) بر اساس پایگاه داده هایی با ۴۶۸ نگاشت شتابنگاری بدست آمده و مورد بحث قرار گرفت.

## Remerciements

Comment peut-on être persan!?

Montesquieu

La question posée par Montesquieu est celle que je me pose toujours!, surtout depuis le temps que je voulais faire mon doctorat en France... pour celui qui vient d'un pays avec un risque très important de séismes majeurs, la réponse pourrait être "Étudier le mouvement fort en Iran!". Un sujet qui n'avait jamais été étudié avant, et en même temps, un travail assez important...

Il y a 5 ans, dans mon mémoire de M.Sc., j'ai écrit "il faut continuer les études sur les mouvements forts en Iran, sur la base de l'ensemble des données de l'Iran, inshaallah...". Aujourd'hui, quand je vois que mon rêve de ce jour-là est devenu une réalité, il faut d'abord que je remercie le bon Dieu, qui m'ai fourni la possibilité de faire ce devoir.

Dans ce travail, qui m'a imposé au départ et à la fin des difficultés majeures, après le bon Dieu qui m'a donné cet esprit amoureux pour travailler pour mon pays(!), il faut que je remercie mon directeur de thèse; M. Pierre-Yves Bard. Pierre-Yves était présent dans ce travail de la première jusqu'à la dernière minute pour m'assister (moralement, scientifiquement, ....etc.) et me montrer le chemin. Je remercie P.-Y. Bard, pas seulement pour diriger ce travail, mais aussi pour m'avoir montré "comment peut-on être humain?"!

Le président de l'IEES (International Institute of Earthquake Engineering and Seismology) à Téhéran (où je travaille), M. Ghafory-Ashtiany m'a fourni tout ce dont j'ai eu besoin. Il a fait vraiment de son mieux et ses efforts ont été vraiment impressionnants: s'il n'y avait pas eu son assistance en Iran, je peux imaginer que le travail que j'ai fait pendant ces trois ans et demi aurait été impossible.

Je remercie les membres de jury, M. Mohammadioun et M. Fukushima, qui ont accepté d'être rapporteurs de ma thèse, M. Campillo, M. Mouroux et M. Hatzefeld qui ont y assisté comme les examinateurs.

Un grand merci à ma famille: mon père; Mohammad, ma mère; Fatemeh, et mon frère,



Mehrdad qui ont été toujours avec moi pendant ce travail, malgré leur absence physique de France. Etre loin d'eux, était mon problème le plus important quand j'étais en France.

Je remercie bien M. G. Poupinet (l'ex-directeur de LGIT) et M. M. Campillo (le directeur actuel du labo) pour m'avoir accepté comme un thésard au sein du LGIT.

Je tiens à remercier M. Regnier et le gouvernement français pour m'avoir fourni une bourse en alternance pour mes séjours en France.

Je remerci BHRC (Building and Housing Research Center), l'organisation qui nous a donné la permission d'utiliser les enregistrements accélérométriques de l'Iran.

Je remercie mes amis à Grenoble, et à Téhéran, pour leur soutien (de différents manière); A. Aboura, M. Abtahi, E. Akbari, M. Akbari-Jokar, A. Azadmanesh, A. Baboli, D. Baumont, R. Bouso, P. Buxton, S. Eshghi, M. Farsi, E. Farzanegan, M. Heydari, M.K. Jafari, A. Jalali, C. Lacombe, D. Maclean, G. Mahmoodi, N. Madjoudj, L. Margerin, H. Mirzaei-Alavijeh, K. Pashaei, S. Shakhesi, M. Shirazian, M. Tatar, M. Zaré (mon père!), M. Zolfaghari, F. Zouesh-tiagh,... et les autres dont j'ai oublié les noms!...

Enfin, un grand remerciement à mes compatriotes, pour leur gentillesse et leur coopération avec notre équipe pendant notre manip (1996-1997) de 20000 km de voyage dans mon cher pays.

Que Dieu protège les iraniens et  
les autres peuples des pays tributaires des  
aléas sismiques... inshaallah!...

## Table des matières

<b>1</b>	<b>Introduction Générale</b>	<b>5</b>
1.1	Le Risque Sismique en Iran . . . . .	6
1.2	Problématique . . . . .	11
1.3	Les Chapitres de ce Mémoire . . . . .	12
<b>2</b>	<b>Le Catalogue des Mouvements forts en Iran</b>	<b>14</b>
2.1	Introduction . . . . .	16
2.2	Determination of the Source Data for each Record . . . . .	17
2.3	Extracting the most Reliable Records . . . . .	23
2.4	Data Correction . . . . .	23
2.4.1	Determination of the appropriate frequency band . . . . .	23
2.4.2	Spectrum shape . . . . .	24
2.4.3	Filtering and Integration . . . . .	25
2.5	Site effects . . . . .	27
2.6	Assigning a Quality Label to each Record . . . . .	30
2.7	Sources of Errors and Uncertainties . . . . .	31
2.7.1	Instrumental and macroseismic epicentral distances . . . . .	31
2.7.2	Focal depths . . . . .	33
2.7.3	Integration of the filtered records . . . . .	34
2.7.4	Earthquake intensities . . . . .	34
2.8	Conclusion . . . . .	35
<b>3</b>	<b>Les Effets de Site</b>	<b>46</b>
3.1	Introduction . . . . .	48
3.2	The methodology . . . . .	49
3.3	An overview on the general situation of the sites and the tests . . . . .	53

20 AOÛT 2003

Univ. J. Fourier - O.S.U.G.  
MAISON DES GEOSCIENCES  
DOCUMENTATION  
B.P. 53  
F: 38041 GRENOBLE CEDEX  
Tél. 04 76 63 54 27 - Fax 04 76 51 40 58  
Mail: ptalour@ujf-grenoble.fr

3.3.1	Receiver function method for strong motions . . . . .	54
3.3.2	Microtremors . . . . .	56
3.3.3	Geoseismic tests . . . . .	56
3.4	The results of the geoseismic tests, microtremors and H/V for Strong Motions . .	57
3.4.1	Sites with a satisfactory agreement between the results of the different methods . . . . .	57
3.4.2	Sites without agreement: failure of the microtremor technique . . . . .	64
3.4.3	A preliminary conclusion on the results of the different methods . . . . .	68
3.5	A Site Categorization . . . . .	69
3.5.1	The Average of Vs for upper 30 meters . . . . .	71
3.5.2	Discrepancies from the defined criteria . . . . .	73
3.5.3	Application to all Iranian strong motion data . . . . .	74
3.5.4	Quality factor for the site determination . . . . .	74
3.6	Conclusions . . . . .	75
<b>4</b>	<b>Études particulières: la source sismique et Kappa</b>	<b>80</b>
4.1	Seismic Moment and Stress Drop for the Strong Motion Accelerograms in Iran .	81
4.1.1	Introduction . . . . .	82
4.1.2	Methodology of the Study: the $\omega^{-\gamma}$ model . . . . .	82
4.1.3	The sources of Uncertainties . . . . .	84
4.1.4	Results . . . . .	84
4.1.5	Application of the method for the records with no reported source . . . . .	88
4.1.6	Conclusions . . . . .	94
4.2	Décroissance de l'amplitude à haute fréquence dans le spectre de Fourier de l'Accélération: coefficient Kappa . . . . .	95
4.2.1	Introduction . . . . .	95
4.2.2	La méthodologie des calculs de Kappa . . . . .	96
4.2.3	Les résultats . . . . .	97
4.2.4	Conclusion . . . . .	102
<b>5</b>	<b>Durée et Énergie des Mouvements Forts</b>	<b>107</b>
5.1	Introduction . . . . .	108
5.2	Seismogenic zones in Iran and site conditions . . . . .	109
5.3	Methodology . . . . .	111

5.4	Results . . . . .	114
5.4.1	Comparison of Strong Motion Intervals: 5%-95% and 5%-75% . . . . .	114
5.4.2	Empirical Relationships for the Strong Motion Duration in Iran . . . . .	118
5.4.3	Attenuation of $a_{rms}$ and $e_a$ . . . . .	131
5.5	Conclusions . . . . .	133
<b>6</b>	<b>L'Atténuation des Mouvements Forts en Iran</b>	<b>141</b>
6.1	Introduction . . . . .	143
6.2	Methodology . . . . .	145
6.2.1	The applied approaches . . . . .	145
6.2.2	Fundamental form . . . . .	145
6.2.3	Ground Motion Parameters . . . . .	147
6.3	The input data-base . . . . .	148
6.3.1	The magnitude values . . . . .	148
6.3.2	Distance parameter . . . . .	149
6.3.3	Geological areas . . . . .	151
6.3.4	Site Categorization . . . . .	151
6.3.5	Fault mechanism . . . . .	152
6.4	Results . . . . .	152
6.4.1	Attenuation coefficients for peak values . . . . .	153
6.4.2	Attenuation coefficients for spectral ordinates . . . . .	157
6.4.3	Nonlinear effects in the Iranian strong motions? . . . . .	168
6.5	Response and Design Spectra for Alborz-Central Iran, and Zagros areas . . . . .	168
6.6	Conclusions . . . . .	172
6.7	Régression en une étape . . . . .	177
6.8	Les études sur la nonlinéarité possible dans les données iraniennes . . . . .	187
<b>7</b>	<b>Conclusion Générale</b>	<b>198</b>
7.1	Introduction . . . . .	199
7.2	Catalogue des mouvements forts en Iran . . . . .	199
7.3	Moment sismique et la chute de contrainte . . . . .	200
7.4	Études des effets de site . . . . .	200
7.5	Énergie et durée des mouvements forts en Iran . . . . .	201
7.6	Atténuation des mouvements forts en Iran . . . . .	202

7.7 Propositions pour la continuation de ces recherches . . . . . 202

8 Bibliographie Générale 205

9 Annexes 217

# Chapitre 1

## Introduction Générale

## 1.1 Le Risque Sismique en Iran

Le plateau iranien (Figure 1.1) est situé entre les plaques Arabie et Eurasie. Le système structurel en Iran est compressif, et la plupart des failles importantes sont chevauchantes avec des composantes de cisaillement. Les régions sismotectoniques de l'Iran (les plus connues) sont le Zagros au sud-ouest du pays, l'Alborz au nord; l'Iran Central; le Koppeh-Dagh au nord-est; le Makran au sud-est et la plaine du Khuzestan à l'extrême sud-ouest. Les études géologiques de l'Iran montrent que la situation en Azarbayjan (au Nord-Ouest du pays) est plus ou moins similaire aux caractéristiques géologiques de l'Iran-Central. Basé sur les données accélérométriques iraniennes actuellement disponibles, nous allons (au point de vue de la source sismique) distinguer la région de Zagros des autres régions iraniennes (avec des durées et des contenus fréquentiels différents).

La figure 1.2 montre la sismicité récente du plateau iranien. La plupart des séismes destructeurs (récents et historiques) en Iran se sont produits dans les régions de l'Iran-Central et d'Alborz; tandis qu'au Zagros les séismes sont plus fréquents avec des magnitudes de niveau moyen ( $M = < 6$ ). Les séismes les plus importants en Iran au cours des vingt dernières années sont le séisme de Sarkhun (Bandarabbas) du 7-3-1975 ( $M_s 6.1$ ,  $m_b 5.9$ ); Vendik (Ghaen) du 7-11-1976 ( $M_s 6.4$ ,  $m_b 5.8$ ); le séisme de Khurgu du 21-3-1977 ( $M_s 7.0$ ,  $m_b 6.2$ ); le séisme de Naghan du 6-4-1977 ( $M_s 6.1$ ,  $m_b 5.6$ ); le séisme de Tabas du 16-9-1978 ( $M_s 7.3$ ,  $m_b 6.7$ ,  $M_w 7.4$ ); le séisme de Ghaen du 16-1-1979 ( $M_s 6.8$ ,  $m_b 6.0$ ); le séisme de Korizan (Ghaen) du 14-11-1979 ( $M_s 6.6$ ,  $m_b 6.0$ ); le séisme de Koli-Bonyabad (Ghaen) du 27-11-1979 ( $M_s 7.1$ ,  $m_b 6.1$ ); le séisme de Golbaf (Kerman) du 11-6-1981 ( $M_s 6.7$ ,  $m_b 6.1$ ); le séisme de Sirch (Kerman) du 28-7-1981 ( $M_s 7.1$ ,  $m_b 5.7$ ); le séisme de Manjil du 20-6-1990 ( $M_s 7.7$ ,  $m_b 6.8$ ,  $M_w 7.3$ ); et le séisme de Ebrahimabad (Firouzabad) du 20-6-1994 ( $M_s 5.7$ ,  $m_b 5.9$ ,  $M_w 5.9$ ) [Les épïcêtres de ces séismes sont indiqués dans la figure 1.2]. La figure 1.3 montre bien que la plupart des épïcêtres des séismes en Iran sont concentrés dans la région de Zagros en sud-ouest, en Iran-Central (sur les frontières des montagnes et des plaines).

Actuellement, les études sur le risque sismique en Iran se concentrent sur les domaines suivants :

- études néotectoniques et connaissance des failles actives.
- installation d'un nouveau réseau (de sismomètres) [un réseau de stations du WWSSN est installé en Iran depuis fin des années 1950].
- Installation de plus en plus d'instruments de mouvements forts en Iran, et remplacement progressive des instruments analogiques anciens pour des instruments numériques.

- Etudes du mouvement fort en Iran; lois d'atténuation; effets de sites.
- Etudes de microzonage sismique dans les grandes villes (Téhéran, Tabriz, ..etc).

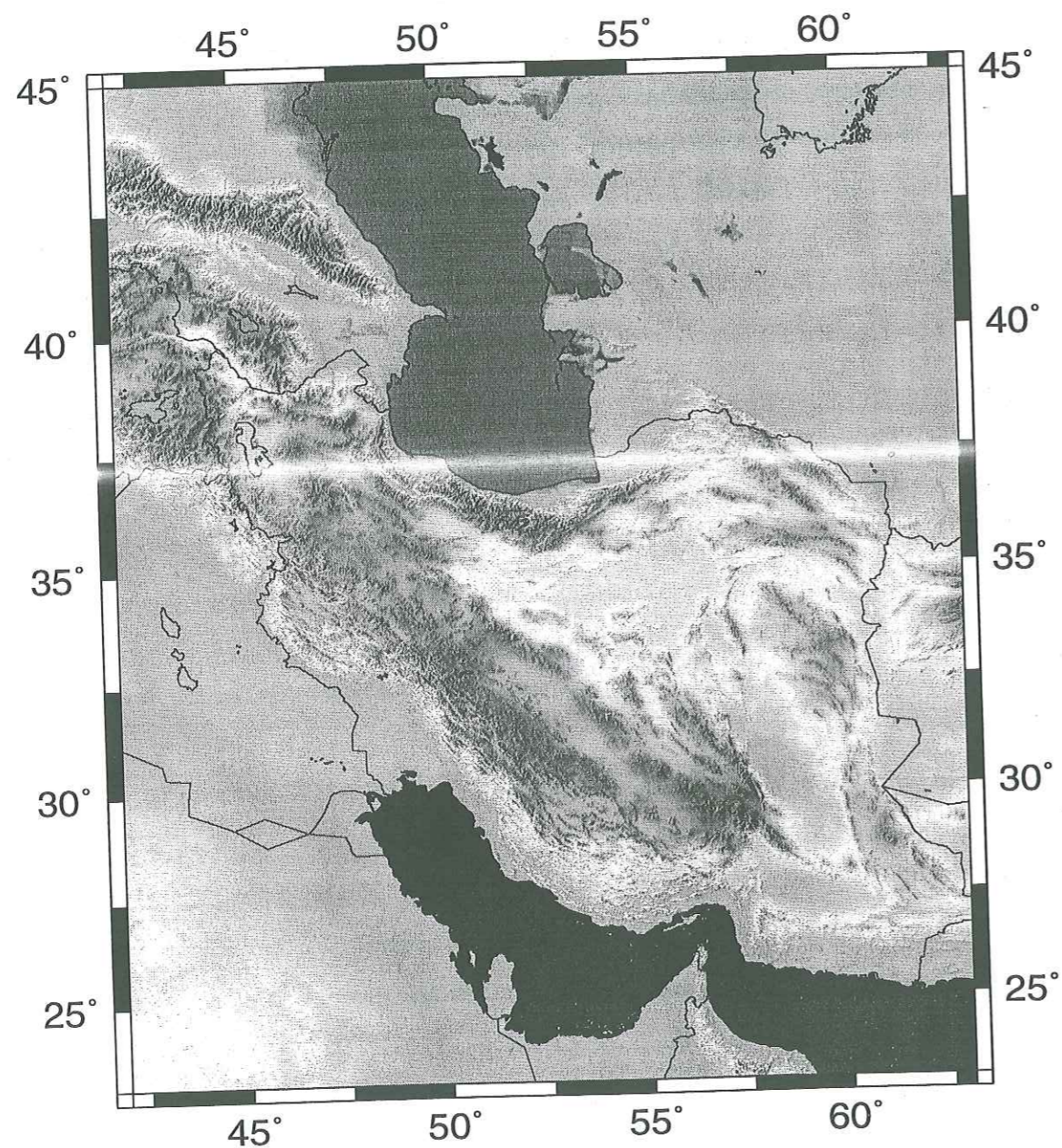


FIG. 1.1 – La carte de la topographie du plateau iranien et des territoires voisins.

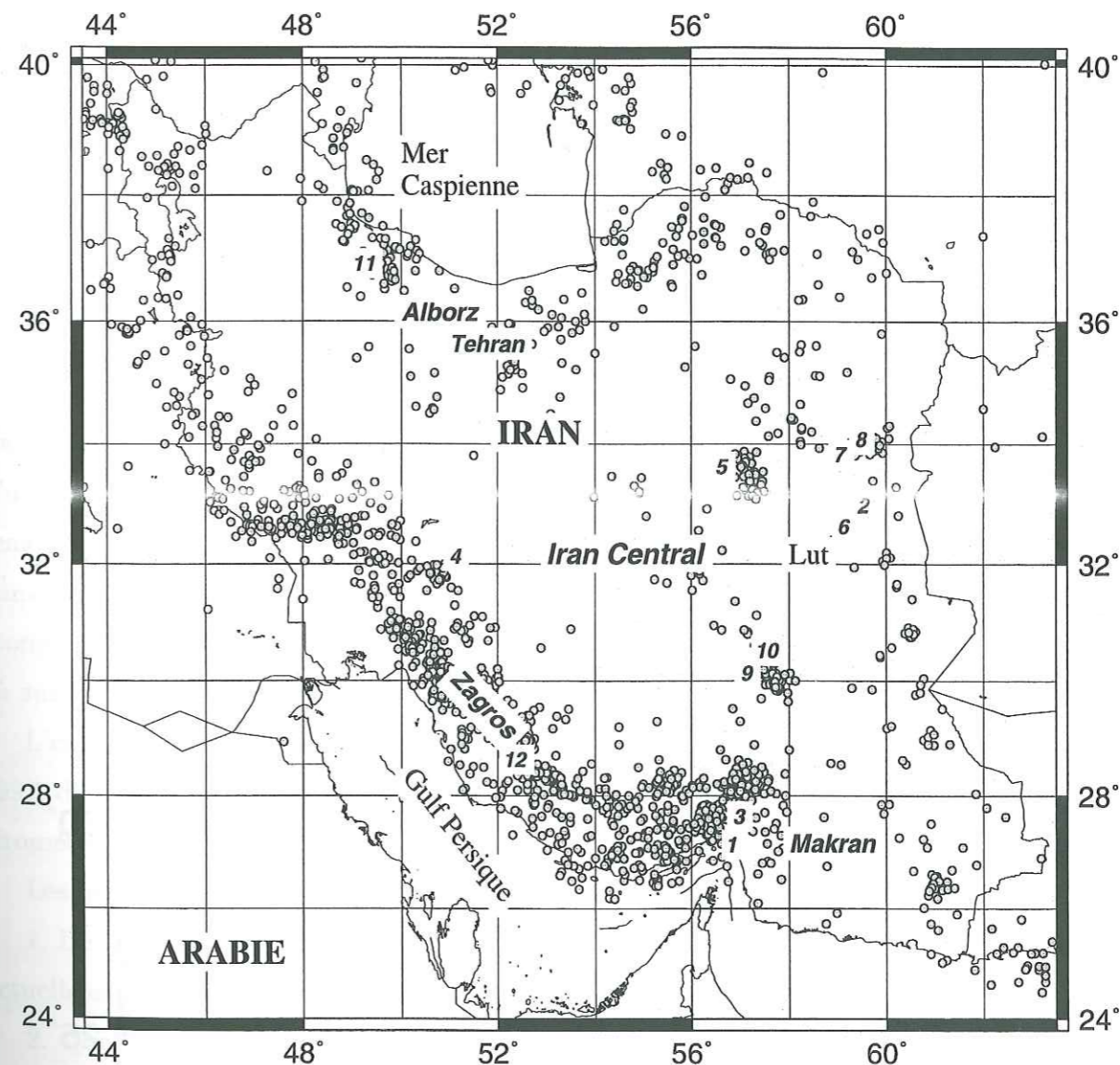


FIG. 1.2 – Les séismes en Iran avec les magnitudes supérieurs à 4.5 de 1965 à 1998; les chiffres sur la carte montrent les épencentres des séismes de 1: Sarkhun, 2: Vendik, 3: Khurgu, 4: Naghan, 5: Tabas, 6: Ghaen, 7: Korizan, 8: Koli, 9: Golbaf, 10: Sirch, 11: Manjil, 12: Ebrahimabad; pour plus de détails regardez le texte.

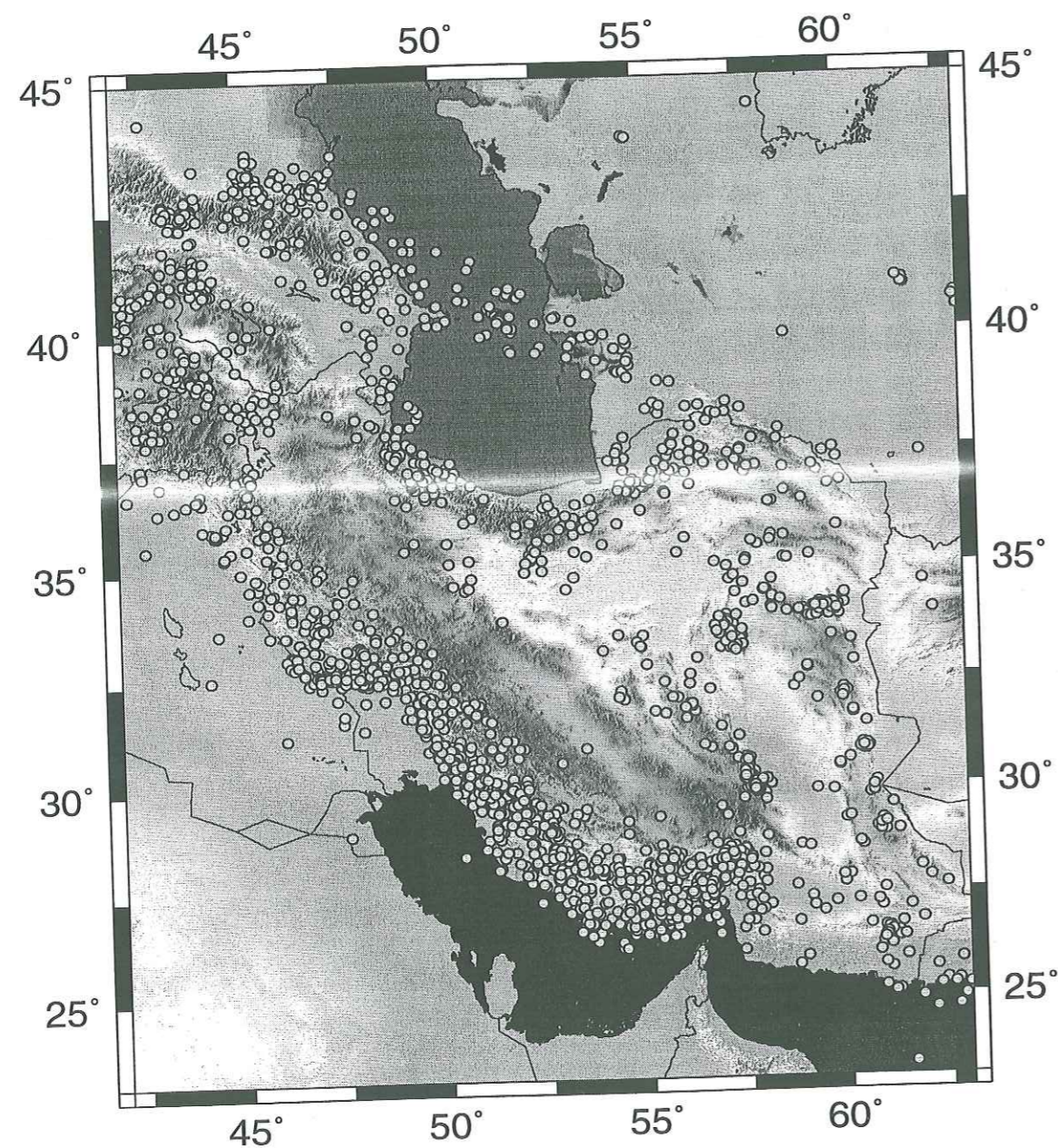


FIG. 1.3 – Les séismes en Iran avec les magnitudes supérieurs à 4.5 de 1965 à 1998, sur fond topographique

## 1.2 Problématique

Le risque sismique a du être pris en compte en Iran pour les nombreux projets de constructions d'ouvrages majeurs en Iran (barrages, ponts, villes nouvelles, tours, constructions souterraines comme les tunnels, le métro de Téhéran et des autres grands villes,... etc.) depuis une vingtaine d'années. Tout ces études se sont déroulées en estimant les sollicitations de dimensionnement sur la base d'enregistrements et/ou de modèles d'atténuations des mouvement forts développés dans d'autres régions du monde (Californie, Japon ou Europe) (Zaré 1995). Il y avait toujours cette discussion sur l'application des loi d'atténuations: est-il possible d'extrapoler une relation d'atténuation développée sur la base des données accélérométriques d'une certaine région? Les spécifications sismotectoniques et physiques différentes de la croûte de chaque région (épaisseur, facteur de qualité, contraintes principales, géologie ...etc) imposent certaine limites à de telles extrapolations. Ce type d'études du risque sismique, sans avoir utilisé les données iraniennes et des modèles basés sur ces données, n'arrivent jamais à manifester l'aléa sismique d'une façon optimum en Iran. Néanmoins, on pense que les analyses du risque sismique en Iran, tenant compte de ces résultats, peuvent être plus réalistes. Les études qui seront présentées dans ce mémoire sont donc d'un intérêt fondamental parce qu'un séisme destructeur, à toute moment ou l'autre, même quand quelqu'un lit ce texte!, peut se produire quasiment n'importe où sur le plateau iranien (l'Iran et ces régions voisins).

L'existence d'un réseau accélérométrique en Iran depuis 1975 (avec 1000 stations à la fin 1997, d'après un rapport du BHRC) permet une étude spécifique en utilisant les données accélérométriques iraniennes.

Les questions importantes auxquelles on voudrait répondre dans cette thèse sont:

1. De combien d'enregistrements accélérométriques de bonne qualité dispose-t-on à l'heure actuelle en Iran?
2. Quels sont les effets de site dans les données iraniennes? Combien de "classes de site" différentes doivent (ou peuvent) être prises en compte?
3. Quelles sont les caractéristiques de source des séismes destructeurs que l'on peut étudier à partir des enregistrements accélérométriques iraniens (moment sismique, chute de contrainte, processus ... etc.)?
4. Est-il possible de distinguer à l'intérieur de l'Iran différentes zones géographiques ou tectoniques, ayant des comportements différents en matière de mouvement forts?
5. Quelles sont les variations de l'énergie et de la durée des mouvements forts dans différentes régions de l'Iran?

6. Quels sont les paramètres d'atténuation en Iran, et quel est le meilleur modèle pour arriver aux résidus minima?

### 1.3 Les Chapitres de ce Mémoire

Ce mémoire comporte neuf chapitres différents :

- Le deuxième chapitre est consacré au catalogue des mouvements forts iraniens: 770 enregistrements accélérométriques iraniens ont été étudiés. Les rapports signal sur bruit ont été calculés pour tous les enregistrements iraniens disponibles. Un filtrage passe-haut et passe-bas est effectué pour éliminer les bruits et les signaux trop bruités. Les caractéristiques des sources sismiques (localisation, magnitude) ont été trouvées pour les enregistrements de qualité convenable, essentiellement à partir des bulletins des organismes sismologiques internationaux, et aussi, chaque fois que c'était possible, des informations locales. Le catalogue présenté dans ce chapitre est composé de 279 données accélérométriques 3 composants, analogues et numériques.

- Le troisième chapitre est consacré à l'étude des effets de sites. Cinquante sites ont d'abord fait l'objet d'un examen attentif, avec la réalisation des mesures géotechniques ou géophysiques spécifiques. 25 sites ont été l'objet de plusieurs types de mesures simultanées: sismique réfraction de surface, profil géotechnique, bruit de fond sismique, tandis que les 25 autres sites faisaient l'objet exclusivement de mesure de bruit de fond sismique. Les résultats de ces mesures ont été comparés à ceux de l'analyse du rapport H/V des enregistrements accélérométriques, et ont conduit à proposer une nouvelle classification en 4 catégories, sur la base du seul rapport H/V. Cette classification s'avère être assez bien corrélée aux valeurs de  $V_s$  dans les 30 premiers mètres.

- Le quatrième chapitre se compose d'études sur le moment sismique, la chute de contrainte et la décroissance haute fréquence. Pour un nombre importants d'enregistrements numériques aucune information locale ou télésismiques ne permet de correspondance avec un événement dûment répertorié. Les magnitudes de moment ( $M_w$ ) ont donc été calculées pour toutes les données (y compris les enregistrements figurant dans les bulletins des organismes internationaux). Les distances hypocentrales ont été estimées par les différences entre les temps d'arrivée des ondes P et S (quand c'était possible). Le calcul de  $M_w$  a fourni un échelle de magnitude, homogène, pour toutes les données. La distance hypocentrale est la seule définition pour les données iraniennes qui peut être à peu près contrôlée avec les données accélérométriques. Ce faisant, avec ces calculs de magnitudes et de distances hypocentrales, 189 données trois composantes ont pu être ajoutées aux 279 enregistrements précédents. D'un autre côté, un ordre de grandeur

pour les chutes des contraintes a pu être estimé, et on observe qu'elles sont représentatives de séismes intra-plaque.

- Le cinquième chapitre est consacré au calcul de l'énergie, de la durée des mouvements forts, et de l'accélération moyenne ( $A_{rms}$ ) et à l'établissement de lois d'atténuation sur ces différents paramètres.

- Le sixième chapitre présente les lois d'atténuation sur les principales caractéristique des mouvements forts, à savoir les valeurs maximales et les valeurs spectrales. Plusieurs formes fonctionnelles ont été analysées, et les régressions ont été établies aussi bien en 1 seule étape qu'en 2 étapes. Les paramètres de ces lois sont présentés pour deux régions du pays (qui semblent montrer des comportements accélérométriques différents) et pour l'ensemble les données iraniennes.

- Le septième chapitre présente un bilan général de ce mémoire. Des suggestions sont formulées pour continuer ce type d'études en Iran et dans les pays voisins.

- La bibliographie générale et l'annexe sont placées dans le huitième et le neuvième chapitres, respectivement.

Les études sur les mouvements forts en Iran présentés dans ce mémoire, constituent un premier pas pour établir en Iran les bases de la « sismologie de l'ingénieur » (Engineering Seismology), un des points très importants pour améliorer la conception parasismique dans ce pays. Cette amélioration sera à la base de toute mise-à-jour des codes parasismiques en Iran.

## Chapitre 2

# Le Catalogue des Mouvements forts en Iran



**Résumé** Les données accélérométriques en Iran seront étudiées dans ce chapitre et présentées dans un catalogue qui comprend les valeurs maximales des mouvements forts et les caractéristiques des sources pour chaque enregistrement. Les enregistrements sont les données pour lesquelles : 1) La qualité de l'enregistrement et de la numérisation (pour les données analogiques) est suffisamment bonne et 2) les caractéristiques de la source auront pu être déterminées à partir des enregistrements télésismiques. Les enregistrements de mouvements forts en Iran sont de deux types: les données analogiques qui sont obtenues par les instruments SMA-1 (Kinematics), et les données numériques enregistrées par les appareils SSA-2 (de même marque). D'après les rapports du BHRC (l'organisation qui s'occupe de réseau accélérométrique iranien) il y avait, à la fin de l'année 1997, 1000 stations installées un peu partout en Iran. Parmi environ 750 enregistrements disponibles (obtenus entre 1974 et 1997), on a choisi 279 enregistrements (qui satisfont les conditions précédentes), dont 169 analogiques et 110 numériques (en trois composantes). Ces données proviennent des différentes régions du pays: 143 du Zagros (ouest et sud-ouest), 78 de l'Iran-Central, 48 de l'Alborz (au nord), 9 de l'Azarbayjan (au nord-ouest) et 1 enregistrement du Koppeh-Dagh (en nord-est). Nous allons donc présenter le premier catalogue de mouvement forts en Iran, qui contient les noms des stations, la catégorie du site, les fréquences de filtrage, les valeurs maximales de l'accélération, de la vitesse et du déplacement, les paramètres de la source [la magnitude ( $M_s$ ,  $m_b$ ,  $M_w$ ,  $M_L$ )], les distances à la source (épicentrale, hypocentrale, et distance à l'épicentre macrosismique), l'intensité, le mécanisme au foyer quand celui-ci était disponible, et un indice de qualité pour chaque enregistrement présenté dans ce tableau.

## The Iranian Accelerometric Data Bank, A Revision and Data Correction

Mehdi Zaré, Pierre-Yves Bard and Mohsen Ghafory-Ashtiani

Article publié dans le "Journal of Seismology and Earthquake Engineering", Vol.1, No.1, pp.1-22

**Abstract** The Iranian strong motion records are studied in order to prepare a catalog to be used as a data base for further studies (for instance empirical attenuation laws). The network was installed in 1974, and now comprises 1000 stations. The instruments are SMA-1 analog (installed before the Manjil earthquake) and SSA-2 digital Kinematics types (after Manjil

earthquake). Out of a total of 450 records with a priori satisfactory quality (well recorded and correctly digitized in the case of the SMA-1 records), a set of 279 records was selected for which it was possible to associate correctly determined source parameters (source magnitudes and epicentral distances): 169 correspond to SMA-1 instruments, and the remaining 110 to SSA-2. The distribution of the records in the different geological/seismotectonics regions are; 143 in Zagros, 78 in Central-Iran/Lut, 48 in Alborz, 9 in Azarbayjan and one record in the Koppeh-Dagh region. The main outcome of this paper is to provide the first strong motion catalog of Iran, with the indication of the site conditions; the frequency band of the reliability of the records, the peak values of acceleration, velocity and displacements, the source parameters (magnitude, epicentral and macroseismic distances), the intensity and finally the fault plane solutions whenever possible.

### 2.1 Introduction

The first Iranian strong motion instruments were installed in 1974. The strong motion network has grown considerably since that time and by the end of 1997 comprises 1000 stations all over Iran, in different geologic conditions. The first instruments were of Kinematics SMA-1 type. The SMA-1 analog recorders have been in use from 1974 until 1991 (the great Manjil earthquake and its aftershocks provided the last important records on SMA-1 instruments). They have been progressively replaced by SSA-2 instruments after the Manjil (1990) earthquake in NW Iran. By the end of December 1997, 640 SSA-2 and 200 SMA-1 instruments were installed mostly in free-field conditions while 58 SSA-2 and 2 SMA-1 instruments were placed on dams all over the country. Several hundred of records have been obtained with this network.

The total number of records (three component accelerograms) which were available for this study were 770 (out of which about 550 SMA-1). These data were distributed by the Building and Housing Research Center of Iran (BHRC) as uncorrected but digitized records. The raw data set distributed by BHRC comprises a relatively complete data set of recordings obtained by the national accelerometric network of Iran since 1974, otherwise we have used some BHRC previously corrected data in order to complete some gaps in the recent data set. Recent records (most of them in the southern Iran; Zagros area) were obtained with the digital network. The digital records are obviously more reliable than the previous analog ones; they include the exact trigger time, and there is no more additional noise brought in by the handy digitalization process. Therefore the amount of reliable SSA-2 accelerograms selected here after about two years (1994-1995) almost equals the number of well-recorded SMA-1 records, although they

relate to a much larger duration; about twenty years (1974-1993).

The previous publications on the Iranian accelerometric data are limited to some reconnaissance reports on the great earthquakes, comprising the uncorrected accelerograms or just the peak values (e.g. Moinfar and Eetemadi, 1982, Moinfar and Adib-Nazari, 1982, Moinfar and Naderzadeh, 1990, Niazi and Bozorgnia, 1992) and the reports presenting a list of the recorded uncorrected accelerograms (BHRC, 1992) or a preliminary processing of the records of one particular event (Moinfar and Shoja-Taheri 1988). The complete listing of the Iranian analog data has been published in 1993 by BHRC, and the SSA-2 accelerograms are published gradually. Some studies on some particular subsets have been already published by Niazi (1986), Shoja-Taheri and Anderson (1988), and Saikia (1994) on the Tabas earthquake of 1978 and in Zaré (1996) on Tabas (1978) and Manjil (1990) earthquakes. Preliminary attenuation studies in Iran have been already performed by Zaré (1995) who has presented the models, developed based on some accelerograms recorded during the great earthquakes in Iran. In another the Iranian data have been compared by the American models is performed by Niazi and Bozorgnia (1990).

The scope of this study was to sort and select accelerograms within this large data set, so as to propose a catalogue of strong motion data in Iran with appropriate and valuable source parameters and site conditions. This catalog (Appendix 1) is the first one to present the well recorded accelerograms in Iran. The catalogue comprises the source and site parameters as well as the maximum values of acceleration, velocity and the displacement for each record. A quality factor is defined as well in this table to indicate the level of reliability of each record.

It should be noticed that during the final stages of the present study, another great earthquake with a magnitude over 7 has shocked the eastern Iran region (Abiz - Ghaen - earthquake of 10 May 1997, Mw7.3) but the recent records from this earthquake were not yet accessible to be included in this study.

In this paper we will present, first, how we have determined the source parameters for each record. The method to select the best (best recorded, more reliable,...) records are explained afterward, and then our methodology to process the accelerograms are presented. The sources of the probable errors are discussed finally.

## 2.2 Determination of the Source Data for each Record

We have chosen a set of 279 records within which we could find minimum source parameters (source magnitudes and epicentral distances) and the best qualities. The selected SMA-1 and SSA-2 accelerographs are shown in Figure 2.1. Figures 2.2 to 2.5 show the distribution of

the accelerometric sites and the instrumental epicenters of the recorded events in the national network, in the northwest, northeast, southwest and southeast of Iran, respectively.

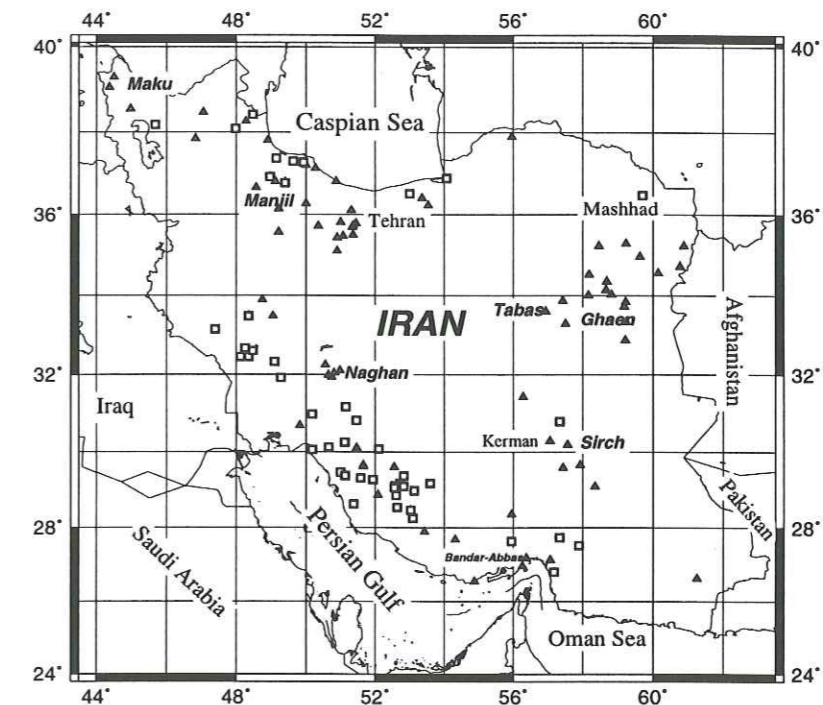


FIG. 2.1 – The locations of the selected accelerometric sites in Iran in this study; the triangles show the analog SMA-1 and quadrangles show the digital SSA-2 instruments.

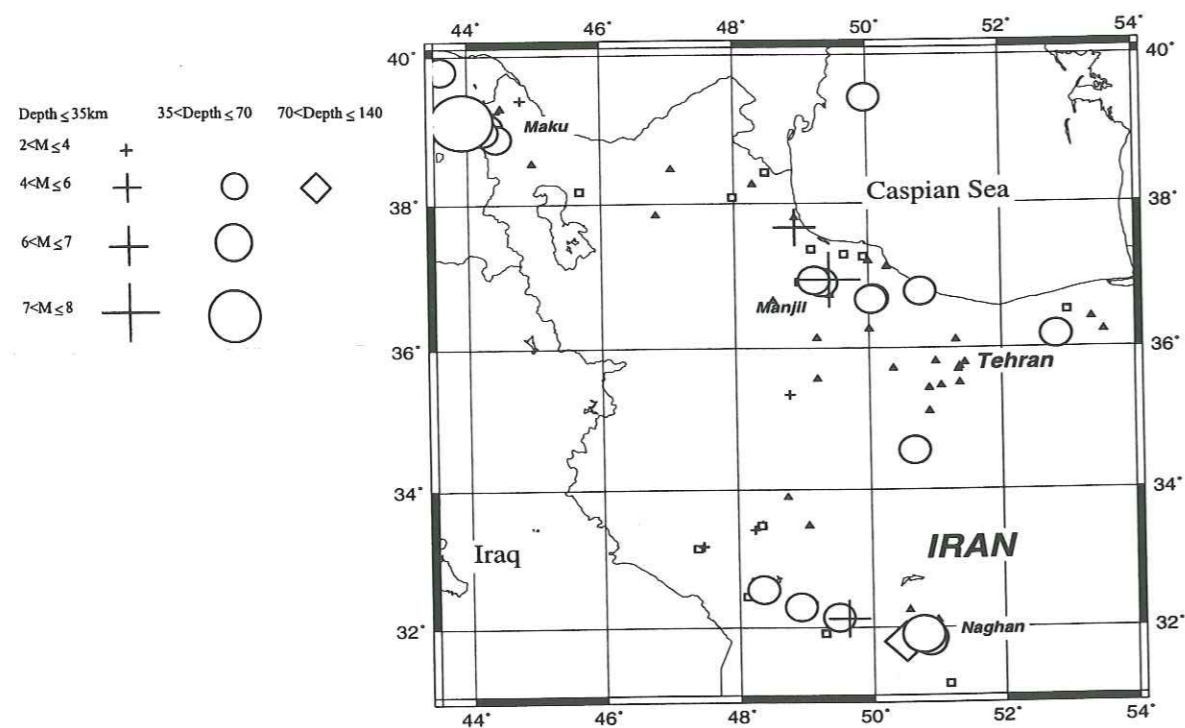


FIG. 2.2 – The location of the strong motion station and the epicenter of the event which a re recorded in these stations in northwest of Iran.

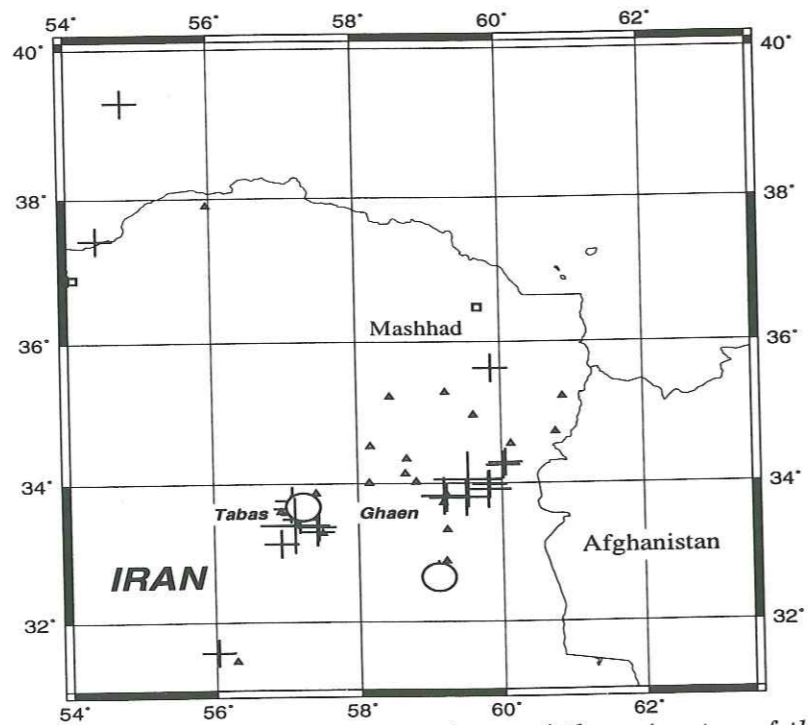


FIG. 2.3 – The location of the strong motion station and the epicenter of the event which a re recorded in these stations in northeast of Iran.

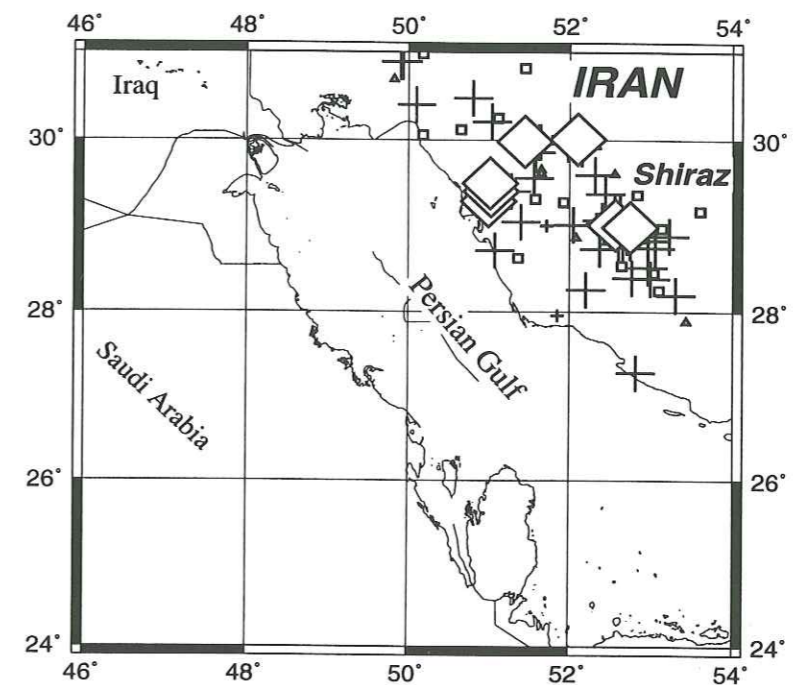


FIG. 2.4 – The location of the strong motion station and the epicenter of the event which a re recorded in these stations in southwest of Iran.

Most of the accelerometric data have been disseminated without corresponding earthquake characteristics (location and magnitude) for each record. Based on the existing data for each record (the peak accelerations, the date and arrival times of the SSA-2 records, or the date of the visit of the operators to change the analog films of the SMA-1 instruments) the causing earthquake is determined. The epicentral locations determined by NEIC and ISC are used in most of the cases. Meanwhile, reports by the national seismic network (Institute of Geophysics, Tehran university; IGTU) and earthquake reports published in the national dailies (if available) are analyzed to check the localities of the macroseismic areas and therefore to have other criteria to check the epicentral distances. Whenever reports on macroseismic epicenters could be found (Ambraseys and Melville 1982; Zaré 1991; 1994; Zaré and Moinfar 1994; Heydari and Zaré 1995; or therefore detail of damage reports in the dailies, or in the NEIC or ISC monthly bulletins) it was possible to have an estimation of the epicentral distances (Appendix 1).

The magnitude of the events are presented as available; the body wave, surface wave and moment magnitudes ( $m_b$ ,  $M_s$  and  $M_w$ , reported by NEIC and ISC) are included, whilst the local magnitudes are given, when available, in the reports by the national seismic network (IGTU).

The focal depths show that most of the recorded events in the Iranian plateau were super-

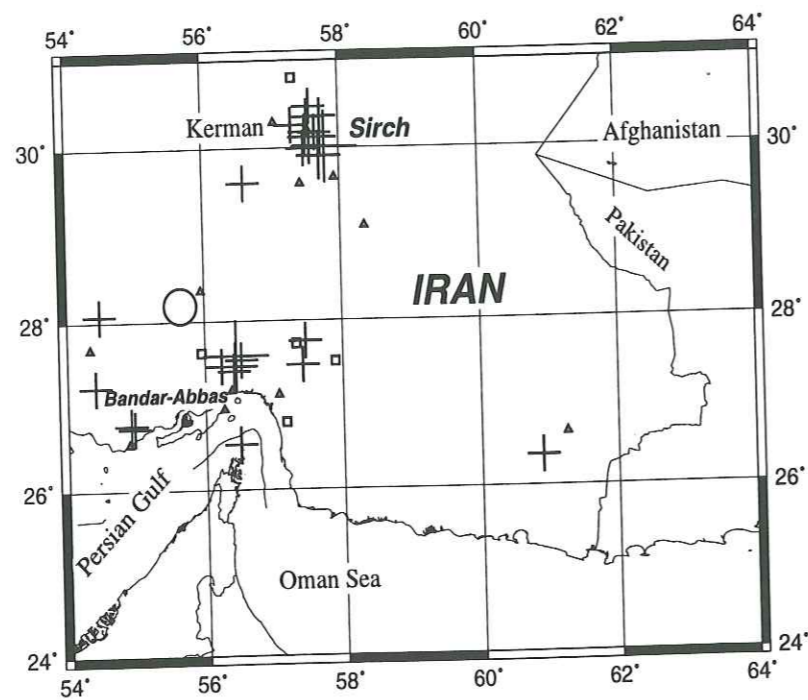


FIG. 2.5 - The location of the strong motion station and the epicenter of the event which are recorded in these stations in southeast of Iran.

ficial. Most of the events had focal depths between 0 and 35 Km (218 records; comprising the depths which are reported '33km', that are the defaults to show the superficial events when it was not possible to determine an exact depth). Forty-one other events have a depth between 35 and 70 Km (in the Zagros area, Alborz, northern Lut, and Azarbayjan - NW Iran - region). Six have a depths between 70 and 140 Km (on the Zagros thrust zone, Southern Zagros and Alborz). There was no depth reported for 12 other events.

The earthquake intensities presented in this work are based on the reported isoseismal maps (Ambraseys and Melville, 1982; Ambraseys, 1988; Berberian et al, 1984; Eshghi et al, 1994; Moinfar and Naderzadeh 1990), but in some cases an estimated intensity was added based on detailed reports that were found in dailies. The intensity values are all presented in MSK scale: when they were reported in another scale, they were converted to this scale using a comparison chart for different intensity values (Japan Technical Committee 4, 1992). The intensity may give an idea of the damage or shaking of an event in an inhabited region. In some cases the landslide reports (as geotechnical evidence) are also used to estimate the intensity; a previous study on the Manjil earthquake (Zaré 1993) has shown that landslides in the form of rock-block slides occurred only in areas with intensities of at least VI MSK. The localities of the most important macroseismic regions, localized in this study, are shown in Figure 2.6. A summary

on these localities is given in Appendix 2.

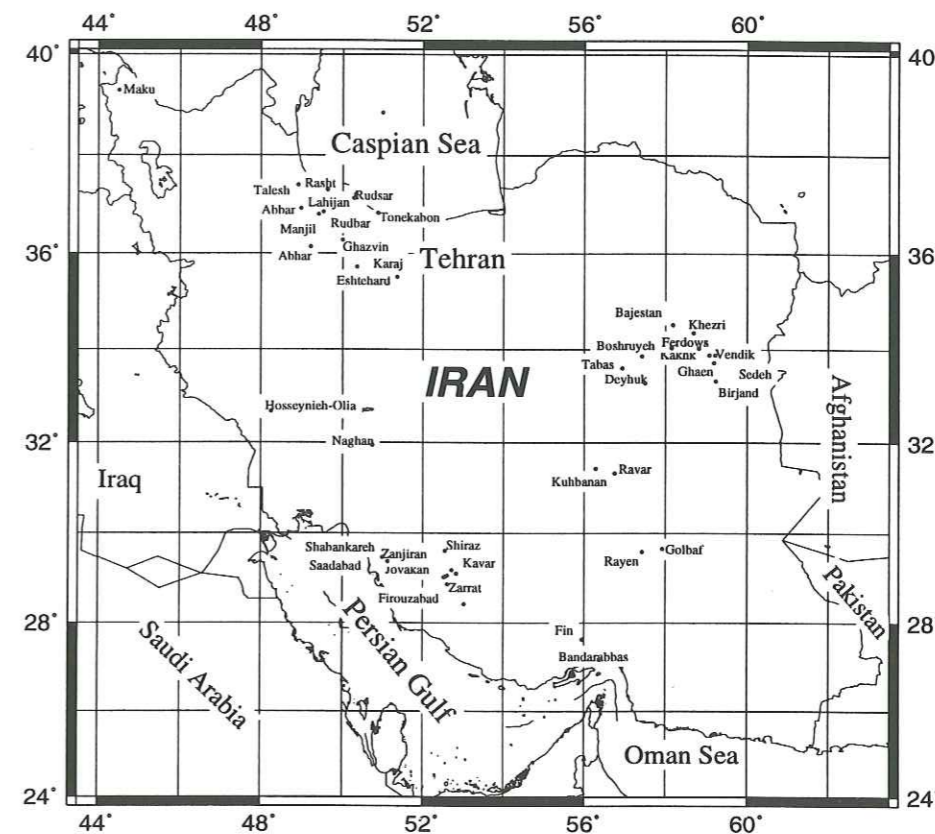


FIG. 2.6 - The selected stations in this study.

The focal mechanisms are reported in Appendix 1 based on the NEIC monthly publications 'Preliminary Determination of Epicenters' as well as the monthly bulletins of ISC. The data presented with reported focal mechanism number 100, of which 40 have strike-slip/reverse solutions, and 31 pure strike slip, 24 pure reverse, 4 pure vertical plane and just one with strike-slip/normal mechanism. Most of the events thus have a strike-slip/compressional mechanism, in agreement with the recent general tectonic activity in the Iranian plateau (by compression between the Arabian plate, in the southwest, and the Turan -Eurasian- plate in its northeast). The deformation is accommodated through the strike-slip and reverse/thrust faults in most of the cases in this plateau. Jackson and McKenzie (1984, 1988) have shown the details of such features of stress and deformation in the Iranian plateau.

## 2.3 Extracting the most Reliable Records

The criteria to select the records are presented below: . Knowledge of the magnitude and source location. The existence of the minimum required source parameters (magnitude and epicentral distance) was necessary to develop the attenuation laws. . Acceptable signal to noise ratio (for the SMA-1 data). Many SMA-1 records had long period noises. The magnitude of the noise was such that it was not possible to distinguish real signal from the noise (especially in the case of the records corresponding to the low magnitude events or the records that were obtained in the far distances from the epicenters).

The amount of low and high frequency noise was verified through the signal to noise ratios. This ratio was calculated for each records. The way to calculate this ratio is described further below.

## 2.4 Data Correction

The data correction (after base-line correction) is carried out through the following steps:

### 2.4.1 Determination of the appropriate frequency band

For each record, the Fourier transform of the signal is computed  $S(f)$  over a length  $t_s$ , as well as the Fourier transform of the noise, computed over a length of  $t_n$ . The normalized signal to noise ratio  $N(f)$  may be shown as :

$$R_{sn} = \frac{\frac{S(f)}{\sqrt{t_s}}}{\frac{N(f)}{\sqrt{t_n}}} \quad (2.1)$$

The threshold level of 3 for  $R_{sn}$  is selected to delimitate the frequency band where the information is meaningful. The example of Bandarabbas record during the Sarkhun earthquake of March 7, 1975 (Ms6.1, mb5.9) that is recorded at an epicentral distance of 28 km (Appendix 1, Figure 2.7) is selected to show the procedure of the correction. This three component accelerometer (raw data) is shown in Figure 2.7 as it results from the digitalization. The window of 30 to 45 sec is selected for noise window  $N(f)$ , and the window between 0 to 25 sec is chosen for signal window  $S(f)$ . The  $R_{sn}$  ratio for this record is presented in Figure 2.8. A part of this spectrum between 0.6 and 20 Hz may be selected as the proper signal frequencies. This

procedure may be too severe when there is no clear « noise » window over the whole record length.

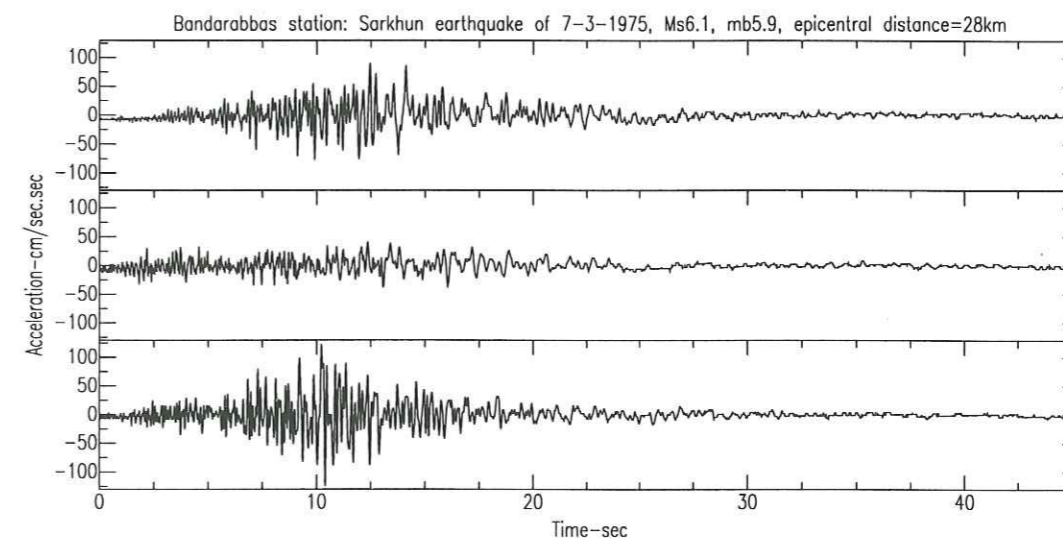


FIG. 2.7 - Three component acceleration time history of Sarkhun earthquake (7-3-1975) recorded in Bandarabbas (before correction and filtering). The middle record is the vertical and the two others are the horizontal components.

### 2.4.2 Spectrum shape

To be sure that the frequency band selected is the dominant signal band, the Fast Fourier Transform (FFT) is calculated for all the records. The FFT for the three components of the aforementioned record is presented in Figure 2.9. According to the ideal shape of the FFT for acceleration, an  $f^2$  shape is expected in the area below the « corner frequency »  $f_c$  and a decaying shape at high frequencies beyond « maximum frequency »  $f_{max}$ . A more or less constant amplitude of the FFT spectrum (below  $f_c$ ) or at high frequencies (beyond  $f_{max}$ ) estimates some low or high frequency noises. In Figure 2.9, the part of the spectra before 0.6Hz and after 20Hz are abnormally high. However these trends might be continued and descend in the ideal slopes in these areas. Therefore these parts may be thought of as noises and the section between these two limits contains the reliable signal. As is shown in this example, the accuracy of the selected

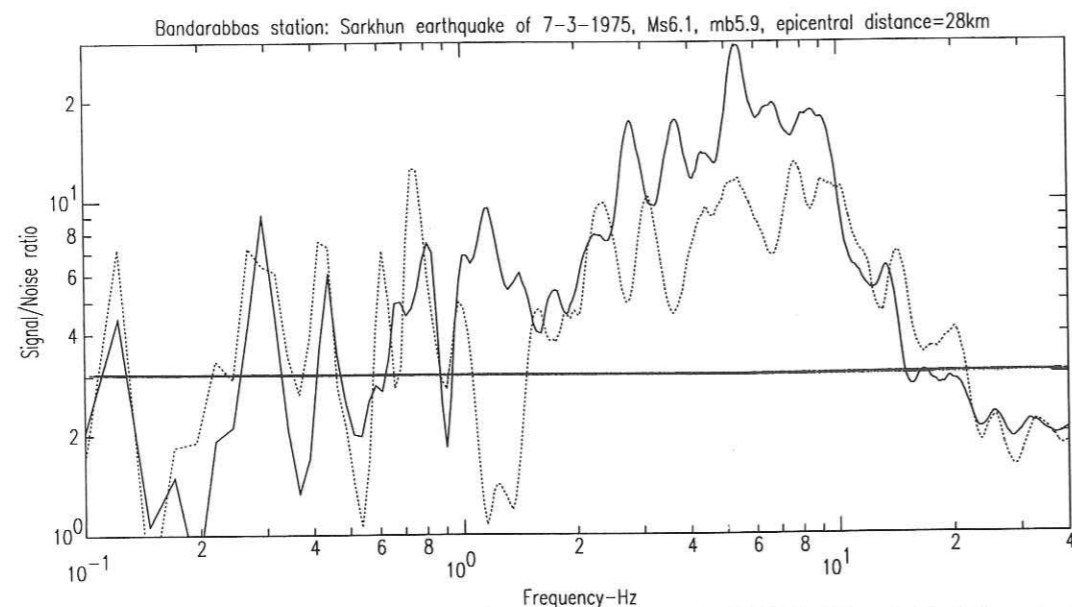


FIG. 2.8 – The signal to noise ratio for the time history in fig2.7. The dotted line is the spectrum for the vertical and the continuous line is for the horizontal components.

windows for the noise and signals, as well as the applied method of signal to noise ratio is verified by checking the spectral shape.

### 2.4.3 Filtering and Integration

Once the reliable frequency band is determined through both signal to noise ratio  $R_{sn}$  and checking of the spectrum shape, the SAC (Seismic Analysis Code) software is used to filter the records in those frequency bands with infinite impulsive response (IIR) filters. The butterworth filter is applied in the present study. This type of filters is a good choice since it has a fairly sharp transition from pass band to stop band, and it has a moderate group delay response. The result of the use of band-pass filtering is shown in Figure 2.10 in the case of Bandarabbas accelerograms during the Sarkhun earthquake. The FFT for this three component record after the filtering (using a band-pass filter with cutoff filters 0.6 and 20 Hz) is presented in Figure 2.11.

The high-pass filters have also been used to eliminate the low frequency (long period) noises from the digital (SSA-2 Kinematics) records although this filter is much less important than for SMA-1 records. For instance, Figure 2.12 shows the three components accelerograms in the

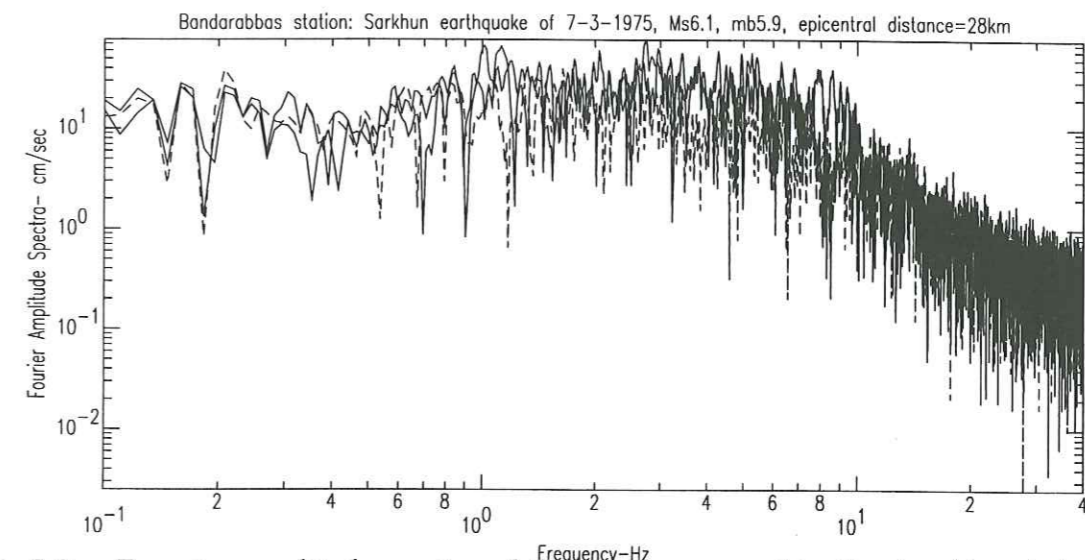


FIG. 2.9 – Fourier amplitude spectra of the Sarkhun record in Bandarabbas, before filtering. The dotted line is the spectrum for the vertical component.

Zanjiran station recorded during the Ebrahimabad earthquake of 20-6-1994. This is the record with the highest acceleration (among the digital records); peak acceleration exceeds 1g. In these cases there were no handy digitalization noises, therefore the filters were selected on the basis of the Fourier spectra to see in which part(s) the FFT spectra differed from the ideal forms before the corner frequency  $f_c$  and after the maximum frequency  $f_{max}$ . These digital recordings have only very small high frequency noise which does not affect significantly peak values (the high frequency noises are generally in the domain of 50 to 100 Hz). Therefore the main attention must be paid to the low frequency noises which are evident before the corner frequency  $f_c$ . The low frequency noises may cause the greatest divergence on the velocity time-histories after an integration on the acceleration time-history. The domain of the low frequency noises may be searched for the example of Figure 2.12 by taking a FFT (shown in Figure 2.13). Even in these transformations some low frequency noises may be seen below 0.3 Hz. Applying a high-pass butterworth filter of 0.3 Hz, one may get the FFT given in Figure 2.14. The filtered acceleration time history is shown in Figure 2.15. The integration on this record after filtering (Figure 2.16) indicates no divergence from the base-line and so a proper filter is selected. The same high-

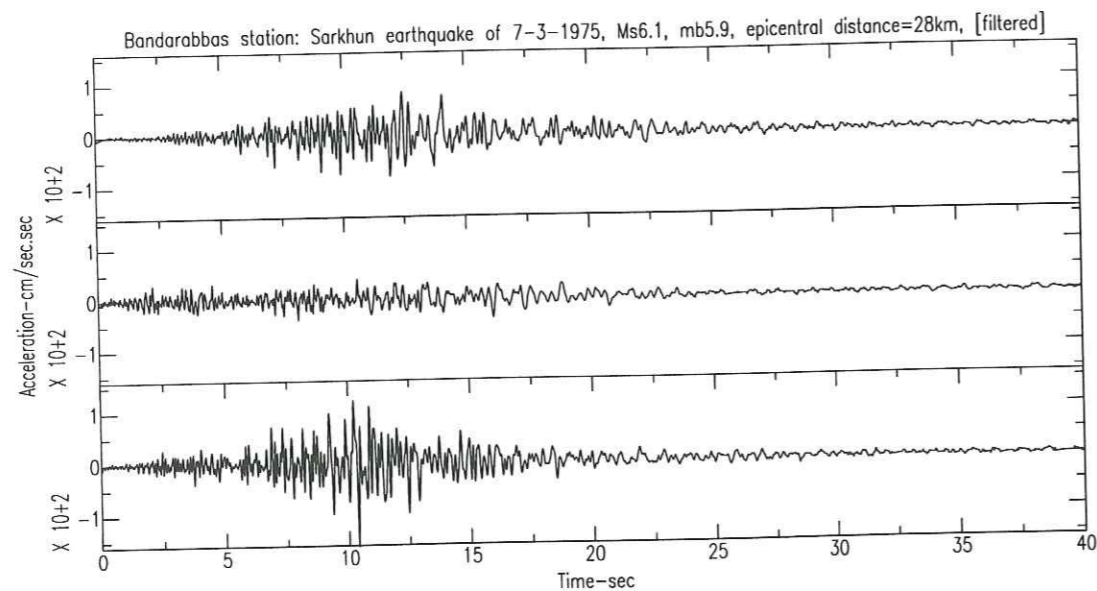


FIG. 2.10 - The corrected and filtered three component acceleration time history in Bandarabbas. The middle record is the vertical and the two others are the horizontal components.

pass filter (0.3 Hz) is applied before the second filtering (on the velocity time-history) and the resultant displacement time-history is shown in Figure 2.17.

The analog corrected record (after filtering) has been integrated to find the velocity and displacement time-histories (Figure 2.18 and 2.19, respectively). It is noteworthy to say that in the present case (Sarkhun earthquake record in Bandarabbas) there was no need to use another filtering before the second integration (to obtain the displacement time-history). As shown in Appendix 1, in most cases a second filtering was needed to obtain the displacement spectra starting and ending on the zero base-line, and with no sharp offset when the recorded samples meet the zero baseline. When these abnormal forms are observed, a second filtering is applied to eliminate these effects.

## 2.5 Site effects

The records are obtained under different soil conditions. As there are no downhole arrays in the country nor any pair of sites in one locality, in most cases there is no possibility to compare

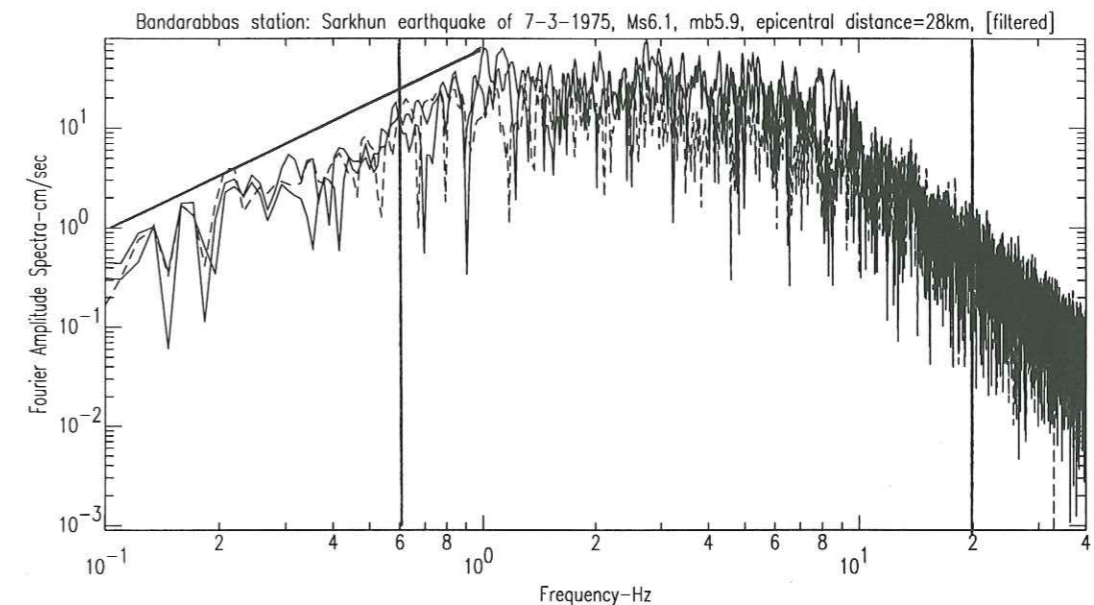


FIG. 2.11 - Filtered Fourier amplitude spectra of the Sarkhun record in Bandarabbas. The dotted line is the spectrum for the vertical component.

empirically the records on soil and on nearby rock outcrops.

Soil conditions are also indicated in Appendix 1. These soil categories were defined after a comprehensive study of soil conditions which is detailed in another paper (Zaré et al 1999a). In brief, site category 1 corresponds to rock and hard alluvial sites, with  $V_s > 800$  m/s over 1st 30m depth and site amplifications (SAM) over 15 Hz. The site category 2 relates to alluvial sites; thin soft alluviums, with  $500 < V_s < 700$  over 1st 30m depth, and  $5 < SAM < 15$  Hz. The site category 3 corresponds to soft gravel and sandy sites, with  $300 < V_s < 500$  over 1st 30m depth and  $2 < SAM < 5$  Hz. Finally the site category 4 relates to soft soil sites; thick soft alluviums with  $V_s < 300$  m/s over 1st 30m depth and  $SAM < 2$  Hz. This preliminary ranking is based both on the studies on 50 sites where geotechnical measurements were performed (compressional and shear wave velocity and microtremor measurements) and three component accelerograms were used to calculate the receiver function for the strong motions. The result of this classification is presented in table-I (Zaré et al 1999a):

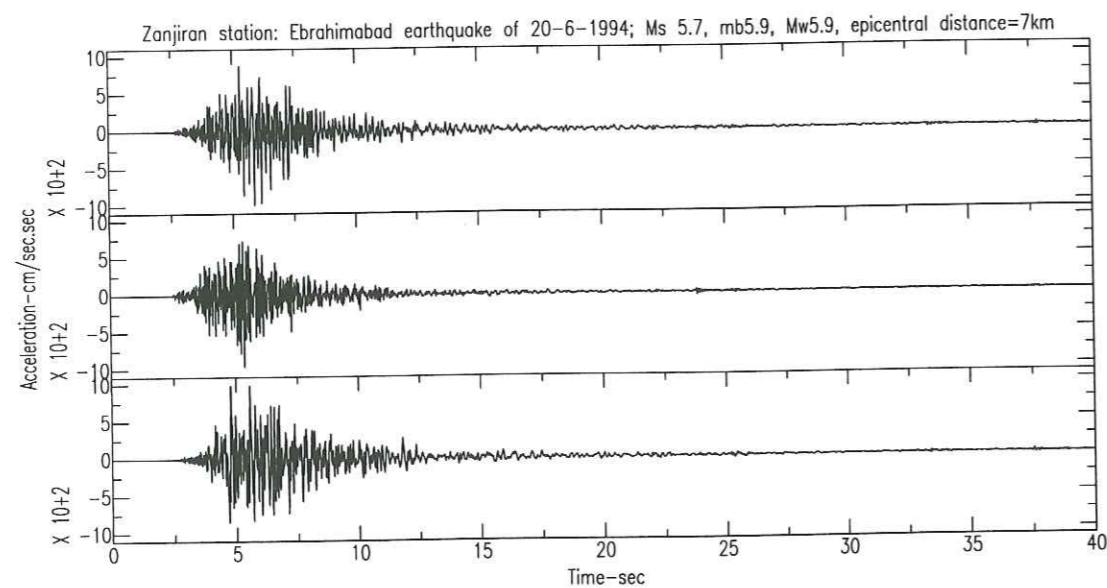


FIG. 2.12 - Three component acceleration time history of the Ebrahimabad earthquake of 20-6-1994 recorded at Zanjiran before filtering. The middle record is the vertical and the two others are the horizontal components.

Table-I: The 4 class site categorization

Group	Frequency Band of the Amplification	$V_{s30}$ m/s	Sites
1	$F \geq 15Hz$	$V_{s30} \geq 700$	Abbar, Deyhuk, Ghaen, Jovakan, Kakhk, Naghan, Saadabad, Tabas
2	$5 \leq F < 15Hz$	$500 \leq V_{s30} < 700$	Kavar, Maku, Manjil, Vendik, Zanjiran
3	$2 \leq F < 5Hz$	$300 \leq V_{s30} < 500$	Fin, Firouzabad, Ghazvin, Golbaf, Rudbar, Zarrat
4	$F < 2Hz$	$V_{s30} < 300$	Abhar, Lahijan, Hosseinieh, Rudsar, Shabankareh, Tonkabon, Talesh

Among the methods that we have used to study the site conditions, the only method that may reveal the site response to ground motions is to study the three component strong motion records. The benefit gained from this method is that we had at least one record in each of the stations and this is the only method which may be applied at each location. The velocity profiles that we measure by the geoseismic methods are limited to the first 30-35 metres; the microtremors have shown important amplifications just in the soft soil sites, and the geoelectric

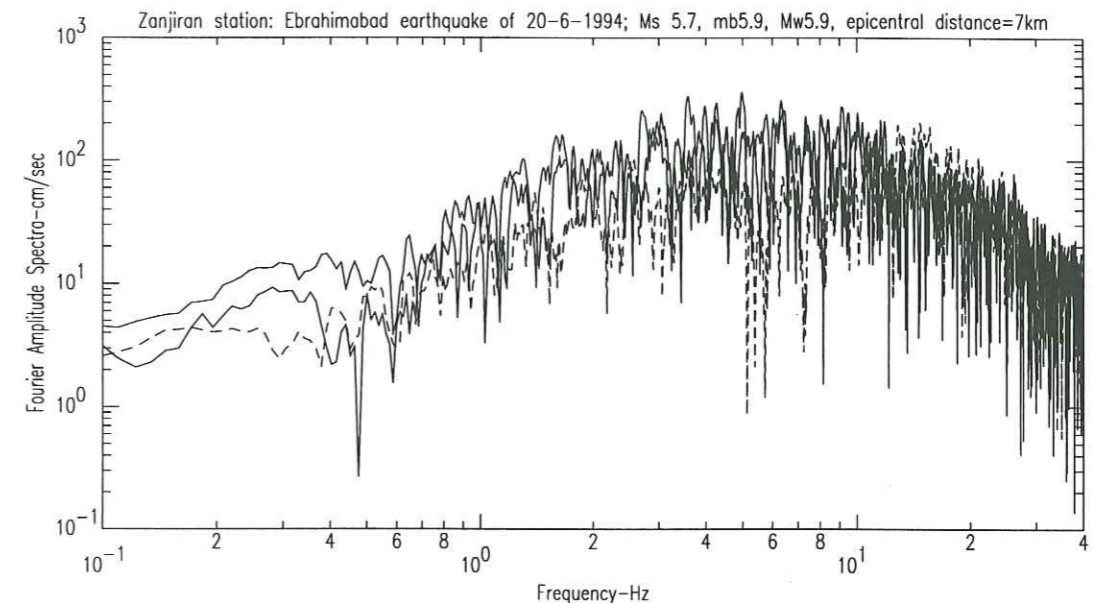


FIG. 2.13 - Fourier amplitude spectra of the Zanjiran record before filtering. The dotted line is the spectrum for the vertical component.

tests do not give the precise measurements to distinguish the different sites. Meanwhile, if there are thick alluvial layers on the surface (with a thickness of more than 30 metres) on a very high velocity layer at greater depths, the H/V spectrum for the strong motion (the receiver function) is the only way to observe such an amplification in low frequencies. In this case the other methods will show just the high velocity alluvium with some amplifications in high to very high frequencies (more than 15Hz).

## 2.6 Assigning a Quality Label to each Record

A four class categorization is used to grade the quality of each record; « A » corresponds to the best quality and « D » to the worst. Four criteria are taken into account for this categorization; 1. The quality of digitalization of the analog records (corresponding generally to low PGA records). 2. The source focal depth (should be unequal to 33 km). 3. The macroseismic epicentral distance. 4. The source mechanism. If these conditions are available for one record, then its label is assigned « A », and in the absence of each of these cases the quality factor



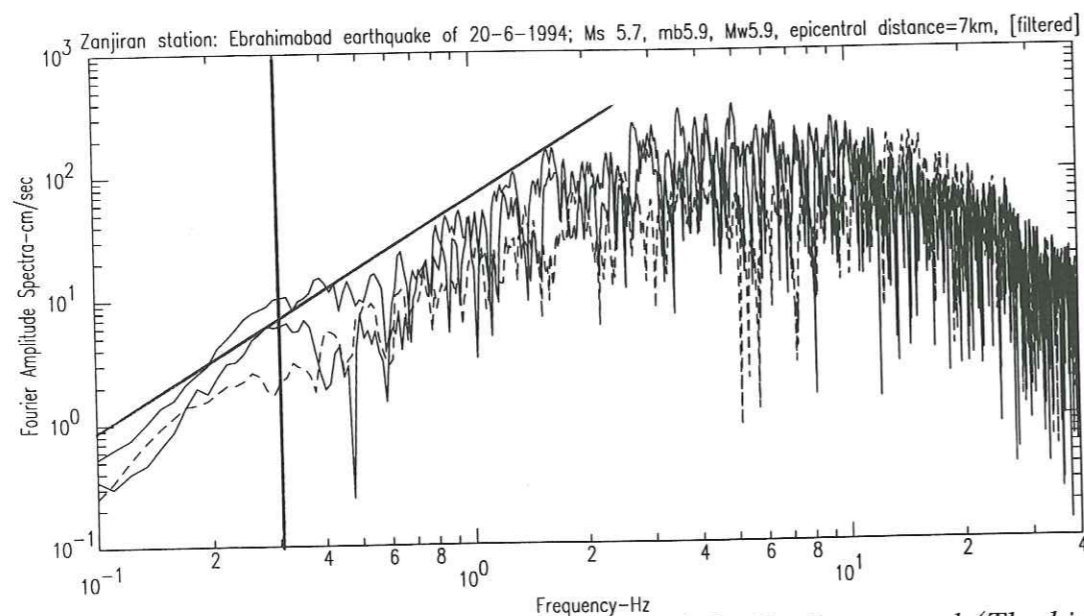


FIG. 2.14 - The filtered Fourier amplitude spectra of the Zanjiran record (The high-pass filter of 0.3Hz is used). The dotted line is the spectrum for the vertical component.

diminishes to « B », « C »,... but the worst records which are chosen had at least the earthquake « magnitude » and the epicentral distance (instrumental) which are referred to as « D ».

## 2.7 Sources of Errors and Uncertainties

Some expected sources of uncertainties during this study may originate from:

### 2.7.1 Instrumental and macroseismic epicentral distances

As most of the source parameters are based on the teleseismic data, an uncertainty may originate from the lack of precision in the epicenters location, and the consequences on the estimates of epicentral distances. According to ISC monthly bulletin, the accuracy of the localization in the last 20 years has been different from about 0.01 (approximately about 1 km in a geographical coordinate such as Iran) for the great earthquakes with magnitudes more than  $M7.0$ , to about 0.15 (approximately about 15 km for such a region) for the earthquakes with magnitudes about  $M4.0$ . We have however the feeling that these precision estimates are very

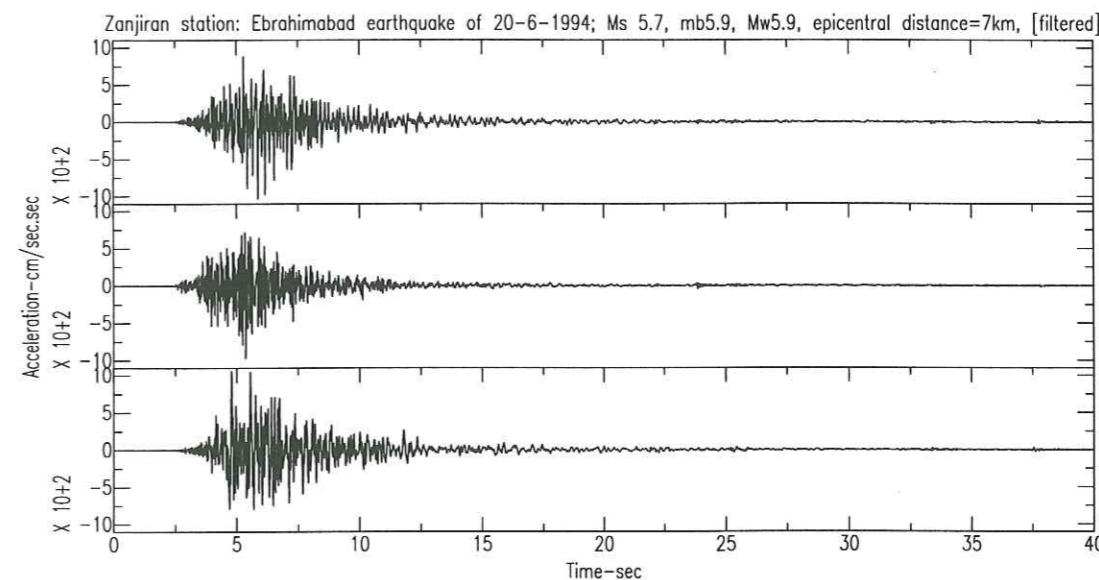


FIG. 2.15 - The filtered three component acceleration time history of the Zanjiran record (The high-pass filter of 0.3Hz is used). The middle record is the vertical and the two others are the horizontal components.

optimistic and should be at least doubled.

The macroseismic epicenters are based on damage reports, whenever available (which is possible only in the inhabited areas), as well as the surface earthquake fault ruptures if there was evidence. Therefore the distances to macroseismic epicenters depend greatly on the presence (or absence) of damage reports, the geographic distribution of the inhabited regions and finally on the presence of the surface rupture. Each of these factors (especially this fact that in most of the cases, the causative fault had no new surface ruptures) may result in the distances to the macroseismic epicenter being uncertain. From this point of view, the great earthquakes are the exceptions (Vendik 1976, Naghan 1977, Ghaen 1978, Tabas 1978, Ghaen 1979, Korizan 1979, Koli-Bonyabad 1979, Golbaf 1981, Sirch 1981, Manjil 1990 and Ebrahimabad 1994), such that the damage reports on these cases are more precise and the causative faults are well known.

For part of the records (mainly SSA-2 which have a pre-event memory) it was possible to estimate the hypocentral distance using the well-known formula:  $D_{hypo} = 8 * (ts - tp)$  Where  $tp$  and  $ts$  are the first arrivals of the P and S waves, respectively. This formula was compared

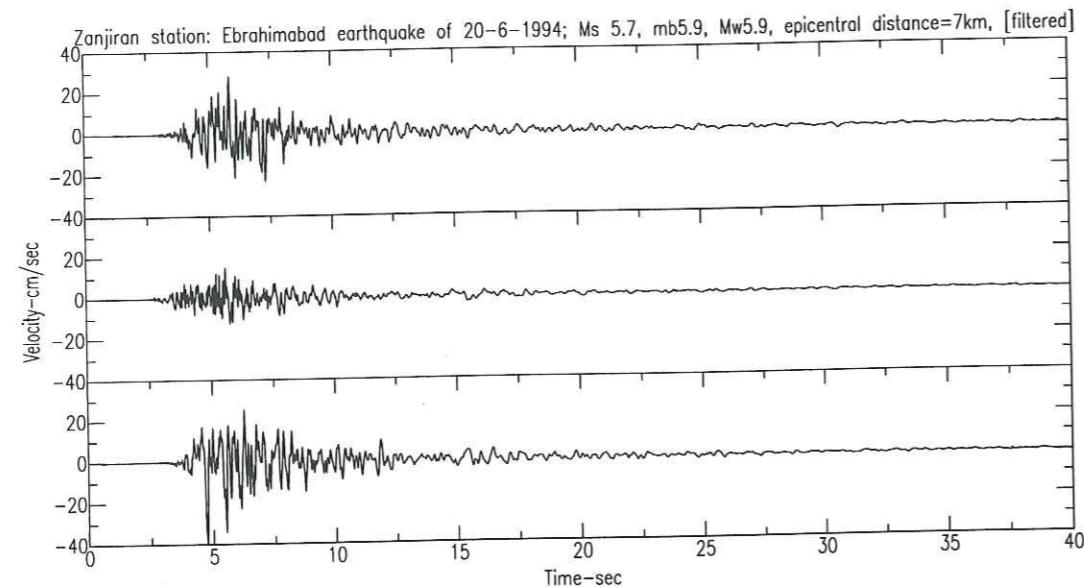


FIG. 2.16 – Three component velocity time history of the Zanjiran record after the integration of the acceleration. The middle record is the vertical and the two others are the horizontal components.

with the epicentral distances and focal depths as inferred for ISC and/or NEIC locations. This distance was not computed for the near-field records of large event, because it was not possible in many cases to identify clearly the P and S waves. As may be seen in Appendix 1, these values are not always consistent with one another. This is another hint that epicenter location in Iran is not very precise.

### 2.7.2 Focal depths

The earthquakes in the Iranian plateau are mostly of the crustal type origin and, as was shown before, most of those considered in this study were superficial (depths less than 35 km). According to the ISC monthly bulletins, the precision of focal depths is different by as much as  $\pm 4$  km for the well determined superficial earthquake (generally the events with the magnitudes more than M6) to  $\pm 30$  km for the poorly determined events (generally the small earthquakes with the magnitudes less than about M4). Therefore, it may be concluded that precision of the focal depths is even less than the precision involved in the location of the

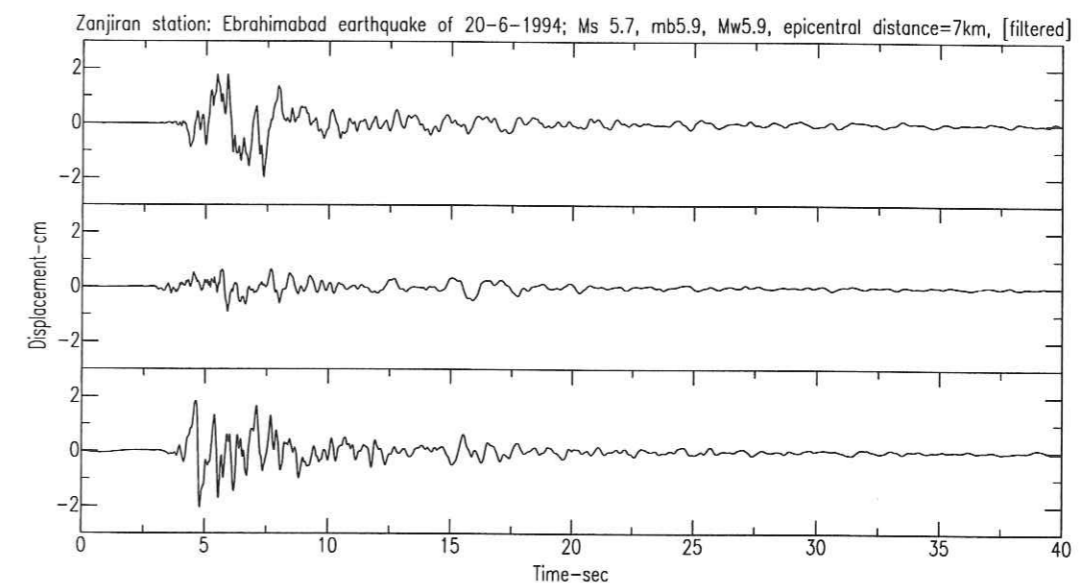


FIG. 2.17 – Three component displacement time history of the Zanjiran record after the integration of the velocity. The middle record is the vertical and the two others are the horizontal components.

epicenter.

### 2.7.3 Integration of the filtered records

The integration to obtain the velocity and displacement time-histories may cause some uncertainties especially for the analog recordings, since the presence of even little high frequency or low frequency noises may cause some differences in the peak values. The high-pass filtering that we applied was intended to eliminate this low frequency noise. This low frequency cut off certainly cuts some signal so that the peak velocity and peak displacement values may be biased (underestimated) in some cases.

### 2.7.4 Earthquake intensities

It has been explained (to determine the macroseismic epicenters) that earthquake intensities are strictly based on observations and reports. According to the qualitative nature of

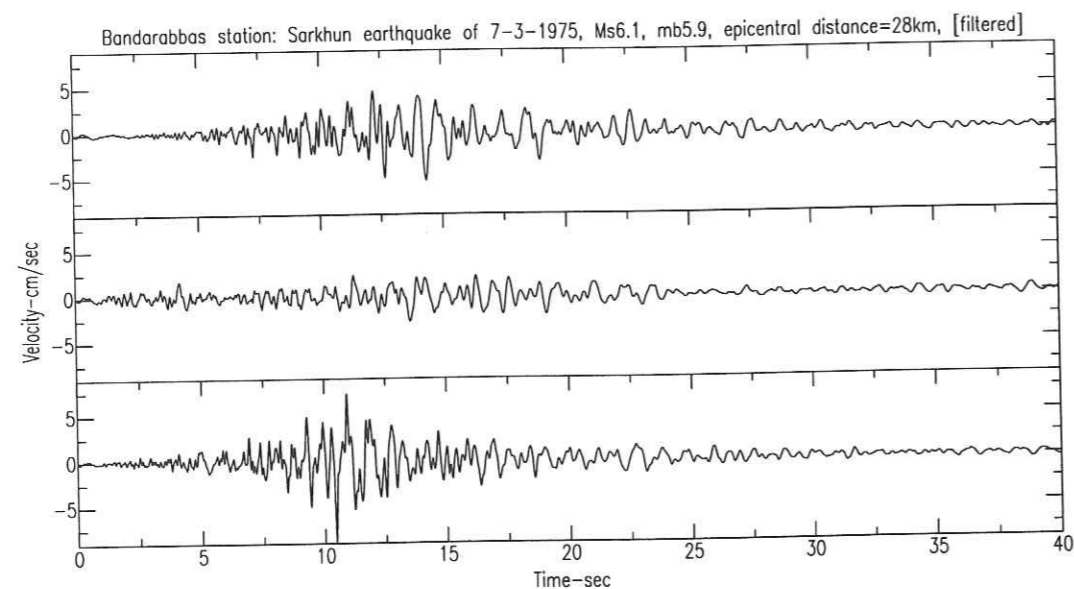


FIG. 2.18 – Three component velocity time history of the Bandarabbas record after the integration of the acceleration. The middle record is the vertical and the two others are the horizontal components.

intensity measurements, different intensities may be presented for one single earthquake by different investigators. On the other hand, in order to compare the different damaged areas with earthquakes with same magnitudes and epicentral distances, we have endeavored to present all the intensities on a single scale (MSK). In this regard, the previously reported intensities on other scales are converted to this scale using the comparison chart of Japan TC-4 (1992). The nature of the intensity measurements and the quality of the reports from the damages or shocked zones, as well as the conversion of the intensities to MSK scale, may be the origin of many uncertainties.

## 2.8 Conclusion

The first Iranian strong motion catalog (Appendix 1) was developed in this study. This catalog comprises the source and site information for each selected three-component record as well as the maximum values of the acceleration, velocity and displacements. The data-set

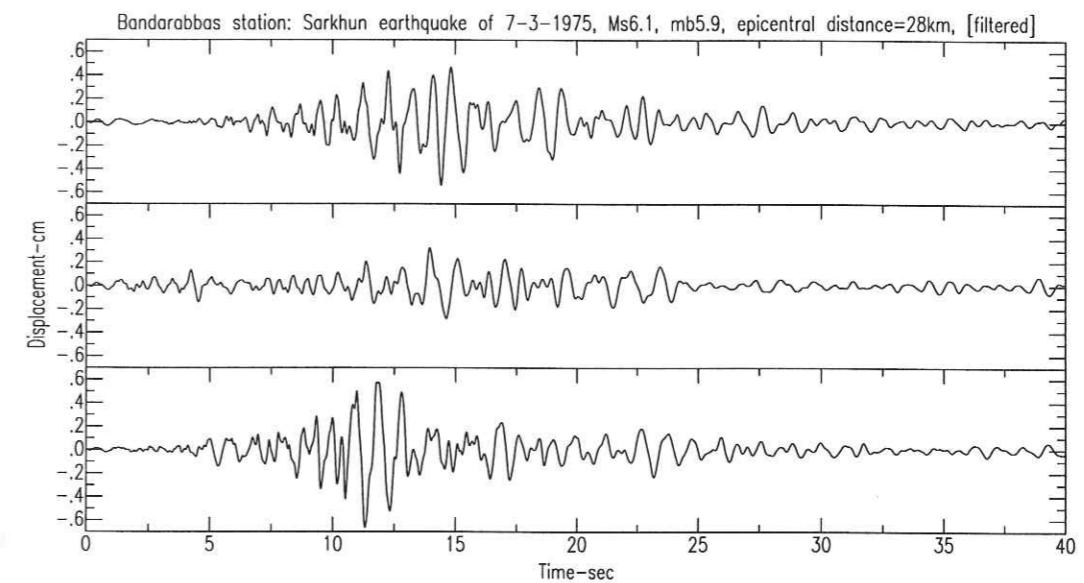


FIG. 2.19 – Three component displacement time history of the Bandarabbas record after the integration of the velocity. The middle record is the vertical and the two others are the horizontal components.

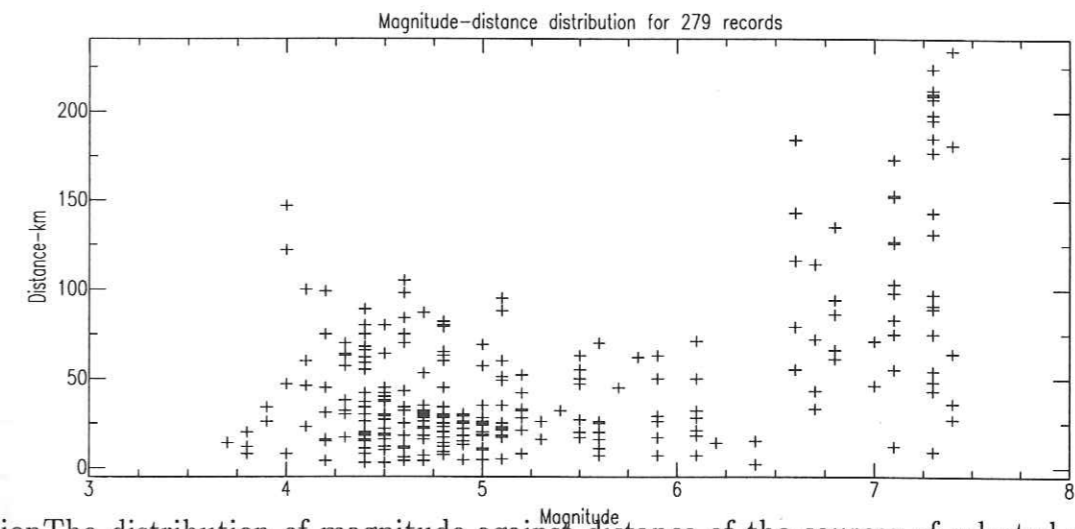
contains the intensity and focal mechanism of the causative events (whenever available). This catalog provides a set of 279 three-component records, with a satisfactory quality and for which we could find their source parameters. There are 169 SMA-1 (analog) and 108 SSA-2 (digital) record in this set. According to the selected sources in this catalog, the geographical distribution of the epicenters indicates that the Zagros region was the most seismically active during the last twenty five years in the Iranian plateau. The most important earthquakes in this catalog are; Sarkhun (Bandarabbas) earthquake of 7-3-1975 (Ms6.1, mb5.9; 3 records for the mainshock and 2 for the aftershock); Vendik (Ghaen) earthquake of 7-11-1976 (Ms6.4, mb5.8; 4 records); Khurgu earthquake of 21-3-1977 (Ms7.0, mb6.2; 2 records); Naghan earthquake of 6-4-1977 (Ms6.1, mb5.6; 4 records for the mainshock and 3 for the aftershock); Tabas earthquake of 16-9-1978 (Ms7.3, mb6.7, Mw7.4; 5 records for the mainshock and 6 for the aftershocks); Ghaen earthquake of 16-1-1979 (Ms6.8, mb6.0; 5 records), Korizan (Ghaen) earthquake of 14-11-1979 (Ms6.6, mb6.0; 6 records) Koli-Bonyabad (Ghaen) 27-11-1979 (Ms7.1, mb6.1; 12 records), Golbaf (Kerman) earthquake of 11-6-1981 (Ms6.7, mb6.1; 3 records), Sirch (Kerman)

earthquake of 28-7-1981 ( $M_s 7.1$ ,  $m_b 5.7$ , 2 records for the mainshock and 6 for the aftershocks), Manjil earthquake of 20-6-1990 ( $M_s 7.7$ ,  $m_b 6.8$ ,  $M_w 7.3$ ; 18 records for the mainshocks and 20 for the aftershocks); Ebrahimabad (Firouzabad) earthquake of 20-6-1994 ( $M_s 5.7$ ,  $m_b 5.9$ ,  $M_w 5.9$ ; 5 records for the mainshock and 6 for the aftershocks).

It must be noticed that there are other good quality recorded three component accelerograms in BHRC collection but they could not be selected in Appendix 1 because they could not be assigned to any particular earthquake [due to the lack of timing on SMA-1 instruments].

The Iranian strong motion data (Appendix 1) are recorded mostly in the Zagros mountains, western Alborz and northern Lut areas. The distribution of the records is shown in (Figure 2.8 in a diagram of the magnitudes against the distances. This figure shows that most of the records are obtained in the magnitude range of  $M 4-5$  and in the distance range of zero to 100 kilometers. The great earthquakes are recorded, as well, in this network (in the range of  $6.5 < M < 8.0$  within a distance range of 5 to 230 km). Therefore, it seems that the attenuation relationships that will be developed on these data will be most reliable in the mentioned ranges of magnitudes and distances. The digital data which will be obtained in the future may fill the gaps between the mentioned ranges. On the other hand, it is still necessary to obtain more data in the near field especially in the range of great events ( $M 6-8$ ), in order to develop reliable analyses in the near field and to perform detailed studies on the source and/or site effects. Until that time, it seems difficult to perform detailed near field studies with the present (especially in the magnitude range of  $M 6-8$ ).

In the capital, Tehran, the strong motion records are mostly limited to the Manjil earthquake corresponding to a distance of about 200 km. No important records were obtained (with high acceleration values) in the regions of country similar to the situation of the Tehran plain. Meanwhile there is concern that a great event may shock the capital in an unpredictable time in the future. Therefore, we suggest strongly the installation of dense accelerometric arrays in Tehran and other major and most hazardous cities of Iran such as Ghazvin, Tabriz, Mashhad, Shiraz, Shahr-e Kord, Naein, Zahedan, Tabas, Kashmar, Gorgan, Kazerun, Birjand, Ardebil and Kerman which have situations comparable to Tehran considering site conditions and distances to the earthquake sources. This would be important to obtain meaningful data-sets for reliable microzonation and hazard studies in Tehran and in the mentioned cities. In general, the Iranian network may provide strong motion data not only for herself, but also to share these data with the other neighboring countries with similar seismic source conditions such as Turkey, Iraq, Afghanistan and Pakistan, as well as with the central Asian and Caucasus republics.



caption The distribution of magnitude against distance of the sources of selected records for the present study.

### Acknowledgements

Many individuals have assisted us in this paper; most notably Mr. Mehdi Heydari (in IIEES) assisted this project to provide the source data. The BHRC (Building and Housing Research Center, Tehran) who have released the raw strong motion records is greatly acknowledged. The financial support in Iran was provided by IIEES, and in France (for the first author) was provided by a French scholarship (Ministère Français des Affaires Etrangères), which are both duly acknowledged. We thank Mr. Mohammad Zaré (the father of first author) who has provided the reports of the Persian dailies on the earthquake damages in Iran during the period of 1974-1996. Our thanks also go to Douglas McLean who has proof-read this text and has given comments to correct the orthography.



Table with columns: No, Code (BHRIC), Station, Site, Filters for processing (1st, 2nd), Peak Ground Acceleration (cm/s²), Peak Ground Velocity (cm/s), Peak Ground Displacement (cm), Macroscopic epicenter (Region), Date, Me, Mb, Ml, Mw, Focal Depth (km), Epicentral Distances (km), Hypocenter Distances (km), Macroscopic epicenter distance (km), Intensity (MSK), Focal Mechanism, Q, Ref.

Table with columns: No, Code (BHRIC), Station, Site, Filters for processing (1st, 2nd), Peak Ground Acceleration (cm/s²), Peak Ground Velocity (cm/s), Peak Ground Displacement (cm), Macroscopic epicenter (Region), Date, Me, Mb, Ml, Mw, Focal Depth (km), Epicentral Distances (km), Hypocenter Distances (km), Macroscopic epicenter distance (km), Intensity (MSK), Focal Mechanism, Q, Ref.



in the site of the Ol d-Lar city in southern Zagros, and are just reported by the local stations of the IGTU. Some 40 aftershocks followed these two main events. Based on some reported minor quake impressions in the Fataviyeh villages and its suburbs, an intensity of III is estimated for the epicentral area.

- Kohan (Kuhbanan) earthquake 11-4-1987 ( $M_s4.5$ ;  $m_b5.0$ ) caused panic among the inhabitants and some damage in form of the rural building collapses in the village of Kohan and the breaking of windows in the city of Kohbanan.

- Gol (Khusf) earthquake 24-11-1987 ( $m_b5.3$ ) caused some damage in the Gol villages and Khusf city in the west and southwest of Birjand.

- Rostamabad earthquake 28-11-1991 ( $M_s5.0$ ;  $m_b5.6$ ;  $M_L5.5$ ) damaged some recently reconstructed buildings (after the great earthquake of Manjil 20-6-1990,  $M_w7.3$  in the same region). Two people collapsed and died in the panic provoked by this shock.

- Ebrahimabad (Firouzabad) earthquake 20-6-1994 ( $M_s5.7$ ;  $m_b5.9$ ;  $M_w5.9$ ) caused severe damages in the central Zagros area between Shiraz and Firouzabad. The quake demolished the most of the buildings in Ebrahimabad, Jovakan and Zanjiran. Some minor damage was observed in Firouzabad (some cracks in walls and minor damages in the rural buildings). Three people were killed in this earthquake (2 in Ebrahimabad and one in Zanjiran).

## Chapitre 3

### Les Effets de Site



**Résumé** Les effets de site sont étudiés dans ce chapitre en utilisant les données de mouvements forts enregistrés par le réseau accélérométrique iranien. Vingt-six sites ont été choisis pour des mesures géosismiques. Le bruit de fond y a été enregistré, ainsi que dans vingt-quatre autres sites où ces mesures ont été les seuls tests réalisés. Des tests géoélectriques ont également été effectués sur les 24 sites où des études géosismiques ont été réalisées, mais ces résultats n'ont pas été utilisés car leur interprétation ne donnait pas de résultats très intéressants. Les rapports spectraux entre les composantes horizontales et verticales (« fonctions-récepteur ») ont aussi été calculés pour tous les enregistrements du catalogue de mouvements forts iraniens (137 sites en tout). Ces rapports ont été la base de notre classification de site, du point de vue de leurs réponses aux mouvements forts, car ils sont les seuls critères qui existent pour tous les sites, et les seuls qui montrent directement les réponses des sites aux mouvements forts. Ce critère de classification résulte d'une comparaison entre les fonctions récepteurs et les résultats des tests géotechniques (géosismique, bruit de fond). En bref, les sites avec les rapports H/V inférieurs à 3 pour toute fréquence inférieure à 15 Hz ont été considérés comme du 'rocher' (classe 1); les sites avec un rapport H/V dépassant 3 dans la bande de fréquence de 5 à 15Hz ont été classés dans la catégorie 2, ceux avec un rapport H/V dépassant de 3 dans la bande de 2 à 5 Hz sont classés en catégorie 3, ceux montrant un rapport H/V dépassant 3 pour les fréquences inférieures à 2Hz ont été classés dans la catégorie 4. Il s'avère que cette classification se corrèle assez bien (dans 70% des cas) avec la valeur moyenne de la vitesse d'onde S sur les 30 premiers mètres,  $V_{s30}$ : pour la classe 1,  $V_{s30} > 700$  m/sec; pour la classe 2,  $500 < V_{s30} < 700$  m/sec; pour la classe 3,  $300 < V_{s30} < 500$  m/sec; et pour la classe 4,  $V_{s30} < 300$  m/sec. Le bruit de fond ne présente qu'un accord très partiel avec ces classifications: dans les sites de type de classe 3 et 4 on trouve les rapports H/V présentant une certaine similarité avec les fonctions-récepteurs. Ce résultat mitigé pourrait être la conséquence des situations topographiques (l'existence de deux chaînes des montagnes importantes dans le plateau iranien) et météorologiques (aride et sec) du pays. La classification présentée dans ce chapitre est le premier travail sur les effets de site accompli à partir du réseau accélérométrique en Iran.

## Site Characterizations for the Iranian Strong Motion Network

Mehdi Zaré, Pierre-Yves Bard and Mohsen Ghafory-Ashtiany

Article publié dans le "Journal of Soil Dynamics and Earthquake Engineering", 1999, Vol.18, no.2, pp.101-123.

**Abstract** 26 sites of the Iranian strong motion network, having provided numerous records of good quality, were selected for a site effect study with the objective of obtaining a reliable site categorization for a later statistical work on Iranian strong motion data. For each site, superficial  $V_p$  and  $V_s$  profiles were measured with refraction techniques, microtremor recordings were obtained and analyzed with the H/V technique and the available three-component accelerograms by the receiver function technique. The aggregation of these results allows the proposition of a four-class categorization based on the H/V spectral ratio of strong ground motions, which demonstrate a satisfactory correlation with S-wave velocity profile. Iran has a particular geological and meteorological situation compared to other seismic countries such as Japan or California; a mountainous country with dry weather condition and low water table in most areas. These conditions result in a relatively small number of sites with low frequency amplification, while many sites exhibit moderate amplifications in the intermediate and high frequency range.

### 3.1 Introduction

The strong motion accelerometric network in Iran is installed throughout the country in different site conditions. The Kinematics SMA-1 analog instruments were initially installed since 1975, and then they have been gradually expanded by the SSA-2 digital instruments since the Manjil earthquake of 1990;  $M_w 7.4$ , in NW Iran. The number of the instruments in this network is 1000 stations (by the end of 1997). The stations have been mainly chosen within the cities or villages for an easy maintenance. However there are no double stations (functioning as a local network on a soil site and its corresponding rock outcrop) to compare easily the soil and rock motions in different earthquakes. Meanwhile, there is no down-hole array, yet, to compare the motions on the surface and on the base rock.

The previous studies on site effects on the strong ground motions in Iran were limited to some, recent, studies on the soil effects on strong motion records during the great earthquakes (Zaré 1994; 1995; 1996a & 1996b). On the other hand, some microzonation case studies were also performed in some great cities in Iran (Jafari et al 1995, 1996).

The scope of this study was to investigate the site effects on the strong ground motions in Iran. It is also tried to select a variety of different soil and geologic conditions in such a

way that at the end of this study, there will be possible to present a site categorization to be used in the seismic hazard studies and the attenuation models for Iran. Meanwhile we hoped to determine a site categorization adaptable to the geological and meteorological situations of Iran. We intended to develop a method that would not be somewhat limited by the depth of the surface deposits. Finally it is tried to suggest a site classification to be mostly reliable and easily applicable (i.e. the site categorization in the United States is based on  $V_{s30}$  which, in our opinion is not optimal; Boore et al. 1997).

In this article the results of a study on the site characterizations of some selected sites of the network are presented. We explain, first, the methodology of the study. Then an overview on the general situations of the sites and the different performed methods are described. The results of the different tests are presented afterward. Finally a 4-class site categorization is introduced.

### 3.2 The methodology

Fifty sites were studied. These sites were chosen from a database of 279 records (already processed and developed; Zaré, et al. 1998). The sites were chosen on the bases of the number and quality of corresponding records, as well as on the amplitude of the recorded motion and its dependence with a great earthquake (to compare cases of the same events). The site studies were carried out with different methods: geoseismic tests to determine the compressional and shear waves in a profile under the station, microtremor studies (with SS-1 instruments and SSR-1 sensors), and geoelectric studies. Finally the site geological observations were performed to understand the geologic frame in each locality (type of the superficial layers, the depth of the water table, etc...). Among the fifty aforementioned sites, in 24 sites microtremor tests were applied, the geoseismic tests were performed in the 26 more important sites (the names of the sites and the results of the performed test are summarized in table I).

Table I: The results of the site effect studies on 138 sites in Iran; comprising 50 sites where the geotechnical tests carried out.

Table I  
The results of the site effect studies, and the site classification for strong motion stations in Iran.

No	Station	Site categorization	Number of records	Site geology	$V_s$ over 1st 30 m ( $m s^{-1}$ )	Amplification of HV on microtremors	Amplification of HV on strong motions	Site based on surface geology (BHRC)	Electric resistivities (ohmm)	Q
1	Abbar	1	5	Stiff alluvium	621	1 2(0.2-20 Hz)	< 4 (2-5 Hz)	3	5-17 (1st 30 m)	A1
2	Abbar	4	1	Silt-clay in surface	263	> 2 (0.2-2 Hz)	> 4 (0.2-0.3 and 1-4 Hz)	4	3-25 (1st 25 m)	A1
3	Aghajari	2	1				> 4 (4-6 Hz)	1		C
4	Ahar	1	1				1-2 (3-10 Hz)	4		D
5	Amirloo (Jirandeh)	3	6				> 4(3-5 Hz)	C		C
6	Andimeshk	1	3				2-3 (3-7 Hz)	2		C
7	Ardal	3	4				> 4 (2.5-3.5 Hz)	2		C
8	Ardebil	4	1				> 4(1-2.5 and 4-5 Hz)	3		C
9	Astaneh	4	1				> 4(0.7-2 Hz)	3		C
10	Avaj	1	2				3(4-7 Hz)	4		D
11	Babakalan (Gachsaran)	2	1				> 4(0.9-1.7 Hz)	C		C
12	Baba-Momir	4	1				> 4(5-6 Hz)	C		C
13	Babonar	2	1	Silt-clay in surface		> 2(2- Hz)	> 4(3-6 Hz)	2		D
14	Bajestan	3	3				1-2(0.7-10 Hz)	4		C
15	Bam	1	1	Sand beach of the Persian Gulf		1-2(1- Hz)	> 4(6-10 Hz)	3		B
16	Bandarabbas (S)	2	3				> 4(3-5 Hz)	C		C
17	Bandar-Deylam	3	1				> 4(0.9-3.5 Hz)	C		C
18	Bandar-lengeh	4	1				1-3(0.7-7 Hz)	2		B
19	Bandar-Torkman	4	1				> 4(2.5-3.5 Hz)	4		C
20	Birjand	1	4	Stiff alluvium		1(0.2-20 Hz)	1-2(1-5 Hz)	2		C
21	Boroujerd	3	1				> 4(1-2.5 Hz)	2		C
22	Boshruyeh	1	1				> 4(5.5-6.5 Hz)	2		D
23	Bostanabad	4	1				> 4(1-2.5 Hz)	C		C
24	Dalin (SE Sepidan-Fars)	2	1				2-3(2-6 Hz)	2		C
25	Darreh-Shahr Ilam	1	1				> 4(8-11 Hz)	C		C
26	Dashtgerd	2	1				> 4(7-11 Hz)	C		C
27	Deh-Balla - N. Farrashband	2	1	Stiff alluvium	826	1 2(0.4-20 Hz)	2-4(2-15 Hz)	2	3-5 (1st 12 m)	A2
28	Delvar	2	1	Hard conglomerate			1-2(1-15 Hz)	1		C
29	Deyhuik	1	3				> 4(2.5-4 and 6.5-8 Hz)	2		C
30	Dez Dam	1	3				> 4(3.5-7 Hz)	C		C
31	Doab (Poje Sefid)	3	5				> 4(1.5-2.5 Hz)	C		B
32	Dorahun	3	1				> 4(0.5-0.65 Hz)	4	20-80 (1st 25 m)	B
33	Doroud	4	1				> 4(5-10 Hz)	3		B
34	Estehard	4	1				1-2(5-8 Hz)	4		C
35	Estakht-Posht	2	1				> 4(5-10 Hz)	1		D
36	Farrashband	1	1				1-2(5-8 Hz)	3		D
37	Farsan	1	1				2-3(0.3-5 Hz)	2		B
38	Ferdows	1	1	Stiff alluvium	480	1(0.4-15 Hz)	> 4(2.5-5 Hz)	2		A1
39	Fin (N. Bandar-Abbas)	3	31	Soft alluvium	478	2-4(4- Hz)	> 4(1.5-4.5 Hz)	3	14-90 (1st 33 m)	A1
40	Firouzabad	3	11	Soft alluvium		2-3(4- Hz)	> 4(2.5-4.5 Hz)	2		C
41	Gachisar	3	3				> 4(2.5-4.5 Hz)	2		C
42	Ghaemiyeh (Chenar-Shahijan)	3	1				> 4(2.5-4.5 Hz)	1		C
43	Ghaen	1	3	Stiff alluvium	867	1(0.6-25 Hz)	2-3(0.4-0.6 and 3-7 Hz)	2	1.5-100 (1st 21 m)	A2
44	Gavbandi	3	1				> 4(3-6 Hz)	C		C
45	Ghaleh-Ganj	1	1				2-3(2-11 Hz)	C		C
46	Ghazvin	3	1	Cohesionless gravel	424	1-2 (4-2 Hz)	3-4(1-5 Hz)	2	10-50 (1st 20 m)	A2
47	Gheshm-Island	1	1				1-2(1.5-8 Hz)	2		C

Table 1 (continued)

No	Station	Site categorization	Number of records	Site geology	$V_s$ over 1st 30 m ( $m s^{-1}$ )	Amplification of H/V on microtremors	Amplification of H/V on strong motions	Site based on surface geology (BHRC)	Electric resistivities (ohmm)	Q
48	Ghir	3	1	Gravel		1(4-15 Hz)	3-4(4.5-5.5 Hz)	1		B
49	Gilvan	1	2				2-3(4-7 Hz)	2		D
50	Golbaf	3	13	Soft alluvium	439	1(4-8 Hz)	> 4(3-5 Hz)	3	4-8 (1st 19 m)	A2
51	Gonabad	4	3	Soft alluvium		1(0.2-40 Hz)	3-4(0.8-1.5 Hz)	3		B
52	Hajiabad	3	1				> 4(3.5-4.5 Hz)	1		C
53	Hassan-Keif	3	1				> 4(2.5-3.5 Hz)			C
54	Hosseiniyeh-Olia	4	11	Soft alluvium	563	1(2(0.2-6 Hz)	> 4(0.3-1 Hz)	1		A2
	Andimeshk								5-30 (1st 25 m)	A1
55	Jovakan	1	30	Soft alluvium in surface	1017	1(2(0.6-9 Hz)	2-3(5-8 Hz)	2		B
56	Kahrizak	4	1	Clay and marl		1(2(0.6-2 Hz)	3-4(0.4-2 Hz)	4		A2
57	Kakhk	1	1	Sandstone	2200	2(4(0.8-10 Hz)	2-3(1.5-6 Hz)	1		B
58	Karaj	1	1	Course grain gravels		1(0.4-25 Hz)	1-3(0.5-10 Hz)	2		C
59	Karkheh Dam	1	1				1-3(1-10 Hz)	1		C
60	Kashmar	3	2				3-4(2-3.5 Hz)	2	6-120 (1st 35 m)	A2
61	Kavar	2	13	Hard conglomerate	946	1(1-11 Hz)	2-4(1-9 Hz)	1		C
62	Kavar Dam	2	4				> 4(4-8 Hz)	4		C
63	Kazerun	2	2				> 4(5-11 Hz)	4		B
64	Kerman	4	2	Soft alluvium			> 4(1.5-3 Hz)	3		C
65	Khaf	2	6				> 4(5-8 Hz)	2		C
66	Khazanun	1	3	Hard conglomerate			2-3(2-7 Hz)	3		B
67	Khezri	1	2				2-3(0.4-4 Hz)	3		C
68	Khonj	1	1				2-3(3-7 Hz)	3		C
69	Khorramabad	2	3				3-4(4-7 Hz)	2		C
70	Khoy	3	1				> 4(4-4.5 Hz)			C
71	Khurmodj	1	1				2-3(3.5-20 Hz)			C
72	Kiasar	2	1				> 4(6-7 Hz)	2		C
73	Kolur	1	1	Soft alluvium			> 4(15 Hz)	4		B
74	Kuhbanan	3	1				3-4(2-6 Hz)	2		C
75	Kuhestak	3	1				> 4(2.5-6 Hz)	1		C
76	Kushk-Nosrat	4	1	Clay and silt	264	1(4(0.8-2 Hz)	3-4(0.8-1.5 Hz)	4	4-10 (1st 10 m)	A1
77	Lahijan	4	1				> 4(3-5 Hz)	2		C
78	Lali	3	8				2-3(0.8-10 Hz)			C
79	Lamerd	1	1				1-2(4-15 Hz)			C
80	Lar -Fars	1	2				2-3(1.5-2 Hz)	2		C
81	Lنده	1	1				> 4(0.1-1.5 Hz)	2		C
82	Mahan	4	1				2-3(1.5-6 Hz)	1		B
83	Maharloo (PTT)	1	1	Soft alluvium in surface	652		3-4(4-8 Hz)	2	13-60 (1st 22 m)	A1
84	Maku	2	4	Fine gravel in surface	589	2-3(6-11 Hz)	> 4(5-7 Hz)	3		C
85	Manjil	2	7				> 4(3-6 Hz)	2		C
86	Maraveh-Tappeh	3	1				3-4(2.5-7 Hz)	2		C
87	Masal	3	3				3-4(0.5-2.5 Hz)	3		C
88	Mashad (Sakht-Azma)	4	1				> 4(2.5-5 Hz)	1		C
89	Masjed-Soleyman	3	1				2-3(1.5-5 Hz)	3		C
90	Minab	1	2				> 4(2.5-6.5 Hz)			C
91	Musian	3	2	Soft alluvium in surface	768	1-2(0.2-25 Hz)	1-2(1-20 Hz)	2	6-200 (1st 25 m)	A1
92	Naghan	1	16				> 4(3.5-7 Hz)	1		C
93	Namin	3	2				3-4(2-6 Hz)			C
94	Nir (Ardebil)	3	2				> 4(3.5-5 Hz)	4		C
95	Noorabad-Mamassani	3	5							C

Table 1 (continued)

No	Station	Site categorization	Number of records	Site geology	$V_s$ over 1st 30 m ( $m s^{-1}$ )	Amplification of H/V on microtremors	Amplification of H/V on strong motions	Site based on surface geology (BHRC)	Electric resistivities (ohmm)	Q
96	Old Lar	1	1				1-2(3-10 Hz)	2		C
97	Pol-Sefid	4	3				> 4(0.2-3 Hz)			C
98	Rasht (Housing Bureau)	3	2	Cohesionless gravel			> 4(2-4 Hz)	3		B
99	Rasht (University)	3	1	Thick fine gravel			> 4(2-2.5 Hz)	2		B
100	Ravar	3	1	Soft soil in surface			3-4(1.5-3.5 Hz)			B
101	Rayen	1	1	Soft soil in surface			1-2(0.2-7 Hz)	2		B
102	Robot-Karim	1	1	Coarse grain gravels			1-2(0.2-2 Hz)	2		C
103	Roshkhar	1	2				1-3(0.8-5 Hz)	4		A1
104	Rudbar	3	22	Cohesionless river gravels	339	1-3(3-7 Hz)	> 4(3.4-5.5 Hz)	3	4-20 (1st 16 m)	A2
105	Rudsar	4	1	Sand beach of Caspian sea	215	1(2(0.4-25 Hz)	> 4(0.25-0.7 Hz)	3		C
106	Rudshur	4	1	Silt and clay in surface			3-4(7-1.5 Hz)	3		A2
107	Saadabad (Borazjan)	1	7	Fine gravel in surface	958	1(2(0.2-2 Hz)	3-4(2.5-9 Hz)	1		C
108	Saman	2	1				> 4(5-11 Hz)			C
109	Sarbaz	2	1				> 4(4.5-6 Hz)			B
110	Sedeh	3	4	Silt and clay in surface			3-4(3-4 Hz)	4		C
111	Sefidabeh (School)	2	1	Hard gravels			> 4(5.5-8 Hz)	2		C
112	Sefidabeh (Microwave)	1	1	Sandstone and shale			2-3(1.5-7 Hz)	1		C
113	Seifabad (S. Kazerun)	1	1				1-2(0.8-1 Hz)	1		C
114	Selseleh	3	1				> 4(3-5 Hz)			B
115	Shabankareh (Borazjan)	4	37	Silty sand in surface	337		3-4(3-6 Hz)	3		C
116	Shabastar	1	3				2-3(2-9 Hz)			C
117	Shahid Yaaghubi Dam (S. Mashhad)	3	1				> 4(3-7.5 Hz)			C
118	Shalamzar	3	2				> 4(3-5 Hz)	4		B
119	Shiraz	4	1	Silt and clay in surface			> 4(0.2-1.1 Hz)	2		C
120	Siah-Cheshmeh	1	3				2-3(4-8 Hz)	4		C
121	Silvaneh	4	1				> 4(0.7-3 Hz)			C
122	Sirch	1	1	Fine gravel in surface			2-3(0.2-15 Hz)	3		B
123	Sisakht	1	4				2-3(7-10.5 Hz)			C
124	Tabas	1	9	Fine gravel in surface	715	-2(0.2-25 Hz)	2-3(1-15 Hz)	2	10-130 (1st 21 m)	A1
125	Talesh	3	5	Clay-silty gravel	514	-3(0.6-2 Hz)	3-4(0.8-4.5 Hz)	4	10-100 (1st 28 m)	A2
126	Tasuj	2	1				> 4(6.5-8 Hz)			C
127	Taybad	4	1				> 4(0.3-0.5 Hz)	3		D
128	Tehran (BHRC)	1	1	Coarse grain gravels			1-2(0.6-15 Hz)	2		C
129	Tehran (Chizar)	1	1	Coarse grain gravels			2-3(2-3 Hz)	3		D
130	Tehran (Sharif University)	1	1	Fine gravel in surface			1-3(1.4 Hz)	2		C
131	Tonkabon	4	1	Artificial soil	209	1-2(0.6-7 Hz)	1-2(2-3 Hz)	3	4-21 (1st 25 m)	A2
132	Torbat-Heydarieh (SH)	3	1				> 4(1.5-2.5 Hz)	2		C
133	Torbat-Jam	1	2				> 4(2-4 Hz)	4		C
134	Vendik	2	10	Fine gravel in surface	597	1-2(0.2-20 Hz)	1-2(3.5-9 Hz)	3	2.5-100 (1st 27 m)	A2
135	Zanjan	1	1				> 4(8-15 Hz)	3		C
136	Zanjiran	2	36	Fine gravel in surface	672	1-1.5(0.3-10 Hz)	2-3(1.5-5 Hz)	1	10-140 (1st 15 m)	A2
137	Zarrat (school)	1	30	Fine gravel in surface	704	1-3(0.2-8 Hz)	3-4(7-11 Hz)	1	5-30 (1st 7.5 m)	C
138	Ziaratali -N. BandarAbbas	1	1				3-4(3-7 Hz)			C

In all of the sites, the obtained strong motion records are studied to obtain their horizontal to vertical spectral ratio (receiver function for the strong motions; RF SMS). Calculating the same ratio for microtremors (H/V ratio for the microtremors; H/V MTS), we have been able to compare the H/V ratio for noises and earthquakes. No geotechnical boring was done through this study, and no data of this type was found in the location of the stations.

Here we have tried to determine the degree of coincidence between different methods of site characterizations. This comparison and likely coincidence were possible especially in sites where we had results from all methods. Finally we describe the factors that may have some affections on site amplifications (besides site geology) which could alter our site characterization results.

### 3.3 An overview on the general situation of the sites and the tests

The locations of each selected site are shown in Figure 3.1. The sites are mostly located in the western and northern Lut area (in central-east Iran), the western Alborz Mountains and the central Zagros region, which correspond to areas hit by the largest events over the last 22 years.

The shear wave velocities in deep layers can not be found by the geoseismic tests; the effective investigation depth for the geoseismic tests is about 30 to 35 meters. The microtremor tests have been proposed, mainly in Japan, to provide some information on site conditions since seismic noise contains surface and body waves which are filtered by surface layers. The geoelectric tests may distinguish very grossly between rock and soil types within a depth of a few tens metres. The results from the geoelectric tests give a range of electric resistivities depending on the ionization of the soil particles. The characteristic resistivities for fine and coarse grain alluviums may juxtapose a lot. It is therefore very difficult to distinguish between different types of sites through the geoelectric tests. Based on the aforementioned reason the results of geoelectric tests will neither be presented here nor be used in the site categorization.

In the absence of down-hole arrays and rock outcrop motions, we have used the H/V method having then an idea of the response of each site to a strong ground motion.

Most of the strong motion sites in Iran are installed on foothills, for the sake of better climate and topographic situations in most areas of the country. On the other hand, in most cases, the sites are alluvial or firm grounds, and the soft soil sites may be found only near the coast (Lahijan, Rudsar and Tonkabon) or in the plains (Talesh, Golbaf, Shiraz and south

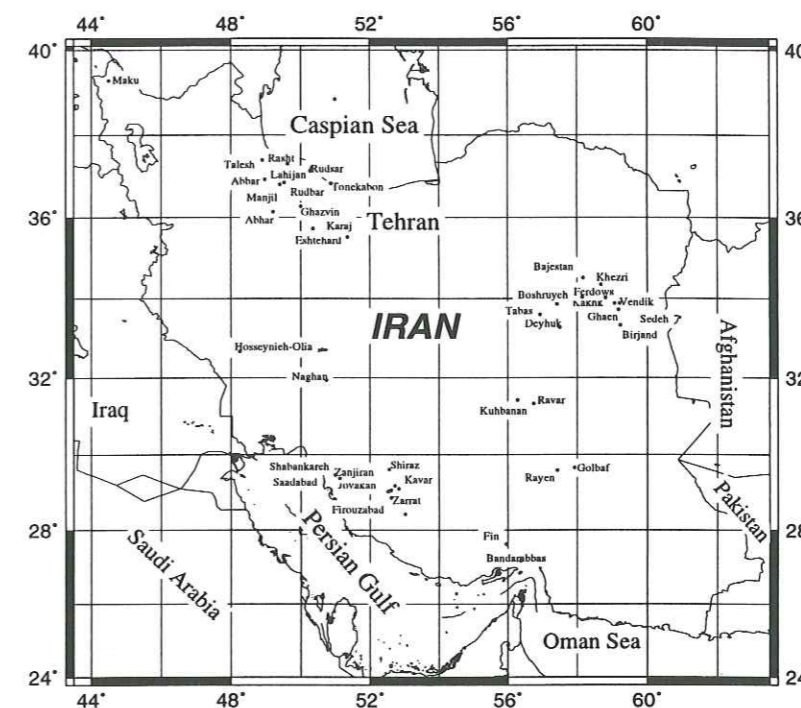


FIG. 3.1 – The locations of the stations which are studied and presented in this paper.

Tehran). A summary of the tests performed in each of 50 sites is presented in table-I. As is shown in the table, in most of these sites a microtremor test was done and in each the local geological situation was observed. The comparison of the local geological observations with the results of the tests may show us the degree of reliability of these observations in each place.

#### 3.3.1 Receiver function method for strong motions

Since there are no station pairs located one on soil and another on rock in a nearby distance, and as there is no down-hole array in the country, we had to use single-station estimates of H/V ratio for site effects. This method, also called the receiver function technique, has been shown to be efficient (Theodulidis et al., 1996, Riepl et al. 1998), in pointing out the site fundamental frequency, and its stability makes it applicable, in principle, even when one single three-component recording is available. The formulation used for the H/V method is based on the spectral ratio ( $R_{hv}$ ) between the smoothed horizontal components and the smoothed vertical component:

$$R_{hv} = \frac{\sqrt{\frac{S_{H1}^2}{2\sqrt{T_{H1}}} + \frac{S_{H2}^2}{2\sqrt{T_{H2}}}}}{\frac{S_v(f)}{\sqrt{T_v}}} \quad (3.1)$$

where  $T_{H1}$ ,  $T_{H2}$  and  $T_V$  are the signal duration for the horizontals and vertical components respectively. Since the same time windows are used the same for all of the components, this relationship might be simplified as;

$$R_{hv} = \frac{\sqrt{\frac{1}{2}S_{H1}(f)^2 + S_{H2}(f)^2}}{S_V(f)} \quad (3.2)$$

In this study, this ratio was considered to be significant only when the signal to noise ratio  $R_{sn}$  for both components exceeds a given threshold value, taken equal to 3. The signal to noise ratio ( $R_{sn}$ ) is computed as:

$$R_{sn} = \frac{\frac{S(f)}{\sqrt{t_s}}}{\frac{N(f)}{\sqrt{t_n}}} \quad (3.3)$$

where  $t_s$  and  $t_n$  are the window duration for the signal and noise parts, respectively. A  $R_{sn}$  ratio over 3 is selected as the proper ratio to distinguish the signal from the noise. The resultant  $R_{sn}$  ratios for two horizontal components are compared with the same ratio calculated for the vertical component in different frequencies.

The implied smoothing is the smoothing proposed by Konno and Ohmachi (1998), which keeps corrects amplitudes whatever the frequency. The stability is found acceptable especially in the sites with many records. The standard deviation of this ratio (RF SMS) is found to be about 1.5. The standard deviations of the digital and the analog records for the RF SMS method are shown in the sites with more than 10 records (Figure 3.2). This figure shows that the standard deviations for the digital records are less than the analog ones, and on the other hand in most cases the standard deviations do not pass 2. Therefore it may be concluded that the use of RF SMS as the main criteria to distinguish the site responses was reliable.

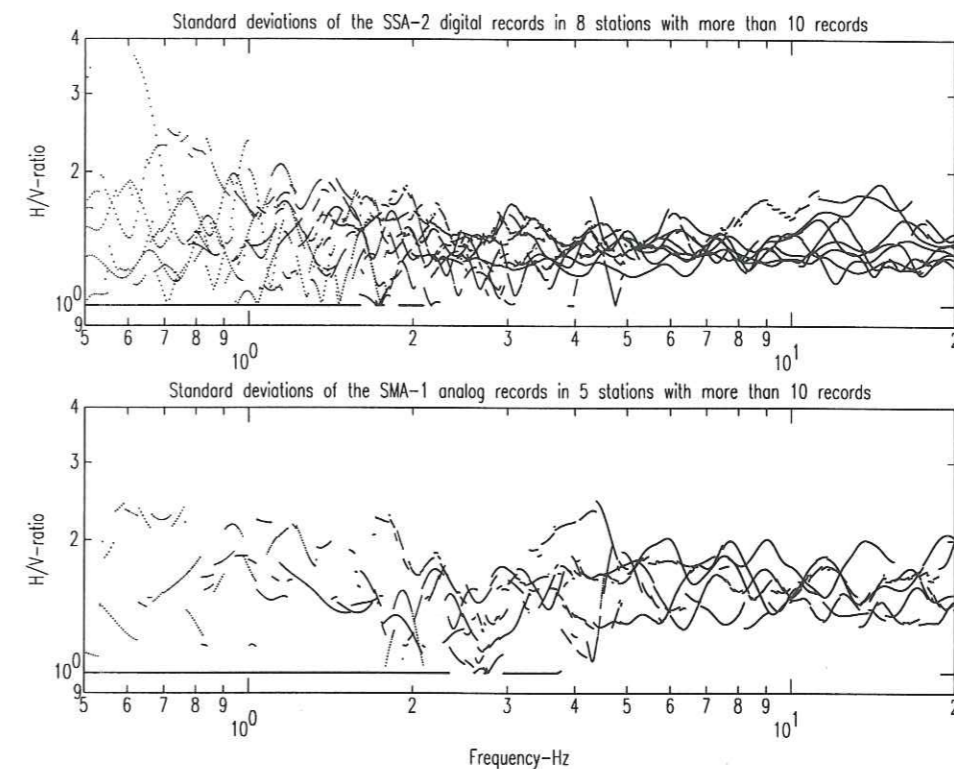


FIG. 3.2 – The comparison of the standard deviations for the digital (SSA-2; a) and analog (SMA-1; b) recorders in the sites with more than 10 records.

### 3.3.2 Microtremors

The microtremor tests are performed in 47 sites, using SSR-1 sensors with a minimum sensitivity of 0.1 Hz. Five windows of 3 minutes duration are selected in each site. In each coordinate, only the best stationary parts of the tremors are considered. The spectral ratio ( $R_{hv}$ ) formulation for the microtremors are the same as the strong motions. The H/V MTS are compared in each site with the relative RF SMS.

### 3.3.3 Geoseismic tests

The geoseismic tests in 26 sites displayed the compressional and shear wave velocities in the superficial first 30 meters of depth using the refraction method. The theoretical transfer function (TTF) could then be computed in each case with 1D programs based on the geoseismic results in each case. There were some cases where the S wave velocities at depth were low (Golbaf, Lahijan). In these cases no velocity contrast may be seen in these depths, meanwhile the receiver function showed the amplifications in low and middle frequencies. No damping measurement

was done at the studied sites.

Since it is necessary to place a row of 24 geophones with the interval distances of 4 to 5 meters to do the geoseismic tests, and according to the location of the stations which are mainly in the central parts of the cities, the tests were not always possible to be done in the same place of the stations. In these cases we have tried to do this test in the nearest possible place. Therefore the velocity profile tests in Deyhuk, Firouzabad, Ghaen Ghazvin, Golbaf, Kavar, Rudbar, Rudsar, Saadabad, Shabankareh, Tabas, Tonkabon and Zarrat are performed in the distances of 200 to 1000 meters away from the location of strong motion accelerographs. This problem might be the source of the incoherence between the strong motion and geoseismic results. The rest of the tests are performed in the distances of less than 200 meter too the stations.

### 3.4 The results of the geoseismic tests, microtremors and H/V for Strong Motions

For twenty-six sites shown in Figure 3.1, some information from the receiver functions, the noise recordings, and the velocity profiles could be simultaneously found from which a theoretical 1D-transfer function for vertically incident S waves could be computed. It has been tried to consider the sites where the most important earthquakes were recorded. Meanwhile, in three sites (Maku, Shabankareh, Tonkabon) a reliable results have not been obtained on the vertical component, and thus the microtremor results were eliminated. In 23 other sites, only performed microtremor test were performed in order to compare them with RF SMS. For some of the sites, a good consistency between all three techniques could be observed, while for some others the agreement was not so close. In particular, the noise results were very disappointing compared with studies made in other countries (Riepl et al., 1998; Duval, 1994; Bard et al., 1997, Lachet et al. 1996).

#### 3.4.1 Sites with a satisfactory agreement between the results of the different methods

A satisfactory similarity between the different methods was obtained only for less than one half of the studied sites. The sites with the best similarities for the different tests are, for instance, Fin (Figure 3.3), Firouzabad (Figure 3.4), Ghaen (Figure 3.5), Jovakan (Figure 3.6), Lahijan (Figure 3.7), Manjil (Figure 3.8), Naghan (Figure 3.9), Rudbar (Figure 3.10), Tabas

(Figure 3.11) and Zanjiran (Figure 3.12). This means that the factors affecting the amplifications were very different. In almost all cases, the peaks on the H/V MTS had low amplitude, much lower than those of the H/V ratio strong motion spectra (RF SMS) and the theoretical transfer functions (TTF). However poor agreement was observed at Lahijan (Figure 3.7) between RF SMS and TTF because the S wave velocity profile was not deep enough. The presence of the low velocity surface layer was essential to find a satisfactory agreement between methods.

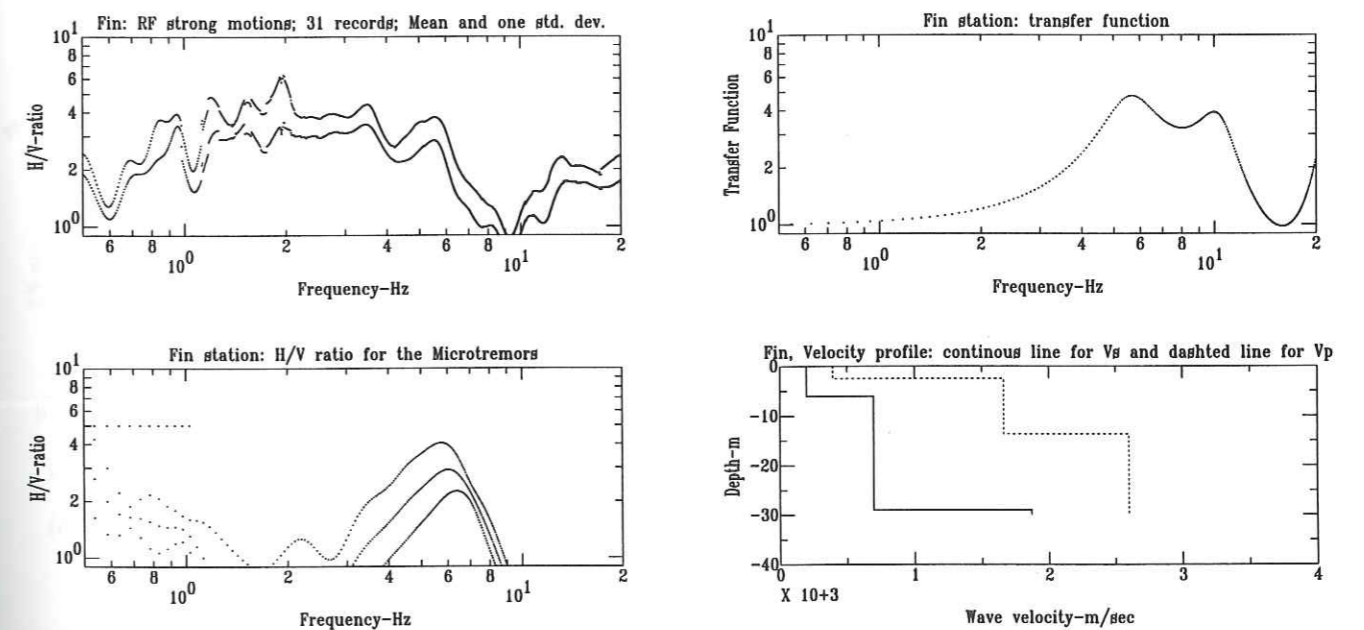


FIG. 3.3 - The results of the site tests in Fin (North Bandarabbas) station (RF SMS, H/V MTS, transfer function and velocity profile).

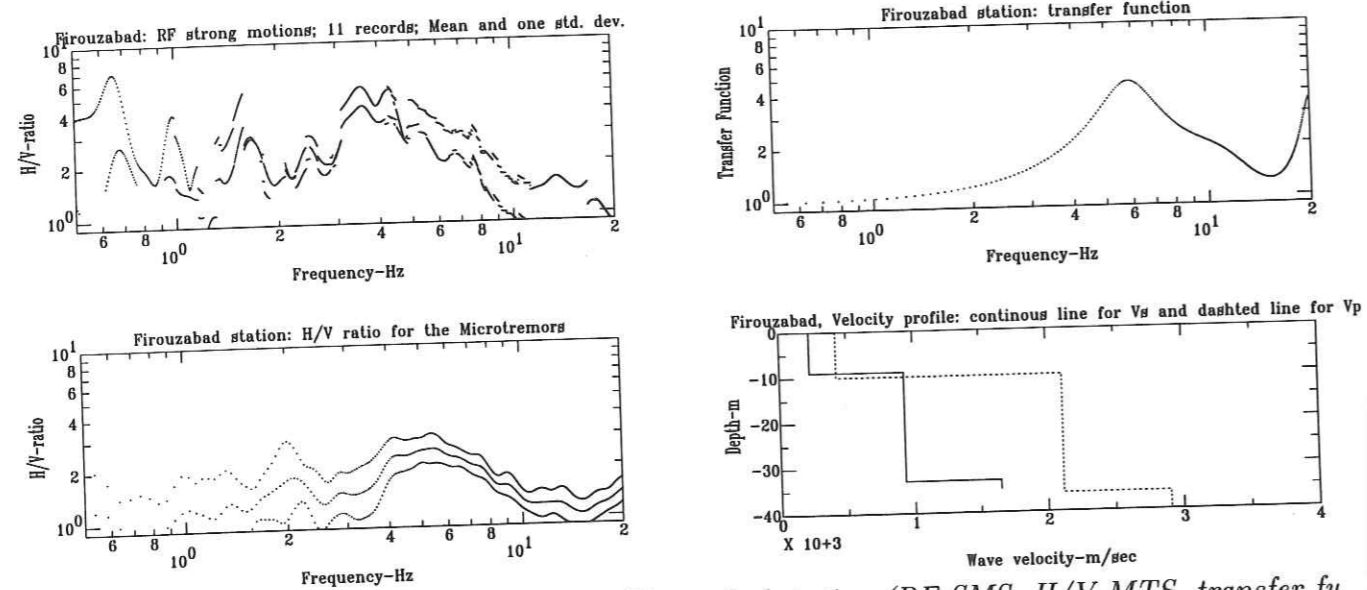


FIG. 3.4 - The results of the site tests in Firouzabad station (RF SMS, H/V MTS, transfer function and velocity profile).

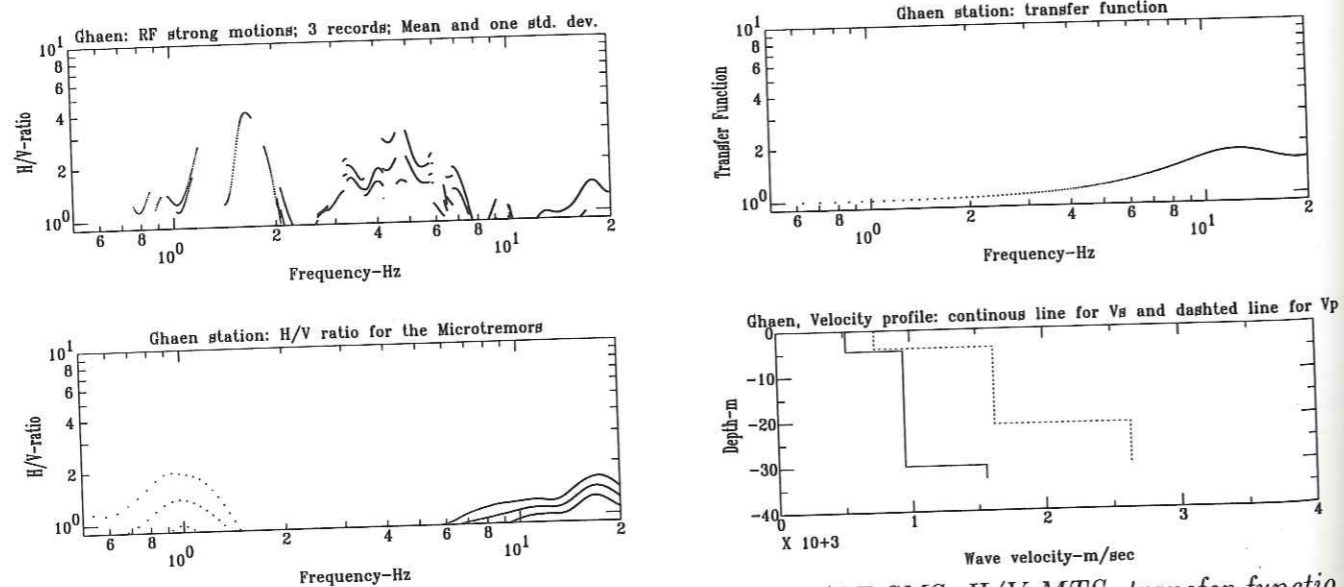


FIG. 3.5 - The results of the site tests in Ghaen station (RF SMS, H/V MTS, transfer function and velocity profile).

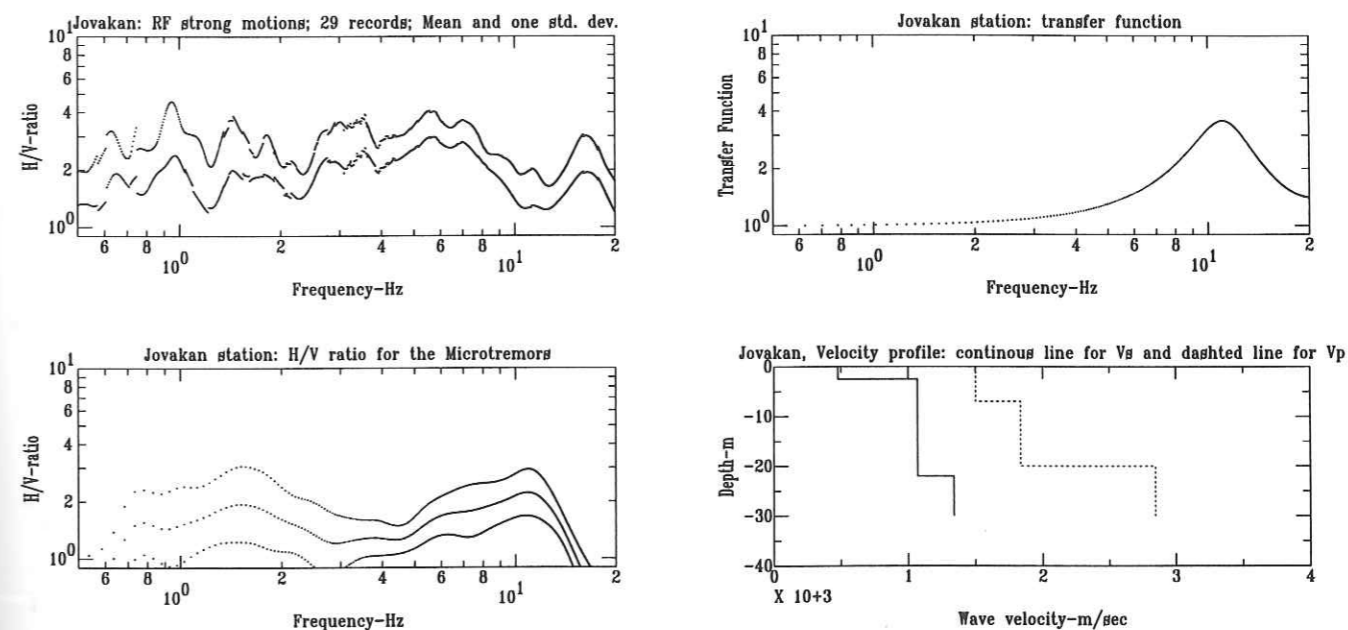


FIG. 3.6 - The results of the site tests in Jovakan station (RF SMS, H/V MTS, transfer function and velocity profile).

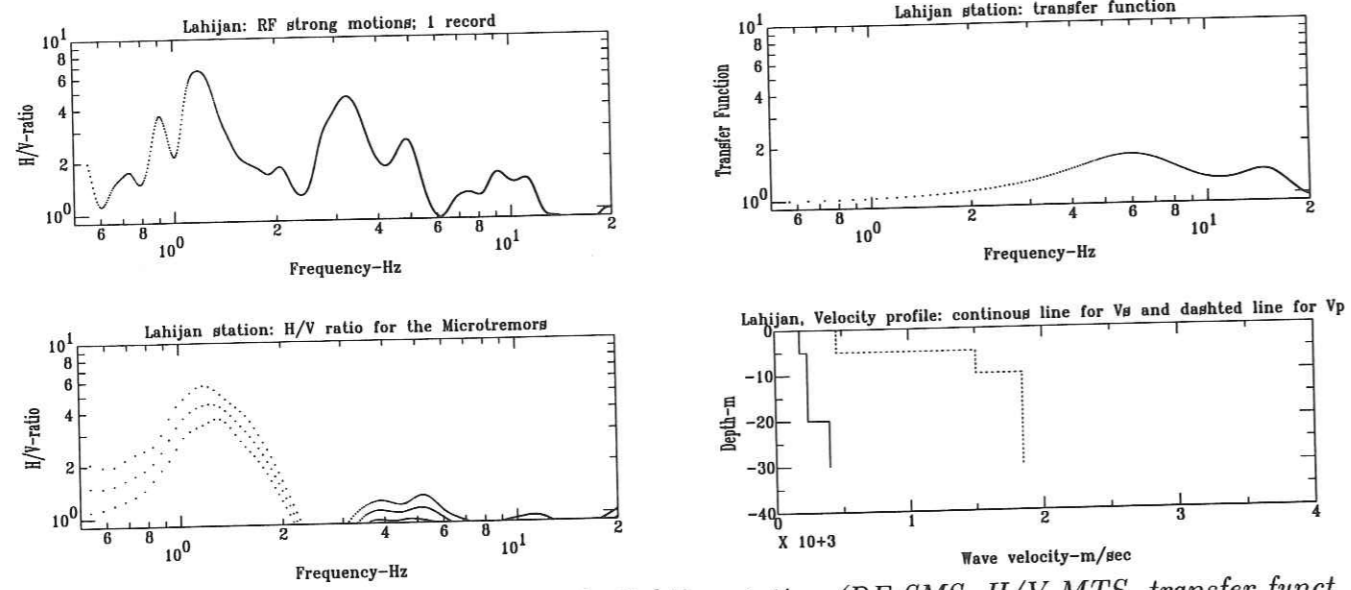


FIG. 3.7 - The results of the site tests in Lahijan station (RF SMS, H/V MTS, transfer function and velocity profile).

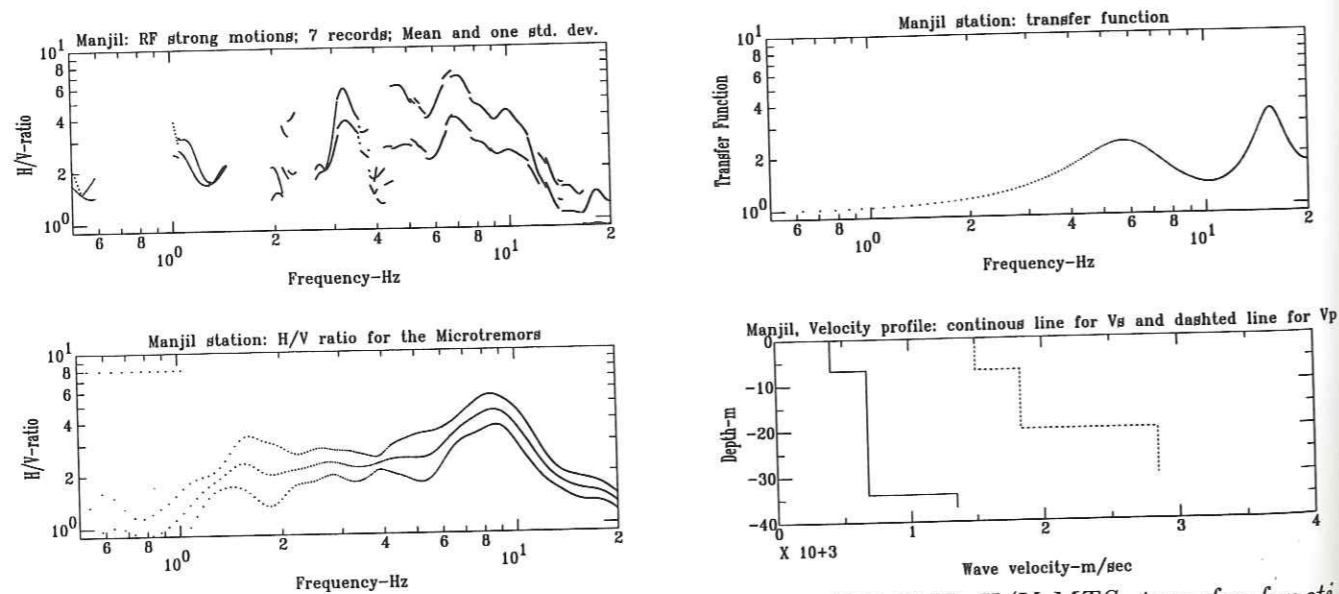


FIG. 3.8 - The results of the site tests in Manjil station (RF SMS, H/V MTS, transfer function and velocity profile).

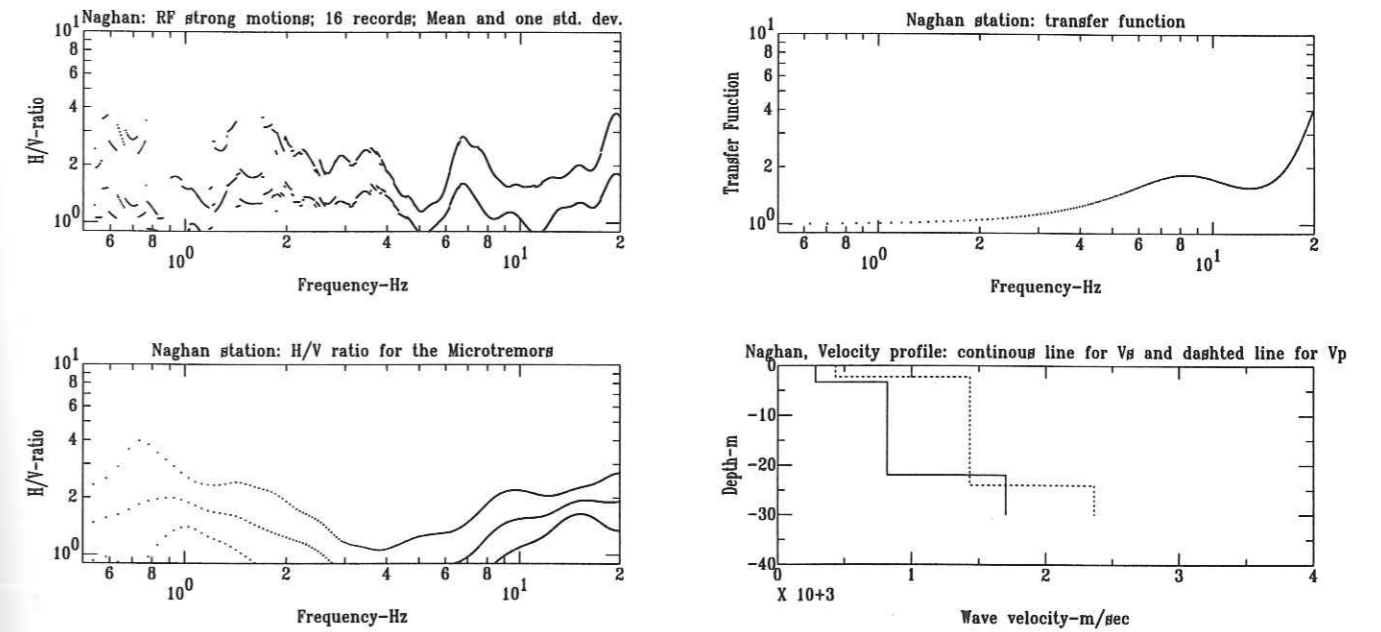


FIG. 3.9 - The results of the site tests in Naghan station (RF SMS, H/V MTS, transfer function and velocity profile).



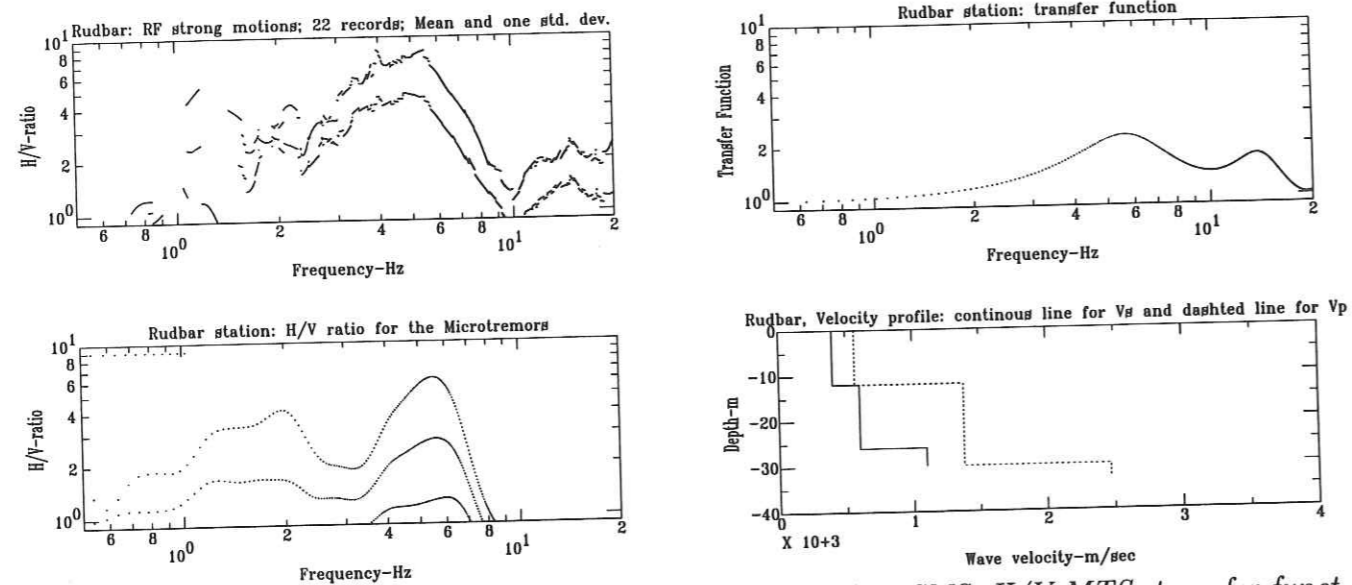


FIG. 3.10 - The results of the site tests in Rudbar station (RF SMS, H/V MTS, transfer function and velocity profile).

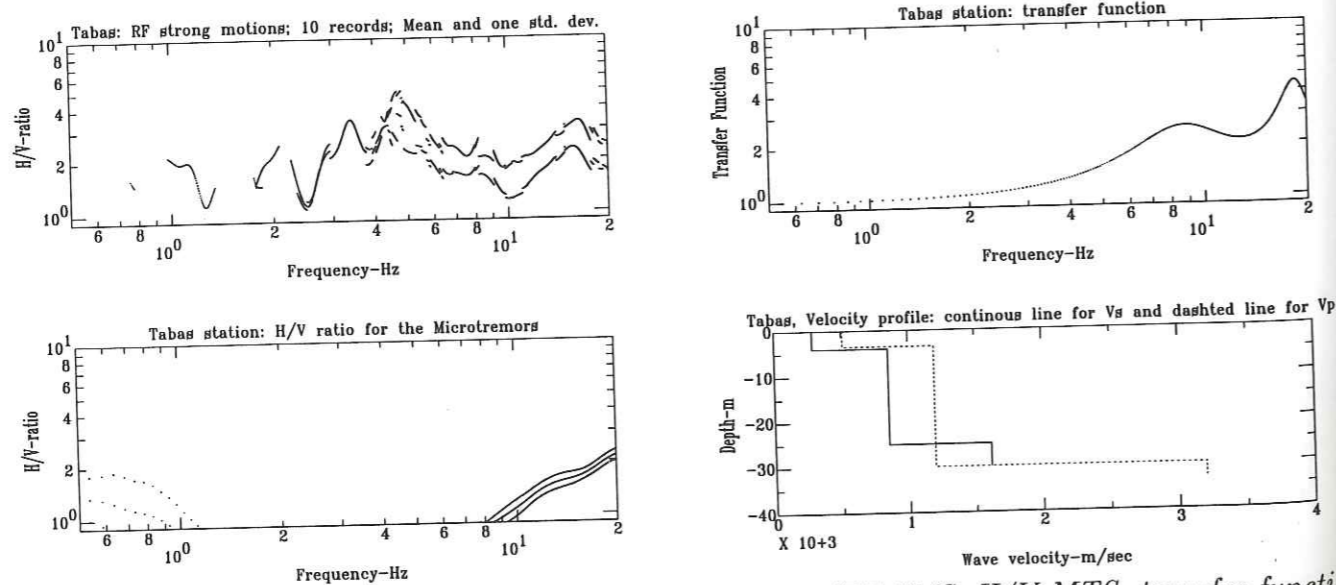


FIG. 3.11 - The results of the site tests in Tabas station (RF SMS, H/V MTS, transfer function and velocity profile).

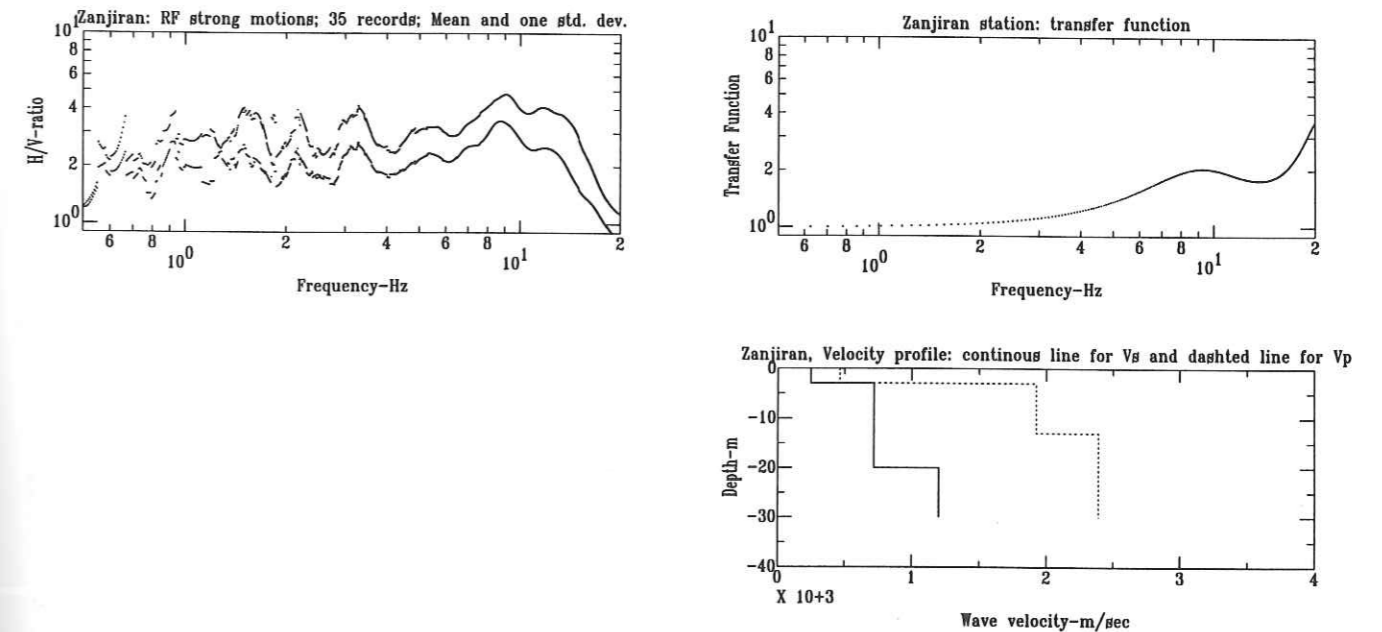


FIG. 3.12 - The results of the site tests in Zanjiran station (RF SMS, transfer function and velocity profile).

### 3.4.2 Sites without agreement: failure of the microtremor technique

Based on the present studies, the results of the microtremor test appear to be reliable just for sites exhibiting significant amplifications at low and/or intermediate frequencies (less than 5 Hz) caused by a low velocity superficial layer. In some of the sites the thick alluvium deposits cause the amplifications in low and middle frequencies (less than 5Hz) on RF SMS, which the H/V MTS did not exhibited the same peaks, for instance in Ghazvin (Figure 3.13). In Rudsar (Figure 3.14) the velocity the transfer function has not shown the peaks in low frequencies (evident on RF SMS). In the soft soil sites, it seems that a high contrast in the superficial layers is needed to cause the evident amplifications in H/V MTS. For example in Golbaf (Figure 3.15) which shows a low average velocity in the first 30 meters (439m/s) the amplifications on the RF SMS may not be seen on the same spectra for the microtremors. A high contrast in about 40 metres depth, with a Vs velocity of about 1500 to 200 m/s is might be sufficient to explain this low frequency amplification in RF SMS in this site.

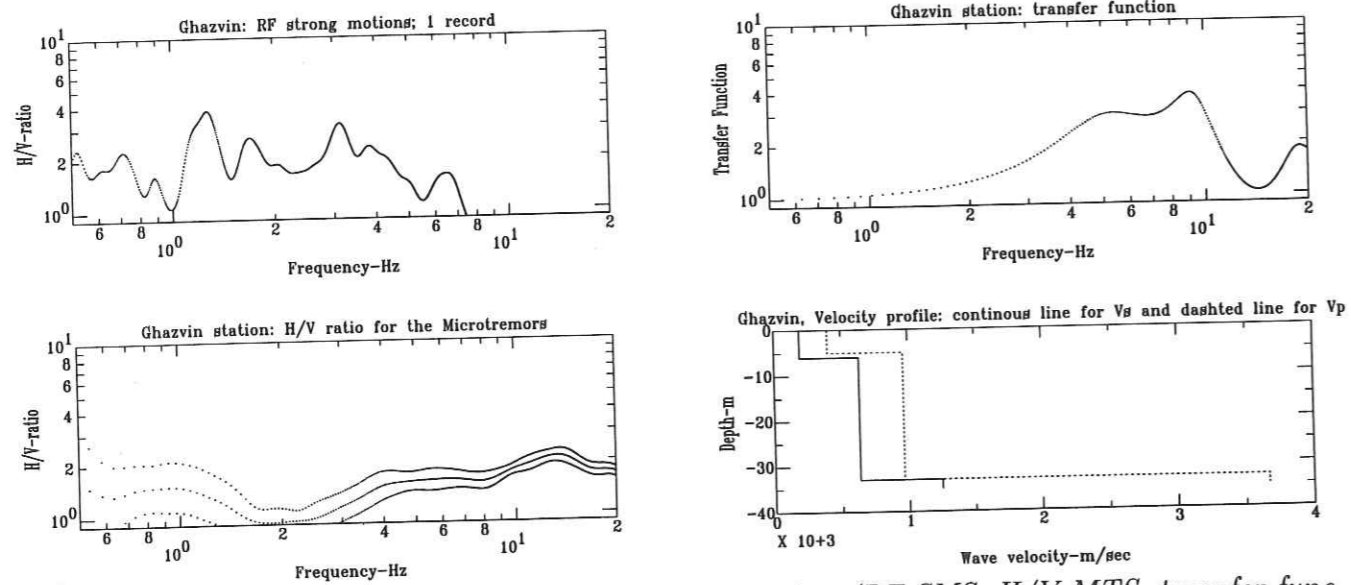


FIG. 3.13 - The results of the site tests in Ghazvin station (RF SMS, H/V MTS, transfer function and velocity profile).

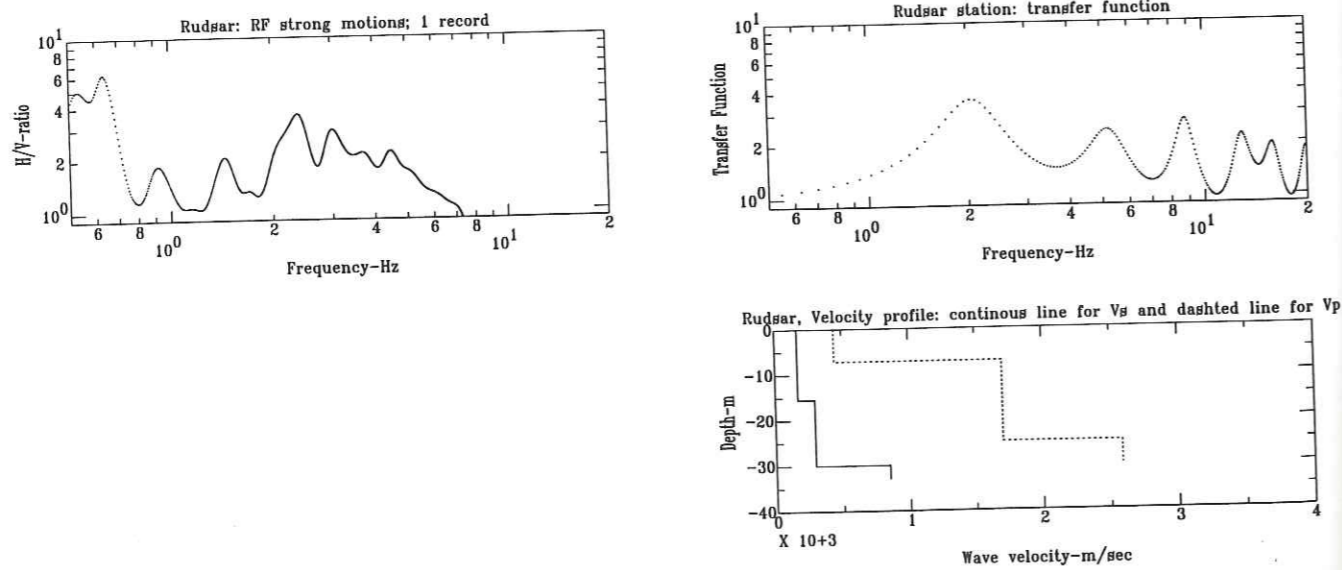


FIG. 3.14 - The results of the site tests in Rudсар station (RF SMS, transfer function and velocity profile).

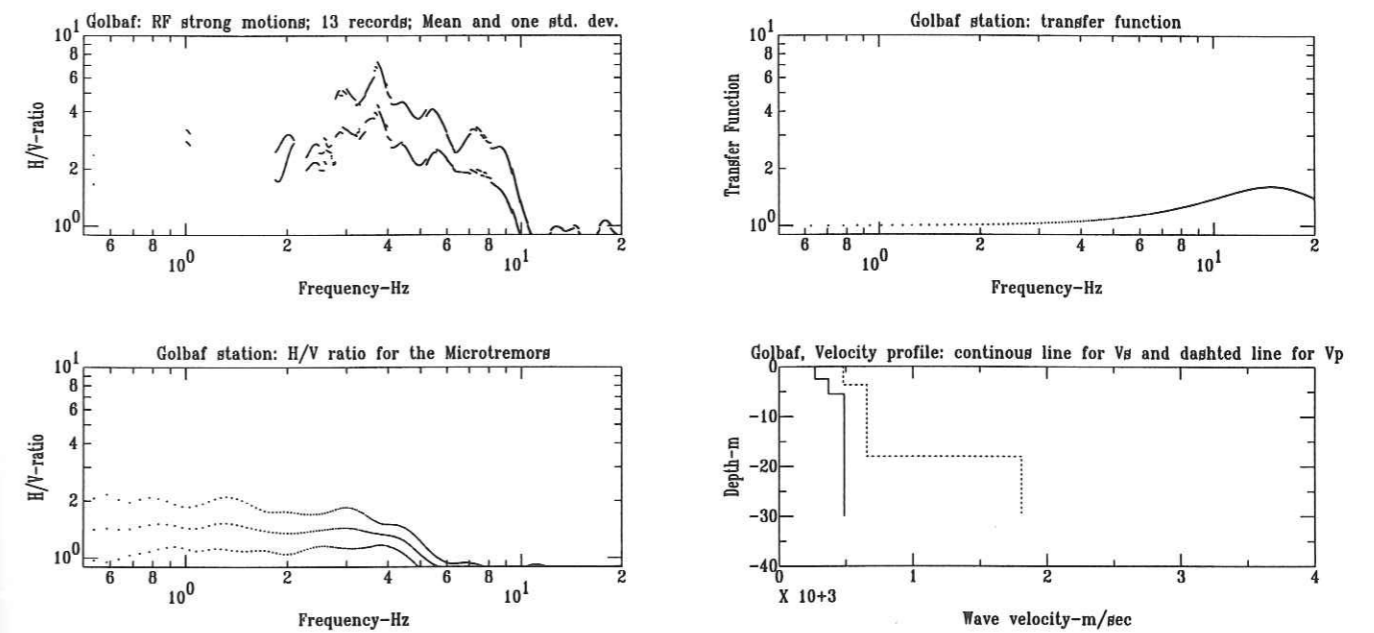


FIG. 3.15 - The results of the site tests in Golbaf station (RF SMS, H/V MTS, transfer function and velocity profile).

There are cases for which there were not each result, however it was possible to compare the amplifications, which may be measured through the H/V MTS and RF SMS. The similarities between H/V ratios for noise and strong motions are observed for instance in Bajestan (Figure 3.16), Sedeh (Figure 3.17), and Shiraz (Figure 3.18). These sites show total accordance between the RF SMS and H/V MTS.

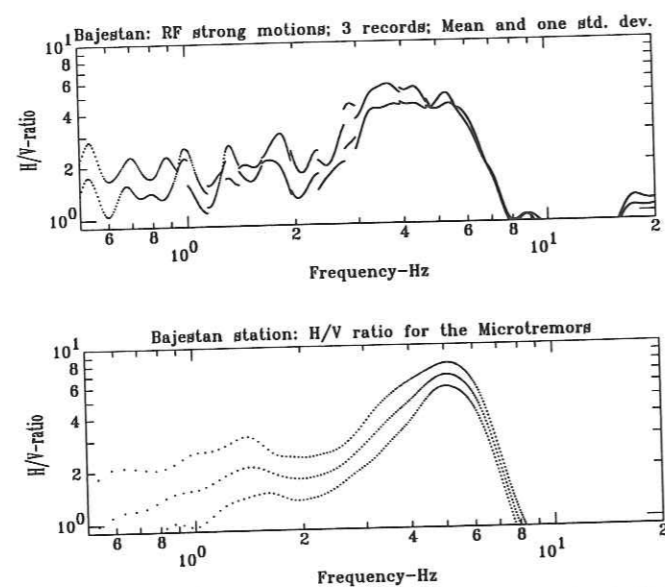


FIG. 3.16 - The H/V ratio results in Bajestan station (RF SMS, H/V MTS).

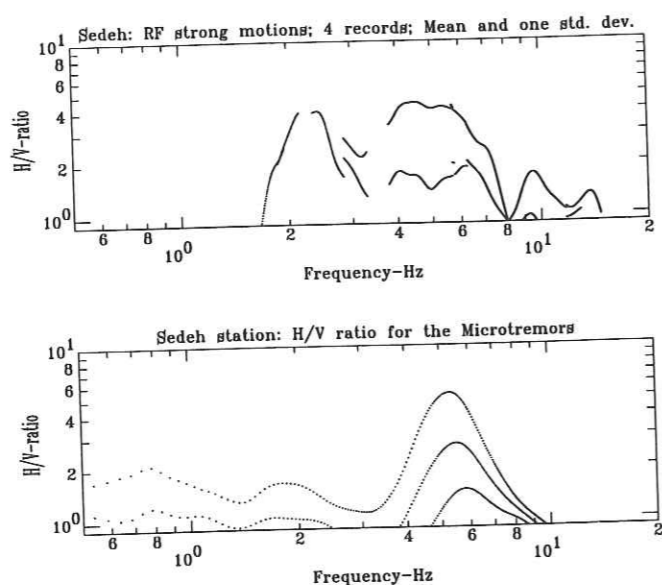


FIG. 3.17 - The H/V ratio results in Sedeh station (RF SMS, H/V MTS).

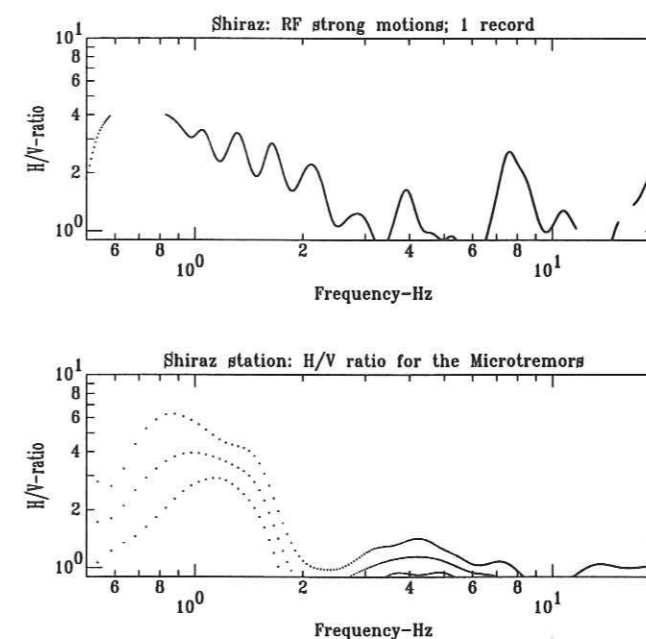


FIG. 3.18 - The H/V ratio results in Shiraz station (RF SMS, H/V MTS).

### 3.4.3 A preliminary conclusion on the results of the different methods

Among the methods that are used to study the site conditions, the only method that may reveal the site response to ground motions is to study the three component strong motion records (RF SMS). The benefit gained from this method is that we had at least one record in each of the stations and this is the only method that may be applied at each location. On the other hand, the RF SMS is a method that does not have the limitations of the other methods. The velocity profiles measured by the geoseismic methods are limited to the first 30-35 metres; the microtremors have shown the important amplifications just in the soft soil sites, and the geoelectric tests do not give the precise measurements to distinguish the different sites. The study on the amplifications based on the 3 component records has another benefit. In the sites where there are thick alluvial layers on the surface (with a thickness of more than 30 metres) on a very high velocity layer at greater depths, the RF SMS is the only way to observe such amplification in low frequencies. In this case the other methods will show just the high velocity alluvium with some amplifications in high to very high frequencies (more than 15Hz).

In addition, the RF SMS is a very stable method (Figure 3.15)

### 3.5 A Site Categorization

The relatively good relationship between the S-wave velocity profiles and the RF results allowed us to propose a multi-class site categorization based on the RF curves. This classification is simply based on the amplitude and level of the highest peak on the RF curve:

- \* site category #1 corresponds to flat RF curves (i.e., peak amplitude below 3-4), or those presenting a peak with an amplitude larger than 3-4 at frequencies beyond 15 Hz
- \* site category #2 corresponds to RF curves presenting a peak with an amplitude larger than 3-4 at frequencies between 5 and 15 Hz
- \* site category #3 corresponds to RF curves presenting a peak with an amplitude larger than 3-4 at frequencies between 2 and 5 Hz
- \* site category #4 corresponds to RF curves presenting a peak with an amplitude larger than 3-4 at frequencies below 2 Hz

According to these criteria, the 26 studied sites are classified and presented later (see 4.1). The RF curves for these sites of each class are depicted in Figure 3.19.

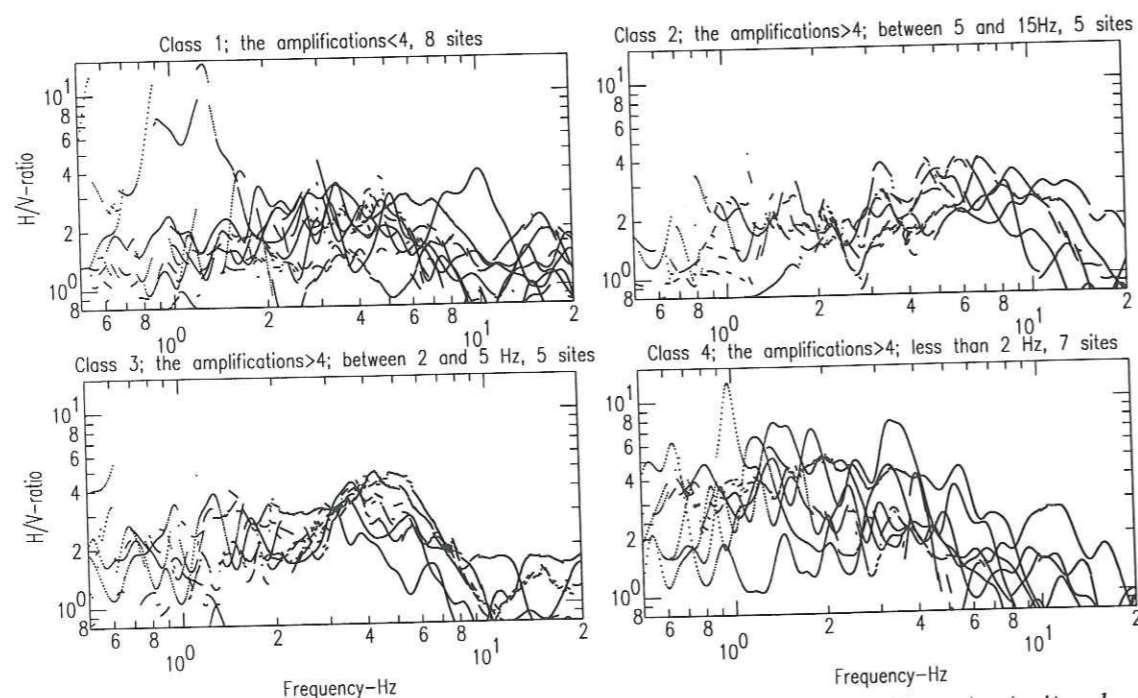


FIG. 3.19 - The comparison of the receiver function for the strong motions in 4 site classes. (the results of 26 sites with the most records).

On the other hand, there are the cases where the RF amplitude is not equal 4 (as it is defined above), but passes 3. In these cases it is tried to observe the results of other tests (if available) to distinguish the site conditions. In such intermediate cases, we have used the Vs and Vp profiles and the microtremor results to decide on the case. However if the peaks did not approach 3 at all, that site is classified as rock site (class 1).

The measured velocity profiles corresponding to each of these classes are grouped in Figure 3.20. The main characteristic of category 1 is that the S-wave exceeds 700 m/s at depths beyond 5 m, although the values may be much lower at very shallow depths (thin layers with resonance frequencies exceeding 15 Hz). On the opposite, the velocity profiles in category 4 exhibit low velocities at surface (below 250 m/s) and at depth (below 500 m/s down to 30 m) except for three "exceptional" sites for which there was a clear discrepancy between velocity profile and RF curve, that we checked several times and could not interpret. Velocity profiles for categories 2 and 3 are intermediate.

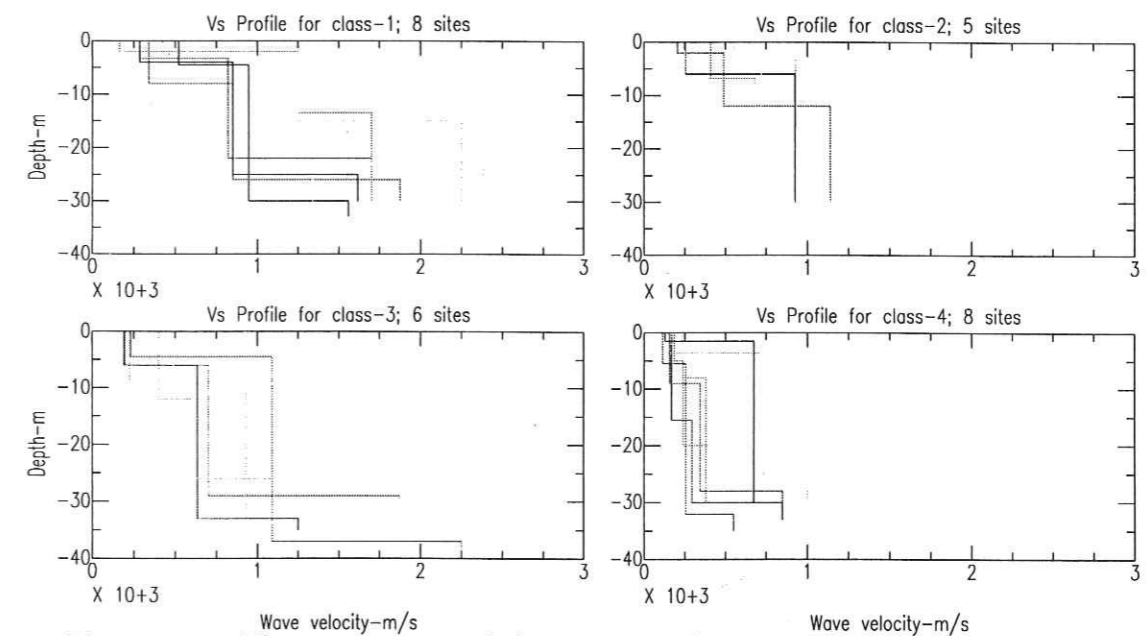


FIG. 3.20 - The comparison of shear wave velocity profiles in 4 site classes.

The microtremor H/V spectra corresponding to each of these 4 categories are displayed in Figure 3.21. It clearly shows that, to the contrary of many published studies, microtremors could not, in our case, point out the fundamental frequency; this negative result may perhaps

be related to the absence of strong impedance contrasts in velocity profiles, except for some class-4 sites. In any case, it requires further work, and probably new measurements, before it can be understood.

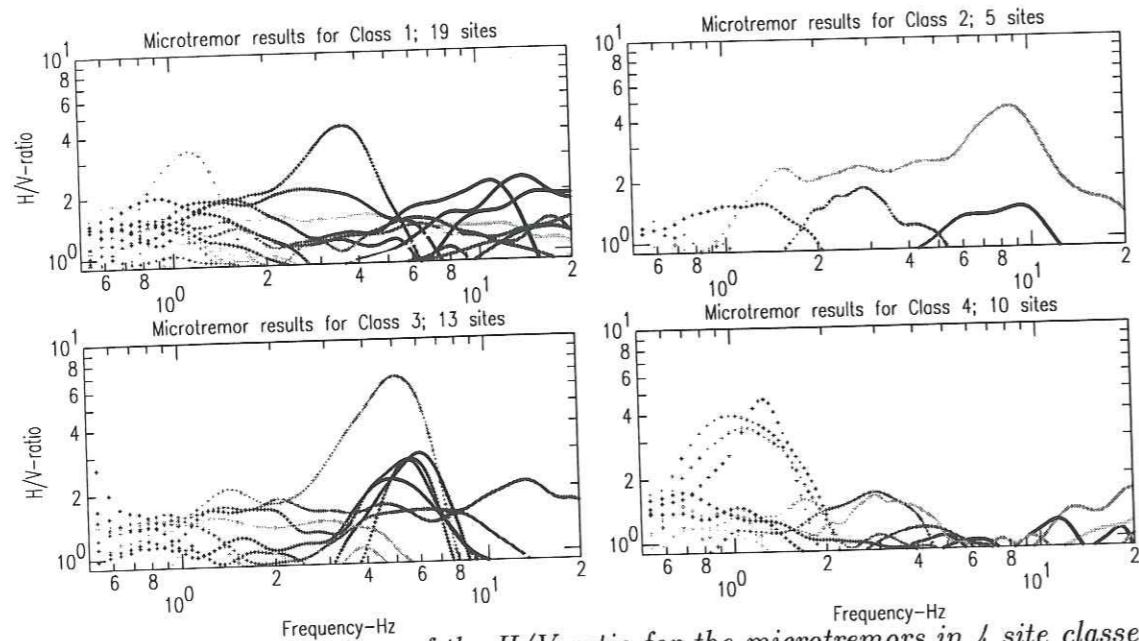


FIG. 3.21 - The comparison of the H/V ratio for the microtremors in 4 site classes.

### 3.5.1 The Average of Vs for upper 30 meters

The average value of shear wave velocity over the topmost 30 metres has been proposed as a criterion to distinguish the site characteristics in response to the ground motions (Boore et al. 1993, Boore et al 1997, NEHRP 1994). Such a criterion has certainly some drawbacks, since it does not take into account the velocity profile at greater depths, which may have a prominent influence on the low frequency response. However, since there was not any other information for the Iranian sites, the relationship between our site categorization and these average velocities  $V_{s30}$  are tested. This average shear wave velocity  $V_{s30}$  is defined as:

$$\frac{30}{V_{s30}} = \frac{h_1}{V_{s1}} + \frac{h_2}{V_{s2}} + \dots + \frac{h_n}{V_{sn}} \quad (3.4)$$

with:

$$h_1 + h_2 + h_3 + \dots + h_n = 30m \quad (3.5)$$

The corresponding values for our 26 sites are listed in Table II, and the distribution of  $V_{s30}$  for different site classes is shown in Figure 3.22. Although the values at depth are much less reliable than at the near surface, we are rather confident in our estimate of  $V_{s30}$  since the "deep" values have only a limited influence in the result. Table II thus points out a rather clear correlation between  $V_{s30}$  and our definition for the site classes 1 to 4, based on RF SMS: our criteria on RF SMS may therefore be almost equivalently replaced by the criteria on  $V_{s30}$ , as indicated in Table III: the correspondence turns out to be valid for 20 out of our 26 studied sites (i.e., 77% of the cases).

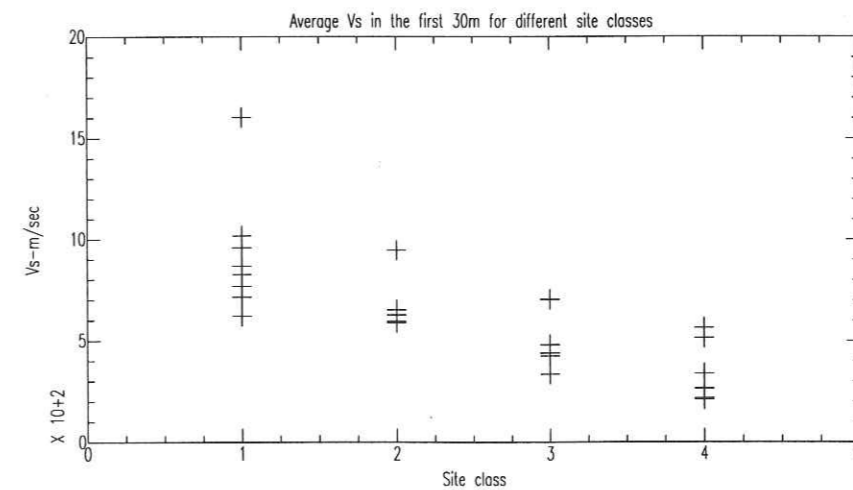


FIG. 3.22 - The distribution of  $V_{s30}$  for four site classes.

Table II: Average velocities for each site, in each category

No	Site	class	$V_{s30}$	No	Site	class	$V_{s30}$
1	Abbar	1	621	14	Fin	3	480
2	Deyhuk	1	826	15	Firouzabad	3	478
3	Ghaen	1	867	16	Ghazvin	3	424
4	Jovakan	1	1017	17	Golbaf	3	439
5	Kakhk	1	1602	18	Rudbar	3	334
6	Naghan	1	768	19	Zarrat	3	704
7	Saadabad	1	958	20	Abhar	4	263
8	Tabas	1	715	21	Hosseinieh	4	563
9	Kavar	2	946	22	Lahijan	4	264
10	Maku	2	652	23	Rudsar	4	215
11	Manjil	2	589	24	Shabankareh	4	337
12	Vendik	2	597	25	Talesh	4	514
13	Zanjiran	2	627	26	Tonkabon	4	209

Table III: The 4 class site categorization

Group	Frequency Band of the Amplification	$V_{s30}$ m/s	Sites
1	$F \geq 15Hz$	$V_{s30} \geq 700$	Abbar, Deyhuk, Ghaen, Jovakan, Kakhk, Naghan, Saadabad, Tabas
2	$5 \leq F < 15Hz$	$500 \leq V_{s30} < 700$	Kavar, Maku, Manjil, Vendik, Zanjiran
3	$2 \leq F < 5Hz$	$300 \leq V_{s30} < 500$	Fin, Firouzabad, Ghazvin, Golbaf, Rudbar, Zarrat
4	$F < 2Hz$	$V_{s30} < 300$	Abhar, Lahijan, Hosseinieh, Rudsar, Shabankareh, Tonkabon, Talesh

### 3.5.2 Discrepancies from the defined criteria

There exist some cases where peaks on RF SMS appear in a frequency band that is not consistent with  $V_{s30}$ . The most important reasons for these discrepancies may be considered in different ways. The source effects may in some cases affect the H/V ratio [for instance, when a station was very close to the earthquake source (such as in Tabas)]. In some other cases one may think that a high velocity layer may be found at depths greater than 30 meters, which could not be imaged by geoseismic methods (i.e. for an average surface velocity of 500 m/s there may exist significant amplifications at low frequencies ( $f < 1Hz$ ) if the corresponding thickness exceeds 125 m).

In the Hosseinieh-Olia station the peaks on RF SMS were observed in the frequency band of less than 2Hz but the  $V_{s30}$  is more than 500m/s (563m/s) (Figure 3.23). The low frequency high amplifications on RF SMS (which may be seen on RF MTS as well) in Talesh (Figure 3.24) and  $V_{s30} = 508m/s$  is also inconsistent with the limits observed for most of the other sites. The most important reasons for these discrepancies may be considered in different ways. The source effects may be more effective than site effects, where the station was very close to the earthquake; the Saadabad records which are obtained in the epicentral distances of 8-16 km (Zaré et al 1998) shows low frequency amplifications which may be associated with directivity effects or near field pulses. The high contrast of a superficial low velocity layer with a very higher velocity sub-layer may cause the lower average value of  $V_{s30}$  in Hosseinieh. There is a superficial layer with  $V_s = 130m/s$  and a thickness of 1.5m situated adjacent to a hard sub-layer with  $V_s = 672m/s$ . In Talesh a high velocity layer might be found at great depth of more than 30 (for a velocity of 730 m/s it might be expected a depth of about 100m to have the amplification of 0.8 to 1Hz). The same situation may be expected for Ghazvin which shows the lower amplifications in 1-2 Hz. If this situation is to be justified with the site effects, a high contrast in a depth of more than 100m is needed.

### 3.5.3 Application to all Iranian strong motion data

The RF SMS method is performed to determine the site conditions for all of the Iranian strong motion data. The result of this application for 138 site (comprising the studied sites) is shown in Table-1. This criterion is applied to categorize the Iranian sites for which strong motion records are available with satisfactory quality. The final statistics corresponding to the 138 sites is as follows: 51 sites are in class 1 (37%), 22 sites in class 2 (16%), 39 sites in class 3 (29%), and 25 sites in class 4 (18%) (Figures 3.22 and 3.26).

### 3.5.4 Quality factor for the site determination

To determine the quality of the information that is developed in this study we have used a quality factor in 4 steps ordered from the best to the worst quality: A to D. If there existed all of the data for a site; the "A" quality was assigned. The order is subdivided to A1 for the coordination between the different results, and A2 for the cases when the H/V MTS or the  $V_{s30}$  contradicted the RF SMS. Otherwise, when there were not the velocity profiles but there

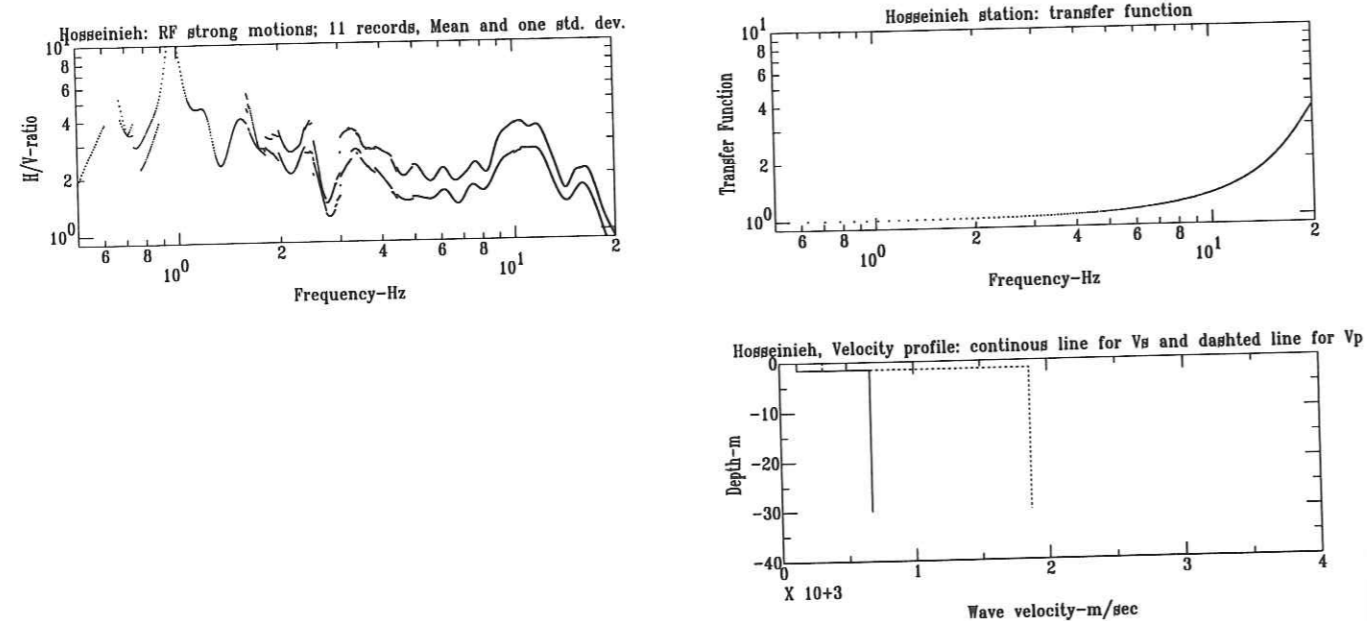


FIG. 3.23 - The results of the site tests in Hosseinieh-Olia station (RF SMS, transfer function and velocity profile).

were all of the other results (H/V MTS and RF SMS) then the "B" quality is marked. If there was just the RF SMS, the "C" is assigned, and in the worst case (when the quality of the record and consequently the quality of the RF SMS was not reliable) "D" is used. These assignments are shown in Table-I.

### 3.6 Conclusions

We conclude that the 26 sites considered in this study may be grouped in four classes: class 1 corresponds to an average velocity  $V_{s30}$  larger than 700 m/s, and no site amplification below 15 Hz; class 2 corresponds to an average velocity  $V_{s30}$  between 500 and 700 m/s, and an RF curve exceeding 3-4 between 5 and 15 Hz; class 3 corresponds to an average velocity  $V_{s30}$  between 300 and 500 m/s, and a RF curve exceeding 3-4 between 2 and 5 Hz; finally class 4 corresponds to soft sites with an average velocity  $V_{s30}$  below 300 m/s, and an RF curve exceeding 3-4 below 2Hz .

This new record based classification may be compared to the previous 4 class classification

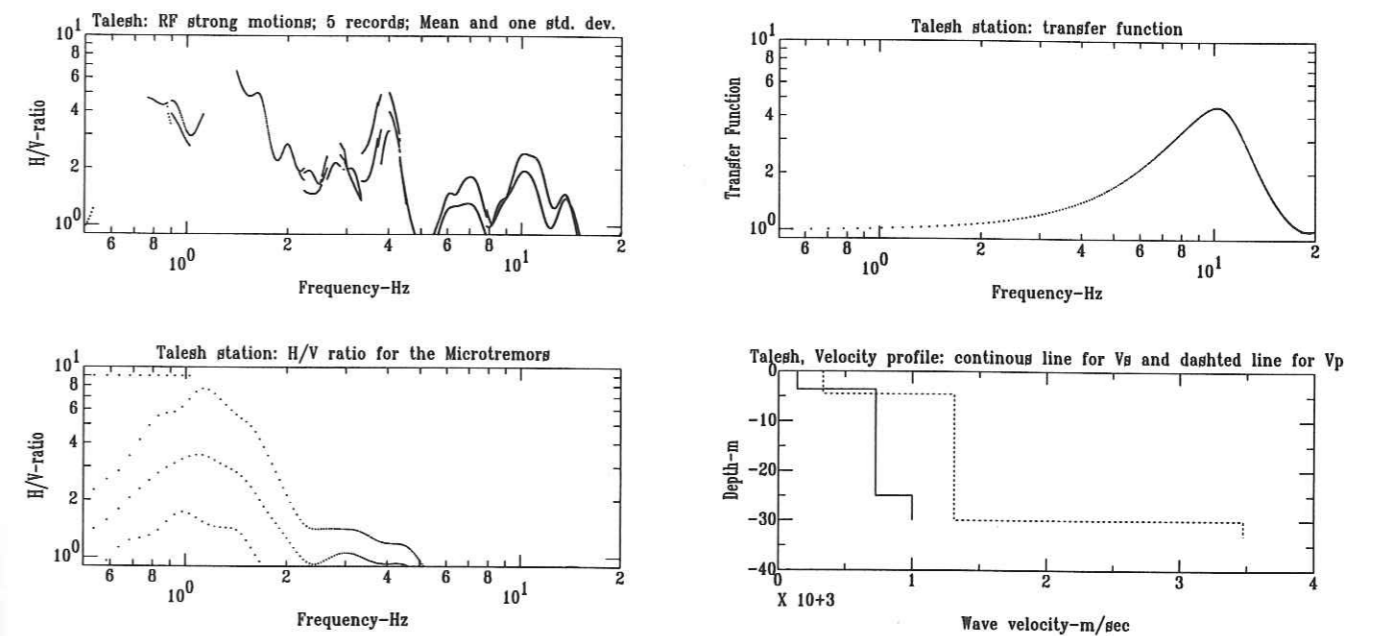


FIG. 3.24 - The results of the site tests in Talesh station (RF SMS, H/V MTS, transfer function and velocity profile).

performed by BHRC (1993) on a pure geological basis: it shows that pure surface geological observations are very poor in assessing the real response of the sites to strong motions. In our study, only in just 22 cases (over the 138 sites; i.e. 16%) the surface geological observations agree with the detailed sites studies (table III, Figure 3.27). In this figure it is shown that the determination of the sites classes based on the surface observation may result in very biased conclusions, such that each site classes may be mistaken for another one.

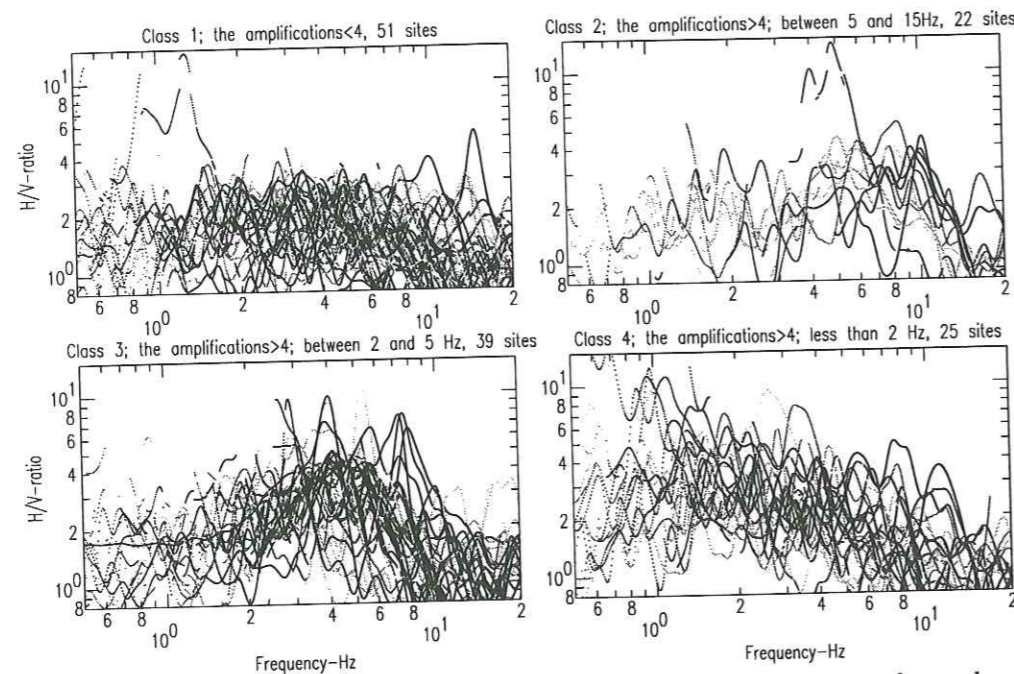


FIG. 3.25 - The results of the RF SMS for all of the 138 sites in four classes.

We insist that the RF SMS method seemed stable for a lot of the studied sites, therefore we have applied this method for the first time as our essential criteria to classify the site responses. Meanwhile the microtremors studies were not consistent with the strong motion results in our studies in Iran, which might be justified with the dry-arid climate mountainous conditions in most part of Iran; in any case the further microtremor tests should be performed. Similar studies might also be conducted in the neighboring countries of Iran; such as Turkey, Pakistan, Afghanistan Iraq, Caucasus and central Asian republics to develop and extrapolate the hazard mitigation results for this seismogenic region. In Iran, future developments of the strong motion network should favor the installation of instruments pairs; one on rock outcrop and another on nearby soil. This will provide the possibility to compare the H/V results with classical site to reference ratio. Other developments may be proposed in the form of "local arrays" for site studies in regions with high seismicity rate, and an important industrial and urban situation. We propose the first array of these series around the important city of Shiraz in southern Iran, where there is a high seismic activity, while a great part of the east of this city is located on soft soils and the underground water level is very high. Another local array with first priority of importance may be proposed for the city of Rasht on the shorelines of the Caspian sea in

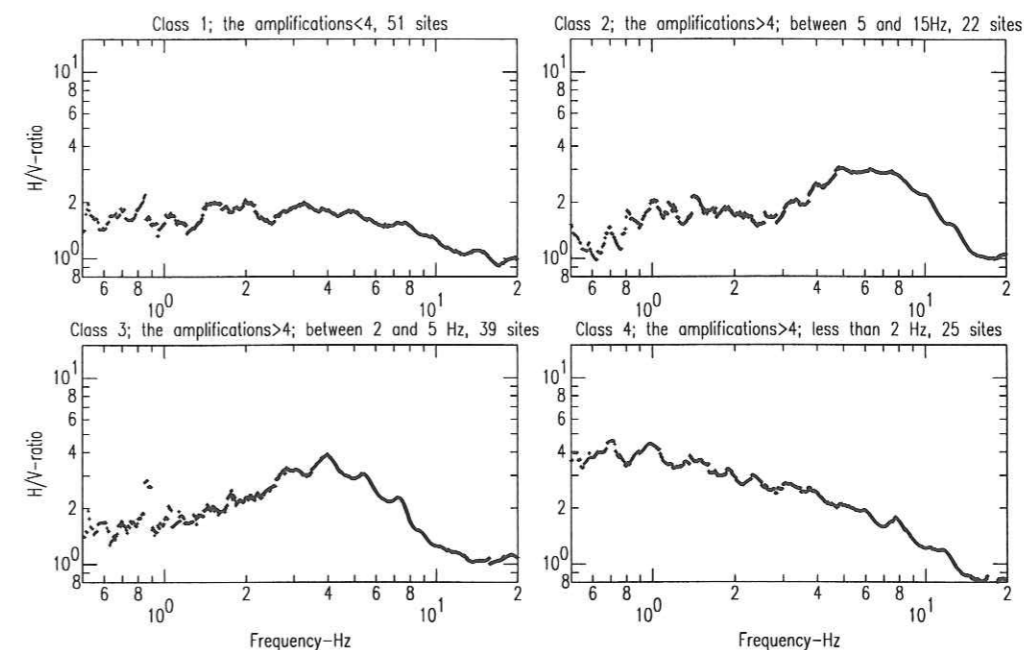


FIG. 3.26 - Average spectra for 4 site classes (using the RF SMS of all 138 sites).

northern Iran (near the epicenter of the Manjil earthquake of 1990; Mw7.3).

Acknowledgement

In this study many individuals have assisted us; most notably Messrs. Shirazian, Azadmanesh, Akbari and Mohseni (in IIEES) who assisted this project in the field studies, and Mirzaei-Alavijeh, Mahmoudi and Jalali in BHRC (Building and Housing Research Center, Tehran) who have completed the geoelectric tests. The financial support in Iran was provided by IIEES, and in France (for the first author) was provided by a French scholarship (Ministère Français des Affaires Etrangères), which are both duly acknowledged. The first author wants to thank F. Zoueshtiagh who has given some suggestions for article layout. Our thanks also go to Douglas McLean who has proof-read this text and has given comments to correct the orthography.

20 AOUT 2003  
 Univ. J. Fourier - O.S.U.G.  
 MAISON DES GEOSCIENCES  
 DOCUMENTATION  
 B.P. 53  
 F. 38041 GRENOBLE CEDEX  
 Tél. 04 76 63 54 27 - Fax 04 76 51 40 58  
 Mail: ptalour@ujf-grenoble.fr



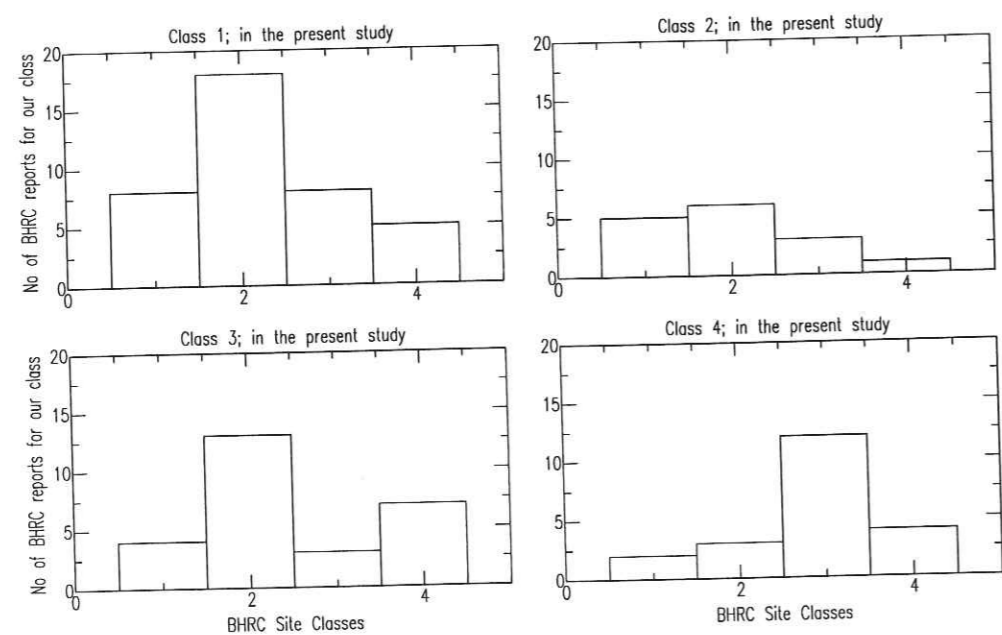


FIG. 3.27 - The comparison of the site classification in this study and that of BHRC (1993); The BHRC site classes are compared to each of the four classes defined in the present st recor

## Chapitre 4

### Études particulières: la source sismique et Kappa

**Résumé** Les enregistrements accélérométriques ont permis l'étude du moment sismique en Iran. Les fréquences-coins des spectres de Fourier et les plateaux des spectres sont mesurés pour un ensemble de 468 enregistrements (de 360 événements), même si les paramètres des sources étaient a priori connus (enregistrements téléseismiques) pour seulement 190 événements. D'autres paramètres de la source sismique comme la fréquence maximale ( $f_{max}$ ), et la chute de contrainte sont calculés et discutés aussi dans ce chapitre. Le moment sismique est utilisé pour déterminer la magnitude de moment, utilisé dans la suite des études sur les mouvements forts. Les valeurs de  $M_w$  sont proches de  $M_s$  pour les magnitudes supérieures à 6.0, et de  $mb$ , pour les magnitudes inférieures à 6.0. Les  $ML$  rapportés par les centres sismologiques iraniens sont plus dispersés mais sont cependant en accord avec les  $M_w$ , surtout pour les magnitudes inférieures à 6.0.

La chute de contrainte pour les séismes en Iran est représentative des régions intra-plaque. Ces valeurs sont entre 30 et 500 bars pour la plupart des séismes. D'autre part l'étude de la dépendance de  $f_{max}$  en fonction de la distance et la magnitude, montre une sensibilité presque similaire avec la magnitude et la distance, avec cependant un coefficient de corrélation un peu plus élevé pour la dépendance avec la magnitude. La dépendance des fréquences-coins en fonction de la magnitude et la distance est aussi étudiée, et on trouve une très bonne corrélation/négative avec la magnitude.

## 4.1 Seismic Moment and Stress Drop for the Strong Motion Accelerograms in Iran

Mehdi Zaré, Pierre-Yves Bard and Mohsen Ghafory-Ashtiany

Article en préparation

**Abstract** The moment magnitude ( $M_w$ ) for the events recorded by the Iranian strong motion network is derived from the corner frequencies and spectral levels measured in the Fourier spectra of the corrected accelerograms. The calculation is done over a data-set of 468 three components time-histories (from 379 events), out of which the teleseismic source data were available for only 190 events. The hypocentral distances are also estimated based on the difference in the arrival times of compressional and shear waves. The comparison of the calculated moment magnitude and the reported teleseismic  $M_s$ ,  $mb$  and  $M_w$ , and local  $ML$  values indicates that the calculated  $M_w$ 's are consistent with the teleseismic  $M_w$ 's; a good approximation is  $M_w = M_s$

for the magnitudes over 6, and  $M_w = mb$  for magnitudes below 6. The  $ML$  values inferred by local seismological networks in Iran (corresponding to magnitudes below 6) exhibit a larger scatter with, however, an average satisfactory agreement. The magnitudes for moderate events (mostly in southern Iran, Zagros region, for which no report existed on their source) are thus estimated by this method. In addition, the estimated stress drops for this data-set (between 30 and 500 bar) correspond better to intra-plate earthquake.

### 4.1.1 Introduction

The purpose of this study is to determine the magnitude of the earthquakes recorded in the Iranian network, for which no teleseismic or local information exists on their localisation and magnitude. The moment magnitude is thus derived from the Iranian strong motion data (corresponding to earthquakes occurred between 1975 and February 1997). The strong motion data in this study were recorded by two types of instruments: the analog SMA-1 instruments have been installed in Iran since 1975, but have been steadily replaced by the digital SSA-2 instruments after the Manjil earthquake of 1990 ( $M_w 7.3$ ). Some 468 three component accelerograms, out of 750 uncorrected records, are selected and filtered. The investigated data set comprises 169 analog and 299 digital records: out of which the source parameters were available only for 279 records (169 analog and 110 digital; Bard et al 1998). Since it was essential to use as much data as possible to establish the attenuation laws for Iran, and the application of a uniform magnitude scale was necessary, the moment magnitudes are calculated.

The earthquake magnitudes in Iran are reported by the international bodies for larger events (PDE monthly reports and ISC bulletins), as well as the local seismologic centers (Institute of Geophysics, Tehran University, IGTU).

In this paper, after a brief outline of method used to calculate the seismic moment, it is applied to the Iranian records for which no teleseismic source data could be found, and the results are presented in a Table (Appendix 4.1). The correlation of the estimated  $M_w$  with the other magnitude scales is indicated. Then, the causes for discrepancies from the ideal model are described. The stress drop estimations are presented as well.

### 4.1.2 Methodology of the Study: the $\omega^{-\gamma}$ model

Haskell (1964) has already proposed a simple source model for the estimation of high frequency ground motions. The simple seismic source models are explained by Aki (1967), and Brune (1970; 1971). In this model, the far field displacement spectrum is characterized by a flat

level  $\Omega$  proportional to  $M_0$  at long periods, a corner frequency  $f_c$  proportional to inverse of the source dimension, and a high frequency spectral decay in the form  $(\frac{f}{f_c})^{-\gamma}$ . Taking the  $\gamma$  values as 2 or 3, we have the  $\omega$ -square or  $\omega$ -cube model, respectively ( $\omega$  is the angular frequency in radians per second, equal to  $2\pi f$ ). Hanks (1982) has shown that with a  $\omega$ -square model, for which the acceleration spectra would be flat after the corner frequency,  $f_c$ , the high frequency decay may in the acceleration spectrum be explained by the attenuation along the wave path. As proposed by Hanks (1979), the displacement spectra may be represented by;

$$\Omega = \frac{\overline{\Omega}_0}{1+(\frac{f}{f_c})^\gamma}$$

where  $\overline{\Omega}_0$  is the value of the low frequency flat part of the displacement spectrum. For far-field S-waves due to a double couple source embedded in an elastic, homogeneous, isotropic half-space, we have:

$$\overline{\Omega}_0 = \frac{1}{4\pi R_h} \cdot \frac{M_0}{\rho} \cdot \frac{1}{\beta^3} \cdot (R'_{\theta\phi}) \cdot F_s$$

where  $\beta$  is the shear wave velocity of the medium,  $\rho$  its density; (around  $2.8 \times 10^3$  kg/m<sup>3</sup>),  $R_h$  the hypocentral distance,  $R'_{\theta\phi}$  the double couple radiation pattern for SH or SV waves (about 0.6 in average),  $F_s$  is the free surface amplification factor (to be taken equal to 2).

The value of the flat part of the acceleration spectrum,  $A_0$ , may be related to  $\overline{\Omega}_0$  with

$$A_0 = \overline{\Omega}_0 \cdot \omega_c^2$$

Hence,  $M_0$  could be written as

$$M_0 = \left( \frac{A_0}{(2\pi f_c)^2} \right) \cdot \frac{4\pi R_h \cdot \rho \cdot \beta^3}{R'_{\theta\phi} \cdot F_s} \quad (4.1)$$

In the following,  $\beta$  is taken equal to  $3 \times 10^3$  m/sec, and  $\rho = 2.8 \times 10^3$  kg/m<sup>3</sup>.

Kanamori (1977) has defined a new magnitude scale based on the seismic moment, that is more reliable measure of the size of the great earthquakes. This scale is defined as:

$$M_w = 0.667 \times \log M_0 - 6.0 \quad (4.2)$$

We used the formula 4.1 and 4.2 to calculate  $M_w$  for the events recorded in Iranian strong motion network.

The static stress drop is related to the moment magnitude and source radius (Kanamori and Anderson 1975). The source radius might be estimated using the Brune model (1970) by:

$$r_0 = \frac{2.34}{2\pi} \cdot \frac{\beta}{f_c} \quad (4.3)$$

$r_0$  is the source radius in meter. For circular faults, the stress drop is related to  $r_0$  with:

$$\Delta\sigma = \frac{7}{16} \cdot \frac{M_0}{r_0^3} \quad (4.4)$$

where  $\Delta\sigma$  is the stress drop, in Pascal ( $1Pa = 10^{-5}$  bar).

### 4.1.3 The sources of Uncertainties

Some essential causes for uncertainties or errors may be classified as follows:

- The pre-event memory does not exist in analog data. Therefore, the determination of the first arrival of P waves, and then the hypocentral distances were difficult for such data in Iran. This difficulty does not exist, fortunately, for most of the digital records.

- The handy digitalization of the SMA-1 records made a lot of problems to pick a corner frequency the  $f_c$  and  $A_0$ .

- In digital records of moderate magnitude events  $M < 4$ , the spectral amplitudes are very low. Therefore, it was sometimes difficult to distinguish the signals from the noises coming from the sensor. The cases with high noise level are eliminated.

- In very high amplitude records of high earthquakes ( $M > 7.0$  distances below 50km), the interferences of different waves make it impossible to identify P and S waves. Therefore, this method of calculation of  $M_w$ , is to be used with caution for such records. The fault distance should be obtained by other means (aftershock studies, for instance).

### 4.1.4 Results

To establish the Iranian strong motion catalogue, some 169 records were selected from a total of 430 three component analog accelerograms (Bard et al 1998a). The first arrival of the P waves was not always clear, therefore it was difficult to calculate the hypocentral distance,  $R_h$  using the difference of S and P arrivals;

$$R_h = 8 \times (t_s - t_p) \quad (4.5)$$

The digital records, which are the main purpose of this article, present more suitable conditions; for 110 digital records the source parameters, were available from teleseismic studies (ISC, NEIC), while for 192 others there were not. A pre-event memory at the beginning of almost all of the SSA-2 records permitted the observation of  $t_p$  and  $t_s$  more easily. On the other hand, the satisfactory quality of digital records provides the opportunity for more precise measurement of the corner frequencies and the flat part of the acceleration spectra.

**An example from a digital record**

A digital (SSA-2) three component accelerogram that is obtained in Hosseinieh village (southern Iran; Figure 4.1) is shown in Figure 4.2. This record was obtained during an earthquake on 31 July 1994, with reported source parameters of  $M_s=5.3$ ,  $m_b=5.3$ ,  $M_w=5.6$ , a focal depth of 43 km according to NEIC, and  $M_L4.5$  (IGTU). Regarding the epicenter coordinates for this event, the epicentral distance for the record would be found as 20 km, and the hypocentral distance at 45km. A closer zoom on the first 6 seconds of the record is indicated in Figure 4.3. The first arrivals for P and S waves,  $t_p$  and  $t_s$ , are estimated at  $1.5 \pm 0.3$  and  $4.7 \pm 0.3$ , respectively, therefore  $R_h$  equals  $25.6 \text{ km} \pm 5 \text{ km}$ . Taking to account highest peaks of the amplitude spectra,  $A_0$  equals  $0.35 \text{ m/sec} \pm 0.15$  (Figure 4.4), and  $f_c$  is measured at  $1.2 \pm 0.3 \text{ Hz}$ . The seismic moment is therefore,  $M_0 = 3.9 \times 10^{17} \text{ N-m}$ . With 4.2, we have  $M_w=5.5 \pm 0.3$ .

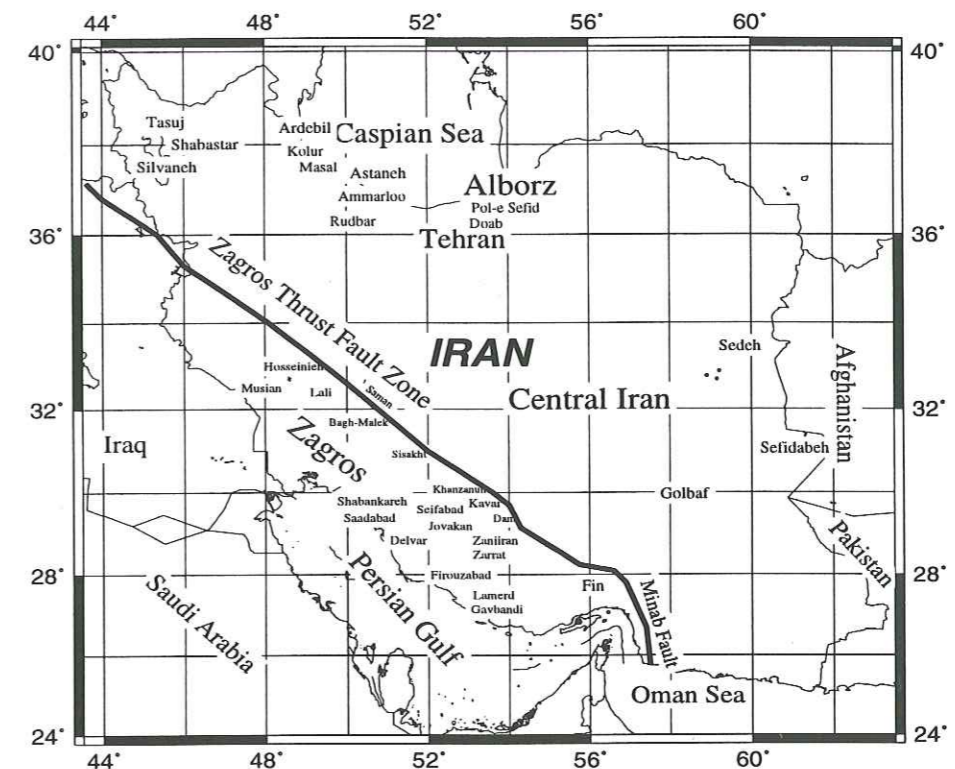


FIG. 4.1 - The locations of the studied selected accelerometric sites in Iran in this paper.

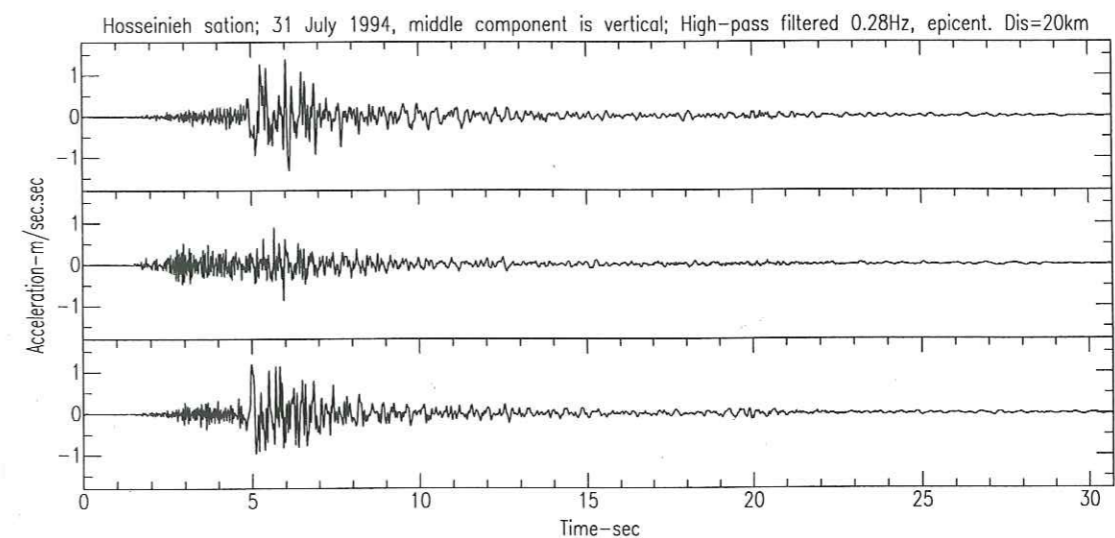


FIG. 4.2 - Hossienieh record of the event of 31 July 1994.

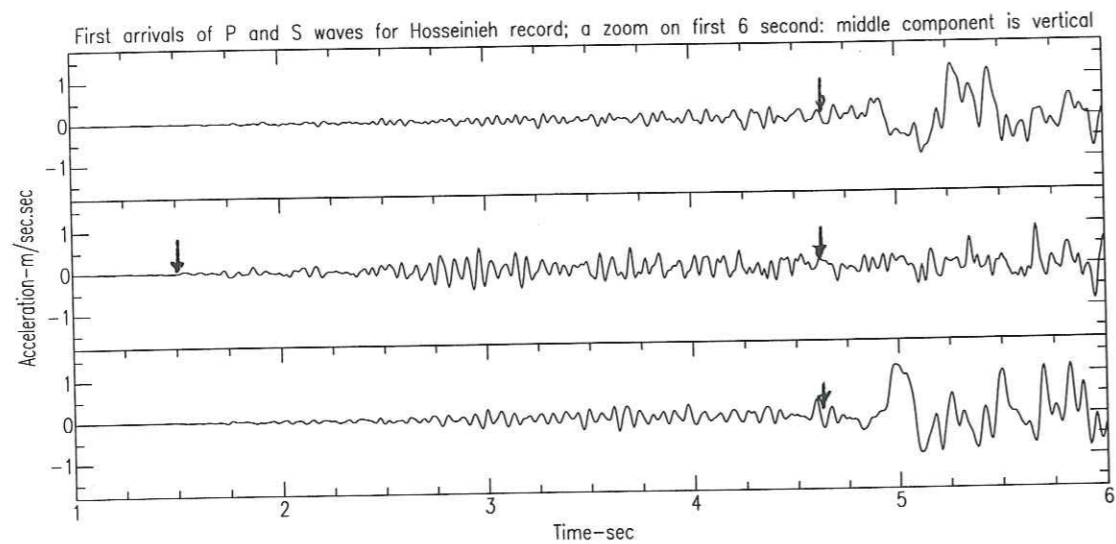


FIG. 4.3 - A zoom on the first 6 seconds of the record in Fig. 4.2; the first arrow at 1.5 seconds for  $t_p$  and the second on at 4.7 seconds for  $t_s$ .

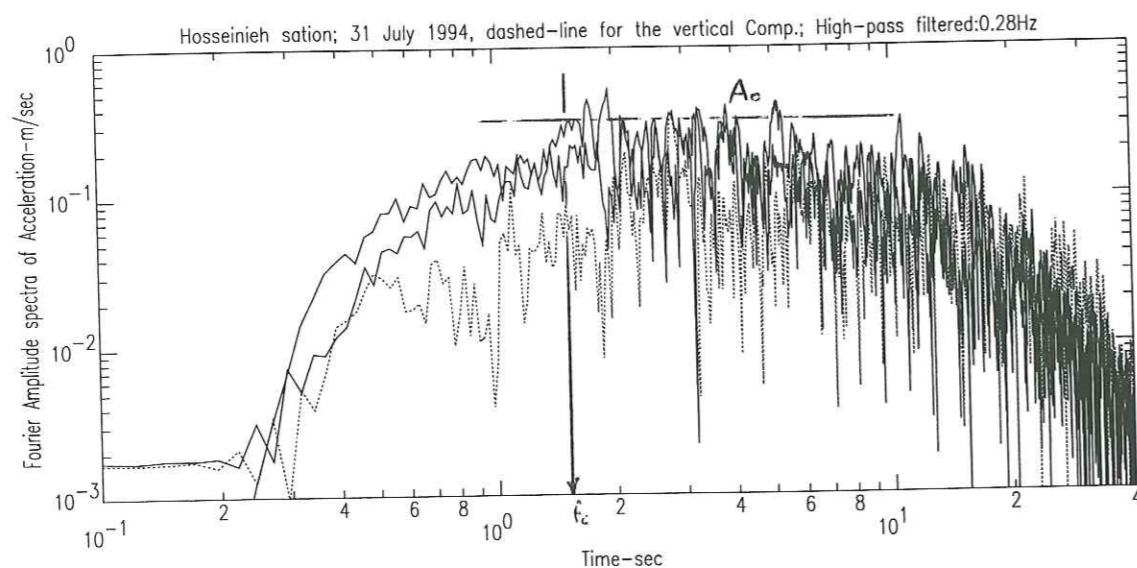


FIG. 4.4 - The Fourier Amplitude Spectra of Acceleration of Hosseinieh record.

#### 4.1.5 Application of the method for the records with no reported source

The recent digital accelerometric data in Iran, recorded after January 1994, contains a lot of records with only the triggering time. To use these data in the attenuation studies, the moment magnitudes and the hypocentral distance are calculated according to the method outlined in the previous section. The results are displayed in Appendix 4.1, listing for each record the BHRC code, the station name, the site class (based on the site classes 1 to 4, already defined by Zaré et al 1999a), the date (as mentioned in the header of the record), the high-pass filter used to avoid the low-frequency noise, the horizontal and the vertical peak ground accelerations (HPGA and VPGA, respectively), the corner frequency, the stress drop in bar, the hypocentral distance and finally the calculated moment magnitude ( $M_w$ ). Most data presented in Appendix 4.1 were recorded in Zagros region, however a few data come from western Alborz in Caspian Sea shoreline, Azarbaijan in NW, as well as some records from eastern Iran (Figure 4.1).

For 27 events, several stations triggered, allowing an investigation on the stability and reliability of this  $M_w$  determination. The results are displayed in Figure 4.5, with stability for the  $f_c$  and stress drop calculation for the same 27 events. This figure exhibits an average standard deviation on moment magnitude of 0.19, corresponding to a factor of  $10^{\frac{0.19}{0.667}} = 10^{0.28} \approx 3$  on seismic moment. The average standard deviations for  $\log f_c$  and stress drop are 0.47 and 8.93, respectively.

#### Comparison of the calculated $M_w$ with reported teleseismic magnitudes

The calculated  $M_w$ 's are plotted against the teleseismic reported  $M_s$ 's,  $m_b$ 's, and  $M_w$ 's and  $M_L$ 's, in Figure 4.6. It is evident that;

- The calculated  $M_w$ 's are consistent with reported teleseismic  $M_w$ 's.
- For magnitudes over 6, the calculated  $M_w$  are in agreement with  $M_s$  values, but for magnitudes below 6, they coincide more with the  $m_b$  values ( $m_b$  values saturate in magnitudes around 6-6.0; Figure 4.7).
- The local magnitudes inferred from the local seismological network in Iran are more scattered but agree however with the calculated  $M_w$  values. These values correspond to magnitudes below 6.

#### Stress Drop estimation

The stress drop is estimated using formula 4.4 and presented in Appendix 4.1. The stress drop depends to the corner frequency,  $f_c$  (4.3 and 4.4). The observed  $f_c$ 's for Alborz-Central

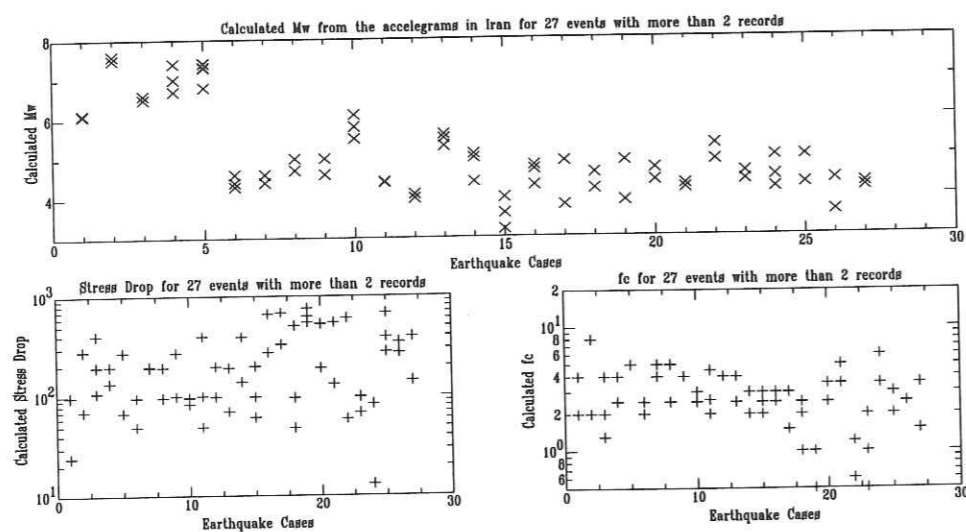


FIG. 4.5 – The stability of the  $M_w$ 's calculated in this study, for 27 cases and  $f_c$  and stress drop for 13 events with more than 2 records.

Iran and Zagros are plotted in Figure 4.8 against  $M_w$ . They are between 1 and 10 Hz for most of the records. No important difference may be seen between these two regions on this limited data-set. The stress drop values are then obtained and traced against  $f_c$  in Figure 4.9 and against  $M_w$  in Figure 4.10. The estimations of the stress drops in Iran are mostly between 30 and 500 bars (3 to 50 MPa). According to Kanamori and Anderson (1975) and Kanamori (1977), they are thus representative for the intra-plate earthquakes.

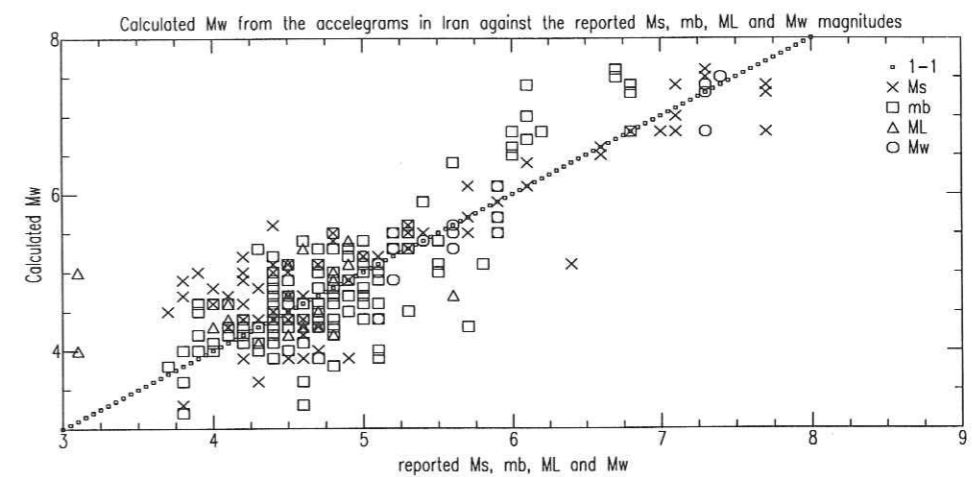


FIG. 4.6 – Comparison between calculated  $M_w$  and the teleseismic and local magnitudes.

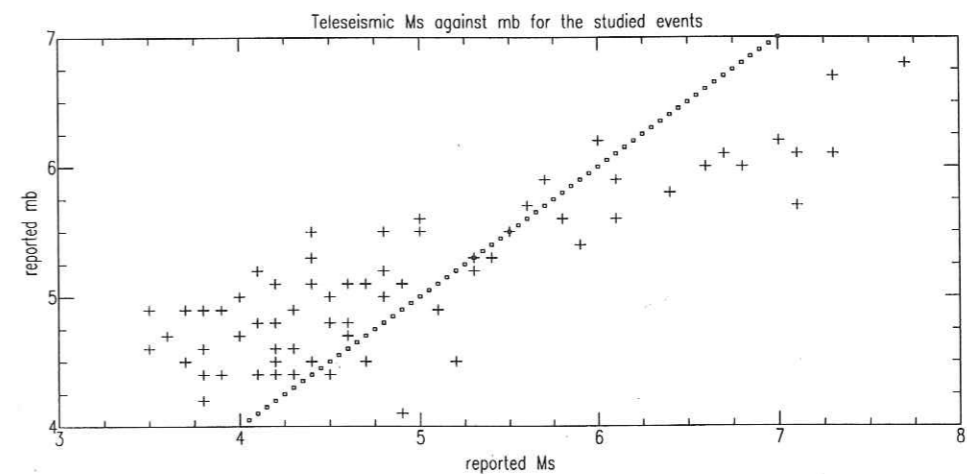


FIG. 4.7 – Comparison between  $M_s$  and  $m_b$  values

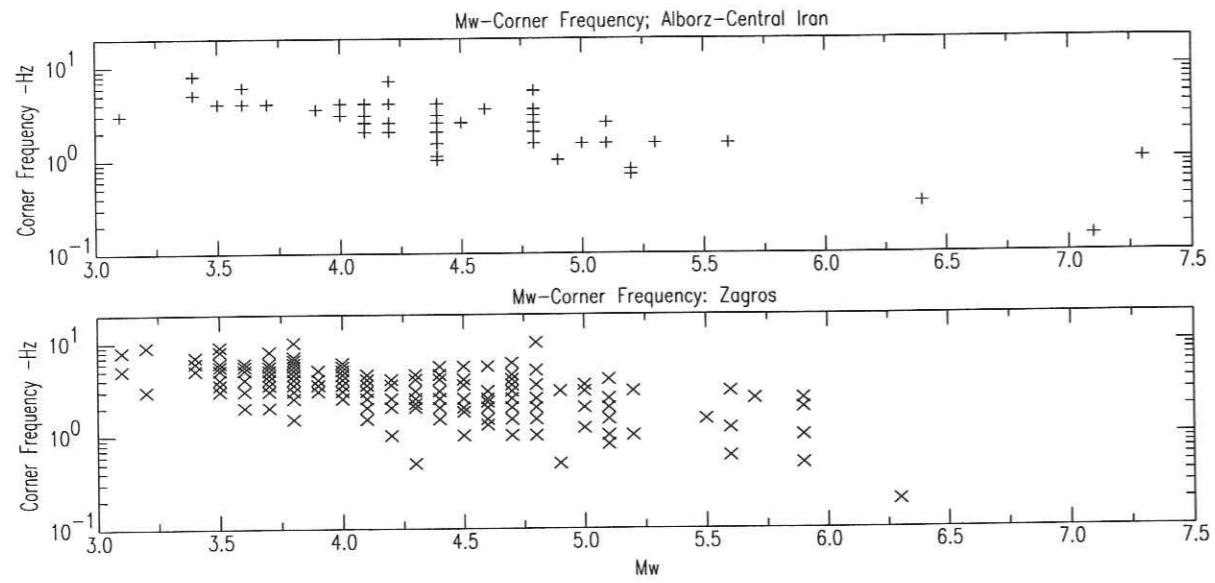


FIG. 4.8 - The observed corner frequencies against  $M_w$  for Alborz-Central Iran and Zagros regions.

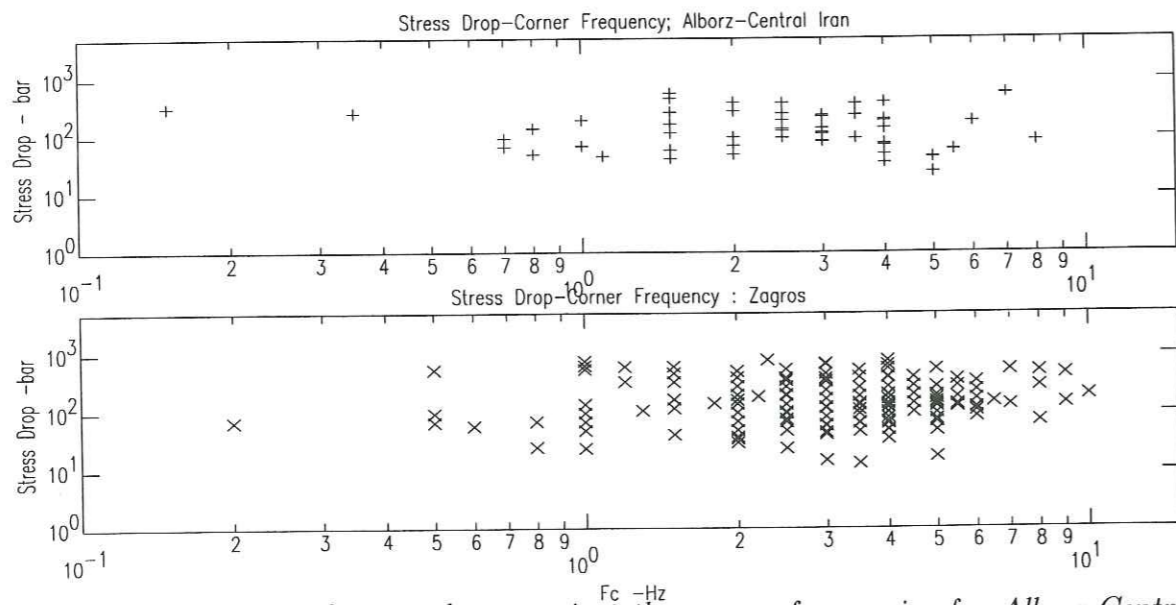


FIG. 4.9 - The estimated stress drops against the corner frequencies for Alborz-Central Iran and Zagros regions.

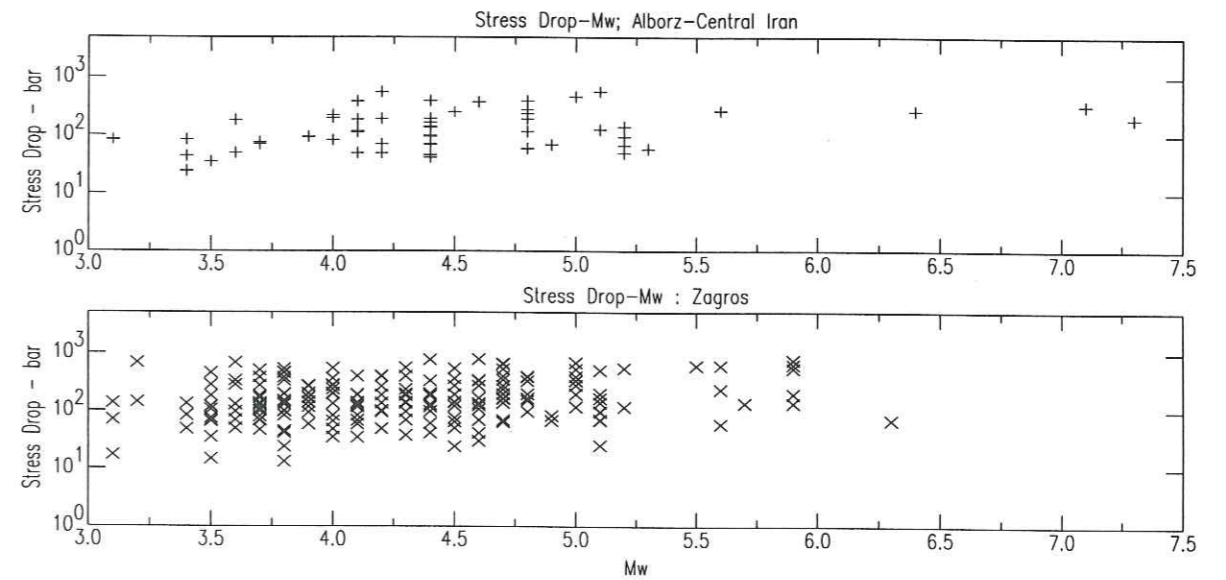


FIG. 4.10 - The estimated stress drops against  $M_w$  for Alborz-Central Iran and Zagros regions.

Dependence of  $f_c$  and  $f_{max}$  to magnitude and distance

The dependence of  $f_c$  and  $f_{max}$  to magnitude and distance is investigated, with the two following relationships :

$$\log f = a \cdot M + c + \sigma_1 \cdot P \tag{4.6}$$

$$\log f = -b \cdot \log R_h + d + \sigma_2 \cdot P \tag{4.7}$$

where a and b are the coefficients of  $M_w$  and  $R_h$ , respectively, c and d are constants and  $\sigma_1$  and  $\sigma_2$  are standard deviation and P percentile. The obtained coefficients are given in Table 4.1 for  $f_c$  and in Table 4.2 for  $f_{max}$ . The correlation coefficient ( $R$ ) for  $f_c$  show that  $f_c$  depends completely to  $M_w$  where no correlation is evident between  $f_c$  and hypocentral distance. The dependence of  $f_{max}$  to  $M_w$  and hypocentral distance is similar (with a slightly higher R for the dependence on  $M_w$ ).

Table 4.1: The coefficients for relationships 4.6 and 4.7, for  $f_c$ .

a	c	$\sigma_1$	R
-0.345	1.940	0.151	0.579
b	d	$\sigma_2$	R
0.295	0.825	0.253	0.001

Table 4.2: The coefficients for relationships 4.6 and 4.7, for  $f_{max}$ , for horizontal and vertical components.

Comp.	a	c	$\sigma_1$	R
Hori.	-0.185	1.781	0.162	0.468
Vert.	-0.130	1.785	0.145	0.469
	b	d	$\sigma_2$	R
Hori.	0.386	1.623	0.167	0.398
Vert.	0.341	1.647	0.148	0.400

4.1.6 Conclusions

The moment magnitudes calculated from the Iranian strong motion data provide satisfactory results: The calculated values are consistent with teleseismic estimates of  $M_w$ , while they agree with Ms for magnitudes larger than 6, and with mb for magnitudes below 6. It becomes therefore possible to use the records from events within low to medium magnitude range (M3-5) in the attenuation studies, even though there does not exist any teleseismic or local report. These data in Iran were recently made available using the new digital SSA-2 network. Of course, it would be better to have an improved seismological network in Iran, so as to locate precisely and have more reliable magnitude determinations. On the other hand, it is suggested to improve the maintenance of the accelerometric network in Iran, so as to systematically assign source characteristics to each strong motion record. In particular the use of a GPS system is recommended to obtain an absolute timing for all the instruments in this network. The present situations, without precise timing, greatly impairs detailed source studies, which is really a pity with so many instruments installed in such an active seismic area.

Acknowledgement

The BHRC (Building and Housing Research Center, Tehran) who have released the raw strong motion records is greatly thanked. A financial support in France (for the first author) provided by a French scholarship (Ministère Français des Affaires Etrangères) is duly acknowledged. Douglas Maclean is greatly acknowledged for controlling the orthography of this article.



## 4.2 Décroissance de l'amplitude à haute fréquence dans le spectre de Fourier de l'Accélération: coefficient Kappa

**Résumé** La décroissance à haute fréquence du spectre de Fourier de l'accélération est étudiée sur les données iraniennes, pour détecter d'éventuelles non-linéarités dans les sols peu rigides. Cette décroissance est caractérisée par le paramètre Kappa (Anderson et Hough 1984), dont la valeur a été estimée seulement pour les données ayant un bon rapport signal sur bruit à haute fréquence. Lorsque  $\kappa$  pouvait être mesuré sur un même site, pour plusieurs enregistrements présentant différents niveaux d'accélération, nous avons étudié les variations de  $\kappa$  avec cette accélération. Nous avons d'autre part repris la classification par site et étudié les variations statistiques de  $\kappa$  (tous les sites d'une même catégorie mélangés) avec le niveau d'accélération, de même que les variations de  $\kappa$  avec le type de site. Les résultats de ces analyses restent très flous:  $\kappa$  semble cependant affecté légèrement quand la rigidité du site diminue, indiquant que  $\kappa$  serait au moins partiellement lié à l'atténuation de proche-surface.

### 4.2.1 Introduction

La décroissance haute fréquence des spectres de Fourier de l'accélération  $A(f)$  est souvent caractérisée par un paramètre appelé  $\kappa$ , correspondant à une décroissance en  $e^{-\kappa f}$ . Deux interprétations existent, liant cette décroissance à l'atténuation de la croûte et du sol (Anderson et Hough 1984, Durward et al. 1996, Hanks 1982, Lacave-Lachet et al. 1998) ou à la source (Papageorgiou and Aki 1983, Gariel et Campillo 1989). Hanks (1982) suppose que la fréquence maximale ( $f_{max}$ ) est induite par l'atténuation anélastique proposée dans une relation entre  $\kappa$  et la distance à la source. Lachet-Lacave et al (1998) reprennent cette interprétation pour détecter des non-linéarités dans les enregistrements obtenus lors de la séquence du séisme de Kobé (1995) au Japon; les sols mous soumis à de fortes accélérations devraient en effet voir leur amortissement augmenter, et donc  $\kappa$  augmenter. À l'opposé, Papageorgiou et Aki (1983) ont montré que la décroissance en haute fréquence serait liée à l'existence d'une zone de collision (non-élasticité de la faille) à l'avant du front de la rupture, dont la taille contrôlerait la fréquence  $f_{max}$ . Gariel et Campillo (1989), en utilisant une approche numérique, ont confirmé que deux facteurs liés à la source peuvent expliquer la décroissance haute fréquence: la présence de cette 'zone de cohésion', mais aussi le ralentissement lissé du front de rupture.

La méthodologie des études sur  $\kappa$  est présentée d'abord. Les relations de  $\kappa$  avec la distance

sont ensuite étudiées pour les différentes régions de l'Iran.

### 4.2.2 La méthodologie des calculs de Kappa

La partie haute fréquence d'un spectre d'accélération peut être représentée comme suite:

$$A(f) = A_1 e^{-\pi \kappa f} \text{ pour } f > f_{max}$$

où  $A(f)$  est le spectre de l'accélération, et  $A_1$  est une constante qui dépend des propriétés de la source, de la distance épacentrale et peut-être d'autres facteurs,  $f$  est la fréquence,  $\kappa$  est le coefficient de décroissance, et  $f_{max}$  est une fréquence au-dessus laquelle la forme spectrale ne peut pas être distinguée de la décroissance exponentielle. En supposant un milieu simple sur un demi-espace élastique, on peut écrire:

$$\kappa = \int \frac{ds}{Q\beta}$$

où  $ds$  est l'élément de rayon sismique,  $Q$  est le facteur de qualité, et  $\beta$  est la vitesse des ondes S.

Cette intégrale peut se décomposer en 2 termes: l'un correspondant à la propagation dans les milieux très superficiels à proximité de la station d'enregistrement et l'autre à la propagation dans la croûte profonde:

$$\kappa = \frac{l_c}{Q(f) \cdot \beta_c} + \frac{h_s}{Q_s \cdot \beta_s}$$

où  $l_c$  est la distance totale parcourue dans la croûte, caractérisée par un facteur de qualité  $Q_c(f)$  et une vitesse d'onde S,  $\beta_c$ ;  $h_s$  est l'épaisseur des milieux superficiels,  $Q_s$  leur facteur de qualité, et  $\beta_s$  leur vitesse d'onde de cisaillement. Selon cette décomposition, le premier terme va produire un coefficient  $\kappa$  qui va augmenter avec la distance source-site ( $l_c$ ), tandis que le second sera sensible aux effets non-linéaires, puisque en un site donné,  $Q_s$  devrait diminuer, et  $\beta_s$  aussi, quand l'accélération augmente beaucoup.

### 4.2.3 Les résultats

Les valeurs de  $\kappa$  ainsi calculées sont représentées en fonction de la distance pour les régions de Zagros, et Alborz-Iran Central et pour 4 catégories des sites différents dans les Figures 4.11 à 4.13, respectivement. Les résultats du Zagros sont très dispersés, et ne correspondent qu'à de faibles distances (la plupart avec  $R_h < 20\text{km}$ ). Ces données viennent des enregistrements plutôt digitaux obtenus pour des séismes de magnitude inférieure à 6 (Figure 4.11). Les résultats en Alborz-Iran Central (pour les séismes des magnitudes de moins de 6, pour comparer avec les données du Zagros, Figure 4.12) montrent des variations moins rapides avec la distance (Figures 4.12 et 4.13). Pour mieux expliquer les valeurs de kappa en champ-proche, il y aurait besoin d'études supplémentaires.

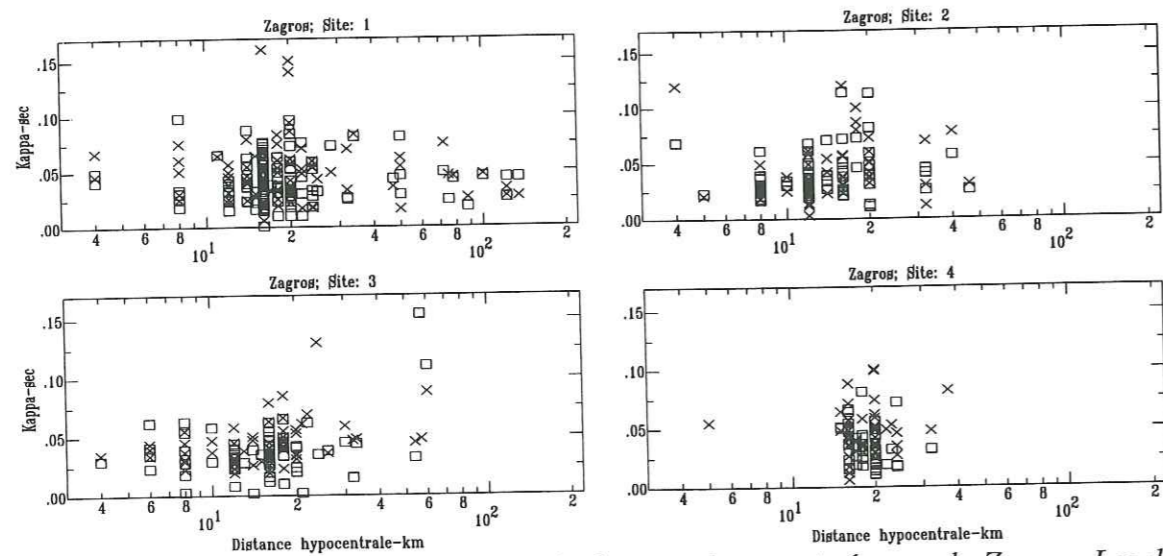


FIG. 4.11 – Les valeurs de  $\kappa$  en fonction de la distance hypocentrale pour le Zagros. Les données sont présentées pour différentes catégories de site. Les croix correspondent aux composantes horizontales et les rectengules aux composantes verticales.

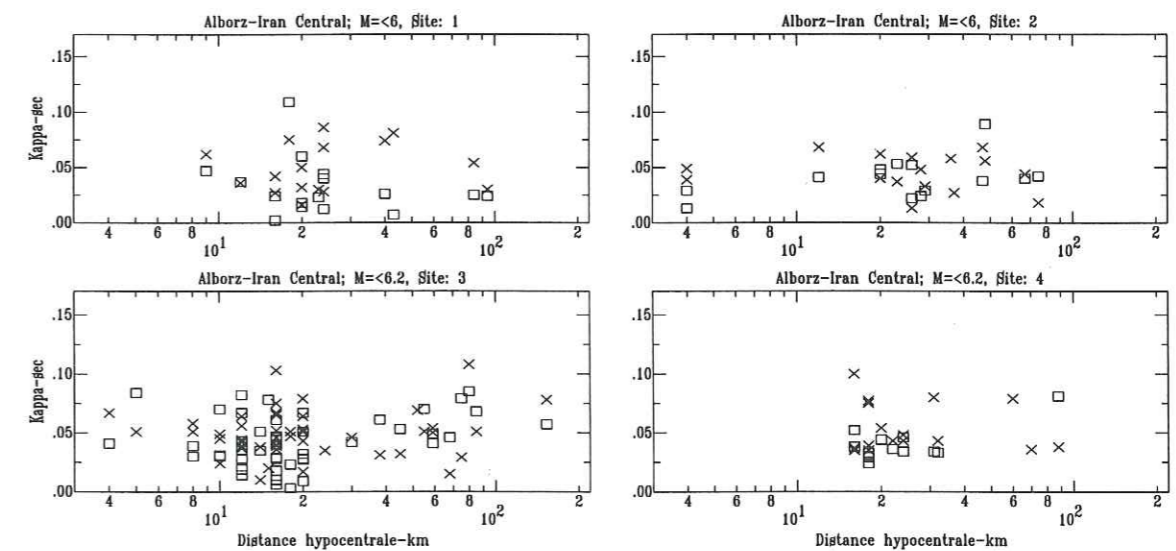


FIG. 4.12 – Les valeurs de  $\kappa$  en fonction de la distance hypocentrale pour l'Alborz-Iran Central; les événements de magnitudes moins de 6. Les données sont présentées pour les catégories différentes de site. Les croix correspondent aux composantes horizontales et les rectengules aux composantes verticales.

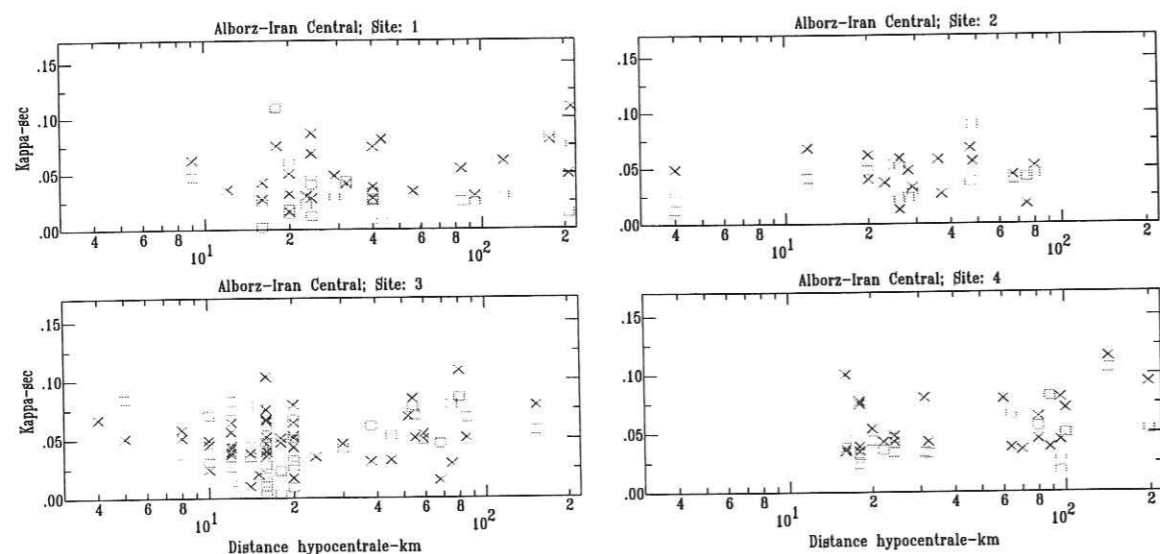


FIG. 4.13 – Les valeurs de  $\kappa$  en fonction de la distance hypocentrale pour la région de l’Alborz-Iran Central (sans limitation de la magnitude). Les données ont été présentées pour les catégories différentes de site. Les croix correspondent aux composantes horizontales et les rectangles aux composantes verticales.

Pour en être sûr, nous avons considéré quelques séismes particuliers pour lesquels nous disposons de plusieurs enregistrements (Ebrahimabad, etc.). La Figure 4.14 pourrait montrer une légère augmentation de  $\kappa$  avec la distance, notamment pour le séisme de Manjil, mais les valeurs varient beaucoup d’un séisme à l’autre, de telle sorte qu’il est impossible de distinguer une dépendance de  $\kappa$  avec la distance pour séismes correspondants. Par ailleurs, les valeurs de  $\kappa$  ont été présentées en fonction de l’accélération maximale pour les sites avec plusieurs enregistrements en Figure 4.15. Ces résultats montrent la variation de  $\kappa$  plus ou moins similaires pour les types différents de sol, et aucune tendance à l’implication de  $\kappa$  avec l’accélération maximale.

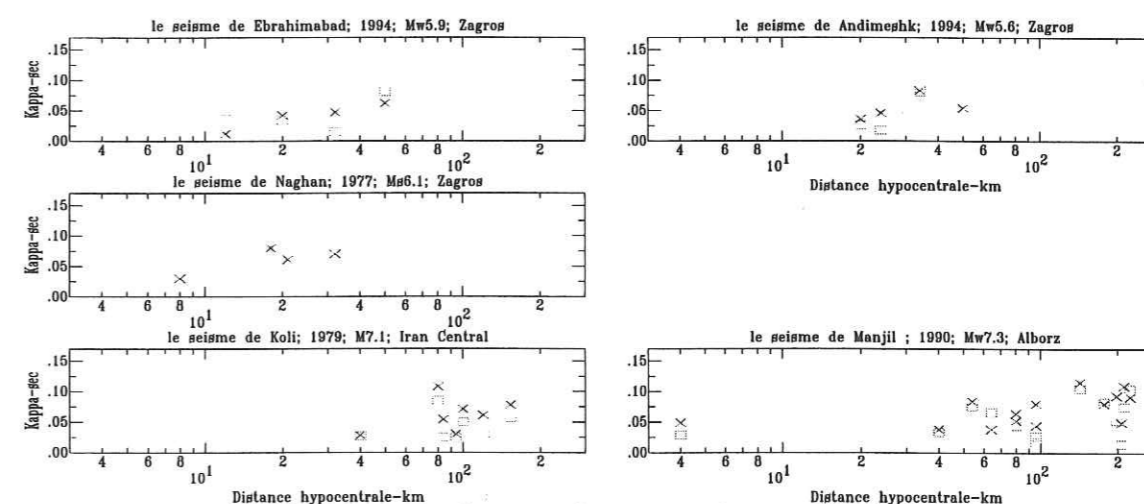


FIG. 4.14 – Variation de  $\kappa$  avec la distance hypocentrale pour les séismes avec les magnitudes supérieures à de 5.9 pour les régions de Zagros, Alborz-Iran Central [Ebrahimabad 1994, Andimeshk, 1994, et Naghan 1977 dans la région de Zagros, et Koli 1979 en Iran Central et Manjil 1990 en Alborz]. Les croix correspondent aux composantes horizontales, et les rectangles aux composantes verticales.

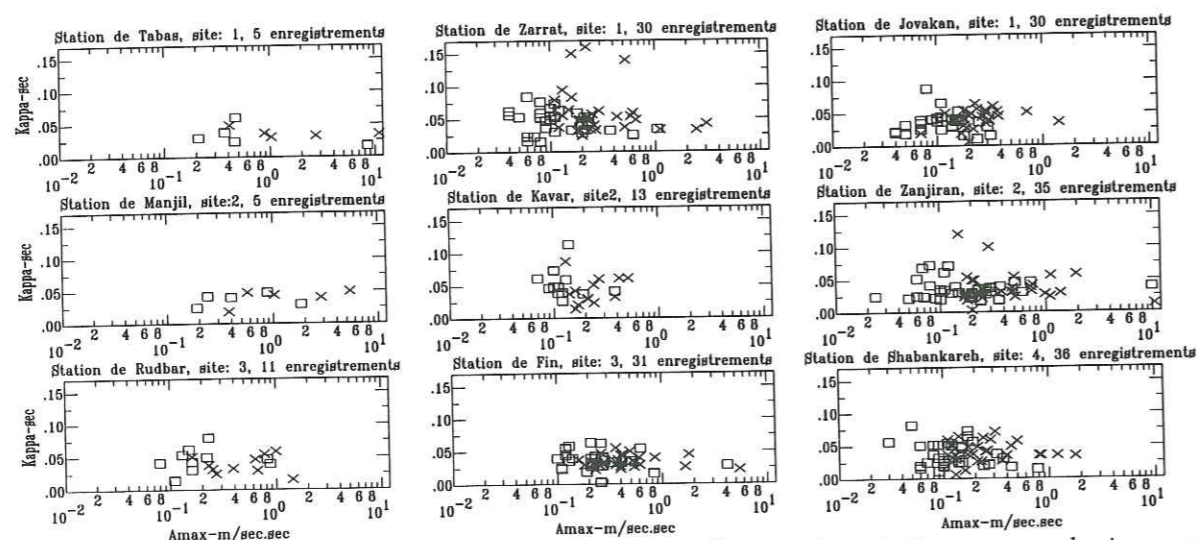


FIG. 4.15 - Variation de  $\kappa$  avec l'accélération maximale pour les stations avec plusieurs enregistrements: Tabas, Zarrat, Jovakan (site 1), Manjil, Kavar et Zanjiran (site 2), Rudbar et Fin (site 3) et Shabankareh (site 4). Les croix correspondent aux composantes horizontales et les rectangles aux composantes verticales.

Ces résultats au  $\kappa$  suggèrent une très faible influence des conditions de site dans les données iraniennes. Concernant un autre faible dépendance avec la distance, nous en concluons que probablement la théorie de Papageorgiou et Aki, et Gariel et Campillo (1989), selon laquelle les effets de source sont prédominants sur le comportement haute fréquence, est plus en d'accord avec ces résultats actuels.

#### 4.2.4 Conclusion

Les études sur le paramètre de  $\kappa$  en Iran montrent essentiellement une très forte dispersion, surtout dans les premiers 20km (surtout dans les données de Zagros) à telle point qu'il est impossible de détecter une tendance. Pour aller plus loin, il faudrait disposer de données de réseaux accélérométriques locaux avec plus des stations numériques, en comparant les données des chocs principaux et des répliques enregistrés sur les sites différents et par des distances différentes. Nous proposons l'observation de la forme de spectre de l'accélération en haute fréquence surtout pour le champ-proche des sources sismiques les plus importantes les plus connues en Iran. Ce type des études particulières permettent de relier  $\kappa$  à l'atténuation superficielle ou profonde.

Appendix 4.1: The Iranian digital records (SSA-2 instruments) for which the source parameters are estimated directly for the records.

No	Code BHRC	Station	Site	Event	HP filter (Hz)	PGA (H1) m/sec2	PGA (V) m/sec2	PGA (H2) m/sec2	f max (H) Hz	f max (V) Hz	fc (Hz)	Stress Drop (Bar)	Ao m/sec	Hypo Dist. (km)	Mw calc.
1	1512-1	Sedeh	3	07/07/94	0.44	.435	.650	.438			2.5	251.6	0.1	16	4.5
2	1505	Sefidabeh (Microwave)	1	1/3/94	0.20	.088	.093	.134	10.0	10.0	2	98.1	0.04	24	4.4
3	1504-1	Sefidabeh (School)	2	1/3/94	0.27	.068	.032	.052			4	24.15	0.006	16	3.4
4	1492-1	Zarrat	1	8/3/94	0.10	.420	.190	.258	12.0	15.0	4	393.5	0.09	16	4.2
5	1503-1	Zanjiran	2	9/3/94	0.24	.191	.105	.193	18.0	18.0	5	193.2	0.06	12	3.8
6	1503-2	Zanjiran	2	9/3/94	0.24	.258	.201	.115	25.0	30.0	8	280.9	0.055	12	3.5
7	1494-1	Kavar	2	11/3/94	0.25	.191	.230	.176	30.0	35.0	2	69.5	0.05	12	4.3
8	1500-1	Zanjiran	2	11/3/94	0.28	.216	.107	.138	10.0	10.0	8	280.9	0.08	8	3.5
9	1500-2	Zanjiran	2	13/3/94	0.25	.178	.104	.109	26.0	30.0	9	142.0	0.03	8	3.2
10	1500-3	Zanjiran	2	14/3/94	0.25	.095	.078	.166	28.0	30.0	4	555.8	0.25	8	4.3
11	1492-3	Zarrat	1	17/3/94	0.14	.728	.272	.613	20.0	25.0	2	195.7	0.10	16	4.6
12	1494-2	Kavar	2	17/3/94	0.25	.145	.080	.223	10.0	15.0	1.3	107.2	0.08	20	4.8
13	1494-3	Kavar	2	17/3/94	0.20	.242	.115	.211	15.0	15.0	2.5	382.3	0.20	12	4.6
14	1500-5	Zanjiran	2	17/3/94	0.23	1.111	.299	.730	18.0	22.0	4	402.6	0.10	16	4.2
15	1500-7	Zanjiran	2	18/3/94	0.25	.099	.061	.198	25.0	30.0	6	118.5	0.045	8	3.5
16	1500-9	Zanjiran	2	19/3/94	0.28	.119	.061	.177	25.0	30.0	5	136.8	0.04	12	3.1
17	1500-10	Zanjiran	2	20/3/94	0.20	.277	.141	.351	20.0	25.0	3	234.5	0.10	12	4.3
18	1500-11	Zanjiran	2	20/3/94	0.30	.153	.136	.182	20.0	25.0	3	83.2	0.035	12	4.0
19	1500-12	Zanjiran	2	21/3/94	0.30	.386	.154	.298	30.0	35.0	4.5	140.8	0.075	8	3.8
20	1492-10	Zarrat	1	12/4/94	0.44	.201	.062	.052	20.0	20.0	7	133.3	0.02	14	3.4
21	1492-12	Zarrat	1	7/5/94	0.25	.153	.066	.166	10.0	10.0	2.5	135.7	0.04	20	4.2
22	1502-1	Zanjiran	2	20/5/94	0.21	.149	.049	.144	15.0	20.0	3	117.5	0.045	16	4.1
23	1502-3	Zanjiran	2	5/6/94	0.21	.112	.081	.235	25.0	28.0	10	194.8	0.025	12	3.2
24	1502-5	Zanjiran	2	6/6/94	0.20	.377	.194	.716	20.0	28.0	4	393.5	0.15	16	4.2
25	1492-17	Zarrat	1	20/6/94	0.25	.214	.078	.227	18.0	18.0	2.2	184.5	0.10	16	4.5
26	1492-18	Zarrat	1	20/6/94	0.20	.090	.038	.129	11.0	15.0	4	197.3	0.045	16	4.0
27	1493-3	Firouzabad	3	20/6/94	0.20	.128	.078	.135	6.0	8.0	2.5	135.7	0.05	18	4.3
28	1492-21	Zarrat	1	21/6/94	0.24	.159	.095	.157	18.0	18.0	4.5	396.8	0.07	18	4.1
29	1518-1	Firouzabad	3	22/6/94	0.40	.359	.073	.084	30.0	30.0	5	17.2	0.015	4	3.1
30	1501-1	Zanjiran	2	23/6/94	0.20	.842	.374	1.092	20.0	22.0	8	501.4	0.11	12	3.7
31	1501-2	Zanjiran	2	23/6/94	0.20	.153	.106	.234	22.0	25.0	8	70.6	0.02	8	3.1
32	1501-3	Zanjiran	2	23/6/94	0.32	.197	.065	.168	22.0	25.0	3	41.7	0.02	12	3.8
33	1501-5	Zanjiran	2	24/6/94	0.27	.248	.097	.476	20.0	22.0	5.5	182.1	0.065	8	3.7
34	1501-6	Zanjiran	2	24/6/94	0.23	.250	.122	.198	25.0	30.0	4	49.6	0.035	5	3.6
35	1501-7	Zanjiran	2	24/6/94	0.23	1.352	.596	1.367	22.0	25.0	2.5	270.6	0.020	8	4.5
36	1501-8	Zanjiran	2	25/6/94	0.24	.154	.073	.214	20.0	25.0	5.5	128.9	0.03	12	3.6
37	1501-9	Zanjiran	2	25/6/94	0.24	.486	.238	.438	25.0	30.0	3.5	263.6	0.15	8	4.2
38	1523-1	Jovakan	1	6/7/94	0.26	.199	.144	.114	20.0	20.0	5	48.6	0.015	12	3.4
39	1523-2	Jovakan	1	7/7/94	0.20	.148	.073	.139	18.0	18.0	2.5	48.2	0.03	12	4.0
40	1523-3	Jovakan	1	7/7/94	0.20	.261	.166	.293	20.0	20.0	4	98.9	0.03	16	3.8
41	1523-4	Jovakan	1	9/7/94	0.20	.339	.153	.233	20.0	20.0	3.5	132.2	0.04	18	4.0
42	1519-1	Zarrat	1	10/7/94	0.20	.133	.050	.099	18.0	18.0	5	272.8	0.05	20	3.9
43	1523-5	Jovakan	1	10/7/94	0.20	.154	.095	.112	18.0	20.0	5	68.5	0.015	16	3.5
44	1518-2	Firouzabad	3	13/7/94	0.20	.126	.076	.080	6.0	10.0	2.5	96.1	0.04	16	4.2
45	1523-6	Jovakan	1	13/7/94	0.20	.288	.158	.263	18.0	18.0	2	49.2	0.06	16	4.2
46	1523-7	Jovakan	1	16/7/94	0.20	.129	.067	.142	18.0	18.0	4	555.8	0.03	16	4.3
47	1523-9	Jovakan	1	18/7/94	0.20	.183	.112	.184	21.0	21.0	2.5	24.1	0.015	14	3.8
48	1523-10	Jovakan	1	20/7/94	0.27	.190	.043	.113	10.0	10.0	4	70.1	0.02	15	3.7
49	1523-11	Jovakan	1	24/7/94	0.21	.129	.180	.224	21.0	21.0	6	83.9	0.025	12	3.4
50	1523-12	Jovakan	1	28/7/94	0.21	.307	.114	.260	21.0	21.0	5	48.6	0.015	12	3.4
51	1523-13	Jovakan	1	29/7/94	0.25	.183	.049	.088	28.0	28.0	5	136.8	0.04	12	3.7
52	1506-2	Hosseinih	4	31/7/94	0.20	.498	.130	.319	9.0	15.0	2	138.6	0.06	20	4.5
53	1506-3	Hosseinih	4	31/7/94	0.20	.146	.094	.257	12.0	18.0	2	69.5	0.04	20	4.3
54	1506-4	Hosseinih	4	31/7/94	0.28	1.786	.470	1.244	5.0	8.0	1.5	463.9	0.30	20	5.1
55	1506-5	Hosseinih	4	31/7/94	0.21	.272	.145	.185	12.0	18.0	1.5	116.6	0.08	20	4.7
56	1506-6	Hosseinih	4	31/7/94	0.21	.191	.060	.155	10.0	12.0	4.5	140.9	0.03	20	3.8
57	1506-7	Hosseinih	4	31/7/94	0.21	.118	.075	.084	15.0	20.0	3	83.2	0.04	18	4.1
58	1506-8	Hosseinih	4	31/7/94	0.21	.261	.141	.349	10.0	12.0	3	234.5	0.09	25	4.3
59	1506-9	Hosseinih	4	31/7/94	0.21	.234	.108	.144	12.0	12.0	3	117.5	0.04	20	4.1
60	1520-1	Kavar	2	1/8/94	0.25	.169	.106	.117	20.0	20.0	4	70.1	0.025	12	3.7
61	1506-10	Hosseinih	4	2/8/94	0.21	.184	.072	.080	18.0	20.0	1.5	41.4	0.03	18	4.4
62	1519-2	Zarrat	1	12/8/94	0.20	.118	.058	.148	12.0	18.0	5	193.2	0.04	15	3.8
63	1523-14	Jovakan	1	12/8/94	0.20	.206	.254	.124	21.0	21.0	4	197.3	0.05	16	4.0
64	1523-15	Jovakan	1	12/8/94	0.20	.380	.140	.338	18.0	18.0	4	197.3	0.05	16	4.0



## Chapitre 5

# Durée et Énergie des Mouvements Forts

**Résumé** Ce chapitre est consacré à l'étude de différents paramètres "énergétiques", c'est à dire liés à l'énergie véhiculée par les accélérogrammes (durée, accélération moyenne quadratique, "énergie"). Comme dans les autres chapitres, une distinction est faite entre Zagros et le reste de l'Iran, et la dépendance de chacun de ces paramètres en fonction de la magnitude, de la distance et des conditions de site est précisée grâce à des régressions. L'influence de ces dernières est d'ailleurs trouvée très faible, surtout pour la durée.

## Duration and Energy Content of the Strong Motions in Iran

Mehdi Zaré, Pierre-Yves Bard and Mohsen Ghafory-Ashtiany

Article soumis au "Journal of Earthquake Engineering"

**Abstract** The energy content and the strong motion duration are studied in Iran. Several parameter [root mean square acceleration,  $a_{rms}$ , the "energy of acceleration",  $e_a$ , proportional to Arias Intensity, and strong motions duration] are calculated for a data-base of 468 three component accelerograms, all recorded during the last 24 years in Iran. Empirical relationships are established for the strong motion duration, as a function of  $e_a$ , PGA on one side, and moment magnitude and hypocentral distances on the others. The dependence of  $e_a$  and  $a_{rms}$  with magnitude and distance is studied as well. Investigations on the possible influence of site conditions on the duration, did not point out any significant dependence in this regard. The probable trends in the results of Zagros region may be studied with more precise data. For such trends, there is no more explanation with this quantity of the data.

### 5.1 Introduction

The strong motion network in Iran has provided a significant amount of records from various regions of the country for the last 24 years. This network was equipped first with Kinometrics SMA-1 analog instruments (1975) which have been gradually replaced and densified with SSA-2 digital instruments after the Manjil earthquake of 1990,  $M_w$ 7.4, in NW Iran. The number of installed instruments in this network was reported to be about 1000 stations by the end of 1997. The stations have been mainly chosen within the cities or villages for an easy maintenance. A

listing of these data is published by BHRC, the organism that maintains this network presently in Iran (BHRC 1993).

The scope of this study is to investigate the energy content of Iranian data, and to derive empirical relationships for the energy-related parameters: strong motion duration,  $e_a$  and  $a_{rms}$ . The data-set used in this study, already presented in Bard et al. (1998), Zaré et al. (1999b), consists of 468 three component records. The source parameters were derived from teleseismic records for 190 events (279 recordings) (Bard et al 1998), while moment magnitudes and hypocentral distances were derived from the strong motion data themselves for 185 events (189 records) (Zaré et al 1999b).

The methodology of the study is explained first. The seismogenic zones in Iran, in view point of the strong motions, are detailed. The relationships for the energy content and duration are discussed. The empirical attenuation relationships are established and presented for the duration,  $e_a$  and  $a_{rms}$ .

### 5.2 Seismogenic zones in Iran and site conditions

The seismotectonics of Iran was first investigated by Nabavi (1976), Berberian (1976, 1977, 1981, ...etc), and more recently in the seismotectonic reports after each destructive earthquake in Iran (i.e. Zaré 1995, Zaré 1997). The main seismogenic zones in Iran are distinguished based on tectonic and neotectonic factors. To define such seismotectonic zones, it is necessary to have sufficient neotectonic diagnosis as well as the seismic source data. Previous works are mostly concentrated on studies on focal mechanisms and focal depths, as well as on seismicity studies (Ambraseys and Melville 1982, Jackson and McKenzie 1984, Berberian 1995, ... etc).

Some differences in seismicity rates are obvious at least between the two regions of Iran: Zagros in SW and west, and Alborz-Central Iran, in the center, north and east (Figure 5.1). The Zagros thrust fault zone is the main geologic frontier between the Zagros and the rest of the country (mainly Central Iran). The time of the event, the distance to source and the exact timing on the digital records (if accessible) were the criteria to attribute each record to the seismic events in these zones. The pre-existing seismic data from Zagros area shows higher seismic activity rate than the other regions. In this area the middle range magnitudes (M4-6) are more frequent (Figure 5.2). In Alborz-Central Iran zone, the earthquake are less frequent with higher magnitudes than Zagros (Figure 5.2), and more destructive. The Tabas earthquake of (1978,  $M_w$ 7.4, Central-Iran) and Manjil earthquake (1990,  $M_w$ 7.3, Alborz belt) are examples of such destructive events. Most of the focal mechanisms in Iran (in Zagros and in other regions)



are compressional and strike slip (Bard et al 1998) in relation with the local plate tectonics context.

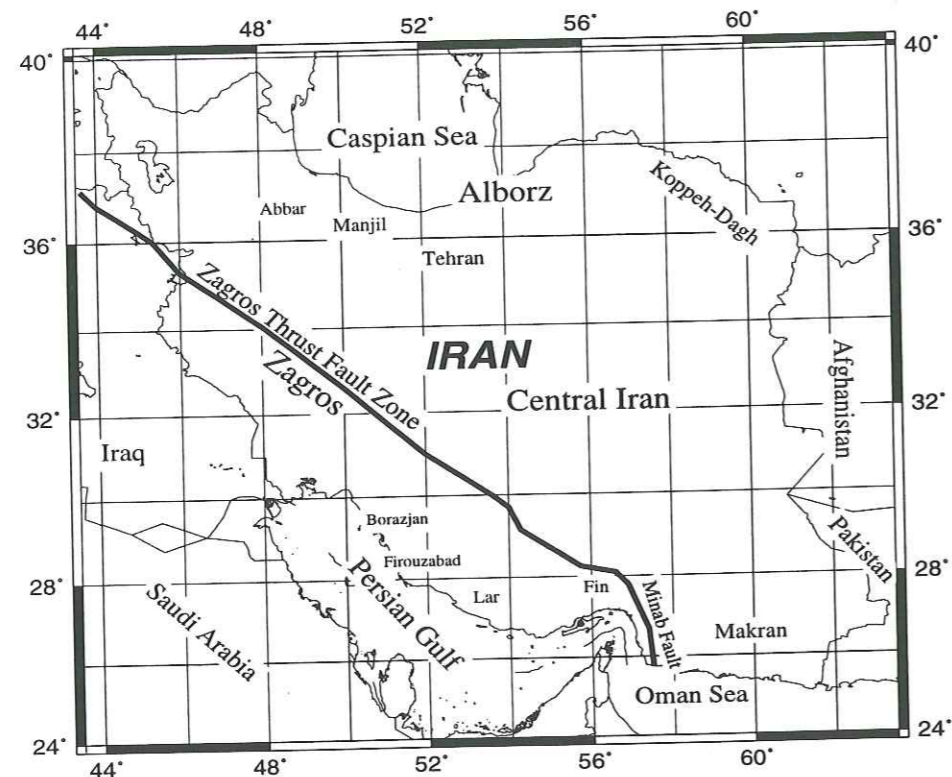


FIG. 5.1 - The studied area; the regions discussed in the text are shown.

The accelerometric data-base of Iran (Bard et al 1998) is not homogeneous; most of the data are recorded in Zagros, but no record exists from Makran (due to the lack of important earthquake in the last decades, and where few stations have been installed). The reasons for the fewer stations in this region were the sparse population in Makran region. Since the most destructive earthquakes have shocked the Alborz and Central-Iran region, the most distant records are obtained in these two regions (Figure 5.2).

The site conditions for the Iranian strong motions have already been studied (Zaré et al 1999a). Site class 1 is defined as sites that do not exhibit any significant amplification below 15 Hz. It corresponds to rock and stiff sediment sites with an average S-wave velocity over the top 30 meters in excess of 700m/sec. Site class 2 is determined as sites for which the receiver function (RF) exhibits a fundamental peak exceeding 3 at a frequency located between 5 and 15 Hz. It was shown to correspond to stiff sediments and/or soft rocks with  $V_{s30}$  between 500 and 700 m/sec. Site class 3 is defined as sites for which RF shows peaks exceeding 3 between 2 and 5Hz, and corresponds to alluvial sites with  $V_{s30}$  between 300 and 500 m/sec. Finally site class 4

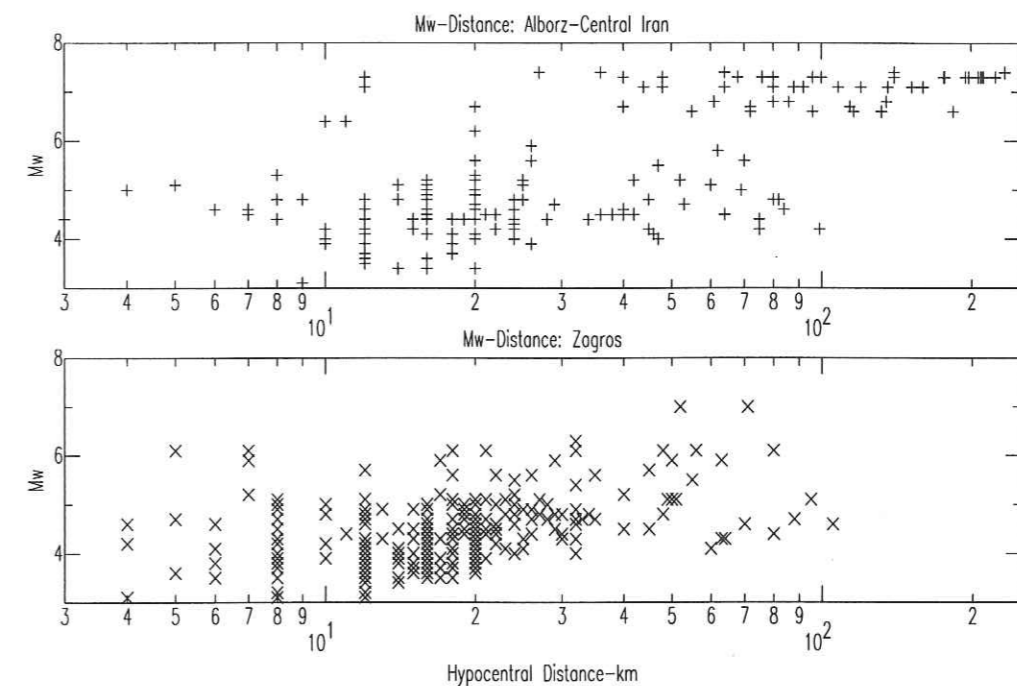


FIG. 5.2 - The  $M_w$ -Hypocentral distance distribution for two areas in Iran.

is defined as sites for which RF exhibits a fundamental peak exceeding 3 below 2Hz, and it may be viewed as corresponding to thick soft alluvium. This ranking was the result of geotechnical measurements on 24 sites (compressional and shear wave velocity and microtremors) and the calculation of the receiver function using the three component accelerograms.

### 5.3 Methodology

The duration of strong motions is defined in different ways. Some authors have used the "bracketed duration" (Bullen and Bolt 1985), which is the elapsed time window between the first and last acceleration excursions greater than a given level (i.e. 0.05g) (Page et al 1975). Another known definition in the earthquake engineering literature is the "cumulative duration" (Bullen and Bolt 1985), which is based on the concept of the cumulative energy obtained by integrating the squared accelerations. In this concept, duration is the time interval required to accumulate a predefined fraction of total energy (95% for Husid et al.,1969; 90% for Trifunac and Brady, 1975; and 70% for some other authors). Trifunac and Brady (1975) take the part between of 5% and 95% of total energy.

The Fourier amplitude spectra ( $A_\omega$ ) of an acceleration time-history,  $a(t)$ , is the absolute value of the Fourier transform of  $a(t)$  (Vanmarke and Lai 1980);

$$A_\omega = \left| \int_{-\infty}^{+\infty} a(t)e^{-i\omega t} dt \right| = \left| \int_0^{t_0} a(t)e^{-i\omega t} dt \right|$$

$\omega$  is the angular frequency in rad/sec,  $i = \sqrt{-1}$  and  $t_0$  is the length of the accelerogram (sec). To explain how the total strong motion energy is distributed over frequency, one may use the squared Fourier amplitude spectrum,  $A^2(\omega)$ . The integral of  $A^2(\omega)$  over the frequencies is a representative for the total strong motion "energy", related to the Arias intensity,  $I_0$  [Arias 1970]. This parameter shows the total energy per unit mass for the entire acceleration record for all single degree of freedom oscillators;

$$I_0 = \frac{\pi}{2g} \int_0^{t_0} a^2(t) dt$$

We have considered here a related formulation:

$$e_a = \int_0^{t_0} a^2(t) dt = \int_{-\infty}^{+\infty} a^2(t) dt = \frac{1}{2\pi} \int_{-\infty}^{+\infty} A^2(\omega) d(\omega) = \frac{1}{\pi} \int_0^{\infty} A^2(\omega) d(\omega)$$

In this article, we name this quality the "energy of acceleration" ( $e_a$ ):

$$e_a = \int_0^{t_0} a^2(t) dt$$

$a_{rms}$  is the square root of the average of the squared ordinates for a given duration,  $t_2-t_1$ , (Udwadia and Trifunac 1974):

$$a_{rms} = \left( \frac{1}{t_2-t_1} \int_{t_1}^{t_2} a^2(t) dt \right)^{\frac{1}{2}}$$

$$a_{rms} = \sqrt{\frac{\Sigma e_a}{t_2-t_1}}$$

McCann and Shah (1979) have defined an evolutionary RMS function (CRF), which represents the average rate of energy as a function of time:

$$CRF(t) = \left( \frac{1}{t} \int_0^t a^2(t) dt \right)^{\frac{1}{2}}$$

CRF allows another definition of duration, (the end of the signal is the time after which CRF(t) decreases).

The cumulative integral of squared acceleration for a record of Manjil earthquake ( $M_w$  7.3, 20 June 1990, hypocentral distance= 40km) obtained at Abbar (site class: rock, Figure 5.1) is shown in Figure 5.3. This record is obtained in Alborz ranges in northern Iran. The duration for this time-history (taking to account the intervals of 5% to 95%) are 31.92 and 35.06 for the horizontals and 35.96 for vertical component, respectively. These values are 8.64 and 20.68 for horizontals and 13.52 for vertical components, respectively, applying the intervals of 5% to 75%.

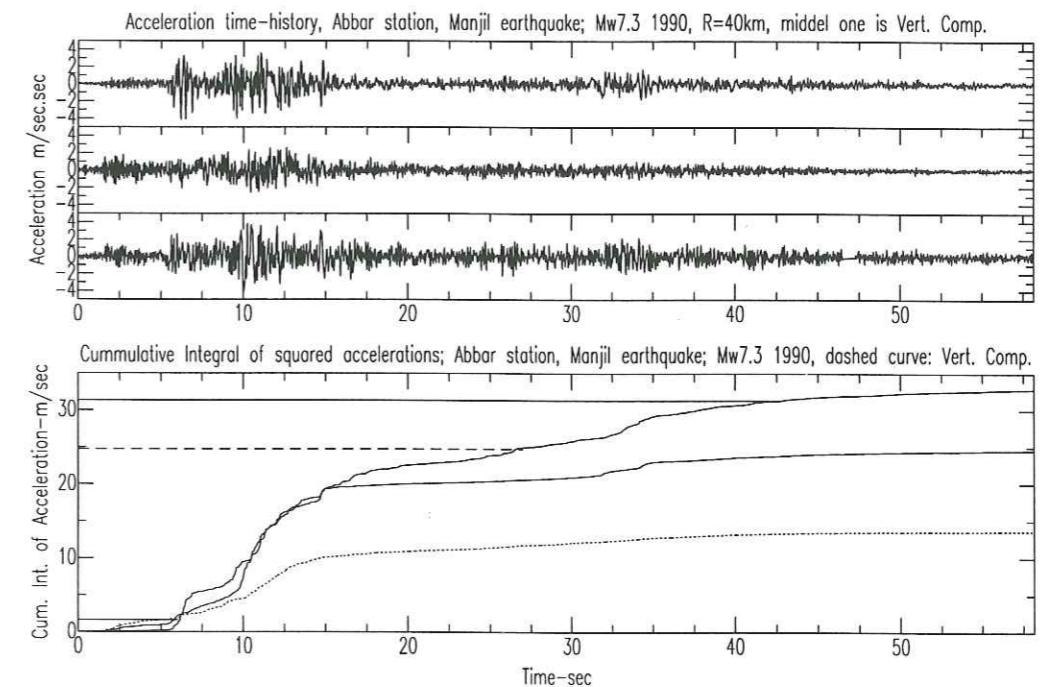


FIG. 5.3 - The time-history of the acceleration (up) and the cumulative integral of squared acceleration (down), for the Abbar record (Manjil, Iran earthquake of 20 June 1990,  $M_w$  7.3). The lines show the 5% and 95% limits, and a dashed line shows the 75% limit for the horizontal component that has the highest values. The vertical component is shown by dotted line as well.

Vanmarke and Lai (1980) have proposed an approximate relationship between the  $a_{rms}$  and PGA based on the random vibration theory:

$$r = \frac{a_{max}}{a_{rms}} \quad (5.1)$$

with  $T_0$  for the strong motion duration and Having

$$e_a = \frac{T_0 \cdot a_{rms}^2}{0.90} \quad (5.2)$$

with an approximation we have:

$$e_a \approx T_0 \cdot a_{rms}^2 \quad (5.3)$$

With (5.1) and (5.2), we have:

$$T_0 = r^2 \cdot \frac{e_a}{a_{max}^2} \quad (5.4)$$

We therefore computed the ratio  $\frac{e_a}{a_{max}^2}$  for all our records, and investigated its relationship with the actual strong motion duration,  $T_0$ . We have studied as well the dependence of  $T_0$ ,  $e_a$  and  $a_{rms}$  as a function of the magnitude and distance.

## 5.4 Results

The results of our calculations are presented in a Table in Appendix 5.1. For each component of the records the values of  $e_a$ , strong motion duration  $T - 0$  and  $a_{rms}$ , are given based on the definition of Udvardi and Trifunac (1974) (5%-75%), and Trifunac and Brady (1975) (5% to 95%).

### 5.4.1 Comparison of Strong Motion Intervals: 5%-95% and 5%-75%

The different intervals of 5% to 95% and 5% to 75% are examined in this study. The general tendency is that: the  $a_{rms}$  values calculated for 5% to 75% intervals, are equal to or larger than  $a_{rms}$  obtained by 5% to 95% intervals (Appendix 5.1).

The relationship for  $a_{rms}$  and the duration values calculated by these two intervals are shown in Figures 5.4 to 5.7. The linear relationship between  $a_{rms1}$  (5%-75%) and  $a_{rms2}$  (5%-95%) is

$$a_{rms1} = b \cdot a_{rms2} + \sigma \cdot P \quad (5.5)$$

where  $b$  is the coefficient,  $\sigma$  is standard deviation,  $P$  is the percentile index. The coefficients for the entire of the data-base are supplied in table 5.1:

Table 5.1: Result of the regression for relationship (5.5)

Data/comp.	b	R(Coef.Corr.)	Sigma
Iranian data (Vert. comp)	1.124	0.981	0.0014
Iranian data (Hori. comp)	1.375	0.981	0.0020

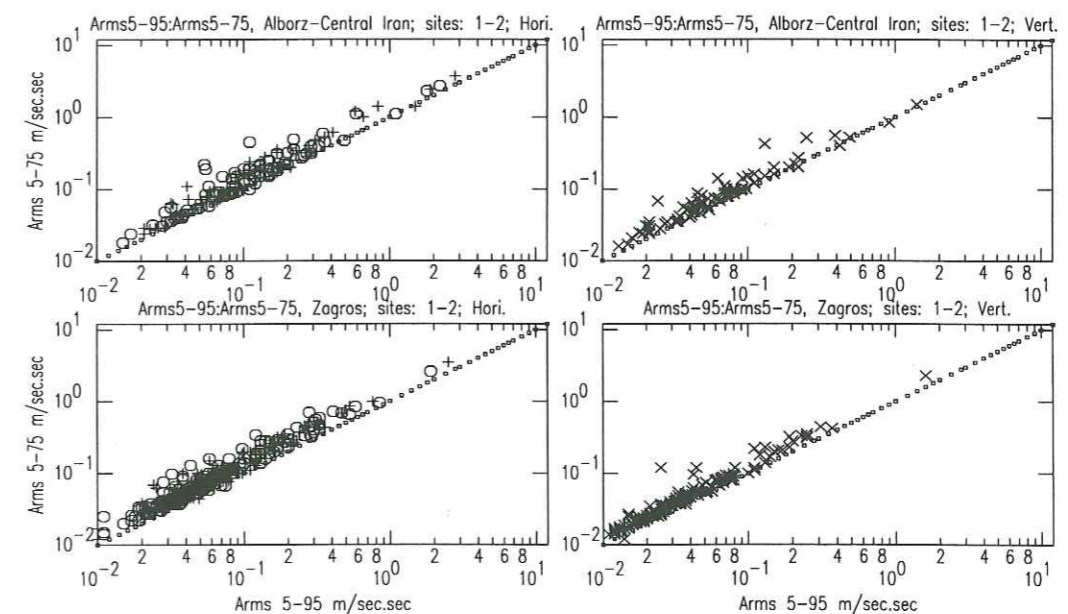


FIG. 5.4 - The  $a_{rms}$  values calculated for different intervals are plotted against each other; site classes 1 and 2, for two areas; two different symbols in the left side figures stand for two horizontal components (Alborz-Central-Iran top, Zagros bottom).

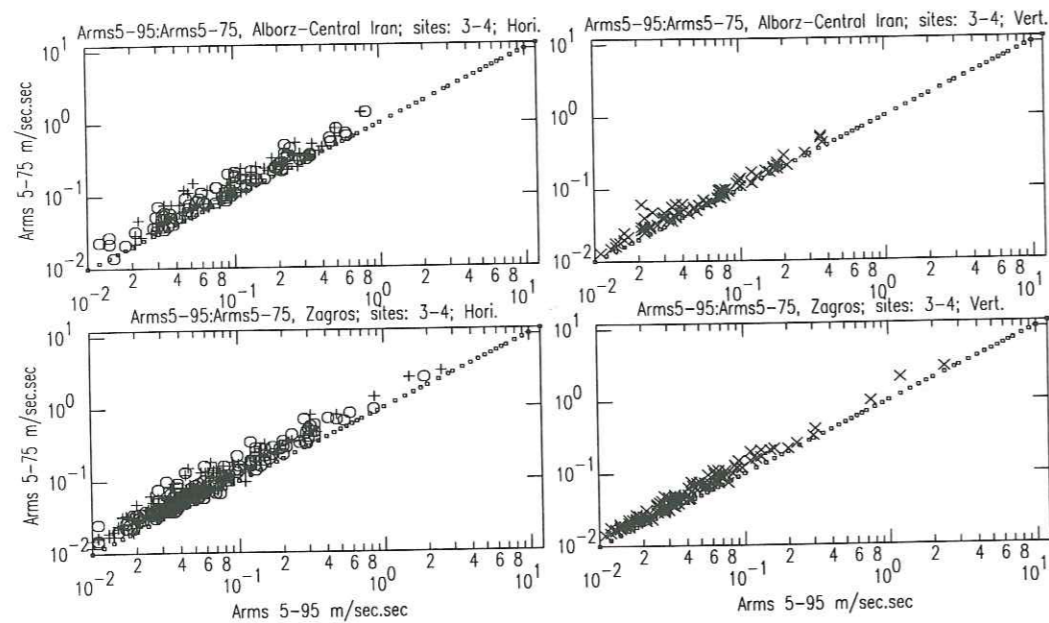


FIG. 5.5 - The  $a_{rms}$  values calculated for different intervals are plotted against each other; site classes 3 and 4, for two areas; two different symbol in the left side figures stand for two horizontal components (Alborz-Central-Iran top, Zagros bottom).

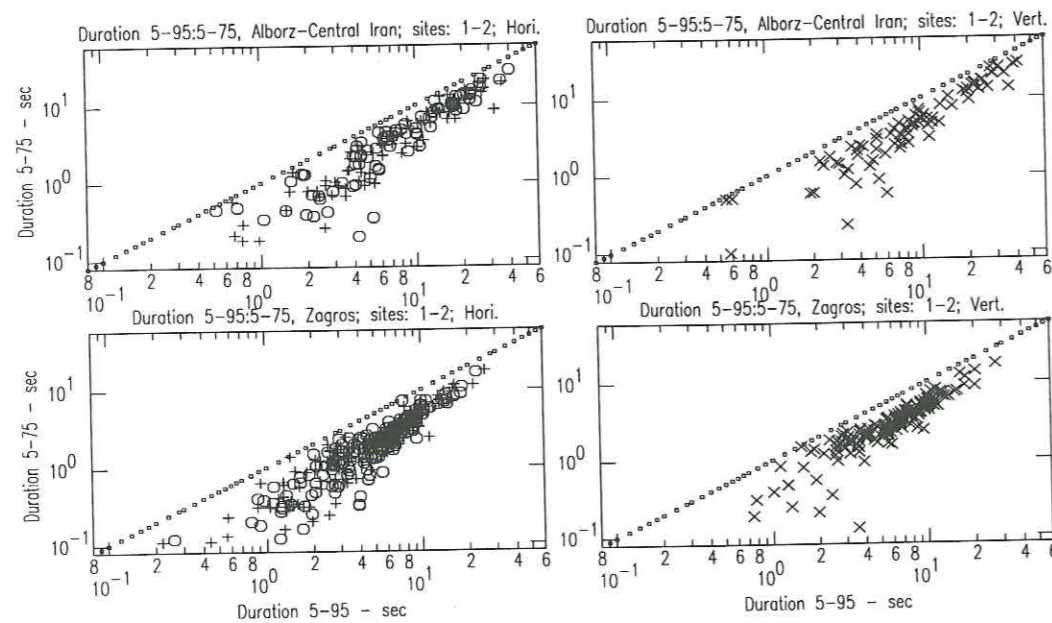


FIG. 5.6 - The strong motion duration values calculated for different intervals are plotted against each other; site classes 1 and 2, for two areas; two different symbol in the left side figures stand for two horizontal components (Alborz-Central-Iran top, Zagros bottom).

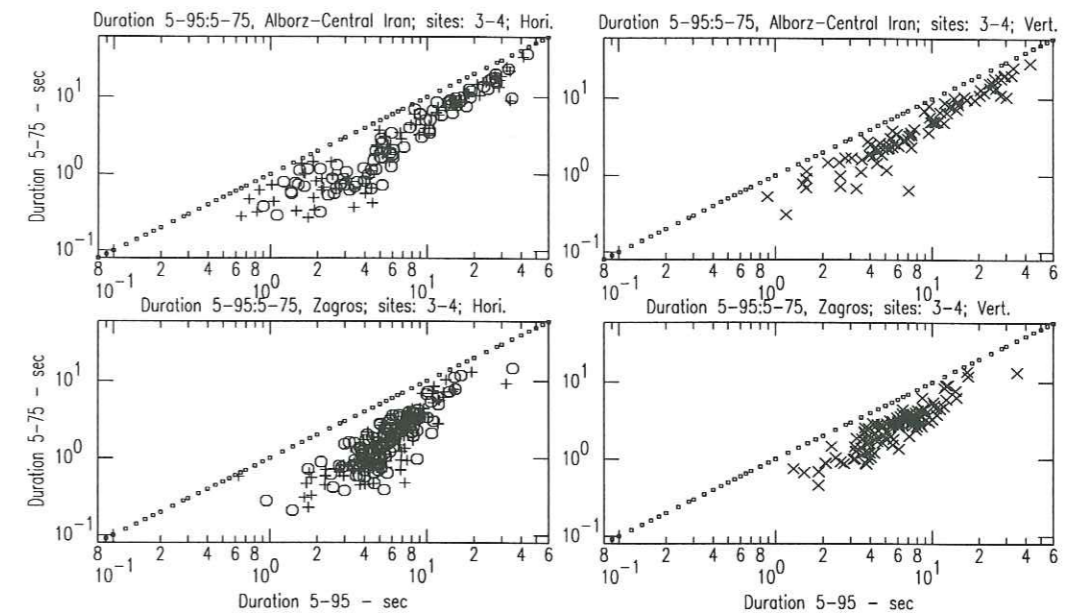


FIG. 5.7 - The strong motion duration values calculated for different intervals are plotted against each other; site classes 3 and 4, for two areas; two different symbol in the left side figures stand for two horizontal components (Alborz-Central-Iran top, Zagros bottom).

The linear relationship for the durations estimated for 5%-75% intervals ( $T_{01}$ : 5-75) and 5%-95% intervals ( $T_{02}$ : 5-95) may be shown in similar way;

$$T_{01} = b \cdot T_{02} + \sigma \cdot P \quad (5.6)$$

The results for such relationship using the entire of the Iranian data are given in table 5.2:

Table 5.2: Result of the regression for relationship (5.6)

Data/comp.	b	R(Coef.Corr.)	Sigma
Iranian data (Vert. comp)	0.578	0.984	1.460
Iranian data (Hori. comp)	0.541	0.927	1.558

In this study, as the differences in data (grouped in four sites classes) were not very clear for  $a_{rms}$  and duration estimations, the data are regrouped in two groups; group 1 which represent the original site classes of 1 and 2, and the group 2 replaced the site classes 3 and 4. The comparison of the duration for group 1 (classes 1-2) and group 2 (classes 3-4) is shown in Figures 5.4 and 5.5 for Zagros and Alborz-Central Iran region. The duration estimations for

site group 2 in Alborz-Central Iran are found in the range of 0.8 to 40 seconds, while in the Zagros region the durations are calculated in the range of 2 to 12 seconds (Figure 5.5). The relationship between the  $a_{rms}$  estimations with the two intervals, for the site groups 1 and 2, for Zagros and Alborz-Central Iran regions, are shown in Figures 5.6 and 5.7.

### 5.4.2 Empirical Relationships for the Strong Motion Duration in Iran

The duration is one of the most important strong motion parameters. Several researchers have declared that the duration and the energy content of the strong motions may reveal the seismic performance of the structures (Jeong and Iwan 1988, Uang and Bertero 1990). Recent developments in different countries provide the possibility to examine the different method to define such parameters using different catalogues (Koliopoulos et al 1998).

#### Attenuation of Duration

To investigate the dependence of duration with  $M_w$  and hypocentral distance, a linear model is first considered. A one-step method is applied, in which all the parameters are determined simultaneously by maximizing the likelihood of the set of observations. This approach, which is used by Joyner and Boore (1993) and Brillinger and Preisler (1984, 1985), led to results comparable with the two-step method (Boore et al 1994). The two-step method is used further in this article to find the attenuation of  $a_{rms}$  and ea.

All of the duration values are plotted against  $M_w$  and hypocentral distances in Figure 5.8. These data similarly shown in Figures 5.9 and 5.10 for the two different geographical zones (Zagros, Alborz-Central Iran) and the two site groups, against  $M_w$  and hypocentral distances, respectively. Such a relationship was already proposed by Trifunac and Brady (1975) as;

$$T_0 = a \cdot M_w + b \cdot X + \sigma \cdot P \quad (5.7)$$

where  $X$  is the hypocentral distance in kilometers. The results of the regression using relationship (5.7) are presented in Table 5.3. The residuals of the predicted  $T_0$  values by (5.7) are shown in Figures 5.11 and 5.12 against hypocentral distance and  $M_w$ , respectively.

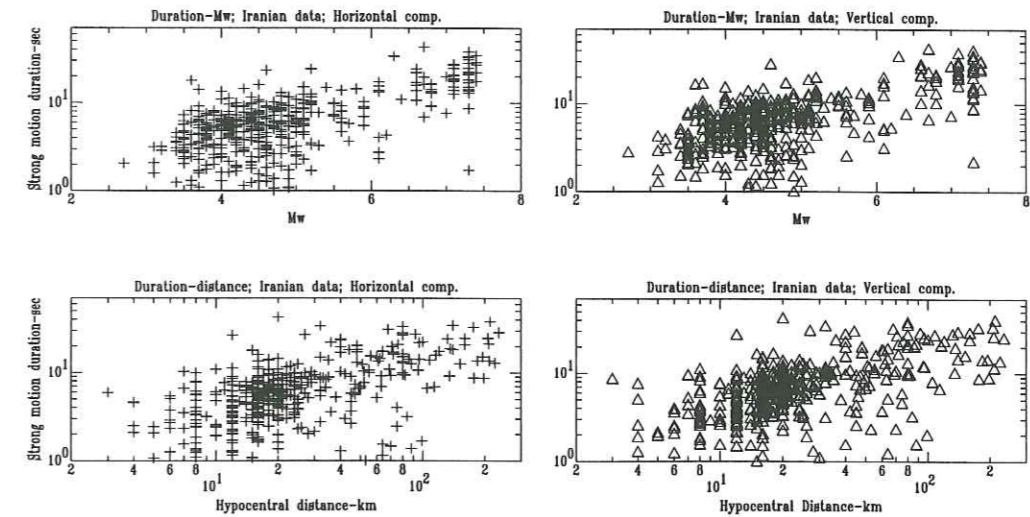


FIG. 5.8 – Distribution of duration values against  $M_w$  (top) and Hypocentral Distances (bottom) for entire data of Iran.

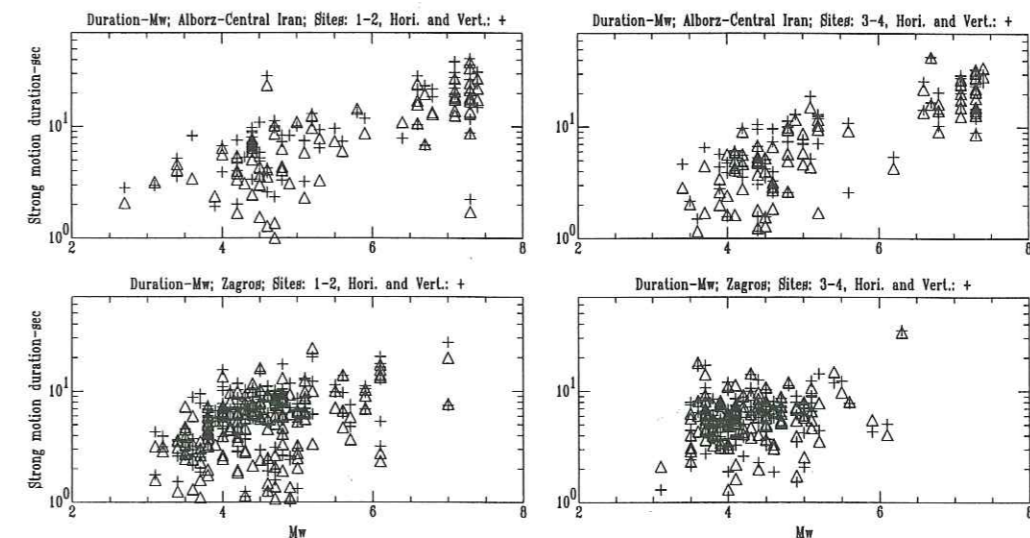


FIG. 5.9 – Distribution of duration values against  $M_w$  for two areas. (triangles for horizontal and crosses for vertical components), left; site group 1, right; site group 2, Alborz-Central Iran; bottom

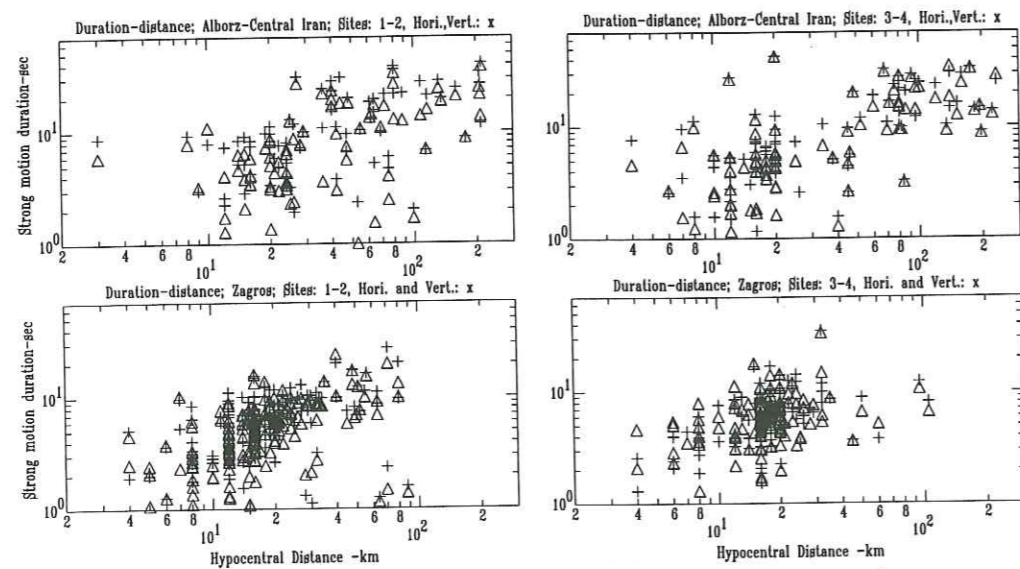


FIG. 5.10 – Distribution of duration values against hypocentral Distances for two areas. (triangles for horizontal and crosses for vertical components), left; site group 1, right; site group 2, Alborz-Central Iran; bottom

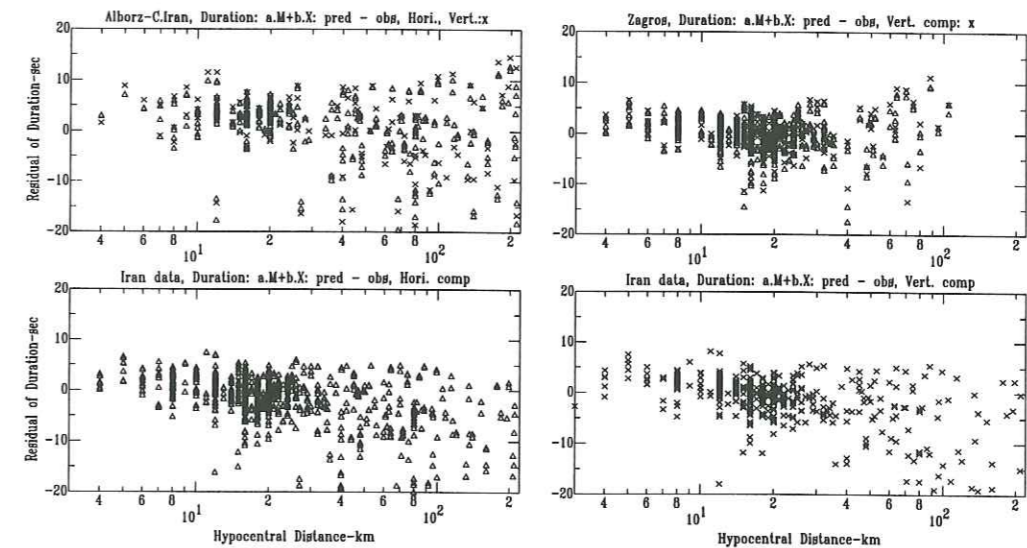


FIG. 5.11 – Residual of the predicted duration values (obtained by relationship 5.7), against hypocentral distances, in Alborz-Central Iran, Zagros and entire of the data base. Horizontal and vertical components are considered. (triangles for horizontal and crosses for vertical components)

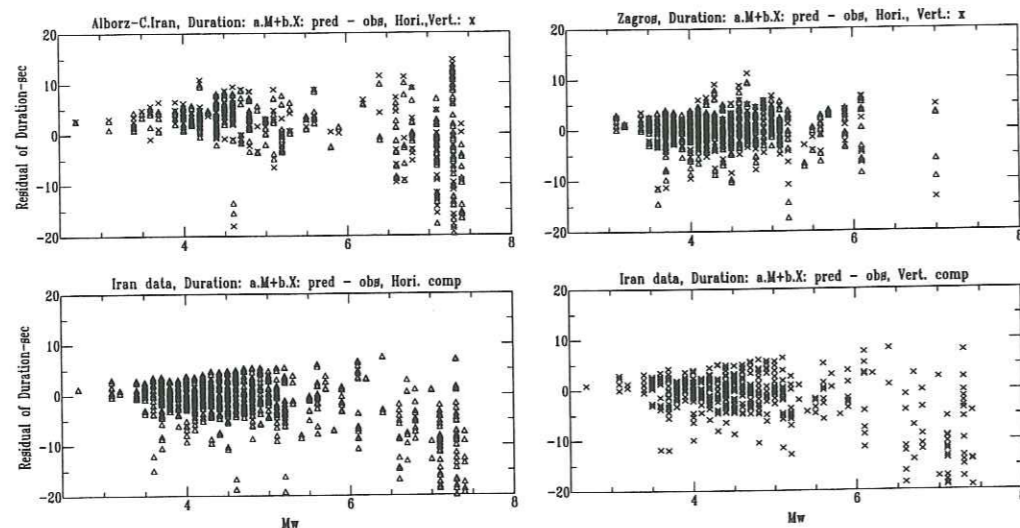


FIG. 5.12 – Residual of the predicted duration values (obtained by relationship 5.7), against  $M_w$ , in Alborz-Central Iran, Zagros and entire of the data base; the horizontal and vertical components are considered. (triangles for horizontal and crosses for vertical components)

Region/comp.	a	b	R(Coef. Corr.)	Sigma
Central Iran, Alborz (Vert.)	1.799	0.053	0.622	5.024
Central Iran, Alborz (Hori.)	1.477	0.052	0.651	6.760
Zagros (Vertical comp.)	1.140	0.084	0.484	3.453
Zagros (Horizontal comp.)	1.085	0.064	0.425	3.326
Iranian data (Vertical)	1.356	0.073	0.676	5.056
Iranian data (Horizontal)	1.181	0.065	0.653	4.730

A slightly different form of the distance-magnitude relationship was also tried, corresponding to formula 5.8, where the  $\log T_0$  and  $\log X$  are replacing the linear terms of 5.7:

$$\log T_0 = a \cdot M_w + b \cdot \log X + \sigma \cdot P \quad (5.8)$$

The coefficients using this equation are presented in table-5.4:

Table 5.4: Result of the regression for relationship (5.8)

Region/comp.	a	b	R(Coef. Corr.)	$10^{\text{Sigma}}$
Central Iran, Alborz (Vert.)	0.111	0.217	0.693	0.277
Central Iran, Alborz (Hori.)	0.097	0.202	0.615	0.338
Zagros (Vertical comp.)	0.046	0.445	0.488	0.219
Zagros (Horizontal comp.)	0.047	0.404	0.410	0.240
Iranian data (Vertical)	0.080	0.323	0.705	0.287
Iranian data (Horizontal)	0.071	0.304	0.637	0.287

The residuals of the  $\log T_0$  predicted values by 5.8 are presented in Figures 5.13 and 5.14, against distance and  $M_w$ , respectively. These results reveal that the Alborz-Central Iran data are more sensible to the variation of the magnitudes, where the Zagros data show more sensibility to the hypocentral distances.

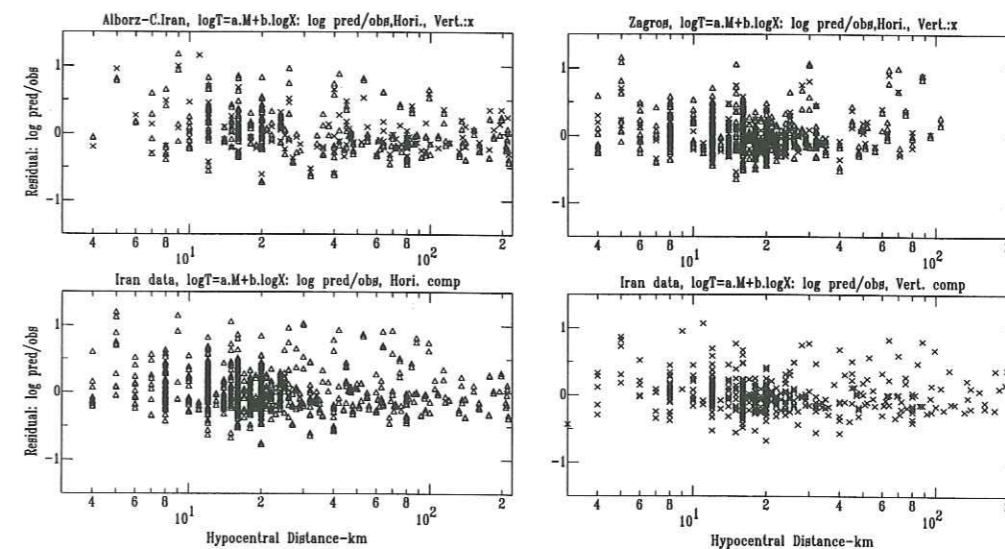


FIG. 5.13 – The residual of the predicted duration values (obtained by relationship 5.8), against hypocentral distances, in Alborz-Central Iran, Zagros and entire of the data base; the horizontal and vertical components are determined. triangles for horizontal and crosses for vertical components

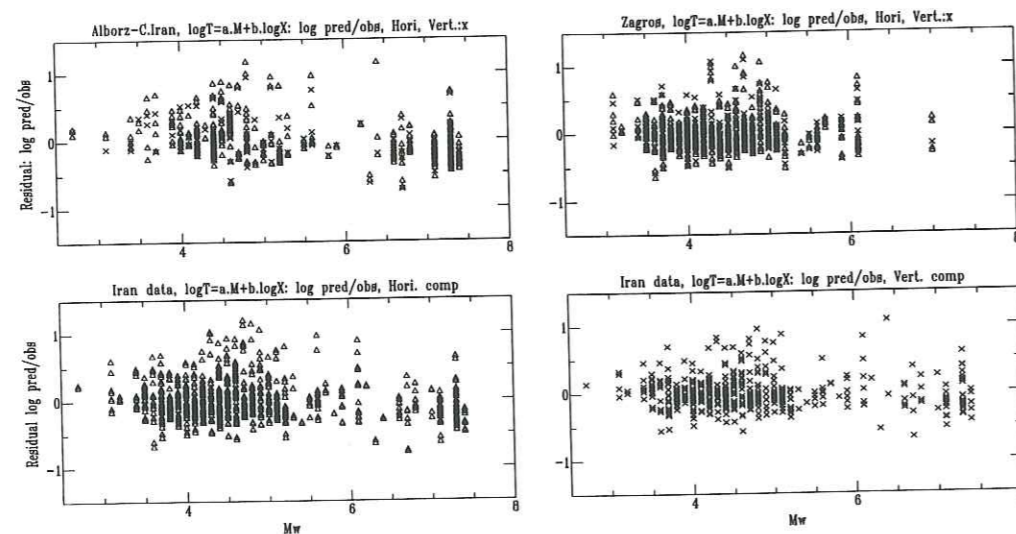


FIG. 5.14 – The residual of the predicted duration values (obtained by relationship 5.8), against  $M_w$ , in Alborz-Central Iran, Zagros and entire of the data base; the horizontal and vertical components are determined. (triangles for horizontal and crosses for vertical components)

As it can be seen in Figure 5.10, the distribution of the duration values against 'distances' are not similar in Zagros and Alborz-Central Iran areas; most of the data in the former area are found at short distances (0 to 50 km). This difference comes from the occurrence of the higher magnitude data in Alborz-Central Iran region. Most of the Alborz-Central Iran data are recorded using the analog, Kinematics SMA-1 instruments, in which the sensibility of the triggering is obviously lower than that of the digital SSA-2 recorders (the instruments that have recorded most of the Zagros data). Hence, it seems that the duration of the strong motions in Alborz-Central Iran area might be systematically under-estimated; because most of the Zagros records are triggered with weaker motions and maybe the instrument have started sooner and stopped later than that might be found with a analog instrument. Therefore, the same regression for relationship (5.8) has been repeated on Alborz-Central Iran data, using only data obtained within 50km, which are representative for the damaging earthquakes (Figure 5.15). The results are shown in Table 5.5;

Table 5.5: Result of the regression for relationship (5.8) for the first 50km (Hypo. Distance)

Region/comp.	a	b	R(Coef. Corr.)	Sigma
Central Iran, Alborz (Vert.)	0.103	0.216	0.505	0.300
Central Iran, Alborz (Hori.)	0.097	0.145	0.392	0.363
Zagros (Vertical comp.)	0.009	0.590	0.489	0.202
Zagros (Horizontal comp.)	0.013	0.536	0.416	0.227
Iranian data (Vertical)	0.010	0.512	0.682	0.234
Iranian data (Horizontal)	0.011	0.552	0.697	0.285

These results indicate slightly lower standard deviation for Zagros and entire of the data-base, while the coefficient of correlation decreasing for all regions, in comparison with the values in table 5.4 (for all distances). The residuals of  $\log T_0$  for the predictions in the first 50km are shown in Figures 5.16 and 5.17.



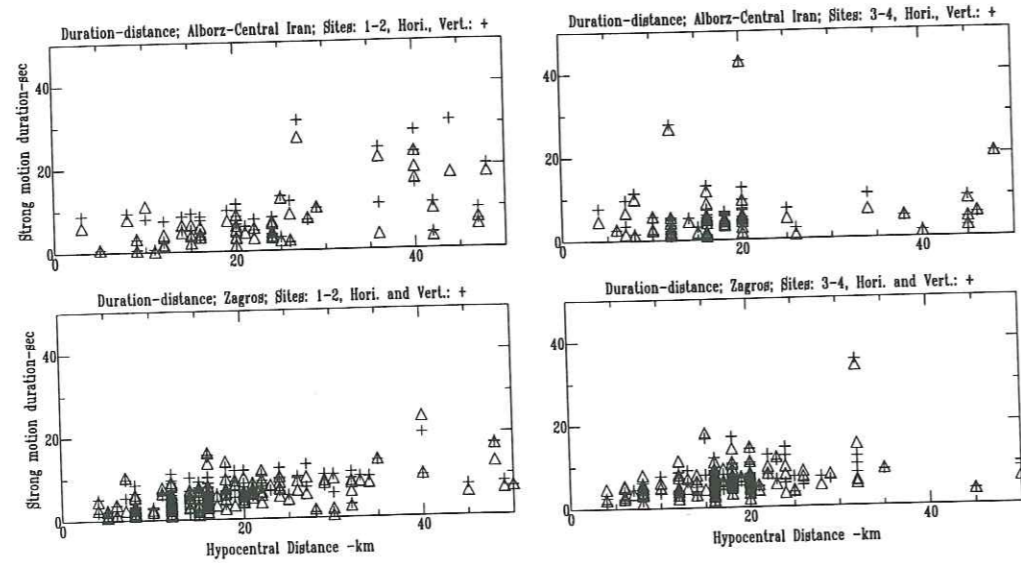


FIG. 5.15 – Distribution of duration values against the hypocentral distances (below 50km) for two areas in Iran. (triangles for horizontal and crosses for vertical components)

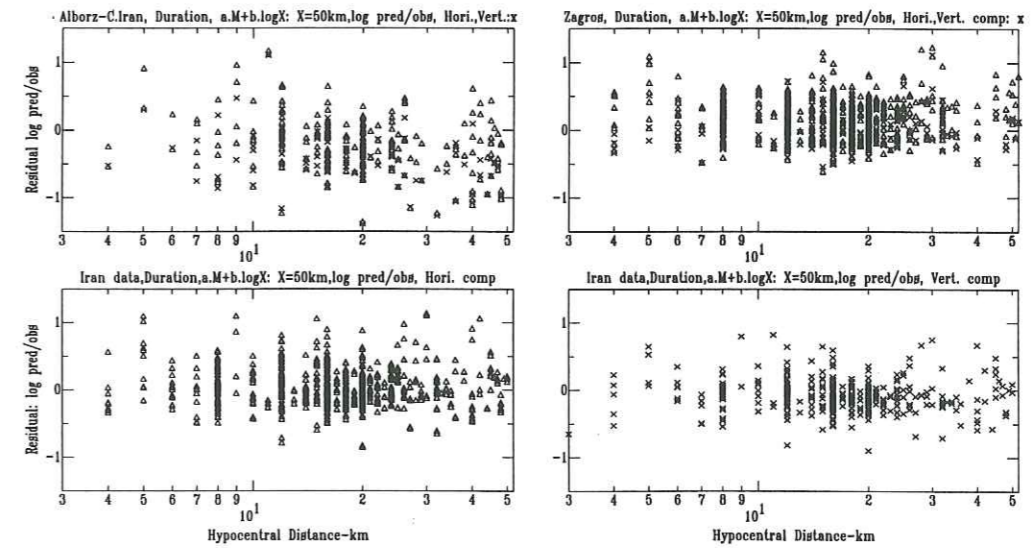


FIG. 5.16 – Residual of the predicted duration values (obtained by relationship (5.8) for first 50km distances), against hypocentral distances, in Alborz-Central Iran, Zagros and entire of the data base; the horizontal and vertical components are considered. (triangles for horizontal and crosses for vertical components)

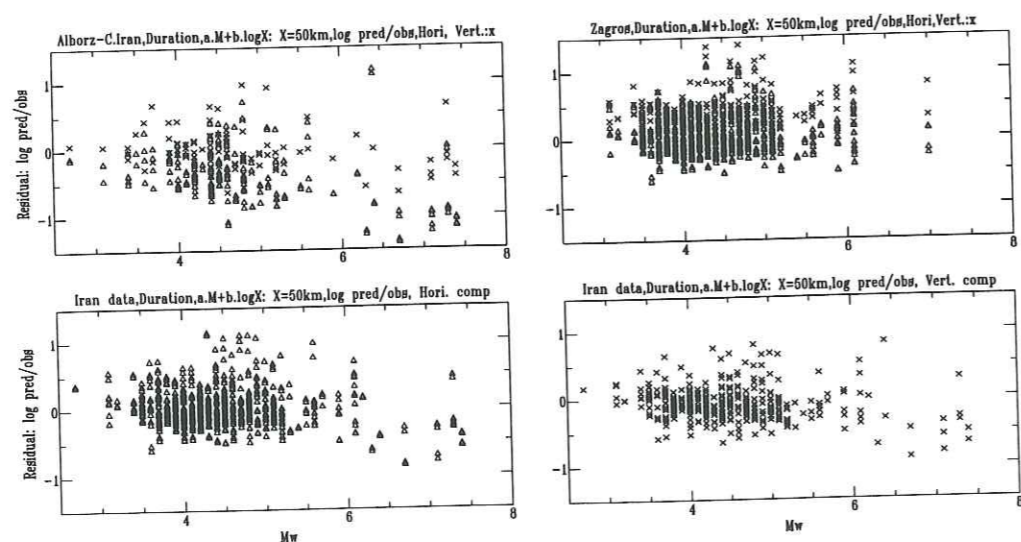


FIG. 5.17 – The residual of the predicted duration values (obtained by relationship (5.8) for first 50km distances), against  $M_w$ , in Alborz-Central Iran, Zagros and entire of the data base; the horizontal and vertical components are determined. (triangles for horizontal and crosses for vertical components)

Duration - energy relationship

The relationship between the duration (measured with the 95% interval) are plotted against the ratio of  $\frac{E_a}{a_{max}^2}$  in Figures 5.18 to 5.20. The data for all sites are separated for Zagros and Alborz-Central Iran in Figure 5.18.

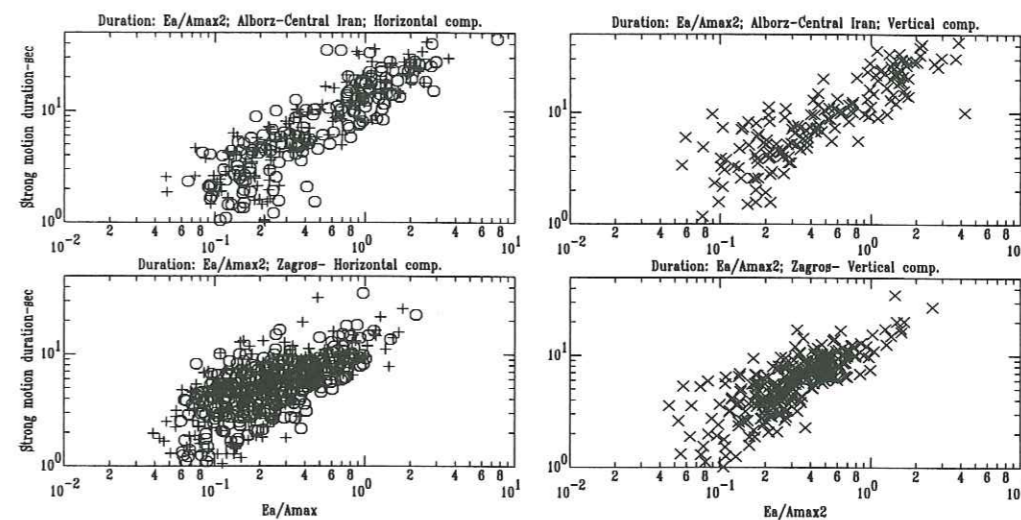


FIG. 5.18 – Strong motion duration, against  $\frac{E_a}{a_{max}^2}$  for two areas in Iran. (two horizontal components; left, and the vertical component; right, Alborz-Central Iran; top, Zagros; bottom, are distinguished)

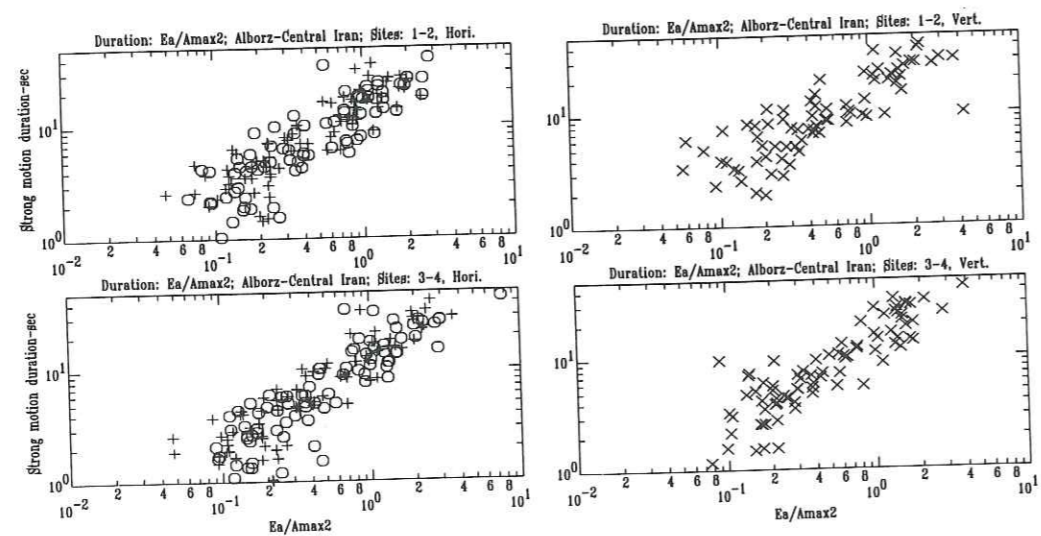


FIG. 5.19 – Strong motion duration, against  $\frac{e_a}{a_{max}^2}$  for two site groups, in Central Iran, Alborz area. (two horizontal components; left, and the vertical component; right, site group 1; top, site group 2; bottom, are distinguished)

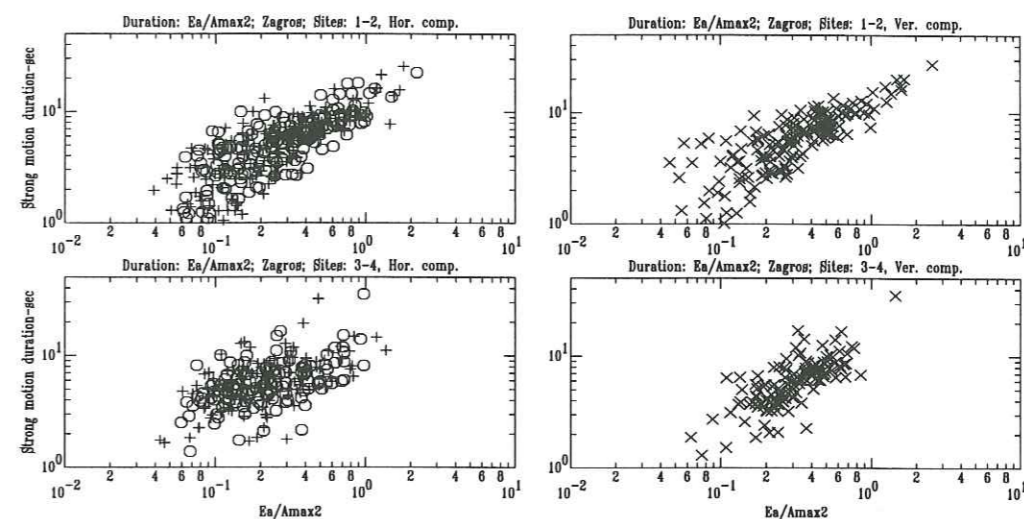


FIG. 5.20 – Strong motion duration, against  $\frac{e_a}{a_{max}^2}$  for two site groups, in Zagros area. (two horizontal components; left, and the vertical component; right, are distinguished)

To establish empirical relationships for the duration, the dependence of the duration is first studied as a function of  $\frac{e_a}{a_{max}^2}$ , as well as the  $M_w$  and hypocentral distances. In all of established relationships, it is tried to find the formula with the best fit to the data. It must be mentioned that since no systematic important difference in view point of the site effect was found on the other parameters discussed here, the site factor is eliminated from our duration relationships.

In the following empirical relationships, the interval of 5%-95% is used to establish the empirical relationships.

The relationship 5.3 may be written as;

$$T_0 = A \cdot \left(\frac{e_a}{a_{max}^2}\right)^b$$

and taking the logarithm of the two sides of this relationship, we have;

$$\log T_0 = a + b \cdot \log \left(\frac{e_a}{a_{max}^2}\right) + \sigma \cdot P \quad (5.9)$$

$\sigma$  is the standard deviation.

Using a one-step method, the regression is done in order to find the parameters a and b for the average of the horizontal components and the vertical component and for Zagros, Alborz-

Central Iran and entire of the data-base. For all of the regressions the correlation coefficient and the standard deviation are presented as well. The results for relationship 5.9, are shown in Table 5.6:

Table 5.6: Result of the regression for relationship 5.9

Region/comp.	a	b	R(Coef. Corr.)	Sigma
Central Iran, Alborz (Vert.)	1.165	0.746	0.827	0.204
Central Iran, Alborz (Hori.)	1.135	0.873	0.858	0.194
Zagros (Vertical comp.)	1.108	0.689	0.811	0.157
Zagros (Horizontal comp.)	1.078	0.603	0.703	0.186
Iranian data (Vertical)	1.140	0.730	0.843	0.176
Iranian data (Horizontal)	1.120	0.713	0.841	0.199

### 5.4.3 Attenuation of $a_{rms}$ and $e_a$

The empirical attenuation relationships for  $a_{rms}$  and the energy of acceleration ( $e_a$ ) are similarly obtained, applying a two-step regression, using the magnitude, distance and the site factors as the dependent variables. The method to establish such relationships for Iran was followed essentially after Joyner and Boore (1981) and Fukushma and Tanaka (1990). This method is used to fit a model to multiple independent variables (magnitude, distance, site,...). Hence, using this method, it is possible to do the regression for the dependence to magnitude and the dependence to distance, as well as the dependence to other terms, separately. In this method the parameters controlling distance and site effects dependence and a set of the amplitude factors, one for each event, must be determined in the first step, by maximizing the likelihood of the set of the observation. The determination of the parameters controlling the magnitude dependence is then performed in a second step, by maximizing the likelihood of the set of the amplitude factors (Joyner and Boore 1993). The applied formula is:

$$\log A = a \cdot M_w + b \cdot X - d \cdot \log X + c_i \cdot S_i + \sigma \cdot P \quad (5.10)$$

where A is the strong motion parameter, a is the coefficient for moment magnitude;  $M_w$ , b is a coefficient related to anelastic attenuation,  $c_i$  is a constant which related to 4 site classes (Zaré et al 1999a),  $S_i$ . The  $d$  coefficient for the  $\log X$  term correspond to the geometrical expansion. This coefficient is fixed to 1 and 0.5 corresponding to pure body and surface waves, respectively.

The coefficients of the regression using the relationship 5.10 are presented in tables 5.7 and 5.8 for  $a_{rms}$  and  $e_a$ , respectively.

Table 5.7: The regression coefficients for  $a_{rms}$ , applying equation (5.10), with  $d=1$ .

Region/comp.	a	b	c1	c2	c3	c4	Sigma
Central Iran, Alborz (Vert.)	0.367	0.0008	-1.836	-1.821	-1.819	-1.785	0.328
Central Iran, Alborz (Hori.)	0.383	0.0010	-1.713	-1.610	-1.677	-1.727	0.350
Zagros (Vertical comp.)	0.438	-0.0036	-2.077	-2.116	-2.022	-1.997	0.352
Zagros (Horizontal comp.)	0.458	-0.0015	-1.992	-1.962	-1.971	-2.034	0.341
Iranian data (Vertical)	0.324	0.0010	-1.553	-1.420	-1.642	-1.514	0.350
Iranian data (Horizontal)	0.317	0.0011	-1.350	-1.081	-1.333	-1.244	0.401

Table 5.8: Regression coefficients for  $e_a$ , applying equation (5.10), with  $d=1$

Region/comp.	a	b	c1	c2	c3	c4	Sigma
Central Iran, Alborz (Vert.)	0.848	-0.0040	-4.509	-4.501	-4.480	-4.359	0.572
Central Iran, Alborz (Hori.)	0.881	-0.0037	-4.353	-4.176	-4.236	-3.286	0.582
Zagros (Vertical comp.)	0.953	-0.0159	-4.777	-4.808	-4.643	-4.556	0.617
Zagros (Horizontal comp.)	0.982	-0.0113	-4.655	-4.543	-4.488	-4.635	0.586
Iranian data (Vertical)	0.802	-0.0036	-4.134	-4.093	-4.370	-4.069	0.591
Iranian data (Horizontal)	0.815	-0.0035	-3.963	-3.678	-3.986	-3.725	0.628

As it is evident from the  $c1$  to  $c4$  coefficients in tables 5.7 and 5.8, the site effects were not very important in these regressions. The attenuation of the estimated values using (5.10) with the coefficients of tables 5.7, estimated for magnitudes of 5, 6 and 7 events on the rock sites are shown in Figures 5.21 to 5.23, for Alborz-Central Iran, Zagros and entire of the data-base, respectively. The results show that taking  $d=1$  (body waves attenuation) induce greater estimations for the near-source distances (less than 20km). Using  $d=0.5$  (surface waves attenuation), larger values are obtained at distances more than 60km, for the Alborz-Central Iran and entire of the data-base; Figures 5.21 and 5.23). According to the lesser data for the greater distances and a conservative approach for the near field distance, it is suggested to use the coefficients with  $d=1$  for  $e_a$  and  $a_{rms}$ . However special studies are recomanded for the near-field of the large magnitude events, using a deterministic approach on the records obtained in similar conditions.

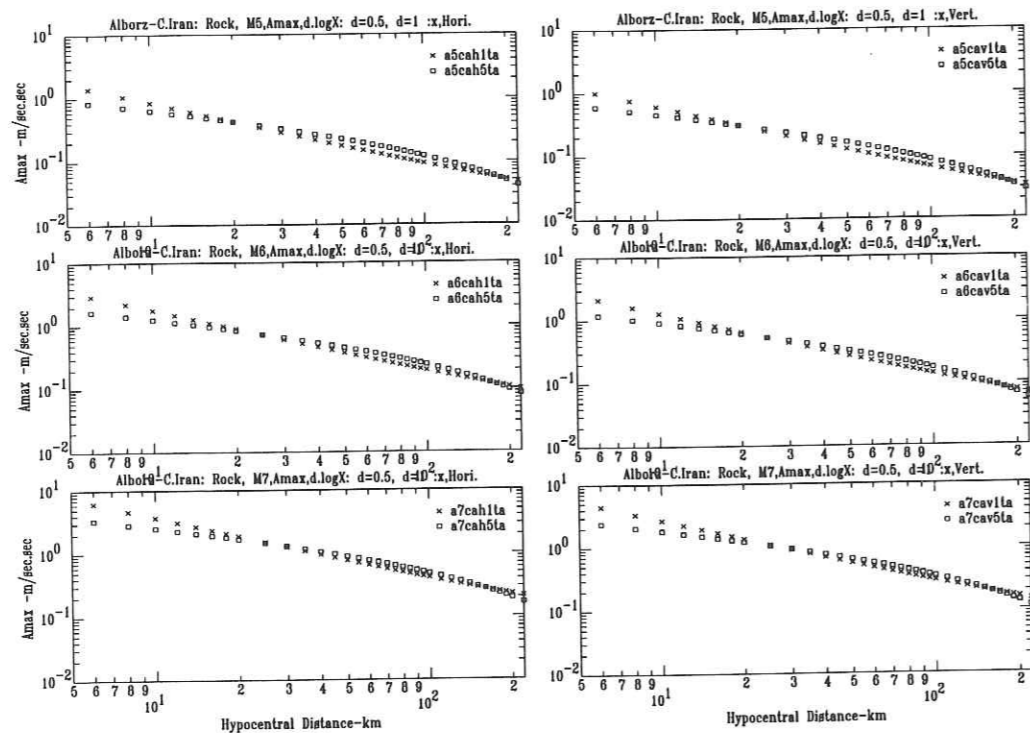


FIG. 5.21 - Attenuation of  $a_{rms}$  with distance for magnitudes 5, 6 and 7, using Alborz-Central Iran data. The results are presented for different  $d$  values (quadrangles for  $d=0.5$ , and crosses for  $d=1.0$ ); horizontal component, left; vertical component, right

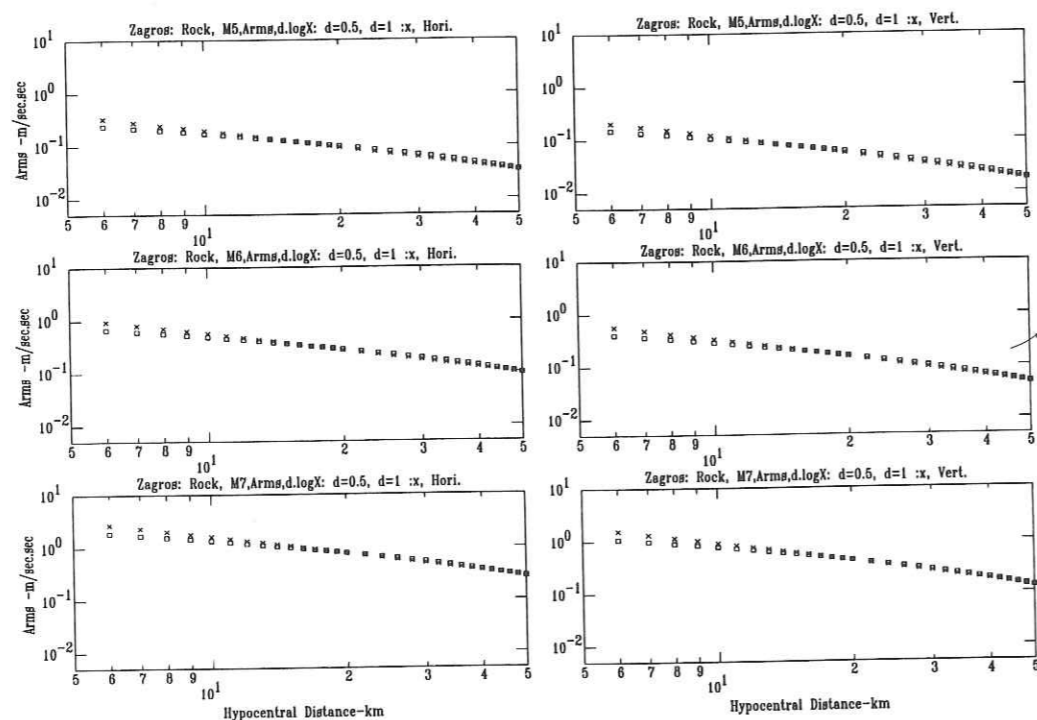


FIG. 5.22 - Attenuation of  $a_{rms}$  with distance for magnitudes 5, 6 and 7, using Zagros data. The results are presented for different  $d$  values. (quadrangles for  $d=0.5$ , and crosses for  $d=1.0$ ); horizontal component, left; vertical component, right

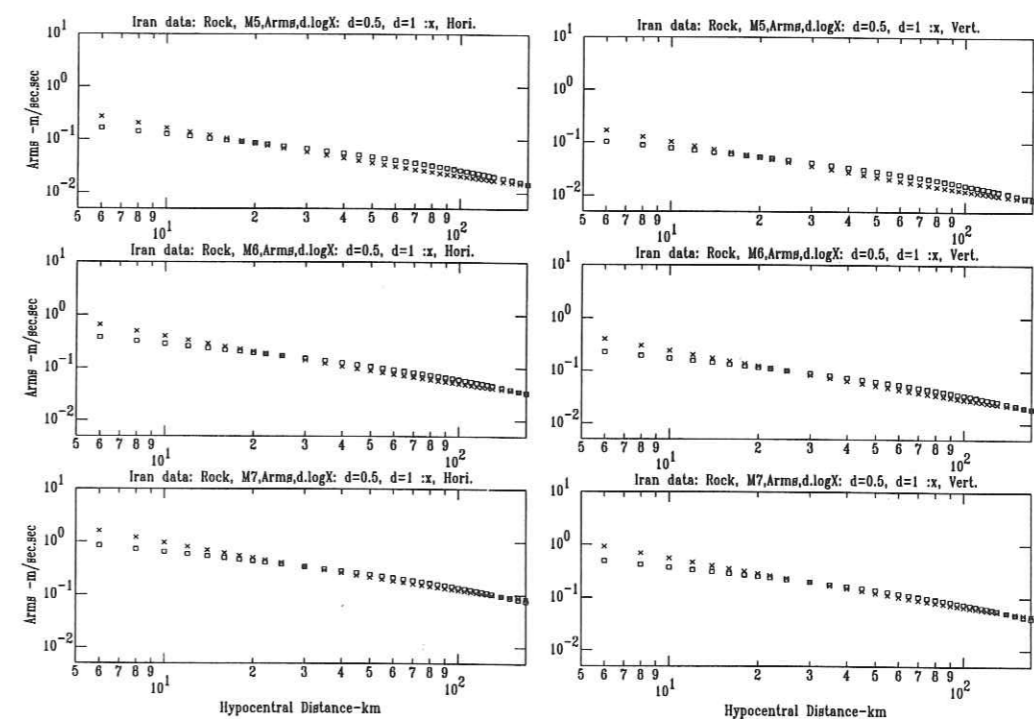


FIG. 5.23 - Attenuation of  $a_{rms}$  with distance for magnitudes 5, 6 and 7, using Iranian data-base. The results are presented for different  $d$  values (quadrangles for  $d=0.5$ , and crosses for  $d=1.0$ ); horizontal component, left; vertical component, right

## 5.5 Conclusions

This article presented investigations on the energy content and the duration values on the Iranian strong motion data. The duration has been calculated using the cumulative integral of the acceleration values. All results are detailed in Appendix 5.1. The conclusions and the propositions for the further studies may be summarized as follows;

- The content of energy of the strong motions is different in Zagros area and the rest of the country). This difference comes partially from the difference in the seismicity rates in Zagros belt, or other reasons (comparing Figures 5.19 and 5.20).

- The Alborz-Central Iran region which represent the seismicity with greater earthquakes recorded in larger distances, shows higher duration.

- According to the distribution of the data which are sub-grouped to Zagros and Alborz-Central Iran groups, and since two probable trends may be assumed in Zagros data, more sophisticated studies may be carried out using higher quality data. Such studies may be followed using the local accelerograph networks to be installed in the high seismic zones (for instance the zones such as Firouzabad, Fin in north Bandarabbas, Lar in southern Fars province or Borazjan in the Bushehr province; Figure 5.1).

- No important influence of site conditions would be detected on duration values. It might come from 95% interval choice.

- The attenuation of  $a_{rms}$  and  $e_a$  show some differences in the estimations in the near and far source distances. The limits for the application of such relationship must be considered in the future: the attenuation coefficients for the Zagros area give proper results in the distances less than 50km, and for the Alborz-Central Iran region in the distances less than 200km. The entire of the data-base might be used in distances up to 170km. The magnitude limits are the  $M_w 3.0$  to  $M_w 7.4$  for Alborz-Central Iran and  $M_w 3.0$  to  $M_w 7.0$  for Zagros region.

### Acknowledgement

The BHRC (Building and Housing Research Center, Tehran) which have released the raw strong motion records, is greatly thanked. A financial support in France (for the first author) was provided by a French scholarship (Ministère Français des Affaires Etrangères) is duly acknowledged. The financial support in Iran was provided by IIEES (International Institute of Earthquake Engineering and Seismology), which is thanked.

Appendix 5.1: The database of the duration/energy content study, developed for the Iranian strong motion and applied in this paper.







Table with 21 columns: No, Record, Station, Site, Date, Mw, R, Dur (H1), Dur (V), Dur (H2), Arms (H1), Arms (V), Arms (H2), Arms (H2), Arms (H1), Arms (V), Arms (H2), Ea (H1), Ea (V), Ea (H2). Rows include records 362-449 from stations like Bandar-Deylam, Lendeh, Rudbar, Astaneh, Shabankareh, Ghir, Ghalieh-Ganj, Lali, Darreh-Shahr, Namin, Khorramabad, etc.

Table with 21 columns: No, Record, Station, Site, Date, Mw, R, Dur (H1), Dur (V), Dur (H2), Arms (H1), Arms (V), Arms (H2), Arms (H2), Arms (H1), Arms (V), Arms (H2), Ea (H1), Ea (V), Ea (H2). Rows include records 450-468 from stations like Shabankareh, Saadabad, Shabankareh, Saadabad, Shabankareh, Shabankareh, Shabankareh, Shabankareh, Shabankareh, Shabankareh, Shabankareh, Shabankareh, Saadabad, Saadabad, Firouzabad, Shabankareh, Shabankareh, Ardebil.

## Chapitre 6

# L'Atténuation des Mouvements Forts en Iran

**Résumé** Les données des mouvements forts en Iran sont utilisées pour établir les lois d'atténuation empiriques pour différents paramètres de mouvements forts:  $A_{max}$ ,  $V_{max}$ ,  $D_{max}$  et les ordonnées spectrales des spectres de réponses. Les variables explicatives sont la magnitude, la distance hypocentrale et les conditions de site. Deux approches ont été essayées pour les régression (une et deux étapes), et les résultats sont très proches l'un de l'autre: les résultats de la première approche (deux étapes) sont présentés d'abord, ensuite viennent ceux de la deuxième approche (une étape). Les résultats de la régression faite en une seule étape sous-estiment les mouvements forts à faible distance ( $< 20km$ ), mais les surestiment pour des distances supérieures à 100km par rapport aux résultats de la régression en deux étapes.

La base de données se compose de 468 accélérogrammes, en 3 composantes, enregistrés au cours des 24 dernières années en Iran. Basé sur ces données, on divise le pays en deux régions géographiques: pour la période d'observation (1975-1997), les plus forts séismes ont eu lieu dans les régions de l'Iran central et dans l'Alborz ( $M > 7$ ), et ont été enregistrés jusqu'à 220km de distance, alors que les séismes du Zagros ont été plus modérés (M4-6), et enregistrés seulement jusqu'à environ 60 km. Cette différence, et une différence possible entre l'atténuation dans ces deux grandes régions, impose des coefficients différents pour les relations d'atténuation. Les effets de site observés à partir de ces régressions ne sont pas très importants, mais malgré tout sont en accord avec la classification de site préalablement choisie. Les effets non-linéaires ont aussi été recherchés dans ces études mais les résultats semblent montrer des phénomènes contraires avec les amplifications d'autant plus grandes que le mouvement est forts; aucune explication exacte n'a pu être trouvée pour cette observation, mais peut-être ces résultats sont la réponse de sites d'alluvions assez raides dans le champ-proche des séismes, quant les niveaux des nappes phréatiques sont très bas. Dans notre proposition pour la poursuite des installations de stations accélérométriques en Iran, nous insistons sur l'importance du problème du champ-proche en Iran. Les réseaux locaux dans les régions à sismicité très importante peuvent aussi fournir les données plus précises pour la suite des études sur la loi d'atténuation en Iran.

## Strong Motion Attenuation in Iran

Mehdi Zaré, Pierre-Yves Bard and Mohsen Ghafory-Ashtiany

Article en préparation pour soumettre au "Bulletin of the Seismological Society of America"

**Abstract** The Iranian strong ground motions data are used to derive the empirical attenuation laws for different strong motion parameters: peak acceleration, peak velocity, peak

displacement, response spectral ordinates. The empirical relationships are established for the strong motion parameters as a function of moment magnitude, hypocentral distance, and a constant parameter representing the site conditions. The one and two step approaches for the regressions are applied, and the results are found to be near to each other, while only the results for the two step approach are presented in this paper. The data set consists of 468 three component accelerograms, all recorded during the last 24 years in Iran. It is split in two subsets corresponding to two geographical areas: during the period of observation (1975-1997), stronger earthquakes occurred in central Iran and Alborz region and were recorded at distances as far as 220km, whereas the Zagros belt experienced only moderate events (M4-6) recorded at distances up to about 60km. This difference, and a probable difference in attenuation between these two main regions, cause different coefficients for the attenuation relationships. The soil effects are considered in the regressions: the resulting site dependence is not very large, but does agree with our previous site classification for Iran.

## 6.1 Introduction

The Iranian strong motion records are obtained by a national network operated by BHRC (Building and Housing Research Center) and installed in different cities and villages throughout the country (Figure 6.1). As it is outlined in a previous paper (Bard et al 1998), this network first consisted of Kinematics SMA-1 analog instruments (1975-1989), which were complemented by numerous SSA-2 digital instruments after the Manjil earthquake of 1990. By the end of 1997, the number of instruments was reported to be 1000 stations, while the location of 386 SSA-2 and 79 SMA-1 stations are reported and plotted in Figure- 1. The stations are mainly installed within cities or villages for easy maintenance. A preliminary listing of the recorded data as of 1993 was published by BHRC. A complete catalog is available in Bard et al 1998).

The attenuation relationships in Iran have never been established using the whole Iranian data set. The purpose of this paper was therefore to fill that gap. The mentioned cleaned catalog is used, that keeps only the data for which the magnitude and epicentral distance are known, and for which the signal to noise ratio is satisfactory. The data set consists of 468 three component records. The source parameters were derived from the teleseismic studies for 279 records (Bard et al 1998) and directly from the strong motion records for the remaining 189 records, using a source model (Zaré et al 1999b). The site conditions were devoted special attention and measurements, which led to a new categorization in four different site classes, on the basis of H/V ratio for strong motion records. Details may be found in Zaré et al 1999a.

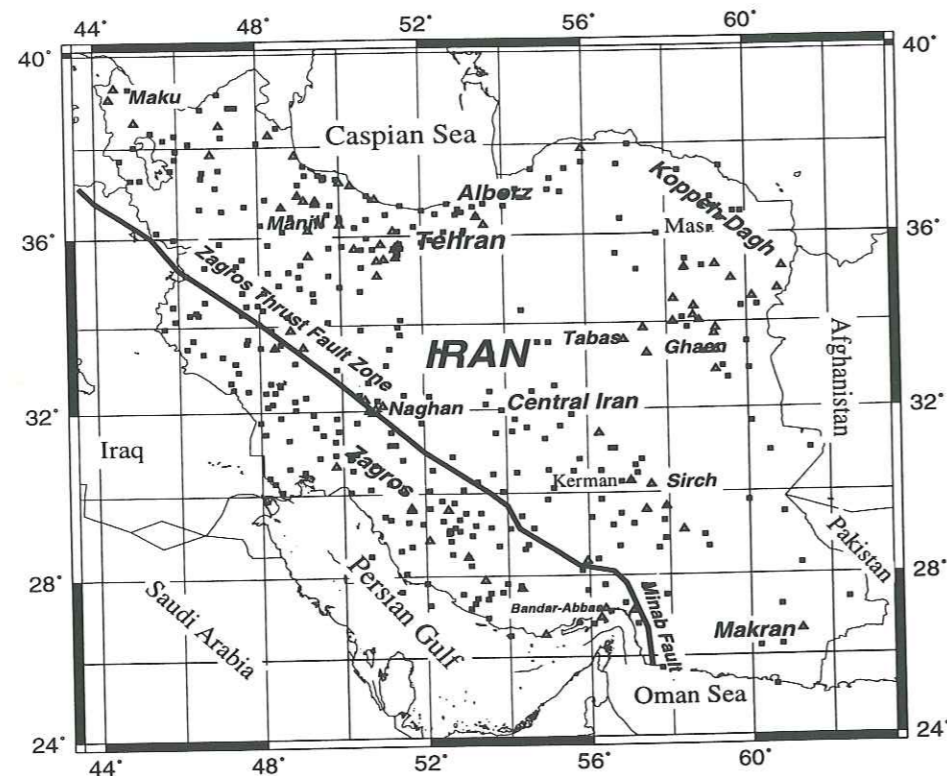


FIG. 6.1 – The strong motion network of Iran (stations installed by the end of 1996) the location of the new instruments are not still reported. The SSA-2 instruments are shown with triangles and the SMA-1 station are marked with quadrangles (special thanks to H. Mirzaei-Alavijeh of BHRC for the location of the new SSA-2 instruments). Iranian seismogenic zones and the Zagros thrust fault zone-Minab fault, which represent the frontier between the Alborz-Central Iran area and the Zagros area, are shown on the map.

The scope of this study is to investigate attenuation laws for the strong motions in Iran, in form of different parameters. An attempt was also performed to look for some difference in the attenuation in different regions. Another scope was to provide the design spectra for sample sites in Alborz (Tehran, on a rock site) and in Zagros (a sample site on the Persian Gulf).

In this article the methodology of the study is explained first, followed by the criteria to establish the data-base. The results of the study are then presented for the various parameters. The coefficients of the regression are presented not only for the spectral values but also for the parameters such as peak ground acceleration (PGA), peak ground velocity (PGV) and peak ground displacement (PGD). All coefficients are presented for horizontal and vertical components and separated for the Zagros and non-Zagros region (Alborz-Central Iran), and finally for the entire of the Iranian data.

## 6.2 Methodology

The establishment of the attenuation relationships for a given region may provide information to be used in other regions with similar characteristics. Meanwhile, it has been repeatedly claimed in recent years that a attenuation relationship, as an empirical model fitted to the data from a specific area, may not be easily used in other regions with different tectonic and crustal specifications (Abrahamson and Silva 1997, Abrahamson and Shedlock 1997).

### 6.2.1 The applied approaches

To establish the attenuation relationships for Iran, the approach presented by Joyner and Boore (1981) and Fukushima and Tanaka (1990) was followed. A two-step regression is used to fit a model to multiple independent variables (magnitude, distance, site,...). In this method the parameters controlling distance and site effects dependence and a set of amplitude factors, one for each event, must be determined in the first step, by maximizing the likelihood of the set of observation. The determination of the parameters controlling the magnitude dependence is then performed in a second step, by maximizing the likelihood of the set of amplitude factors (Joyner and Boore 1993).

Another possible approach is the one-step method, in which all the parameters are obtained simultaneously by maximizing the likelihood of the set of observations. This approach, which is used by Joyner and Boore (1993) and Brillinger and Preisler (1984, 1985), yields similar results to the two-step method for the spectral ordinates using the north-western American data (Boore et al 1994).

### 6.2.2 Fundamental form

The genuine form of the dependence is:

$$\log A = a \cdot M_w + b \cdot X - d \cdot \log X + c_i \cdot S_i + \sigma \cdot P \quad (6.1)$$

where  $A$  is the strong motion parameter,  $a$  is the coefficient for magnitude  $M$ ;  $b$  is the coefficient related to the anelastic attenuation with distance  $X$ ;  $c_i$  is a constant depending on the sites class  $S$ ;  $\sigma_i$  is the sigma value of 84 percent ( $P = 1$ ), to be added to the mean (50 percent values;  $P = 0$ ). The  $d$  coefficient for the  $\log X$  term is introduced to allow a geometrical

expansion which may be different from the body wave dependence. In this study the moment magnitude  $M_w$  is used for  $M$  and hypocentral distance is used for  $X$  (except for two cases which will be explained later). The site conditions are divided in 4 categories according to Zaré et al 1999a. In many of the computations presented below,  $d$  is set equal to 1, so that this regression formula is similar to:

$$y = \frac{k}{X} \cdot e^{-qX}$$

where  $k$  is a function of  $M$ , and  $q$  is a constant. This form represents a simple point-source geometric expansion with constant ( $Q$ ) anelastic attenuation. We have examined the  $X^{-d}$  form, as shown in equation 6.1, such that:

$$y = \frac{k}{X^d} \cdot e^{-qX} \quad (6.2)$$

Joyner and Boore (1981) have shown that such form should apply only to a harmonic component of the ground motion, and not to the peak values, however its application to the peak values (determining empirically) would be a proper approximation.

Ambraseys (1995) proposed attenuation relationships for Europe using the same model. He eliminated the anelastic attenuation coefficient term  $b \cdot X$ , for the vertical component estimations claiming that for the vertical records (of European data) of magnitudes  $M_s$  4.0-7.9 and the focal depths less than 30km, a two-step regression was found to be inadequate in size to determine both the anelastic and geometric distance terms (Ambraseys 1995, Ambraseys and Simpson 1996). The distance term used by Ambraseys in the mentioned papers and by Joyner and Boore (1981), Boore et al (1997) is:

$$X = (R^2 + h^2)^{0.5}$$

where  $R$  is the distance to the surface projection of ruptured area, and  $h$  is the focal depth. Fukushima and Tanaka (1990) and Fukushima et al (1988) have defined the term of

$$X = (R + j \cdot 10^{e \cdot M})$$

where  $R$  is the rupture distance,  $j$  and  $e$  are the coefficients to be filtered, and  $M$  is the surface wave magnitude. This expression should reduce to  $X = R$  for large distances. Hardly

and Helmberger (1980) have shown that near the faults, little geometrical attenuation exists. Therefore they suggested a functional form of the effective attenuation versus distance, for the strike-slip earthquakes. For this function, we have:

$$X = [R + C(M)]^{-t}$$

in which  $X$  is the modified epicentral distance for the near source earthquakes,  $R$  is the epicentral distance,  $C(M)$  is a function of magnitude and  $t$  is a coefficient. This function is used by Campbell (1981) to present the attenuation relationship for the near-field strong motions:

$$PGA = a \cdot \exp b \cdot M [R + C(M)]^{-j}$$

The near-field attenuation is a function of the fault dimensions, therefore Esteva (1970) has shown that the parameter relating the fault rupture dimensions scales exponentially with magnitude;  $C(M) = c_1 \exp(c_2 \cdot M)$ .

### 6.2.3 Ground Motion Parameters

The regressions were performed for various ground motion parameters;  $PGA$ ,  $PGV$  and  $PGD$ , and for the spectral accelerations ( $S_a(T)$ ). The regression on  $S_a(T)$  was fulfilled for 146 different frequencies and 5 percent of damping (between 0.1 and 50 Hz, periods between 0.02 and 10 seconds; see Annexe 9.1) such that more point are applied for low frequencies in comparison with the high frequencies. The general form of the attenuation relationship for the spectral acceleration ( $S_a$ ) is;

$$\log S_a(T) = a(T) \cdot M_w + b(T) \cdot X - d \cdot \log X + c_i(T) \cdot S_i + \sigma(T) \cdot P \quad (6.3)$$

This relationship has the same form as equation 6.1, just the spectral acceleration and the coefficients  $a$ ,  $b$ ,  $c$  and  $\sigma$  are functions of the period ( $T$ ). Caillot (1992) used a slightly different form of such formula with the Neperian logarithm of  $S_a(T)$  and eliminating the term related to the anelastic attenuation coefficient, while adding a coefficient to observe the geometric expansion for the Italian data:

$$\ln S_a(T) = a(T) \cdot M_w + b(T) \cdot \ln X + c_i(T) \cdot S_i + \sigma(T) \cdot P$$

### 6.3 The input data-base

The data-base used as the input for this study consists of 468 three components accelerograms (169 analogs by SMA-1 instruments and 299 digitals by SSA-2 recorders, Appendix 6.1), recorded between 1975 and February 1996 by the national network (Figure 6.1). This data-base comprises 279 analog and digital records with fairly well known source parameters (Bard et al 1998) and 189 other digital accelerograms which were very well recorded, and for which no source data was directly available. The moment magnitude and hypocentral distance for these records have thus been estimated directly from the strong motion records. The hypocentral distance was obtained from the S-P time difference, while the seismic moment was directly calculated from the level of acceleration spectra plateau and the corner frequency (Zaré et al 1999b).

The magnitude range for the whole data set is  $2.7 = M \leq 7.4$  while the range for hypocentral distances is  $4 \leq X \leq 240\text{km}$  (Figure 6.2). The focal depths range is 9-133km but the focal depth determination is very imprecise and the majority of the events are shallow (Bard et al 1998a). The two horizontal components of each record are included separately in the study, therefore the number of the horizontal records entered to the regressions was twice the vertical ones.

#### 6.3.1 The magnitude values

The magnitude used here is the moment magnitude, to give a uniform and reliable scale. The moment magnitude was systematically calculated for the well recorded earthquakes (with little noise). When it was not possible to calculate  $M_w$  precisely because of the high noise level, other magnitudes were converted to  $M_w$  using the correlation with  $M_w$  specifically derived for Iran (Zaré et al 1999b). According to this correlation,  $M_w$  is taken equal to  $M_s$  for magnitudes greater than 6 and equal to mb and ML for magnitudes less than 6. Ambraseys and Free (1997) showed for a European data-base (including a few Iranian data) that such correlation exists between  $M_s$  and  $M_w$  not only for the moment magnitude relationship (Hanks and Kanamori 1979, used in Zaré et al 1998b) but also for a new empirical non-linear relationship established by them.

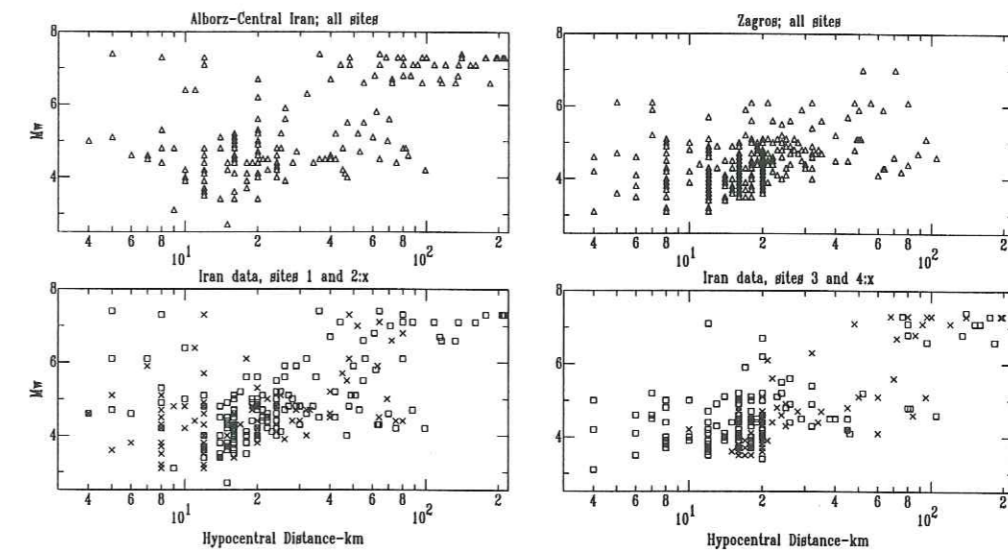


FIG. 6.2 – The statistics of the Iranian data for Alborz-Central Iran, Zagros and entire of the data; the attribution of the records to the site classes is shown for the entire of the data.

#### 6.3.2 Distance parameter

When discussing the choice of the "distance parameter" one must keep in mind the significant uncertainties in teleseismic epicenter localizations and large uncertainties in determining focal depths for the Iranian earthquakes. It is important however to define this parameter so that the future use of the attenuation law will be easy.

The focal depths for most of the Iranian records (below  $M_w 6.0$ ) are estimated using the teleseismic reports, because of the lack of a dense seismic array in Iran. This situation is similar even for some larger events ( $M_w > 6.0$ ). Kadinsky-Cade and Barazanji (1982) showed that for the Zagros data in southern Iran, there is a discrepancy between the depths reported by ISC and those of NEIC. Neglecting the values of 33km (depth at which events are arbitrarily located when the iteration process used in their location yields large residuals), the ISC depths are systematically reported to be greater than the NEIC depths.

The only earthquakes with  $M_w$  greater than 6.0 for which the focal depths are constrained by waveform observations are:

- The Sarkhun earthquake, 7 March 1975 ( $M_s 6.1$  depth=11km);
- The Khurgu, earthquake, 21 March 1977 ( $M_s 7.0$ , depth=12km) (both by Jackson and

Mckenzie 1984);

- The Naghan, earthquake, 6 April 1977 ( $M_s 6.1$ , depth=43km), (Ni and Barazanji 1986);
- The Tabas, earthquake, 16 September 1978 ( $M_w 7.4$ , depth=10km, Berberian 1982);
- The Manjil, earthquake, 20 June 1990 ( $M_w 7.3$ , depth=19km, Eslami and Mozaffari 1992, and 14km, Berberian et al 1992);

We have decided to define the distance variable for the regression as the "hypocentral distance". This distance is controlled by the difference in the arrivals of the compressional and shear wave for each record. Such information is available without any ambiguity only with the SSA-2 digital records, since the SMA-1 instruments do not include any pre-event memory.

In the cases of near-source records (such as the Tabas record obtained at 5km distance from the Tabas 1978 earthquake fault, and Abbar record in the Manjil 1990 earthquake at 8km distance to fault zone), it was impossible to distinguish the phases and the first arrivals, so we have taken the distance to the fault zone ( $R_f$ ) as our variable  $X$  (which has more physical concept than hypocentral distance;  $R_h$ ). Ambraseys and Sbrulov (1998) indicated that in the near-field cases (such as Tabas record) the point-source model may over-estimate the predictions of peak values and spectral ordinates. They showed that the over-parameterization of the attenuation model may not reduce variability of the predictions from point-source models, however they suggested a better understanding of source location, direction and thickness of the non-seismogenic zone for the near-field records.

On the other hand, the Tabas record exhibits a very specific near-source spectra, such that it was estimated that an important directivity effect was probable on this record (Zaré 1996). It is hence suggested that for magnitudes greater than  $M_w 7.0$ , and distances less than 20km, and magnitudes greater than  $M_w 6.0$  with distances less than 10km as well, the prediction of strong motion parameter should deserve a special study, for instance through a search of corresponding near-source records in the Iranian data-set or in another data-set which represents similar seismotectonic characteristics. In such conditions near-field records might be studied by a deterministic approach to predict the probable strong motion parameters.

Since the differences between the hypocentral and epicentral distances are not too large for shallow earthquakes (less than 35km depth), it is suggested that in further use of the presented attenuation laws in this article, the "surface distance to fault" be replaced in the formula whenever the estimation of the depth of the seismic source is impossible. We propose that such surface projected distance might give a good estimation of the hypocentral distances.

### 6.3.3 Geological areas

The Iranian data falls into two geological groups; the Zagros data and Central Iran and Alborz data (Figure 6.1). The Zagros thrust fault zone (Figure 6.1) is the main geologic frontier between the Zagros and non-Zagros regions. The pre-existing seismic data from Zagros area shows higher seismic activity rate than the other regions. In the Zagros area middle range magnitudes ( $M 4-6$ ) are more frequent. In Alborz-Central Iran zone earthquakes are less frequent but have generally higher magnitudes than Zagros, and are therefore more destructive (Tabas earthquake, 1978, Central-Iran; and Manjil earthquake, 1990, Alborz). The Zagros thrust fault zone is the main geologic frontier between these two areas. On the other hand, the Zagros data are mostly recorded in the near-field distances (below 60km), while there exist records at distances greater than 220km in Alborz-Central Iran region. The time of the event, the distance to source and the exact timing on the digital records (if accessible), the magnitude of the corresponding event and the amplitude of the records were the main criteria to attribute each record to the seismic events in these zones. Since the strong motions are limited to relatively near distances, and most of our records were obtained within 50km (Figure 6.2), the events are distinguishable for each of the mentioned zones.

### 6.3.4 Site Categorization

Site conditions are considered through the categorization in four site classes on the basis of the receiver function (Zaré et al 1999a). Site class 1 is defined as sites that do not exhibit any significant amplification below 15 Hz. It corresponds to rock and stiff sediment sites with an average S-wave velocity over the top 30 meters in excess of 700m/sec. Site class 2 consists of sites for which the receiver function (RF) exhibits a fundamental peak exceeding 3 at a frequency located between 5 and 15 Hz. It was shown to correspond to stiff sediments and/or soft rocks with  $V_s 30$  between 500 and 700 m/sec. Site class 3 consists of the sites for which RF shows a peak with an amplitude exceeding 3 between 2 and 5Hz, and corresponds to alluvial sites with  $V_s 30$  between 300 and 500 m/sec. Finally site class 4 is defined as sites for which RF indicates peaks with amplitudes greater than 3 at frequencies below 2Hz, and it may be viewed as corresponding to thick soft alluvium. This ranking was the result of geotechnical measurements on 50 sites (compressional and shear wave velocity, microtremors) and the calculation of the receiver function for strong motions using three component accelerograms. This categorization shows some similarity to that of Boore et al (1993, 1994) (based on the average  $V_s$  for the top 30m) for the northwestern American data. The average  $V_s$  limits to distinguish the site classes

in Boore et al (1993,1994) reports are 180 m/sec, 360 m/sec, 750 m/sec and greater than 750 m/sec (to be compared with our values of 300, 500 and 700 m/sec).

### 6.3.5 Fault mechanism

According to the regional tectonic conditions of Iranian plateau, the fault mechanisms of most of the earthquakes are compressional, strike-slip or a combination of these two mechanisms. In an earlier study (Bard et 1998), it was shown that out of the 100 focal mechanisms of the records that are available, 40 correspond to strike-slip/reverse mechanisms, 31 to pure strike slip, 24 to pure reverse and 4 to pure vertical plane. Hence further usage of the attenuation law in this article should be limited to the sources with such mechanisms. It must be noted that since the time of installation of the Iranian accelerometric network, no earthquake with a normal (extension) fault solution has been recorded in this network.

## 6.4 Results

The results of regressions are presented in the form of spectral ordinates and the peak values. The values of the coefficients and the residuals between the predicted and the observed values for the maximum of the strong motion parameters (PGA, PGV and PGD) are estimated. The predicted spectra are presented for two different situations in Zagros and Alborz-Central Iran, and the smoothed (design) spectra to be proposed. The representative spectra are calculated using the attenuation laws for the spectral accelerations ( $S_a$ ).

As explained before for the equations 6.1, 6.2, and 6.3, surface wave-like attenuation may be reproduced applying  $d = 0.5$  for  $d \cdot \log X$ . To find the lowest possible standard deviation, different values are examined for  $d$ , and the lowest sigma value were obtained for  $d = 0.3$  on the vertical components and  $d = 0.1$  for the horizontal components. These variations may be investigated further to find the other effective factors in the attenuation in the Iranian crust. However we will present here only the calculations with  $d = 0.5$  and  $d = 1$ , because of their physical meaning in relation with surface and body waves, respectively.

The calculations on the response spectra are limited to the frequency bands for which a good signal to noise ratio ( $R_{sn}$ ) could be found. The accelerometric data are already band-pass filtered, considering a  $R_{sn}$  fixed to be 3 (Bard et al 1998, Zaré et al 1998b). Therefore in the frequency bands for which  $R_{sn}$  was lower than 3, the accelerogram is considered to be noisy and the spectral values are eliminated from the calculations. The sum of the selected point for

the regressions after such sieving is shown in Figure 6.3. According to this figure, the records in Alborz-Central Iran which were mostly analog (SMA-1) records contained a lot of noise and suffered more from the filters, while the Zagros data which are mostly digital show proper signals.

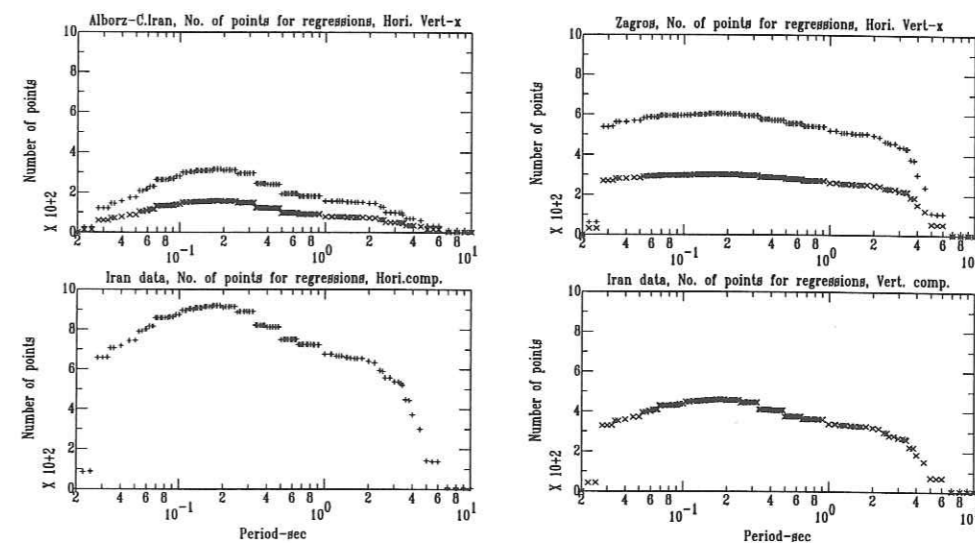


FIG. 6.3 - Number of spectral values after eliminating the values with low signal to noise ratios.

### 6.4.1 Attenuation coefficients for peak values

The strong motion parameters (A value in equation 6.1) selected in this section are PGA, PGV and PGD. Other parameters (energy and duration) were investigated in a separate study (Zaré et al 1999b).

The values of the coefficients of the regression for PGA, PGV and PGD in equation 6.1 are shown in Tables-6.1 to 6.3. The attenuation curves (Figures 6.4, 6.5 and 6.6) are presented for Alborz-Central Iran, Zagros and the Iranian data (entire of the data-base). The Iranian strong motion data show some differences in at least two main regions: Zagros and Alborz-Central Iran (Tables-6.1 to 6.3).



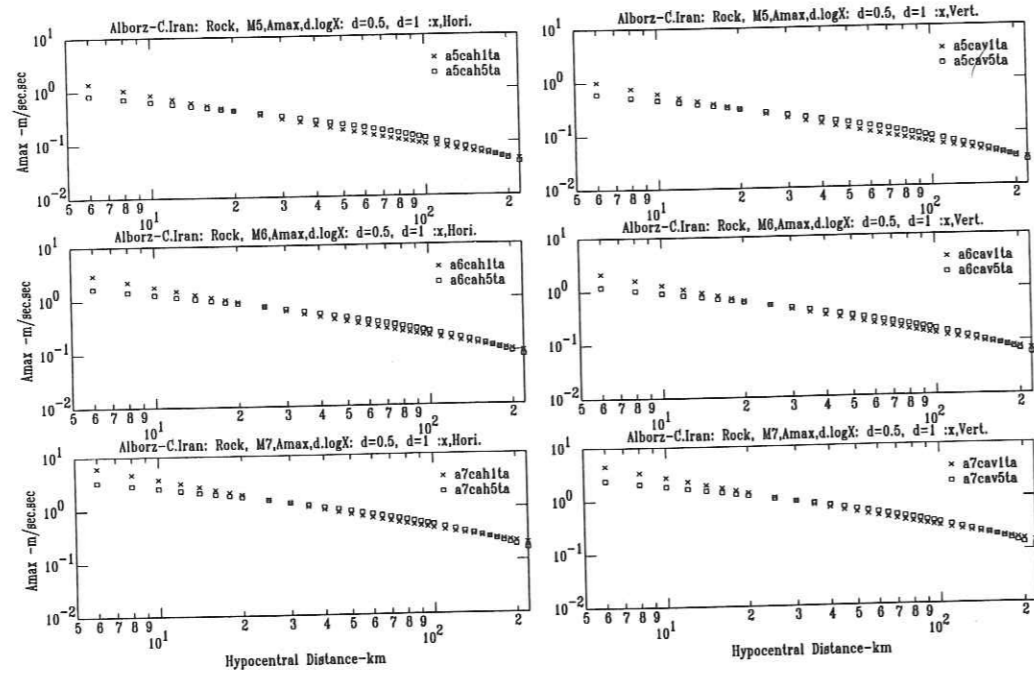


FIG. 6.4 – Attenuation of PGA with distances for magnitudes 5.0, 6.0 and 7.0, in Alborz-Central Iran, left: horizontal and right: vertical components; quadrangle:  $d=0.5$ , cross:  $d=1$ .

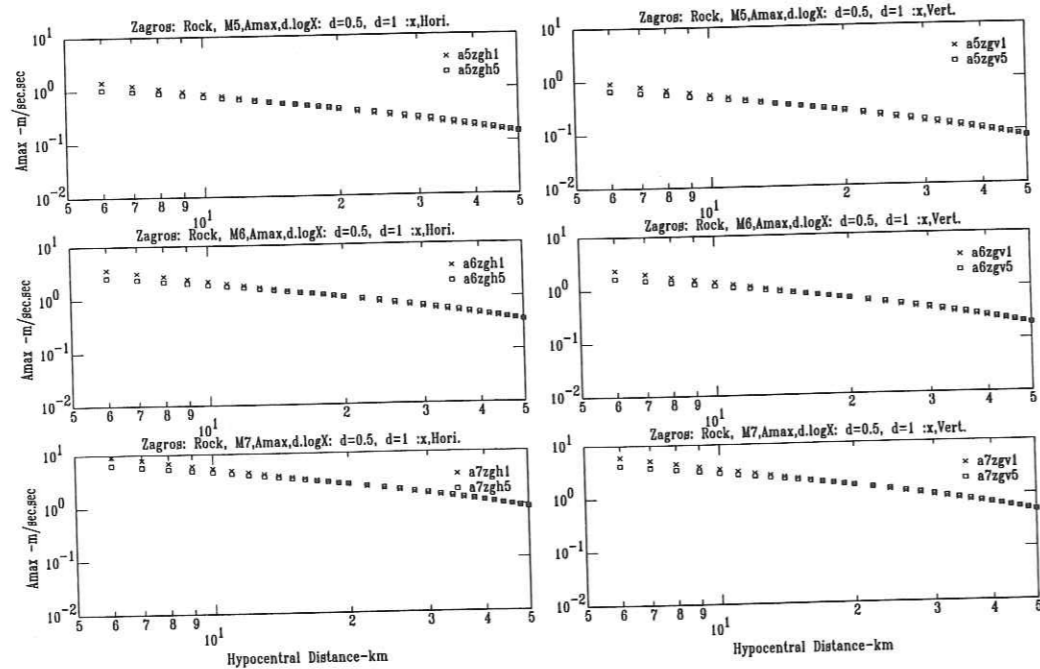


FIG. 6.5 – The attenuation of PGA with the distances for the magnitudes 5.0, 6.0 and 7.0, for Zagros.

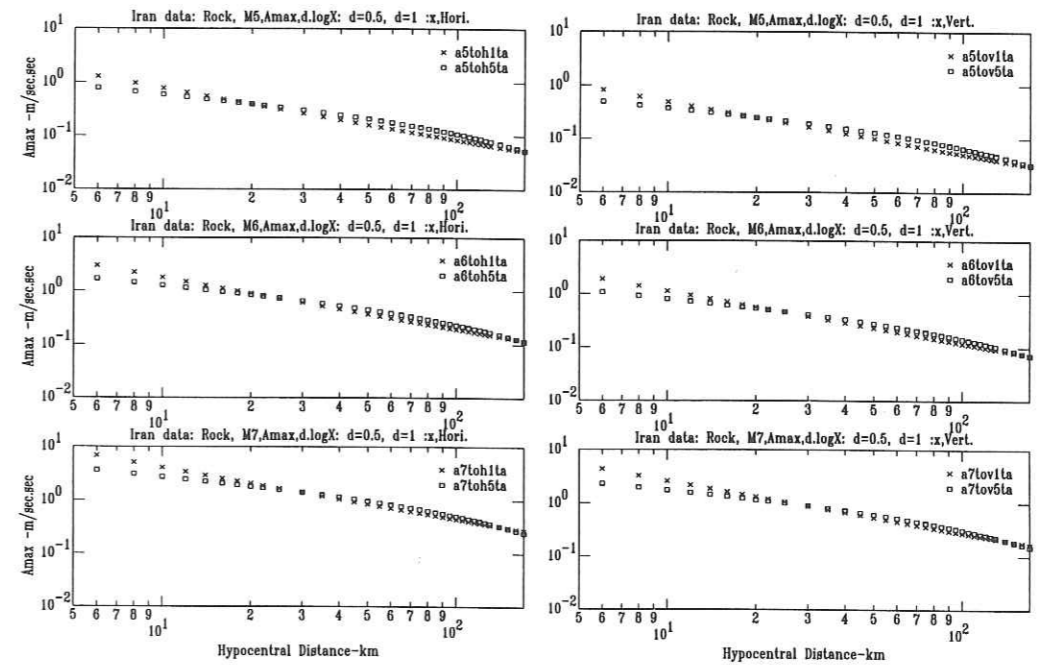


FIG. 6.6 – The attenuation of PGA with the distances for the magnitudes 5.0, 6.0 and 7.0, for the entire of the data-base.

The regressions were performed for  $d = 0.5$  and  $d = 1$ , but the coefficients are just presented for  $d = 1$ , because the differences between the sigma values in these two case were not significant. The most important differences between these two cases is observed for the PGA values in Alborz-Central Iran data at distances less than 20km (Figure 6.4), where the regressions with  $d = 1$  give the higher values for PGA.

Table 6.1: The coefficient for the attenuation of PGA, applying equation 6.1

Region/comp.	a	b	c1	c2	c3	c4	Sigma
Central Iran, Alborz (Vert.)	0.322	-0.0003	-0.828	-0.754	-0.971	-0.788	0.352
Central Iran, Alborz (Hori.)	0.322	-0.0004	-0.688	-0.458	-0.720	-0.585	0.394
Zagros (Vertical comp.)	0.406	-0.0038	-1.262	-1.333	-1.230	-1.777	0.356
Zagros (Horizontal comp.)	0.399	-0.0019	-1.047	-1.065	-1.020	-0.975	0.329
Iranian data (Vertical)	0.362	-0.0002	-1.124	-1.150	-1.139	-1.064	0.336
Iranian data (Horizontal)	0.360	-0.0003	-0.916	-0.852	-0.900	-0.859	0.333

Table 6.2: The coefficient for the attenuation of PGV, applying equation 6.1, for 381 cases

Region/comp.	a	b	c1	c2	c3	c4	Sigma
Central Iran, Alborz (Vert.)	0.466	0.0014	-3.108	-3.178	-3.328	-3.069	0.363
Central Iran, Alborz (Hori.)	0.471	0.0006	-2.865	-2.896	-2.969	-2.737	0.360
Zagros (Vertical comp.)	0.612	0.0028	-4.011	-4.101	-3.984	-3.917	0.319
Zagros (Horizontal comp.)	0.588	0.0040	-3.627	-3.651	-3.632	-3.502	0.315
Iranian data (Vertical)	0.548	0.0018	-3.675	-3.761	-3.702	-3.610	0.336
Iranian data (Horizontal)	0.538	0.0014	-3.335	-3.360	-3.348	-3.224	0.338

Table 6.3: The coefficient for the attenuation of PGD, applying equation 6.1, for 346 cases

Region/comp.	a	b	c1	c2	c3	c4	Sigma
Central Iran, Alborz (Vert.)	0.828	-0.0029	-5.861	-6.127	-6.023	-5.753	0.521
Central Iran, Alborz (Hori.)	0.828	-0.0036	-5.694	-5.837	-5.771	-5.352	0.489
Zagros (Vertical comp.)	0.784	0.0084	-6.043	-6.164	-6.144	-6.109	0.312
Zagros (Horizontal comp.)	0.797	0.0086	-5.893	-5.973	-5.954	-5.743	0.334
Iranian data (Vertical)	0.830	-0.0003	-6.051	-6.213	-6.163	-6.081	0.337
Iranian data (Horizontal)	0.829	-0.0010	-6.831	-5.942	-5.899	-5.645	0.388

The 'b' value, which represents the anelastic attenuation, was found to be the positive in some cases in Tables 6.1 to 6.3. Such abnormal values is to be connected to the fixed values of 1 or 0.5 in the  $\log X$  term in our regressions. The 'b' values, however, are very low. The residuals between the recorded and observed values of each of the parameters are shown in Figures 6.7 to 6.12, against the hypocentral distance and  $M_w$ . These residuals are presented for  $d = 0.5$  and  $d = 1$  (in equation 6.1), and it is evident that the difference of the residuals for  $d = 0.5$  and  $d = 1$  is not significant. In some cases (Figures 6.7, 6.9 and 6.11) lower residuals might be seen at greater distances for values calculated with a  $d = 0.5$ , especially for Alborz-Central Iran data. However these differences are not very large. The difference of the sigma values are found to be very low (for  $d=0.5$  and  $d=1$ ), while the sigma values are lower for  $d=0.5$  (for Iranian data, sigma values for the horizontal components, for logarithm of PGA is found to be 0.333 and 0.318 while for logarithm of PGV they are 0.338 and 0.317 and for logarithm of PGD, they are 0.388 and 0.362 for  $d=1$  and  $d=0.5$ , respectively).

Univ. J. Fourier - O.S.U.G.  
 MAISON DES GEOSCIENCES  
 DOCUMENTATION  
 B.P. 53  
 F. 38041 GRENOBLE CEDEX  
 Tél. 04 76 63 54 27 - Fax 04 76 51 40 58  
 Mail: ptalour@ujf-grenoble.fr

20 AOÛT 2003

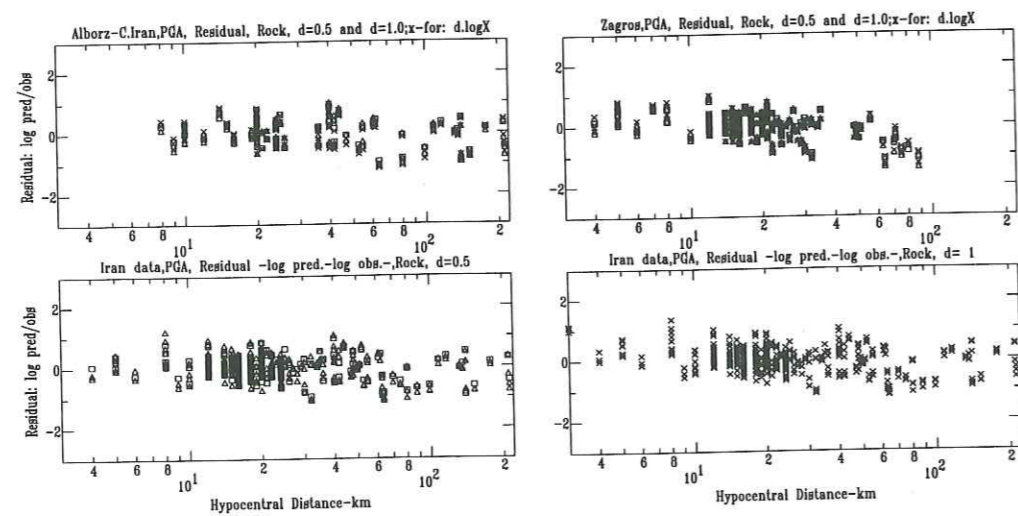


FIG. 6.7 - The residual ( $\log$  predicted -  $\log$  observed) of the PGA against distance, on rock sites, for Alborz-Central Iran, Zagros and entire of the data-base; the results are shown for  $d = 0.5$  (quadrangles) and  $d = 1$  (crosses) for Alborz-Central and Zagros; the  $d=0.5$  and  $d=1.0$  results are separated for Iran data (below).

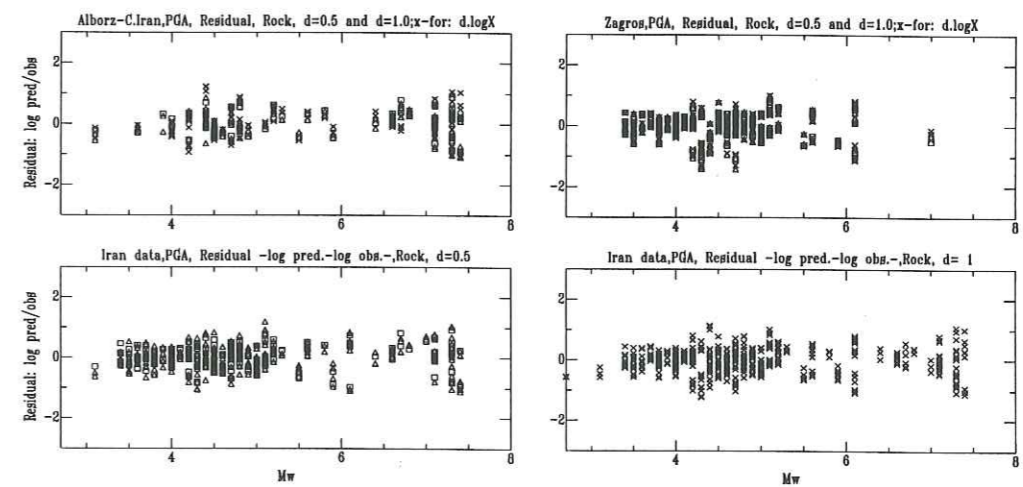


FIG. 6.8 - The residual ( $\log$  predicted -  $\log$  observed) of the PGA against  $M_w$ , on rock sites, for Alborz-Central Iran, Zagros and entire of the data-base; the results are shown for  $d = 0.5$  (quadrangles) and  $d = 1$  (crosses) for Alborz-Central and Zagros; the  $d=0.5$  and  $d=1.0$  results are separated for Iran data (below).

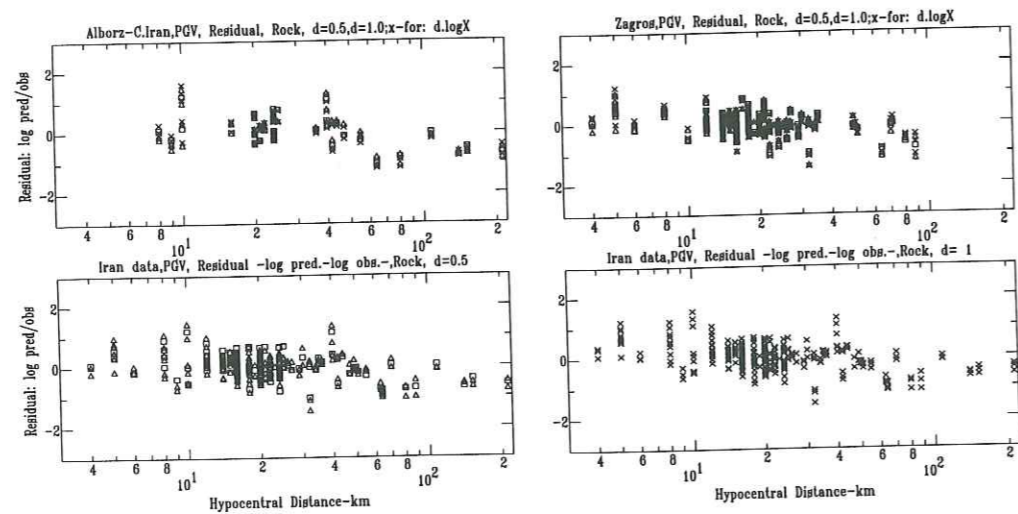


FIG. 6.9 – The residual (log predicted – log observed) of the PGV against distance , on rock sites, for Alborz-Central Iran, Zagros and entire of the data-base; the results are shown for  $d = 0.5$  (quadrangles) and  $d = 1$  (crosses) for Alborz-Central and Zagros; the  $d=0.5$  and  $d=1.0$  results are seperated for Iran data (below).

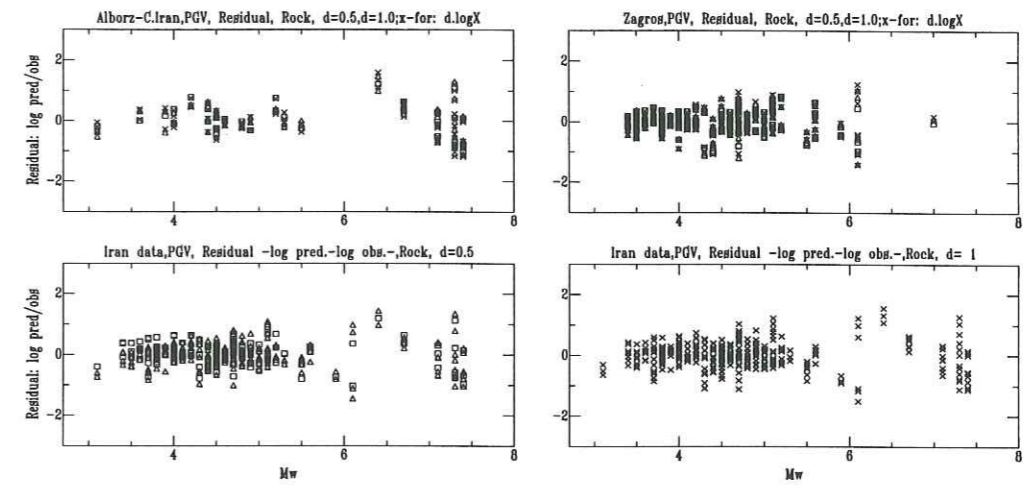


FIG. 6.10 – The residual (log predicted – log observed) of the PGV against  $M_w$  , on rock sites, for Alborz-Central Iran, Zagros and entire of the data-base; the results are shown for  $d = 0.5$  (quadrangles) and  $d = 1$  (crosses) for Alborz-Central and Zagros; the  $d=0.5$  and  $d=1.0$  results are seperated for Iran data (below).

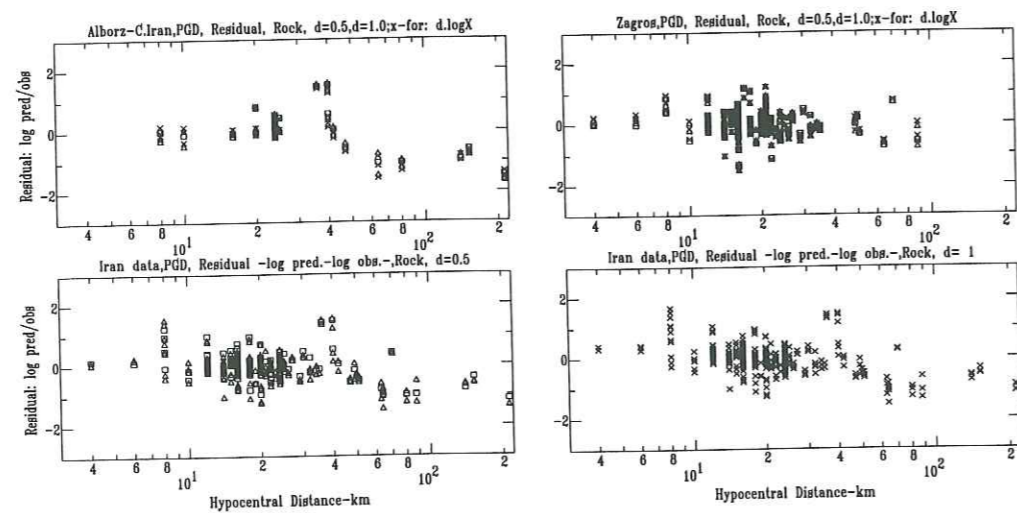


FIG. 6.11 - The residual (log predicted - log observed) of the PGD against distance, on rock sites, for Alborz-Central Iran, Zagros and entire of the data-base; the results are shown for  $d = 0.5$  (quadrangles) and  $d = 1$  (crosses) for Alborz-Central and Zagros; the  $d=0.5$  and  $d=1.0$  results are separated for Iran data (below).

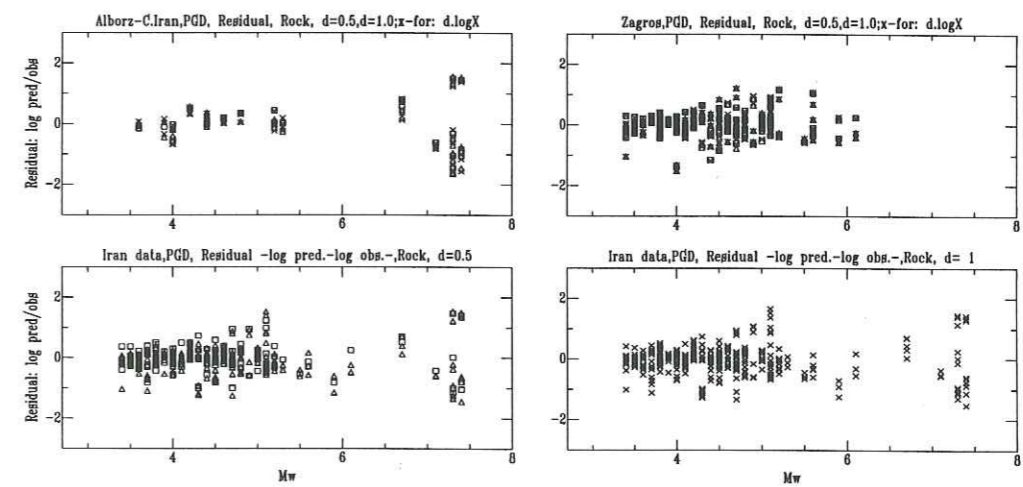


FIG. 6.12 - The residual (log predicted - log observed) of the PGD against  $M_w$ , on rock sites, for Alborz-Central Iran, Zagros and entire of the data-base; the results are shown for  $d = 0.5$  (quadrangles) and  $d = 1$  (crosses) for Alborz-Central and Zagros; the  $d=0.5$  and  $d=1.0$  results are separated for Iran data (below).

### 6.4.2 Attenuation coefficients for spectral ordinates

The acceleration response spectra are calculated for all the records, keeping just the frequency bands with a  $R_{sm}$  ratio greater than 3. According to Figure 6.3, the analog records (most of the Alborz-Central Iran data) are much noisy at long periods, leading to a low number of useful data (Figure 6.13). The coefficients of  $a$ ,  $b$  and  $c1$ , as well as the amplification of the second, third and fourth site classes ( $c2 - c1$ ,  $c3 - c1$  and  $c4 - c1$ ) are presented separately for Alborz-Central Iran, Zagros and whole Iran, for different periods between 0.05 to 4 seconds (Figures 6.13 to 6.16).

The values for  $d = 0.5$  are shown only for entire of the Iranian data (Figure 6.16). The values of sigma are generally lower for  $d = 0.5$  in all periods, but still for the spectral values, such difference is not large. Finally, according to the difference between the results with  $d = 1$  and  $d = 0.5$  in the near-field and the fact that using  $d = 0.5$  will underestimate parameters in near-field area (Figure 6.4 to 6.6), it is proposed to take  $d = 1$  in this paper, which may be a more conservative approach. Additional strong records in near-field conditions in Iran are needed for more detailed investigations.

According to Figure 6.3, the reliable period bands for the different regions are 0.05 to 1 seconds for Alborz-Central Iran and 0.03 to 3 sec for the Zagros data. Therefore the great instability for the Alborz-Central Iran results after 0.5sec (Figure 6.13) might be understood.

The  $a$  values increase when the period increases (Figures 6.13 to 6.16), which means an increasing magnitude dependence with longer periods as expected.

The positive  $b$  values for very large periods (beyond 3sec) might correspond to insufficient data (Figures 6.13 to 6.16). On the other hand, the negative  $b$  values at short periods may be an indication that attenuation of body waves were dominant, which in consequence gives more realistic values (negative sign for the coefficient of anelastic attenuation). The frequency content of the Zagros data is meaningful for such behavior; the Zagros records are representative for higher frequency, for which the body waves are more dominants. The same discussion might be done for the Iranian data (Figures 6.15 and 6.16) while the tendency for the positive 'b' values is evident when the period increases.

The site coefficients are consistent with the detailed site study on the Iranian strong motion sites (Zaré et al, 1999a). Amplifications at short periods ( $< 0.2sec$ ) for the site class 2, in middle range periods (0.2 to 0.5 seconds) for site class 3, and and large periods ( $> 0.5sec$ ) for site class 4, for most of the cases, do agree with the previous defined limits. However, the discrepancies from these limits seem to be significant for  $c3$  and  $c4$  for Alborz-Central Iran data

(Figure 6.13).

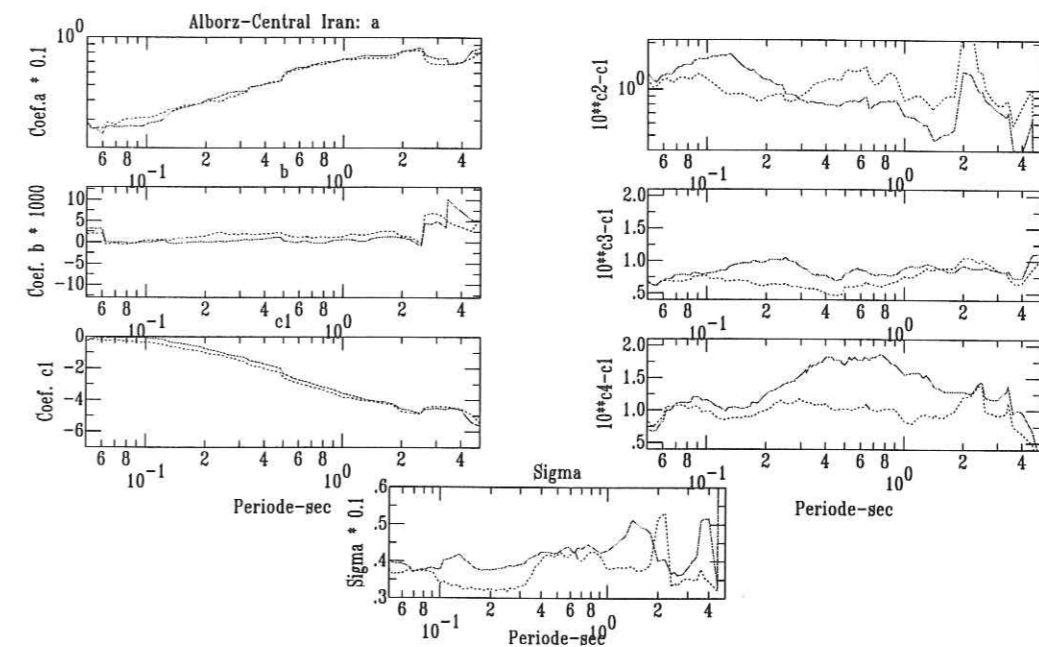


FIG. 6.13 - Coefficients of the regression (difference from  $c1$ ) (equation 6.3) against period, for the Alborz -Central Iran data. The site coefficients of the regression against period, for the Alborz-Central Iran data are given as well; solid lines :horizontal components, dotted line: vertical components.

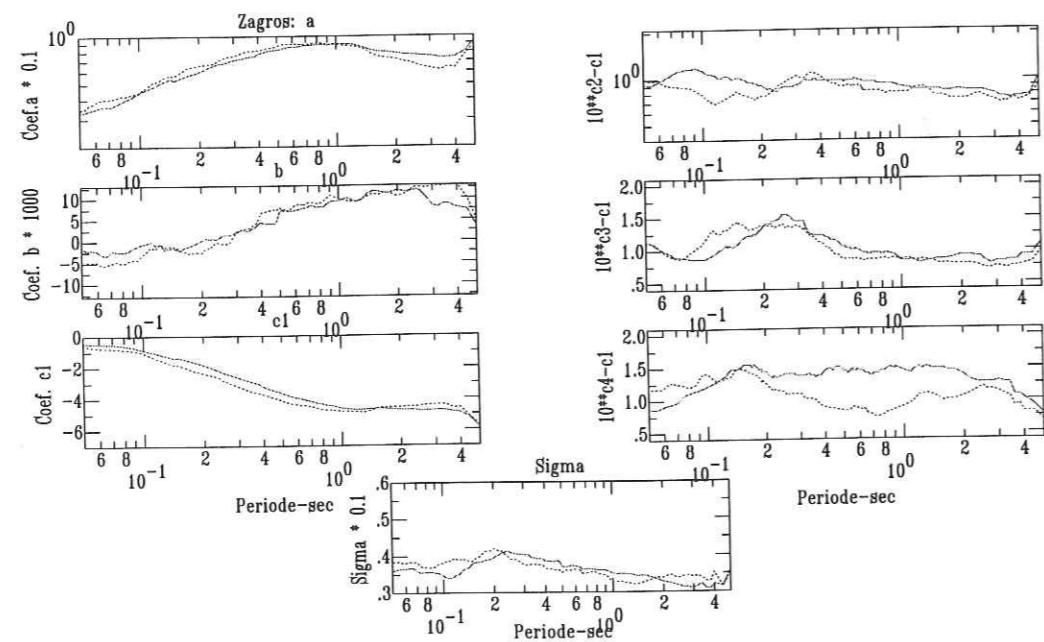


FIG. 6.14 - Coefficients of the regression (difference from  $c_1$ ) (equation 6.3) against period, for the Zagros data. The site coefficients of the regression against period, for the Zagros data are given as well; solid lines: horizontal components, dotted line: vertical components.

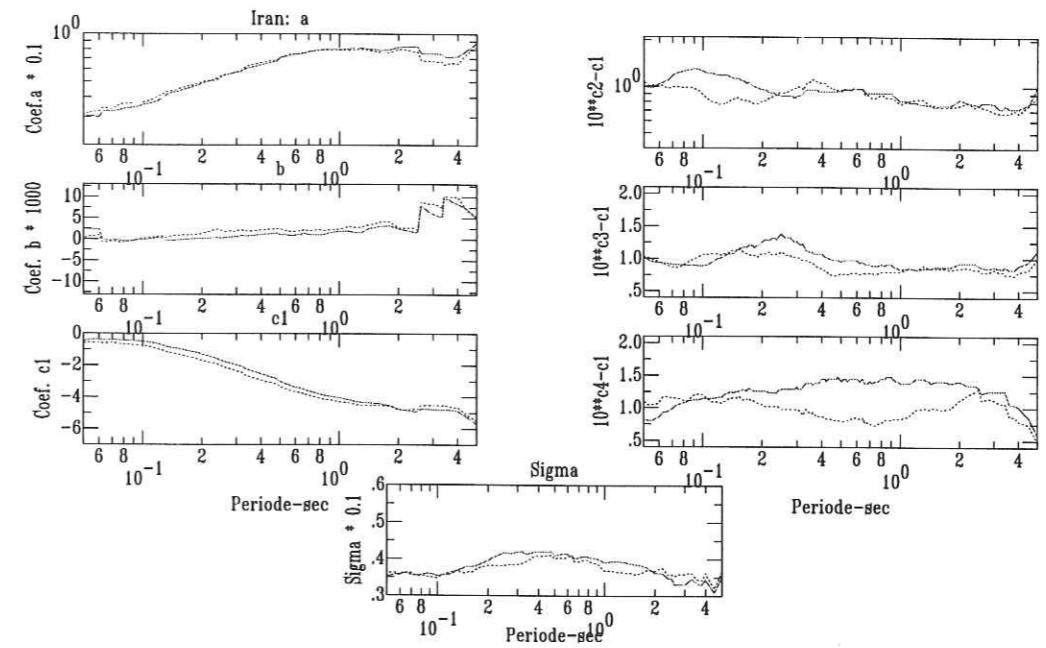


FIG. 6.15 - The coefficients of the regression (difference from  $c_1$ ) (equation 6.3) against period, for the Iranian data, for  $d = 1$ . The site coefficients of the regression against period, for the Iranian data, for  $d=1$  are given as well; solid lines: horizontal components, dotted line: vertical components.

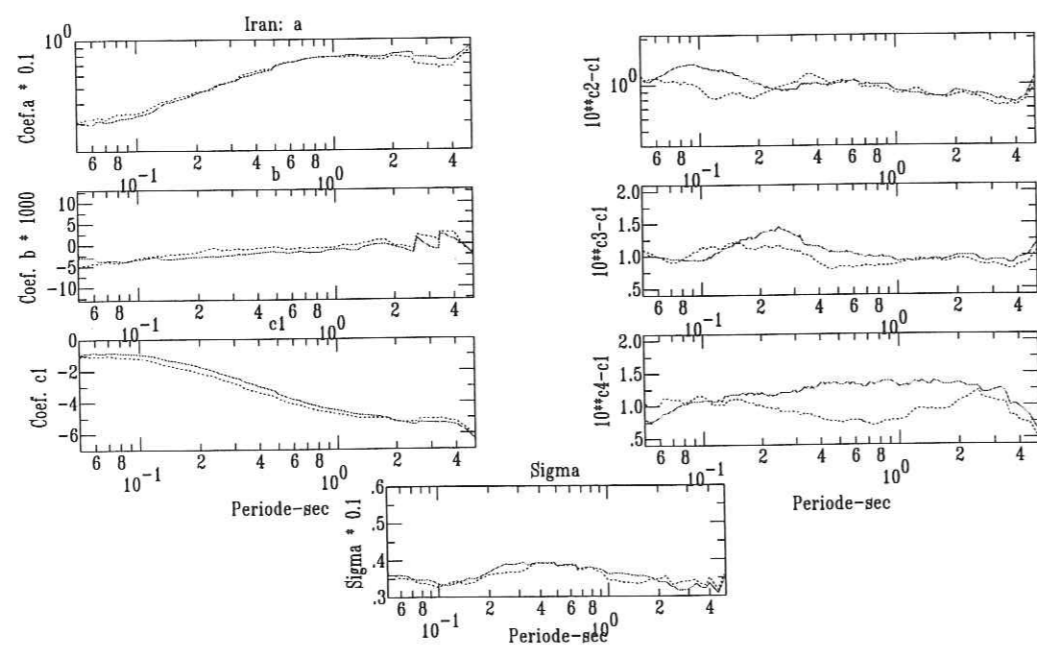


FIG. 6.16 - The coefficients of the regression (difference from  $c_1$ ) (equation 6.3) against period, for the Iranian data, for  $d = 0.5$ . The site coefficients of the regression against period, for the Iranian data, for  $d=0.5$  are given as well; solid lines :horizontal components, dotted line: vertical components.

Differences between Alborz-Central Iran and Zagros data may be also observed in i) lower duration data for and lower magnitude (but more frequent) earthquakes in Zagros (Zaré et al 1999b) which cause probably the abnormal positive  $b$  values at high frequencies, and more rapid attenuation of strong motions in this region, and ii) the higher  $a$  values specially in middle periods in Zagros, which might be induced by the reason told for previous item. On the other hand, since there are more records in the Zagros region, site amplifications for class 3 are more evident for Zagros data (Figure 6.14) than for Alborz-Central Iran data (Figure 6.13).

### 6.4.3 Nonlinear effects in the Iranian strong motions ?

The possible non-linear effects were looked for investigating the variation of the residuals as a function of PGA. In case of a soft soil (site class 4), a decrease of the high frequency content due to the non-linearity would be expected, which should reflect in an overestimation through prediction ( $prediction > observation$ ). Simultaneously we would expect a reverse effect at long periods ( $observation > prediction$ ). Such effects were looked for at several period values (0.1sec, 0.2 sec, 0.5 sec, 0.67sec, 1.0sec, 1.25sec, 2.0sec and 5.0sec). The difference between the observed values in the stations of class 4 and the predicted values (using  $d = 1$  for  $d \cdot \log X$ ) on the rock sites (for the same stations) are displayed in Figure 6.17 for the entire of the data-base. The difference between the observed and predicted values for the site class-4 are presented as well. These results show clear trends, with underestimation of spectral levels for really strong motions, and overestimation at moderate levels, whatever the period. This result was expected only at long periods, and we have no explanation for these observations at short periods.

## 6.5 Response and Design Spectra for Alborz-Central Iran, and Zagros areas

The coefficients for spectral values based on the whole Iranian data set are applied to estimate the response spectra of accelerations and the velocities for some typical near and far field situation on rock site conditions (Figure 6.18). The mean and mean plus one sigma values are calculated for magnitudes of  $M_w 6.0$  at a distance of 10 km, and  $M_w 7.4$ , at distances of 20km and 100km, with  $d = 0.5$  and  $d = 1$ . The selection of the magnitude of 7.4 was made according to the highest magnitudes occurred in Iran since the beginning of the strong motion measurements in Iran (Tabas earthquake of 1978,  $M_w 7.4$ ).

The difference between  $d=0.5$  and  $d=1.0$  is clear only at short distances (10 and 20 km),



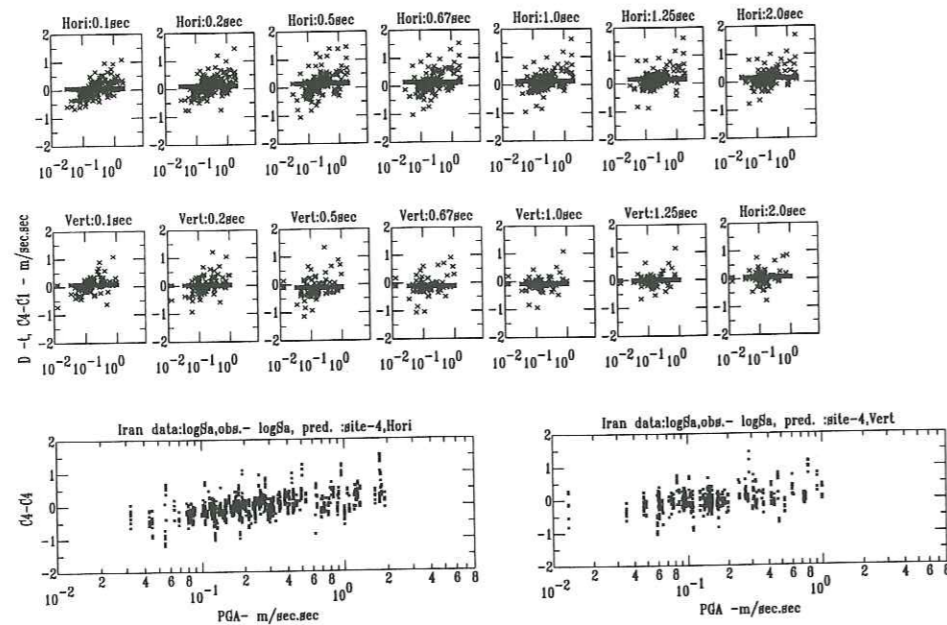


FIG. 6.17 - Difference between the observed spectral acceleration values at class-4 sites and the corresponding predicted values on rock sites, for horizontal and vertical component for the entire of the data-base. The differences between observed and predicted values on rock sites are shown as well.

with larger spectral values for  $d = 1$ . At 100km distance, results are almost the same. To show the results for different coefficients provided for Alborz-Central Iran, Zagros and entire of the data-base, the PGA values are looked for a magnitude of 7.0 with two different distances: The PGA values obtained with the coefficients in table-6.1 ( $d = 1$ ), for a magnitude of 7.0 and a hypocentral distance of 20km are found to give  $1.870m/sec^2$ ,  $2.546m/sec^2$  and  $2.032m/sec^2$  for Alborz-Central Iran, Zagros and entire of Iran data-base, respectively. With the same magnitude, and for a hypocentral distance of 50km, we obtain  $0.770m/sec$ ,  $0.897m/sec$  and  $0.833m/sec$  for the mentioned data-bases respectively.

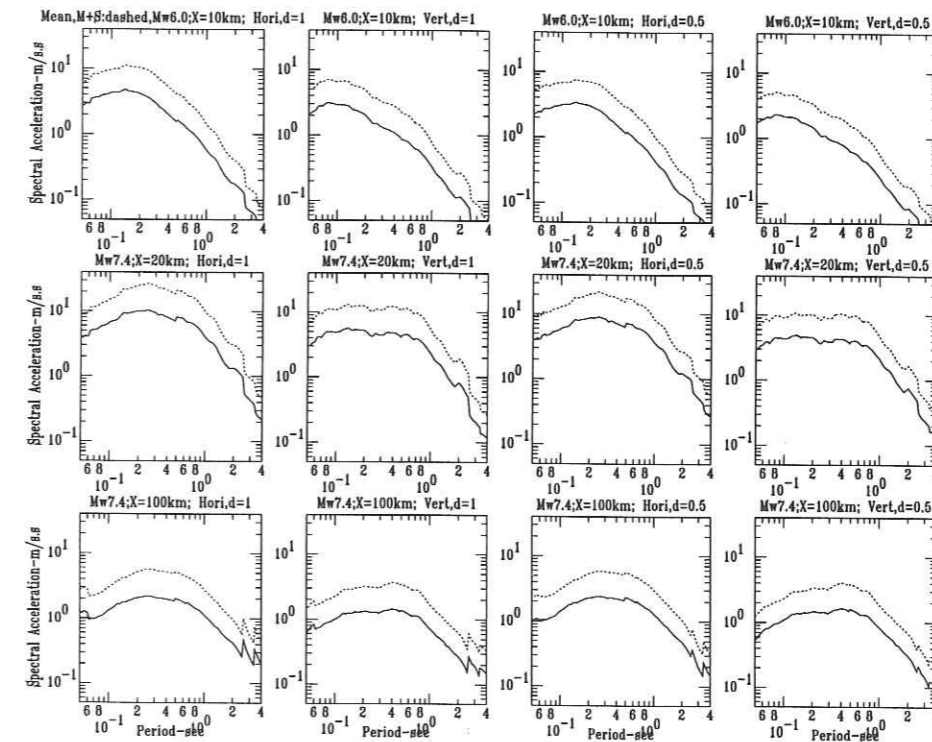


FIG. 6.18 - Representative response spectra calculated using the coefficients for the Iranian data ( $d = 0.5$  and  $d = 1$ ), for  $M_w 6.0$ , and  $7.4$ , for 10 and 20km and 100km distances, respectively: for the 3 cases (Top:  $M_w=6.0$ ,  $X=10km$ ), (Middle:  $M_w=7.4$ ,  $X=100km$ ) and (Bottom:  $M_w=7.4$ ,  $X=100$ ); solid line: mean and dotted line: mean +  $\sigma$ , two left for figures  $d=1.0$  (horizontal and vertical) and two right figures for  $d=0.5$  (horizontal and vertical).

Based on the results for the spectral ordinates, we will presents some response and design spectra for two different sites in Iran. The design spectra to be presented, is based on the response spectra of the records for a rock site in Tehran and a alluvial site in coastal area of the Persian Gulf (southern Zagros), with a average  $V_s$  in top 30m of 550m/sec (site class 2). To estimate the earthquake magnitude an empirical relationship for Iran is applied. This relationship is established using the fault rupture data coming form 22 earthquake faults (the events since 1336 till 1994) in Iran (Zaré 1995). This relationship predicts the moment magnitude having the fault rupture length:

$$M_w = 0.91 \cdot \ln L_R + 3.66 \quad (6.4)$$

where  $L_R$  is the rupture length in km. According to the mentioned study, in average, the rupture length might be estimated as about 0.37 of the total length of a major Iranian earthquake fault.

The main seismic sources nearby Tehran are North-Tehran fault and the Mosha fault. Taking a 120km segment of the Mosha fault and using equation 6.4, a magnitude  $M_w$ 7.1 is found for a rock site for northern Tehran. The intersection of the Mosha and the North-Tehran faults (in the Kalan Village in NE of Tehran) has a distance of the 35km with Tehran.

A floating earthquake scenario for Zagros belt is considered. The highest magnitude occurred in Zagros during our period of observation (Khurgu 1977) was Ms7.0. The thickness of the crust is estimated to be 15km for the Coastal region in southern Zagros (based on the geological maps), therefore considering an earthquake at the bottom of the crust, such depth may be taken as the hypocentral distance. These parameters are used to select the response spectra for our site in the coastal region of Persian Gulf. The specifications of the selected records are shown in Tables 6.4 and 6.5 .

Table 6.4: Selected records to find the design spectra in Tehran:

Code BHRC	$M_w$	Hypocentral Distance(km)	Site
1082-1	7.4	36	1
1083-1	7.4	64	1
1084-1	7.4	5*	1
1107	6.8	61	1
1118	6.6	55	1
1139	7.1	44	1
1362-1	7.3	40	1

\*:Tabas earthquake: Distance to the Fault zone

Table 6.5: Selected records to find the design spectra in a coastal area of Persian Gulf (southern Zagros):

Code BHRC	$M_w$	Hypocentral Distance(km)	Site
1006-1	6.1	48	2
1050-1	7.0	52	2
1058	6.1	18	2
1291-1	5.7	45	2
1491	5.7	12	2
1498	5.9	63	2
1502-9	5.9	9	2

All of the spectral acceleration and velocity values (calculated for a damping of 0.05) are normalized to PGA and PGV of each record and shown in Figure 6.19. To normalize the spectral velocities, the velocity spectral values for each record are divided by the observed PGV for that record. The mean and mean plus one sigma values are presented in Figure 6.20 and the smoothed spectra are given in Figure 6.21. According to high earthquake hazard in Iran, a conservative approach is applied to fit the smoothed spectra for these two examples (Figure 6.21). The higher spectral values are obvious for the design spectra in Tehran in longer periods, while in Zagros coast the spectra show more important values for shorter periods.

## 6.6 Conclusions

The attenuation of the strong ground motions in Iran was studied for the first time in this article. The regression coefficients are presented for the peak values and the spectral ordinates, which are generally in agreement with the coefficients presented by Joyner and Boore (1981), Boore et al (1993, 1994, 1997) and Fukushima et al (1995) for other regions of the world. Meanwhile the results of this study are in agreement with the Ambraseys attenuation relationships for Europe (comprising some few Iranian records) (Ambraseys 1995, Ambraseys and Simpson 1996). The conclusions are summarized below:

- The attenuation of the strong motions in Iran follows the general form of the attenuation of the strong motions in Mediterranean attenuation (Caillot 1992, using the Italian data, and Ambraseys 1995, for the European data). This general accordance might be studied more precisely if the location of the foci for the earthquakes was determined using the local networks in Iran.

- The attenuation seems to be different for, at least, two regions of Iranian plateau; the Zagros area and the Alborz-Central Iran region (Figure-3). The seismicity, strong motion duration

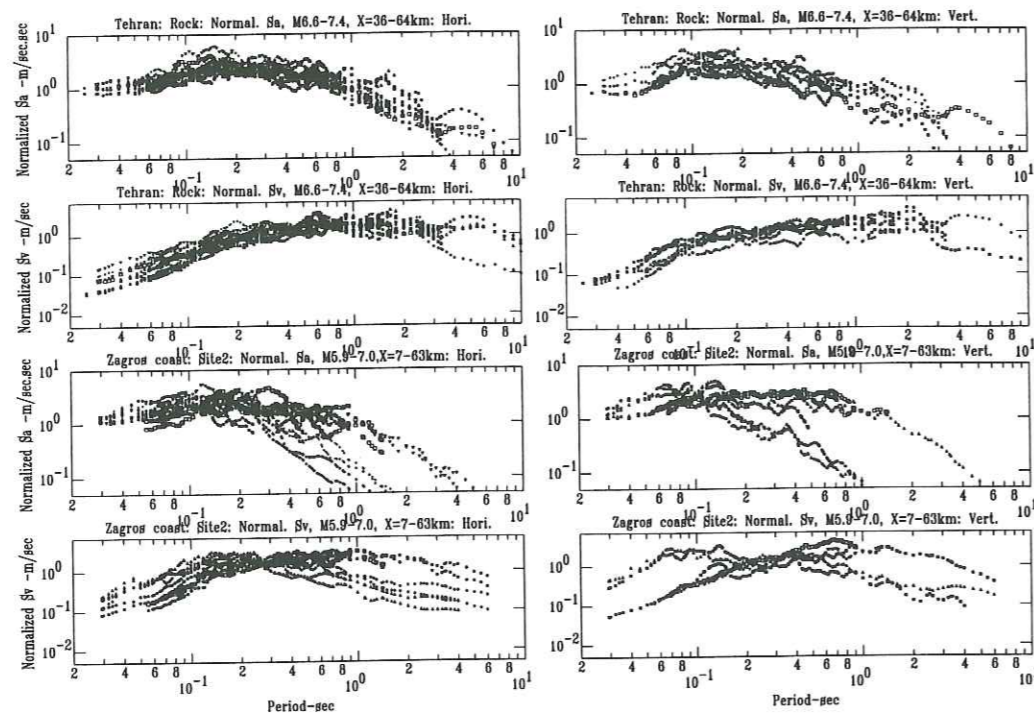


FIG. 6.19 – The normalized response spectra for a rock site in Tehran and an alluvial site in the Zagros coastal region on the Persian Gulf (specification for the spectra are given in Tables-6.4 and 6.5).

and the crust specifications seems to be one of the major factors for this evident difference. On the other hand, the response spectra for the Zagros region are rich in short periods, while the larger period amplitudes may be seen in the Alborz- Central Iran data.

- The site factors, which are obtained for 4-class site categorization of Iran, do not contribute too much except for PGD. This may come from the meteorological and topographic situation of the Iranian plateau: most of the Iranian territory is dry and arid and most of the urban areas are located on the alluvial fans, nearby the foothills.

- The attenuation term of the body waves and surface waves studied using a different coefficient for the geometric expansion term ( $\log X$ ); the difference for these two cases was not too much, but the higher values obtained with  $d = 1$  (body waves) in the near field distances (less than 20 hypocentral distances). The surface wave attenuation ( $d = 0.5$ ) gives the higher values in greater distances. This difference may be observed especially for the Alborz-Central Iran data.

- The near-field records are still very few in the Iranian network especially for large earthquakes ( $M_w > 6.0$ ) to investigate the near-source strong motions in Iran. The Tabas record (Tabas earthquake) and the Abbar record are the only records obtained in distances less than

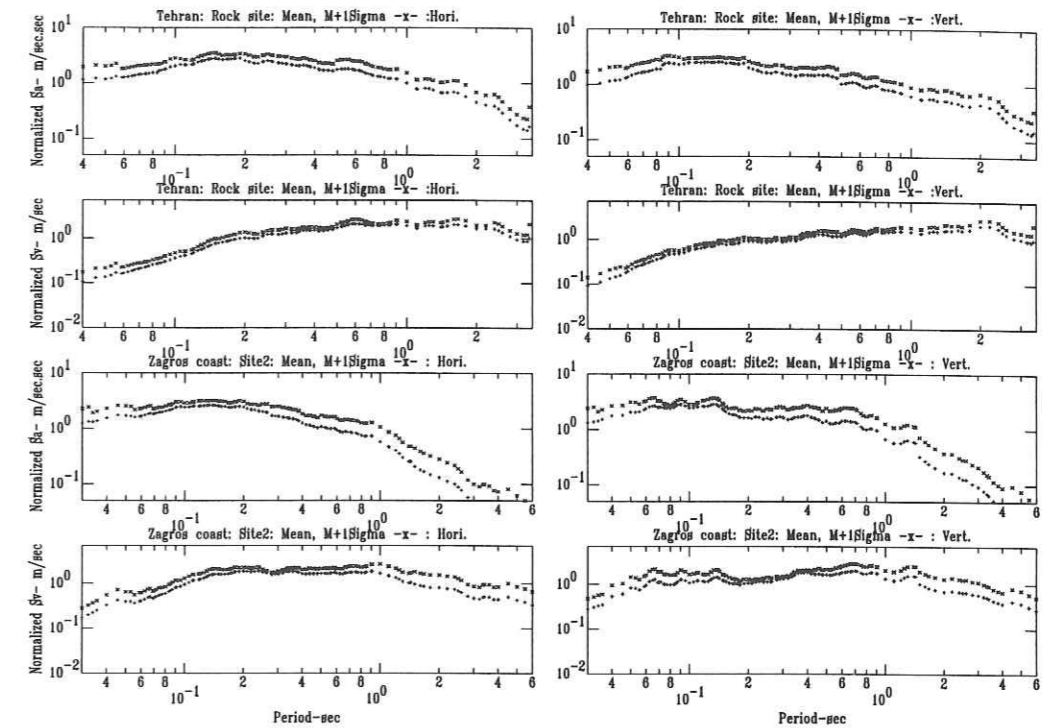


FIG. 6.20 – The mean and mean plus one sigma of the response spectra presented in Fig:6.19

10km the surface fault ruptures for an earthquake of magnitude greater than  $M_w 7.0$ . This problem causes a limitation in the use of the attenuation laws presented in this paper: for the near-source cases, it is suggested to select strong motions recorded in similar situations with a deterministic approach (hypocentral distances less than about 20km, or nearest distance to the fault rupture of 10km for the sources with magnitudes greater than 7.0).

- Strong motion attenuation studies should be continued in Iran to investigate the unknown aspects of this important subject, not only to be used to seismic risk studies in Iran and its neighboring countries, but also to contribute to strong motion studies in the east-Mediterranean and European region. The main subjects suggested for future investigations are listed below;

- The attenuation parameters such as absorption coefficient ( $\kappa$ ) and the quality factor ( $Q$ ) might be investigated with more precise data to be provided with the dense network which is expanding actually in Iran. Such studies may reveal clearly the causes for the different features of the attenuation in the crust of the Iranian plateau.

- The uniform hazard spectra for Iran might be studied, based on a precise seismicity study on Iran. Furthermore, the response spectra should be classified for each defined limit for the magnitude and distance values.

- The focal depth of seismic events in Iran should be determined, *a priori*, using a dense and online seismic network (to be installed in Iran). In the absence of such data, a large uncertainty

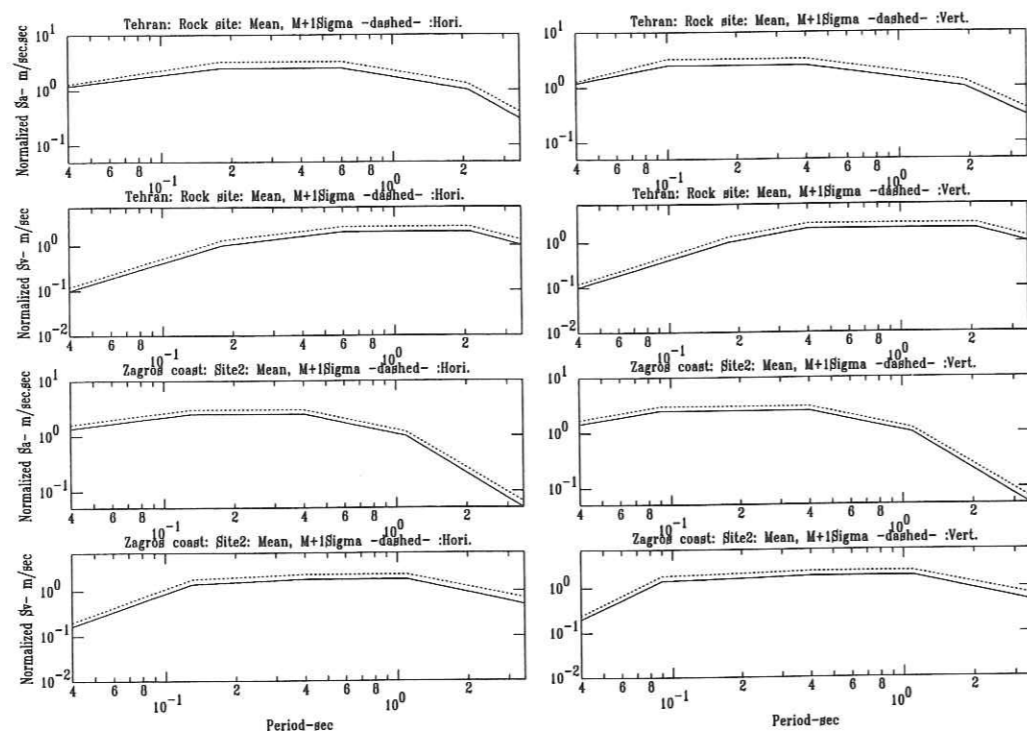


FIG. 6.21 - The smoothed spectra for the response spectra shown in Fig:6.20

will remain for the distance determinations. Such studies may help to compare the Iranian attenuation models with the other models.

- To develop the existing accelerometric network in Iran, the site and seismicity characteristics should be considered for the site selections. The installation of more instruments in the region which are sparsely populated but show high seismicity (like Makran and eastern Iran), may provide valuable information to be used everywhere.

- The studies on micro-earthquakes using the empirical Green functions for the capital of the country (Tehran), where no great and near earthquake was recorded in recent years but the seismic risk is very important, could be useful to estimate the earthquake strong motion for this city. Such estimations should be compared with real earthquakes in regions with similar condition.

- The near-source strong motions should be studied, using the dense arrays to be installed around quaternary faults. Because of the water-supply problem, most of the cities, villages and the industrial centers in Iran are located on or nearby the borders of the hills and plains, where a lot of the quaternary faults are located. Such a situation highlights the need for a better understanding of the near-fault strong motion.

- Advanced source studies should be conducted in Iran. The directivity effect was an important amplification factor in the Tabas earthquake. On the other hand, the rupture modeling

may reveal the nature of the source processes in the destructive earthquakes in Iran. The first priority for such studies would be an absolute and simultaneous timing of the accelerometric network.

- The Iranian attenuation relationships should be compared with the neighboring countries relationships. The best possibility for such study is now to study the strong motions in Turkey (Anatolian plateau), which is geologically in the continuation of the Iranian plateau, and for which the strong motion data are now available.

- The site effect parameters might be studied more precisely for the attenuation models in Iran. Pairs of the stations on alluvium and nearby rock outcrop, as well as the down-hole arrays would help to understand better site effect in Iran. Using the present information, neither a more sophisticated definition of the site parameters nor the over-parameterization of the site factors would be helpful for a better understanding of the site effects. Such studies might be completed with a comparison with the similar study in highly seismic region, where strong motion and site effects are properly recorded and studied (such as Japan).

- The attenuation of macroseismic intensities might be studied more using the historical reports, which are accessible for Iran with a great civilized history and cultural heritage. Such studies may give a general view of the attenuation of the strong motion in the history (especially for the regions where strong motions are not yet recorded).

#### Acknowledgements

J. Christophe Gariel in IPSN (Institut de la Protection et la Sécurité Nucleaire, CEA, France) kindly hosted the first author for a short term technical visit, to work on the Attenuation law within the BERSSIN team. The discussions with him, F. Cotton and B. Hernandez were useful to establish the attenuation law for Iran, that is greatly thanked. The BHRC (Building and Housing Research Center, Tehran), who released the raw strong motion records is greatly thanked. The location of the new digital instruments were provided by Mr Hossein Mizaei-Alavijeh from BHRC, which is appreciated. A financial support in France (for the first author) was provided by a French scholarship (Ministère Francais des Affaires Etrangere) and acknowledged. We acknowledge as well Poppy Buxton who has controlled the text in view point of the English orthography.

### 6.7 Régression en une étape

Nous avons voulu ici simplement comparer les résultats obtenu avec deux types de régressions, une et deux étapes. Nous avons pour cela utilisé le logiciel STATISTICA. L'ensemble des données (déjà étudiés avec les régression dans deux étapes, discuté avant dans ce chapitre) ont été utilisées dans la régression dans une étape avec la même relation déjà utilisée:

$$\log A = a \cdot M_w + b \cdot X - d \cdot \log X + c_i \cdot S_i + \sigma \cdot P \quad (6.5)$$

Les valeurs des coefficients de cette relation sont présentées dans le tableau 6.6 pour les paramètres différents ( $A_{rms}$ ,  $e_a$ ,  $A_{max}$ ,  $V_{max}$ ,  $D_{max}$ );

Tableau 6.6: Les valeurs des coefficients de la régression en appliquant la relation 6.5 pour les paramètres différents;

Paramètre/comp.	a	b	c1	c2	c3	c4	Sigma	R
$A_{rms}$ , Vertical	0.320	0.0029	-1.675	-1.650	-1.655	-1.647	0.327	0.566
$A_{rms}$ , Horizontal	0.343	0.0027	-1.576	-1.466	-1.537	-1.610	0.339	0.607
$e_a$ , Vertical	0.767	-0.0005	-4.233	-4.208	-4.198	-4.120	0.564	0.415
$e_a$ , Horizontal	0.807	-0.0005	-4.104	-3.913	-3.982	-4.072	0.567	0.535
$A_{max}$ , Vertical	0.307	0.0025	-0.937	-1.951	-0.948	-0.902	0.330	0.638
$A_{max}$ , Horizontal	0.311	0.0023	-0.749	-0.685	-0.729	-0.715	0.328	0.682
$V_{max}$ , Vertical	0.508	0.0040	-3.550	-3.631	-3.567	-3.517	0.325	0.689
$V_{max}$ , Horizontal	0.501	0.0035	-3.216	-3.238	-3.221	-3.135	0.331	0.828
$D_{max}$ , Vertical	0.750	0.0038	-5.787	-5.947	-5.887	-5.877	0.352	0.769
$D_{max}$ , Horizontal	0.766	0.0023	-5.627	-5.738	-5.686	-5.491	0.353	0.781

Les résidus des entre valeurs prédites et valeurs observées sont présentés dans les Figures 6.22 à 6.26. Les valeurs prédits des paramètres  $A_{rms}$ ,  $e_a$ ,  $A_{max}$ ,  $V_{max}$  et  $D_{max}$ , en utilisant les coefficients de tableau 6.6 avec la relation 6.5 (la régression dans une étape) ont été comparés avec les résultats de la méthode de la régression dans deux étapes (pour les même paramètres et le même jeu de données; l'ensemble des données iraniennes; Figures 6.27 à 6.31). Ces comparaisons montrent que les deux régressions prédisent les valeurs comparatifs pour une gamme de distance de 20-80km. A moins de 20km, la régression en une étapes sous-estime les paramètres de mouvements forts par rapport à la régression en deux étapes. Cette situation est inversée aux distances supérieurs à 80km. De plus, les estimations de  $V_{max}$  et  $D_{max}$  avec la régression en une étape, montrent une augmentation avec la distance, évolué de la distance de 80km qui

est illogique. Cette perturbation peut être considérée comme due à l'insuffisance des données à grande distance. Cela peut donc montrer que la méthode de régression en une étape est plus sensible à l'homogénéité de la distribution des données avec la distances, alors que cette condition est moins évidente pour la régression en deux étapes (Figures 6.27 à 6.31).

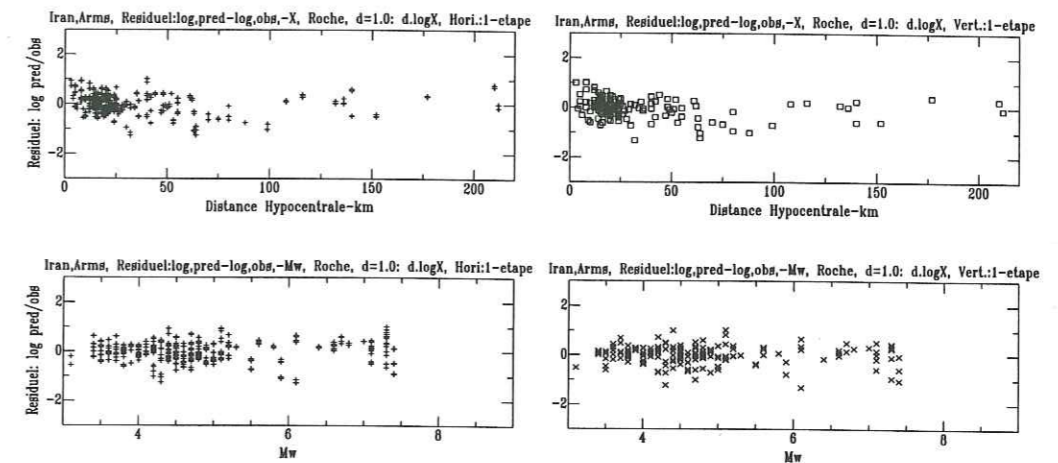


FIG. 6.22 – Le résiduel ( $\log$  prédit-  $\log$  observé) de  $A_{rms}$  en fonction de la distance hypocentrale et de la magnitude, pour l'ensemble des données iraniennes avec  $d=1.0$

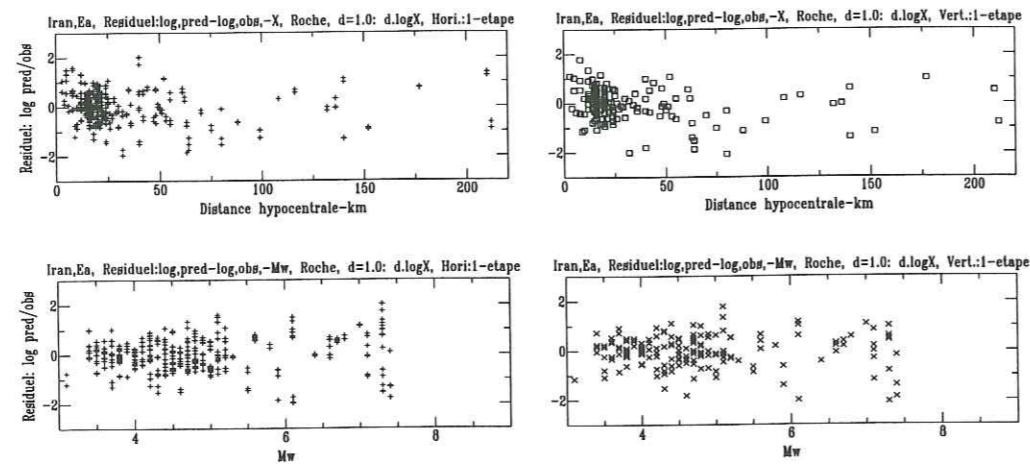


FIG. 6.23 – Le résiduel (log prédit- log observé) de  $e_a$  en fonction de la distance hypocentrale et de la magnitude, pour l'ensemble des données iraniennes avec  $d=1.0$

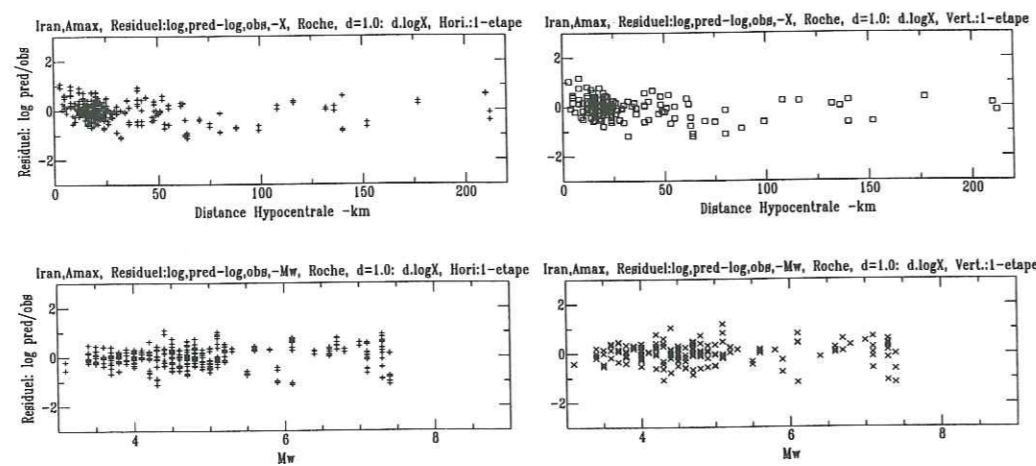


FIG. 6.24 – Le résiduel (log prédit- log observé) de  $A_{max}$  en fonction de la distance hypocentrale et de la magnitude, pour l'ensemble des données iraniennes avec  $d=1.0$

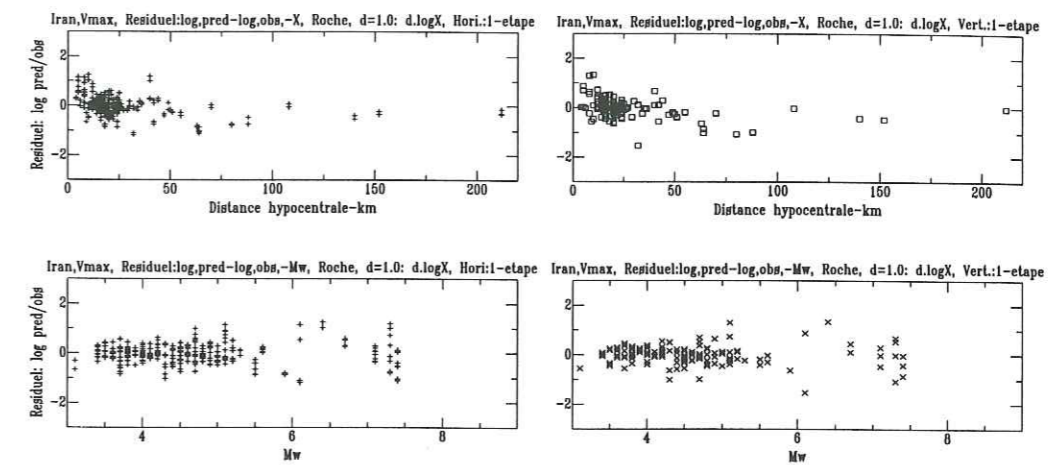


FIG. 6.25 – Le résiduel (log prédit- log observé) de  $V_{max}$  en fonction de la distance hypocentrale et de la magnitude, pour l'ensemble des données iraniennes avec  $d=1.0$

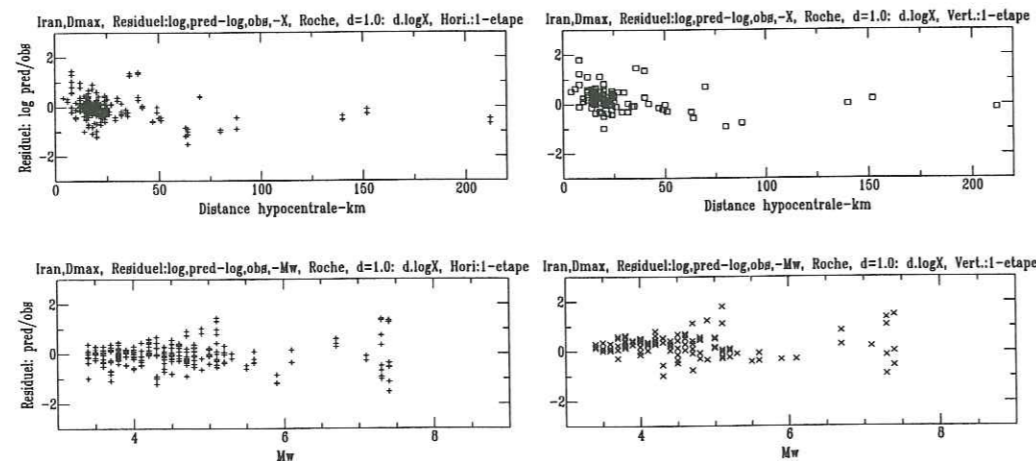


FIG. 6.26 – Le résiduel (log prédit- log observé) de  $D_{max}$  en fonction de la distance hypocentrale et de la magnitude, pour l'ensemble des données iraniennes avec  $d=1.0$

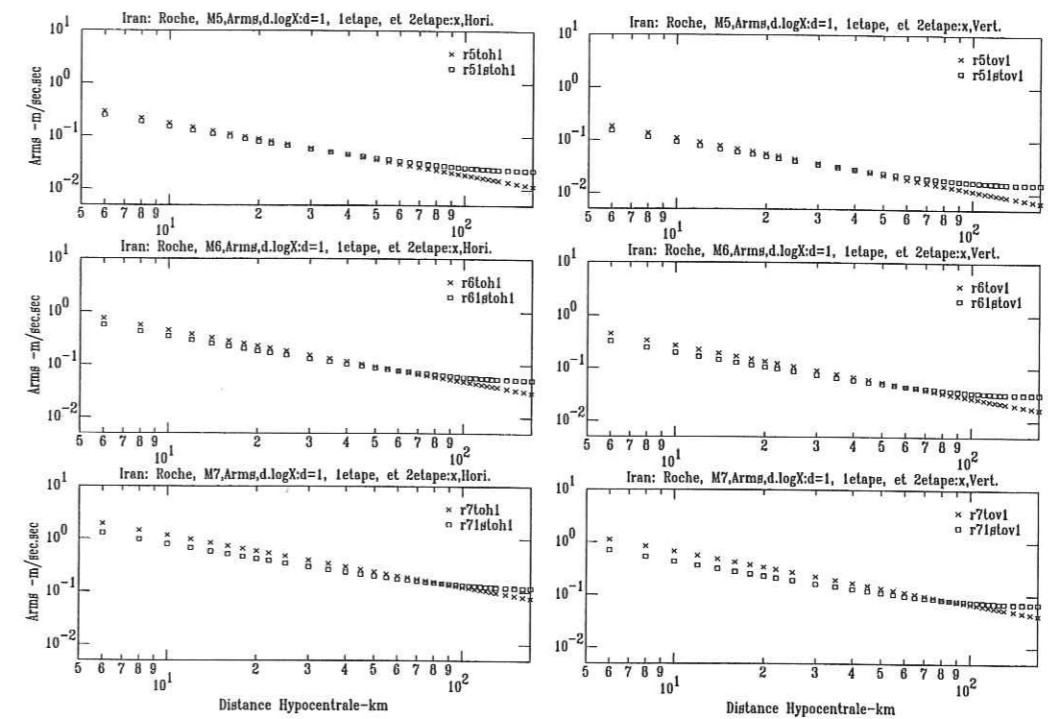


FIG. 6.27 – L'atténuation de  $A_{rms}$  en fonction de la distance hypocentrale pour les magnitudes de 5.0, 6.0 et 7.0, basé sur les résultats de la régression en une-etape (les rectangulaires) et en deux-etape (les croix) pour l'ensemble des données iraniennes.

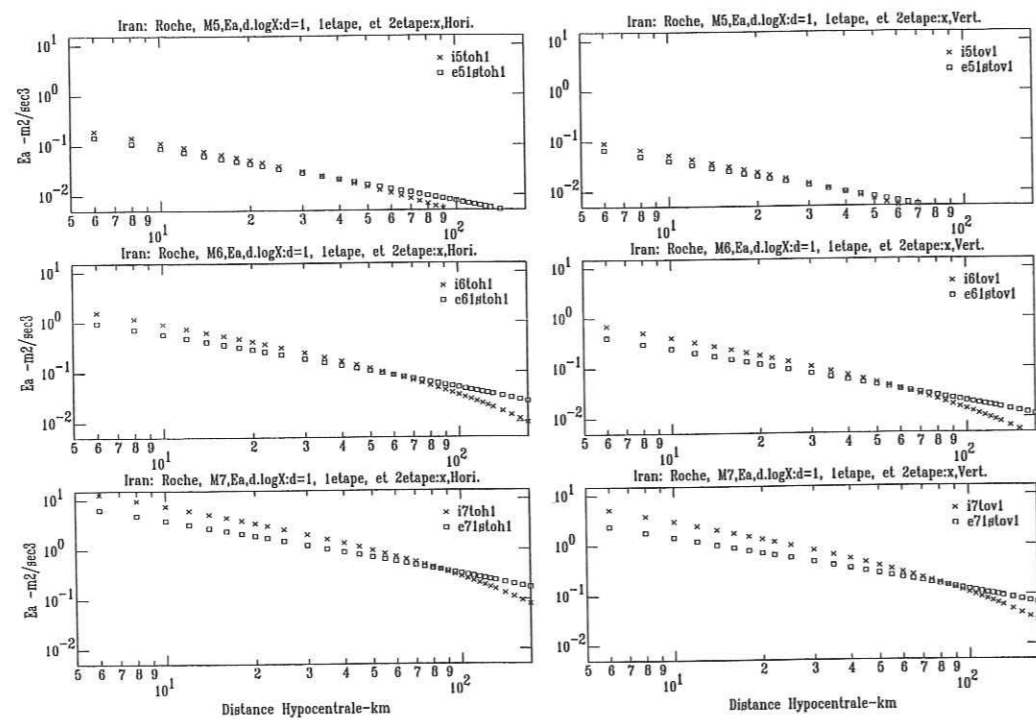


FIG. 6.28 - L'atténuation de  $e_a$  en fonction de la distance hypocentrale pour les magnitudes de 5.0, 6.0 et 7.0, basé sur les résultats de la régression en une-étape (les rectangulaires) et en deux-étapes (les croix) pour l'ensemble des données iraniennes.

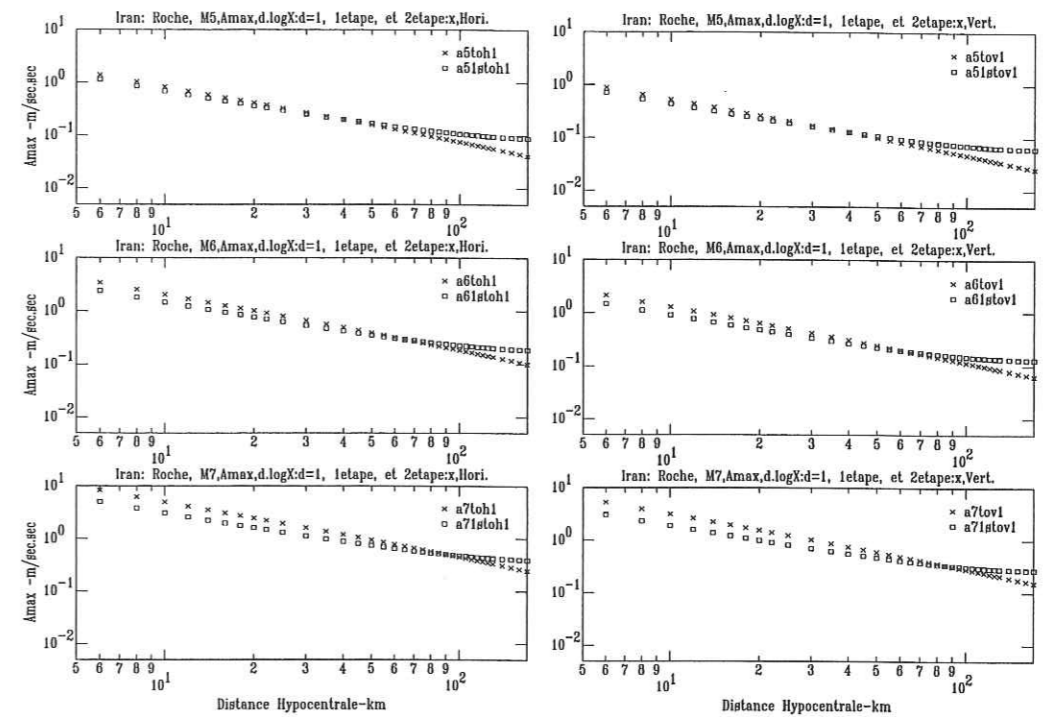


FIG. 6.29 - L'atténuation de  $A_{max}$  en fonction de la distance hypocentrale pour les magnitudes de 5.0, 6.0 et 7.0, basé sur les résultats de la régression en une étape (les rectangulaires) et en deux-étapes (les croix) pour l'ensemble des données iraniennes.



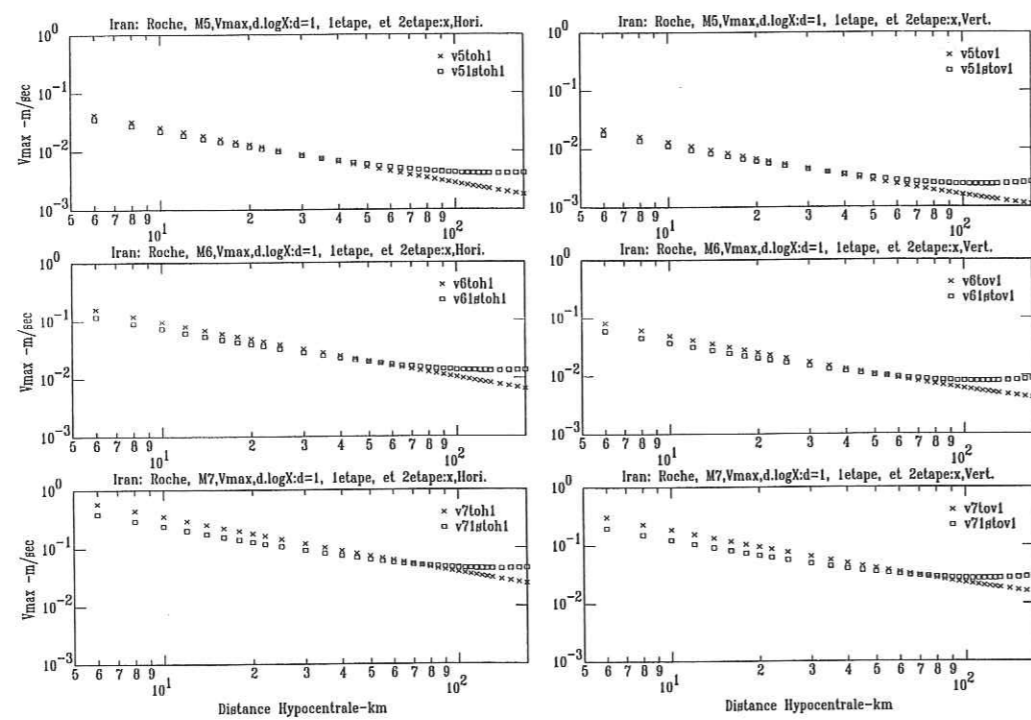


FIG. 6.30 - L'atténuation de  $V_{max}$  en fonction de la distance hypocentrale pour les magnitudes de 5.0, 6.0 et 7.0, basé sur les résultats de la régression en une-étape (les rectangulaires) et en deux-étapes (les croix) pour l'ensemble des données iraniennes.

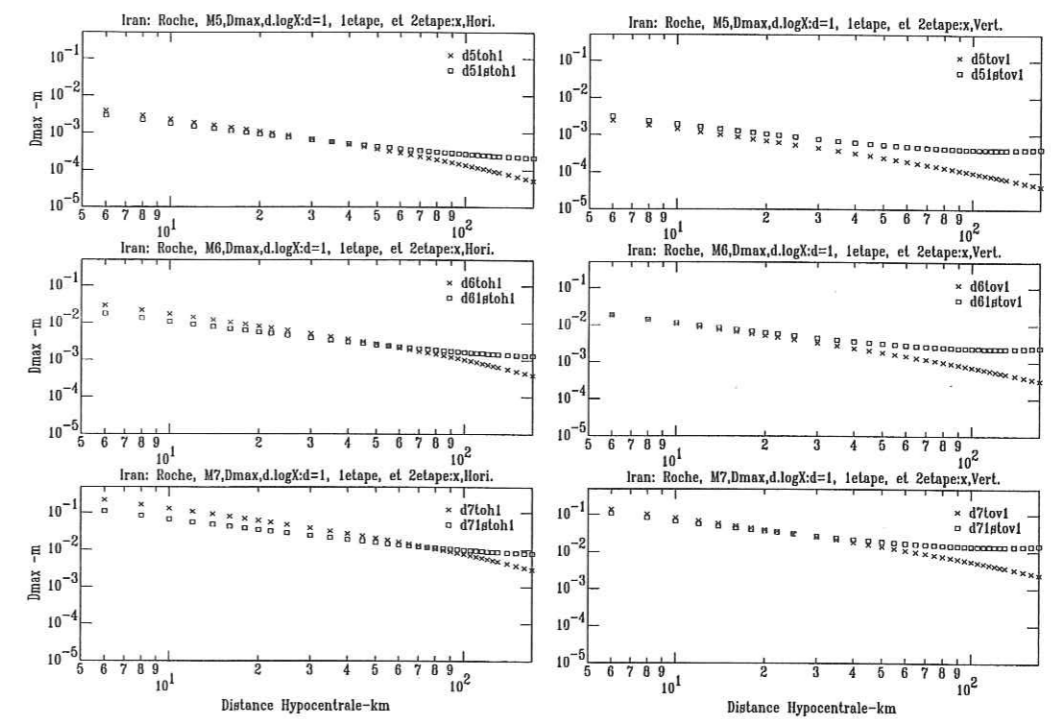


FIG. 6.31 - L'atténuation de  $D_{max}$  en fonction de la distance hypocentrale pour les magnitudes de 5.0, 6.0 et 7.0, basé sur les résultats de la régression en une-étape (les rectangulaires) et en deux-étapes (les croix) pour l'ensemble des données iraniennes.

Une autre forme de cette relation est étudiée qui ne se sert plus de l'atténuation anélastique et de l'expansion géométrique, mais en cherchant la meilleur décroissance "logarithmique" avec la distance:

$$\log A = a \cdot M_w - b \cdot \log X + c_i \cdot S_i + \sigma \cdot P \quad (6.6)$$

Les résultats des calculs en utilisant cette formule-la sont présentés dans le tableau 6.7:

Tableau 6.7: Valeurs des coefficients de régression en appliquant la relation 6.6;

Paramètre/comp.	a	b	c1	c2	c3	c4	Sigma	R
$A_{rms}$ , Vertical	0.308	0.581	-2.081	-2.048	-2.047	-2.081	0.320	0.407
$A_{rms}$ , Horizontal	0.319	0.539	-1.992	-1.863	-1.929	-2.023	0.327	0.489
$e_a$ , Vertical	0.728	0.889	-4.275	-4.240	-4.236	-4.187	0.570	0.162
$e_a$ , Horizontal	0.752	0.768	-4.168	-3.959	-4.036	-4.167	0.570	0.226
$A_{max}$ , Vertical	0.286	0.571	-1.327	-1.324	-1.317	-1.317	0.324	0.398
$A_{max}$ , Horizontal	0.281	0.547	-1.135	-0.050	-1.092	-1.129	0.317	0.479
$V_{max}$ , Vertical	0.500	0.447	-4.118	-4.172	-4.107	-4.108	0.317	0.487
$V_{max}$ , Horizontal	0.480	0.434	-3.759	-3.750	-3.732	-3.708	0.319	0.539
$D_{max}$ , Vertical	0.722	0.357	-6.393	-6.501	-6.453	-6.510	0.339	0.509
$D_{max}$ , Horizontal	0.729	0.471	-6.080	-6.148	-6.105	-5.978	0.343	0.411

### 6.8 Les études sur la nonlinéarité possible dans les données iraniennes

La possibilité des effets de nonlinéarité sous forte accélération a été analysée par l'études des résidus des valeurs maximales de l'accélération ( $A_{max}$ ). Ces résidus logarithmiques (logarithme des valeurs observées moins logarithme des valeurs prédites) sont représentés en fonction des valeurs de  $A_{max}$  observées pour les 4 sites différents et pour les deux types de régression (1 et 2 étapes)(Figures 6.32 à 6.35). Ces figures montrent une claire augmentation des résidus avec l'augmentation des valeurs de  $A_{max}$  observés, et une décroissance avec l'augmentation des Amax prédits. Cet effet est contraire a l'effet attendu, qui devrait être une décroissance de l'amplification à forte accélération. Cette observation peut s'interpréter comme la conséquence de la situation géologique du pays: la plupart des sites accélérométriques sont situés sur les alluvions raides et secs et sur les 25 ans d'existence du réseau accélérométrique iranien aucun

séismes ne s'est produit dans les régions côtières (où se trouvent les sols mous). Selon ces résultats, il faut donc insister encore sur la nécessité d'être prudent dans l'applications des lois d'atténuation présentées dans cette étude; pour les site à faible distance de forts séisme.

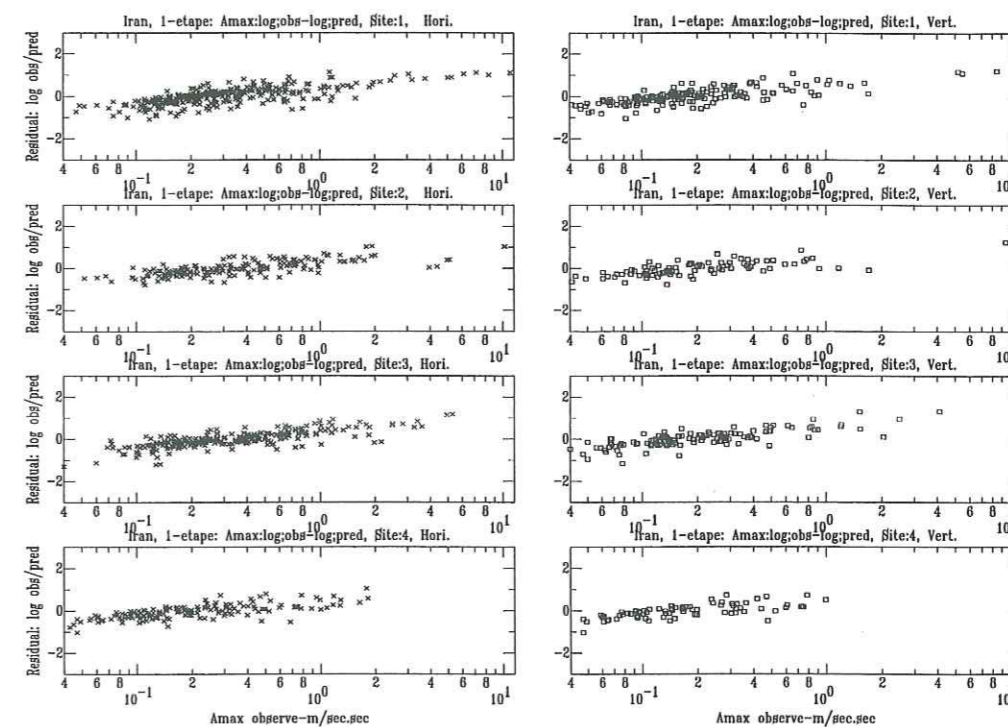


FIG. 6.32 – Les résiduels (log observé - log prédit) de  $A_{max}$  en fonction de  $A_{max}$  observé pour les catégories différents des sites en utilisant de la régression en une-étape, pour l'ensemble des données iraniennes

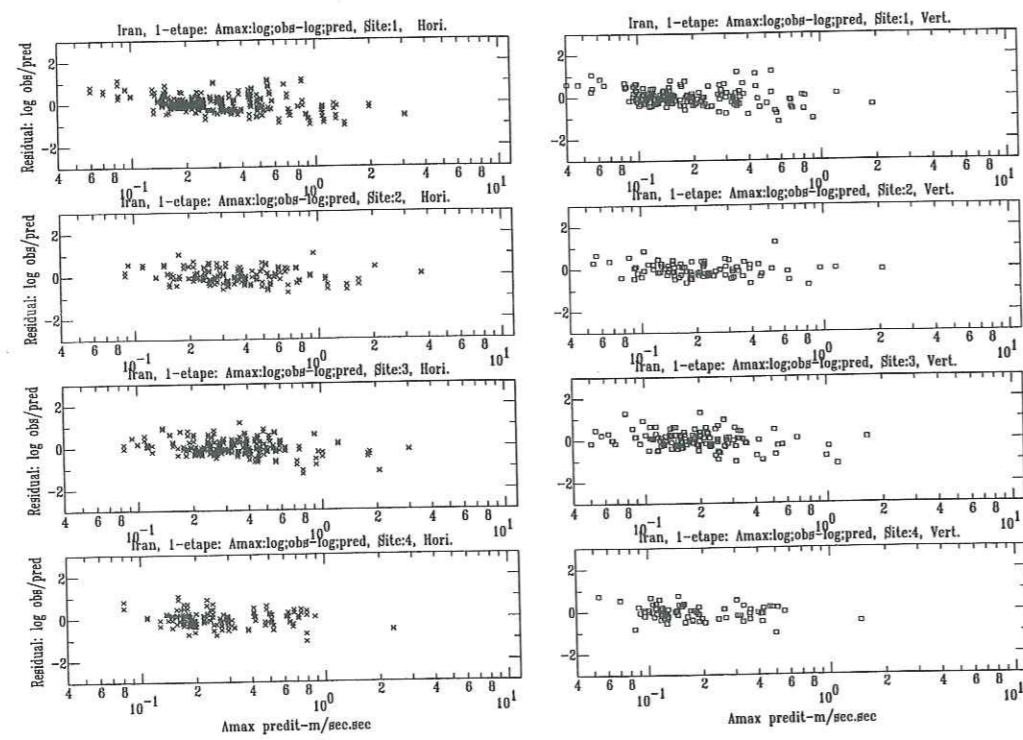


FIG. 6.33 – Les résiduels (log observé - log prédit) de  $A_{max}$  en fonction de  $A_{max}$  prédit pour les catégories différents des sites en utilisant de la régression en une-étape, pour l'ensemble des données iraniennes

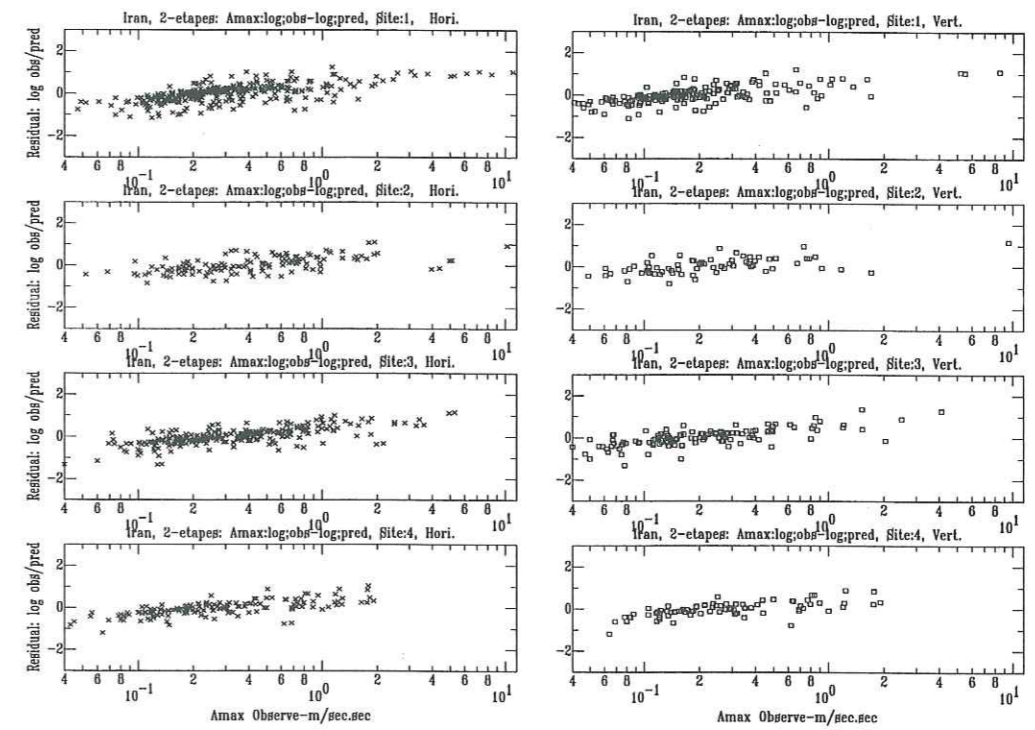


FIG. 6.34 – Les résiduels (log observé - log prédit) de  $A_{max}$  en fonction de  $A_{max}$  observé pour les catégories différents des sites en utilisant de la régression en deux-étapes, pour l'ensemble des données iraniennes

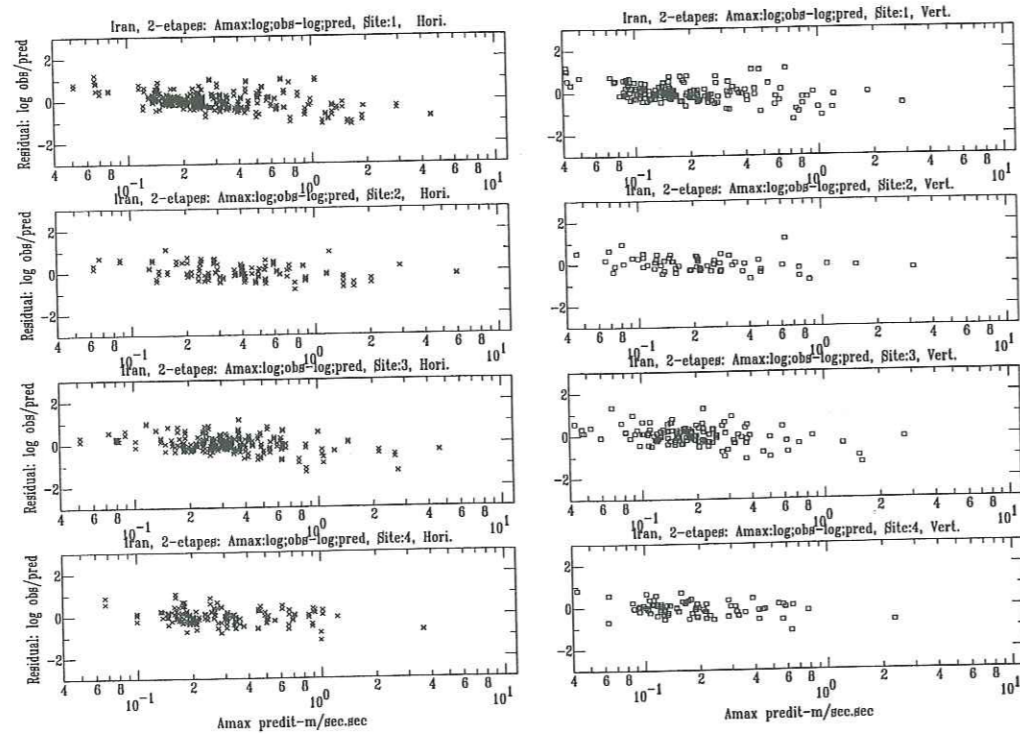


FIG. 6.35 – Les résiduels ( $\log$  observé -  $\log$  prédit) de  $A_{max}$  en fonction de  $A_{max}$  prédit pour les catégories différents des sites en utilisant de la régression en deux-étapes, pour l'ensemble des données iraniennes

Pour examiner si cette dérive non-linéaire inverse à l'effet attendu était due à une mauvaise prise en compte de l'expansion géométrique, nous avons influé sur les lois d'atténuation des ordonnées spectrales en modifiant le coefficient  $d$ , et en étudiant les variations des résidus lorsque  $d$  varie de 0.5 à 3.0. Les écarts-type pour ces estimations sont présentés sur la Figure 6.36; on peut conclure que, quelque soit la période, le plus faible écarte-type est obtenu pour  $d=0.5$ . Ce résultat peut indiquer que les grands résidus pour les forts valeurs de  $A_{max}$  n'ont rien à voir avec la valeur de  $d$ , et ne contribuent donc pas d'une manière représentative à la forme de la loi d'atténuation.

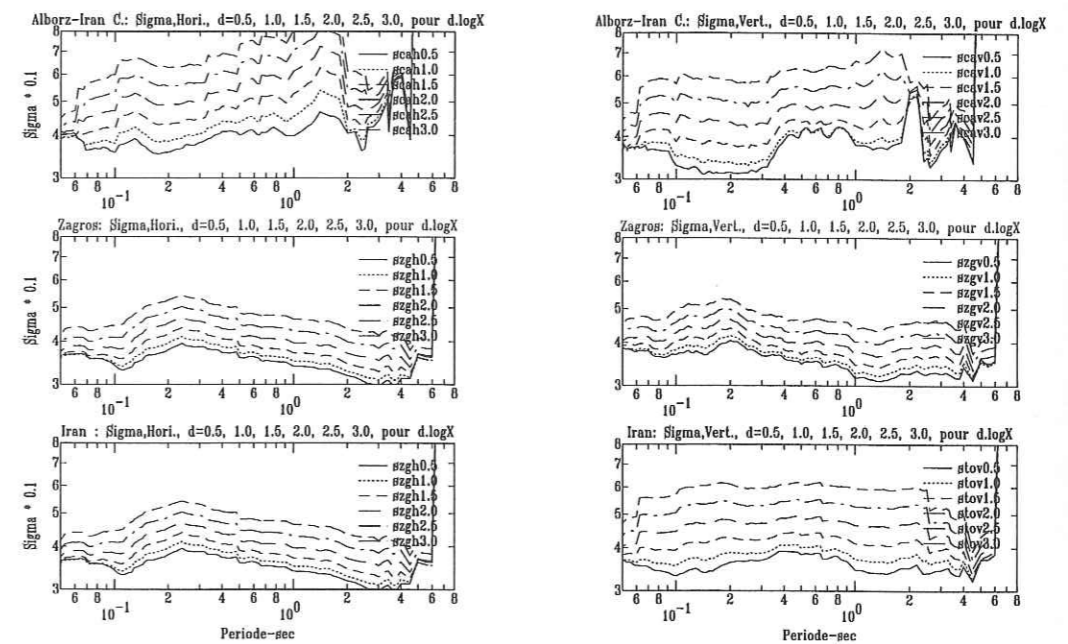


FIG. 6.36 – Les valeurs différents de Sigma avec  $d$  de 0.5 à 3.0 pour les régressions en fonction des périodes différents. Les résultats ont présentés pour les régions de l'Alborz-Iran Central, le Zagros, et l'ensemble des données iraniennes







## 7.1 Introduction

Ce mémoire a été consacré aux investigations sur les mouvements forts en Iran. Le premier catalogue des mouvements forts a été établi au cours de ce travail, et plusieurs études "de base" sur ces données ont été effectuées. Le catalogue des données iraniennes des mouvements forts fournit une base de données très riche de cette région du monde qui possède une forte sismicité. Le réseau accélérométrique iranien, installé depuis 24 ans, fournit des informations sur les propriétés des séismes forts en Iran. Le réseau est toujours en cours de développement, surtout depuis le séisme de Manjil du 20 juin 1990. L'installation de stations sur différents types de sols a fourni la possibilité d'étudier les effets de site. Une classification des sites pour montrer leur réponse aux mouvements forts a été présentée. Dans ces études, l'énergie des mouvements forts et la durée ont été examinées. Les lois d'atténuations pour les mouvements forts ont été présentées pour les valeurs maximales et pour les valeurs spectrales.

Nous résumerons tout d'abord les principales conclusions de chaque thème, puis des suggestions générales pour continuer les études de "sismologie de l'ingénieur" en Iran seront exposées.

## 7.2 Catalogue des mouvements forts en Iran

Un catalogue des mouvements forts en Iran a été donc fourni. Ce catalogue donne les informations correspondant aux sources et aux sites des enregistrements accélérométriques. Les valeurs maximales de l'accélération, de la vitesse et du déplacement pour chaque enregistrement ont été présentées en compagnie des paramètres de la source pour l'événement correspondant à chaque enregistrement. Les données pour lesquelles on pouvait retrouver la source sismique par les bulletins téléseismiques (279 enregistrements en trois composantes) sont composés de 169 enregistrements analogues (SMA-1) et 108 enregistrements digitaux (SSA-2). La plupart des données iraniennes viennent de la région de Zagros, par contre il y a très peu d'enregistrements dans les régions comme Makran, Koppeh-Dagh et l'est de l'Iran (car ces régions sont très peu peuplées). La plupart de ces données correspondent à des séismes de magnitude 4 à 6, et à des distances comprises entre 0 et 80 kilomètres. Il existe également des enregistrements de séismes majeurs (comme le séisme de Tabas du 1978, et de Manjil du 1990) avec les magnitudes de plus de 7, qui ajoutent les données pour des distances de plus de 150km au catalogue présent. L'achèvement de ce catalogue s'est effectué en prenant en compte les 189 données digitales (en trois composantes) pour lesquels aucune information téléseismique ne pouvait être trouvée.

## 7.3 Moment sismique et la chute de contrainte

Les moments sismiques ont été calculés pour toutes les données, y compris les données pour lesquelles les rapports téléseismiques n'existent pas. Le niveau de l'amplitude maximale sur les spectres de Fourier de l'accélération ( $A_0$ ) et les fréquences coin ( $f_c$ ) ont été calculés. Les distances hypocentrales pour tous les enregistrements ont été estimées à partir des différences des arrivées des ondes P et S. Une échelle homogène de magnitude ( $M_w$ ) a été choisie basée sur les résultats acquis pour les moments sismiques. Les magnitudes de moment ( $M_w$ ) supérieures à 6.0 sont en accord avec les magnitudes d'ondes de surface ( $M_s$ ), et les  $M_w$  inférieures à 6.0 sont proches des magnitudes d'ondes de volume ( $m_b$ ). En utilisant ce critère, les magnitudes de moment ont été estimées à partir de leur  $M_s$  ou  $m_b$  (si leur magnitude était inférieure ou supérieure à 6.0), même pour les données pour lesquelles le calcul de  $M_w$  n'était pas possible. Cette homogénéisation était nécessaire pour les régressions qui sont effectuées pour la suite. Les chutes de contraintes ont été également étudiées, pour la première fois en Iran, en appliquant les résultats des mesures des fréquences coin et des amplitudes de spectres de Fourier des données. Les valeurs des chutes de contrainte pour les séismes iraniens, tombent bien dans le domaine des chutes de contrainte déjà présentées pour les séismes intra-plaque.

## 7.4 Études des effets de site

Les effets de sites dans les données iraniennes ont été étudiés en utilisant les résultats des investigations géotechniques. Des tests de profil de vitesse des ondes S et P, de mesures de bruit du fond et des profils géoélectriques ont été effectués en 26 sites, choisis en fonction de nombre d'enregistrements. Les tests de bruit du fond ont été réalisés également dans 24 autres sites. Les rapports H/V ont également été calculés pour tous les enregistrements (même pour ceux qui viennent des stations pour lesquelles les investigations géotechniques- géophysiques ont été faites). Les bandes de fréquences de l'amplification ont été utilisées pour distinguer les réponses variées des différents sols aux mouvements forts. Cette classification en 4 classes a été comparée aux résultats des profils des ondes S et P pour les 30 premiers mètres de profondeur (qui est en général la base des classifications des effets de sites dans les codes américains). Il y a un accord, dans 70% des cas, entre ces deux résultats: la classe 1 est le site le plus dur, avec les amplifications du rapport H/V ( $R_{H/V}$ ) de moins de 3, ou plus de 3 dans les fréquences de plus de 15 Hz avec les  $V_s$  dans premier 30m de plus de 700m/s, la classe 2 concerne aux sites avec les amplifications du  $R_{H/V}$  plus de 3 pour les fréquences compris entre 5 au 15Hz avec les  $V_s$



pour le premier 30m entre 500m/sec et 700 m/sec, la classe 3 est composée des sites avec des amplification du R H/V plus de 3 pour les fréquences entre 2 et 5 Hz avec les Vs dans premier 30m entre 300m/sec et 500 m/sec, et la classe 4 est consisté des sites avec les amplification plus du R H/V de plus de 3 dans les fréquence de moins de 2Hz avec les Vs 1er 30m de moins de 300m/sec (le site le plus mou). Cette classification a été la première dans les catégorisation des effets de sites du point de vue de leur réponse aux mouvements forts, dans laquelle les rapports H/V sont utilisées.

Les rapports H/V pour le bruit de fond (effectués pour 50 sites) ne sont que rarement en accord avec les rapports H/V des enregistrements de mouvement forts pour les mêmes sites. Cela peut être dû à la situation météorologique et topographique du plateau iranien. Les seuls exemples pour lesquels les rapports H/V des bruits du fonds montrent les amplifications dans les même bandes de fréquence que les rapports H/V de mouvements forts, sont les sites de classe 4, qui sont soit en bord de mer (comme les site de Lahijan et Rudsar), soit sur les sols mous d'épaisseur importante (Bajestan et Shiraz).

Les non-linéarités éventuellement ont été analysés en calculant de différences entre les observations sur les sites 3 et 4. Les valeurs observées pour les basses fréquence sont significatives pour ces effets, qui doivent être l'objet des prochaines études en Iran. On propose donc l'observation précise des mouvement forts dans les régions très sismiques (comme Zagros) sur les sols de types 3 et 4 (les sols mous) en utilisant les réseaux locaux. Les limites qui viennent des données doivent être respectés pour l'utilisation de ces lois: il faut appliquer les lois de cette thèse, pour une estimation optimum, dans les magnitude de 3 à 7 dans Zagros et 3 à 7.4 dans le reste de pays, et les distance de 10 à 50km dans Zagros et 20 a 200 pour le reste de pays. Les études déterministes spécifiques pour le champs proche (distance inférieure à 10km) doivent être utilisées.

## 7.5 Énergie et durée des mouvements forts en Iran

La durée est un paramètre d'énergie (l'énergie de l'accélération) proporsionnel à l'intensité d'Arias, et l'accélération moyenne quadratique ( $a_{rms}$ ) ont été étudiées. Les durées sont différentes en Zagros et dans le reste du reste du pays. Ce problème vient probablement de la sismicité eblement des autre facteurs.  $\kappa$  a été étudié séparément pour les données iraniennes, et les résultats ont été plus ou moins différents pour la région de Zagros et pour le reste du pays, mais cette différence n'est pas très claire. Les atténuation de Arms et d'énergie de l'accélération ( $e_a$ ) ont été également présentés dans ce chapitre. Les régressions sur les valeurs de la durée

donnent un écart-type moins fort quand on utilise les données obtenues pour des distances hypocentrales inférieur à 50km (où la plupart des données ont été enregistrées).

Les conditions des sites se sont avérés sans influence significative sur la durée.

Les estimations des modèles empiriques d'atténuation de  $A_{rms}$  et  $e_a$  pour les ondes de volumes et les ondes de surface sont différents surtout dans les premiers 20 km, où justement les valeurs prédites avec le coefficient des ondes de volume sont plus élevés.

## 7.6 Atténuation des mouvements forts en Iran

Les lois d'atténuation en Iran ont été présentées non seulement pour les valeurs maximales de l'accélération, de la vitesse et du déplacement, mais aussi pour les valeurs spectrales des l'accélération. Ces lois sont fournies séparément pour les régions de Alborz-Iran Central, Zagros, et pour l'ensemble des données iraniennes. Les régressions ont été faites en utilisant les paramètres explicatives comme la distance hypocentrale, la magnitude  $M_w$  et les coefficients de sites (pour l'ensemble des 4 classes présentées).

A partir des observations sur les sites 3 et 4, les valeurs observées pour les basses fréquence sont significatifs pour les effets inattendus. Ces effets doivent être étudiés dans les prochaines investigations en Iran. Une étude sur les basses fréquences basée sur les observations des mouvements forts dans les régions très sismique (comme Zagros) sur les sol de types 3 et 4 (les sols mous) en utilisant les réseaux locaux serait intéressante à mener.

Les limites qui viennent des données doivent être respectées pour l'utilisation de ces lois: il conviendra de n'appliquer les lois de cette thèse, que pour les distances comprises entre 10 et 50km dans le Zagroso (et magnitude comprise entre 4 et 6.5), et des distances comprises entre 20 et 200km dans l'Iran-Central (magnitude comprise entre 4 et 7.4). Les études déterministes spécifiques sont recommandés pour le champ-proche.

## 7.7 Propositions pour la continuation de ces recherches

Les études sur les mouvements forts en Iran peuvent être développées dans plusieurs directions différentes. Mais au préalable, il est nécessaire de consolider et d'étendre le réseau accélérométrique en Iran, de façon à fournir une base des données plus riche. Les propositions pour la continuations des études en « Sismologie de l'ingénieur » en Iran sont classifiées comme suit:

1. Le réseau sismographique du pays doit absolument être développé de façon à ce que les épicentres des événements sismiques en Iran soient localisés précisément. Ce problème est très important pour poursuivre les études des atténuations et de l'aléa sismique en Iran, parce que tant que les localisations ne sont pas précises, la détermination et la définition des distances pour les lois d'atténuation ne pourront pas être améliorées.

2. Des réseaux accélérométriques locaux peuvent être installés dans les régions très actives (comme le Zagros) pour étudier les effets de sites ou de source avec les méthodes différentes. Dans ces réseaux locaux, les comparaisons des résultats des méthodes numériques et expérimentales seront possibles. Les régions côtières de la mer Caspienne et du golfe Persique sont les plaines où l'on trouve des sols mous avec une nappe phréatique assez superficielle: nous les proposons donc en priorité pour ces réseaux locaux. Ils peuvent aussi faire l'objet d'installations spécifiques dans les plaines de Gilan et de Mazandaran au nord, et Khuzestan au sud, et les plaines du sud de Téhéran, de l'est de Shiraz, au nord et à l'ouest de Bandarabbas, au sud de Tabriz, ... etc.).

3. L'installation d'un récepteur horaire sur toutes les stations pour les obtenir en temps absolu peut fournir les données nécessaires pour l'analyse de la rupture. En utilisant ce paramètre spectral, l'estimation préliminaire des zones macrosismiques sera possible avec un réseau dense.

4. Le filtrage des enregistrements accélérométriques en Iran doit se faire avec les estimations des spectres de signaux et du bruit. Les données disponibles, auparavant en Iran, quoique nombreuses, ont pu conduire à des mauvaises interprétations, voire à des erreurs en raison de l'inadéquation des traitements réalisés.

5. La distribution des données iraniennes sur le réseau « Internet » peut fournir l'occasion d'échange des données avec les scientifiques internationaux. Aujourd'hui, la communication entre les chercheurs des pays différents, qui ont des approches variées, est essentielle.

6. Les meilleures données peuvent être utilisées pour des estimations plus précises de l'énergie, de la durée, du moment sismique, du facteur de qualité ( $Q$ ) et du facteur d'absorption ( $\kappa$ ). Ces types de calculs peuvent aider à une meilleure compréhension des effets de source, de propagation et de site. Ces études peuvent aussi conduire à la possibilité d'un zonage en Iran de point de vue de l'atténuation des mouvements forts.

7. Le spectre d'aléa sismique uniforme devraient être étudié en Iran sur la base d'une étude précise de la sismicité de l'Iran.

8. La sélection de nouveaux sites des stations accélérométriques en Iran doit être effectuée en considérant la situation géologique et sismologique des différentes régions de pays. En particulier des paires de stations proches (une sur l'alluvions et l'autre sur le rocher) peuvent fournir les

données pour les études expérimentales des effets de site.

9. Les études sur le champ-proche sont essentielles pour l'Iran. A cause de l'approvisionnement en eau, presque partout en Iran, les villes et les villages sont édifiées au pied des montagnes ou collines, où la nappe phréatique est très superficielle. Ces endroits correspondent en fait à la plupart des failles quaternaires. Donc beaucoup de zones urbaines se trouvent à proximité immédiate de sources importantes.

10. Les données accélérométriques des pays voisins (surtout Turquie, Arménie, Azarbayjan) peuvent être le sujet d'études comparatives. Les situations géologiques en Iran et en Turquie sont similaires. Ce type d'études peut aider les investigations de l'aléa sismique dans la région méditerranéenne.

11. Enfin, l'étude de l'atténuation des intensités macrosismiques serait souhaitable aussi pour l'Iran. On propose la calibration de l'échelle européenne de EMS98 pour une étude plus précise sur les intensités en Iran. Les destructions historiques pourraient alors indiquer l'aléa sismique dans un pays comme Iran, qui a un grand héritage culturel, historique et archéologique.

## Chapitre 8

### Bibliographie Générale

- Abrahamson N.A. and K.M. Shedlock (1997), Overview (special issue of SRL on the Attenuation of Strong motion), *Seism. Research Let.*, Vol. 68, No.1, pp.9-24.
- Abrahamson N.A. and W.J. Silva (1997), Empirical Response Spectral Attenuation Relationships for Shallow Crustal Earthquake, *Seism. Research Let.*, Vol. 68, No.1, pp.86-93.
- Aki, K. (1967), Scaling law of Seismic spectrum, *J. Geoph. Res.*, Vol.72, pp.1217-1231.
- Ambraseys N.N. (1988), *Engineering Seismology, Earthquake Eng. and Structural Dyn.*, Vol.17, No.1, pp.1-105.
- Ambraseys N.N. (1995), The Prediction of Earthquake Peak Ground Acceleration in Europe, *Earthquake Eng. Struct. Dyn.* Vol.24, pp.467-490.
- Ambraseys N.N., and M. W. Free (1997), Surface Wave Magnitude Calibration for European Region Earthquakes, *Journal of Earthquake Eng.* Vol.1, No.1, pp.1-22.
- Ambraseys N.N. and C.P. Melville (1982), *A History of Persian Earthquakes*, Cambridge University Press.
- Ambraseys N.N., and K. A. Simpson (1996), Prediction of Vertical Response Spectra in Europe, *Earthquake Eng. Struct. Dyn.* Vol.25, pp.401-412.
- Ambraseys N.N., and M. Srbulov (1998), A Note on the Point Source Approximation in Ground Motion Attenuation Relations, *Journal of Earthquake Eng.* Vol.2, No.1, pp.1-24.
- Anderson J.G. and S.E. Hough (1984), A Model for the Shape of the Fourier Amplitude Spectrum of Acceleration at High Frequencies, *Bul. of the Seis. Soc. of America*, Vol.74, No.5, pp.1969-1993.

- Arias A. (1970), A Measure of Earthquake Intensity, in *Seismic Design of Nuclear Power Plants*, R.J. Hansen Editor, M.I.T. press.
- Bard, P.-Y., Duval A.-M., Lebrun B., Lachet C., Riepl J., and Hatzfeld D. (1997), Reliability of H/V Technique for Site Effects Measurement: An Experimental Assessment, SDEE'97, Proc. Of the Eight International Conf. on Soil dynamics and Earthquake Eng. , Istanbul, in press, 8p.
- Bard, P.-Y, M. Zaré and M.Ghafory-Ashtiany (1998), The Iranian Accelerometric Data Bank, A Revision and Data Correction, *Journal of Seismology and Earthquake Engineering*, Vol.1, No.1, pp1-22.
- Berberian M. (1976), Contribution to the Seismotectonics of Iran, (PartII), *Geol. Sur. Iran*, Rep. 39, 518p.
- Berberian M. (1977), Contribution to the Seismotectonics of Iran, (PartIII), *Geol. Min., Sur. Iran*, Rep. 40, 300p.
- Berberian M. (1981), Active Faulting and Tectonics of Iran, , In: H.K. Gupta and F.M. Delany (Editors), *Zagros-Hindu Kush-Himalaya Geodynamic Evolution*, *Amr. Geophy. Union*, *Geodyn. Ser.*, Vol.3, pp.33-69.
- Berberian M. (1982), Aftershock tectonic of the Tabas-e-Golshan (Iran) Earthquake Sequence: A Thick and Thin skinned Tectonic' Case, *Geoph. J. R. astr. Soc.*, Vol.68, pp.499-530.
- Berberian M.et al. (1984), Field and Teleseismic Observations of the 1981 Golbaf-Sirch Earthquakes in SE Iran, *Geoph. J. R. ast. soc.* Vol.77, pp. 809-838.
- Berberian M. (1995), Master Blind Thrust Faults hidden under the Zagros Folds: Active Basement Tectonics and Surface Morphotectonics, *Tectonophysics*, Vol.241, pp. 193-224.

Berberian M., M. Qorashi, J.A. Jakson, K. Priestley and T. Wallace (1992), The Rudbar-Tarom Earthquake of 20 June 1990 in NW Persia: Preliminary field and Seismological Observations, and its Tectonic Significance, *Bul. of Seismological Soc. of America*, Vol.82, No.4, pp.1726-1755.

Boore D. M., W.B. Joyner and T.E. Fumal (1993), Estimation of Response Spectra and Peak Accelerations from Western North American Earthquakes: An Interim Report, U. S. Geol. Survey, Open-file report: 93-509. 72.p.

Boore D. M., W.B. Joyner and T.E. Fumal (1994), Estimation of Response Spectra and Peak Accelerations from Western North American Earthquakes: An Interim Report, U. S. Geol. Survey, Open-file report: 94-127. 40.p.

Boore D. M., W.B. Joyner and T.E. Fumal (1997), Equations for Estimating Horizontal Response Spectra and Peak Acceleration from Western North American Earthquakes: A Summary of Recent Work, *Seism. Research Let.*, Vol. 68, No.1, pp.128-153.

Brillinger D.R. and H. K. Priestler (1984), An Exploratory Analysis of the Joyner-Boore Attenuation Data, *Bul. of Seismological Soc. of America*, Vol.74, No.4, pp.1441-1450.

Brillinger D.R. and H. K. Priestler (1985), Further Analysis of the Joyner-Boore Attenuation Data, *Bul. of Seismological Soc. of America*, Vol.75, No.4, pp.611-614.

Brune, J.N. (1970), Tectonic stresses and the spectra of seismic shear waves, *J. Geoph. Res.*, Vol.75, pp.4997-5009.

Brune, J.N. (1971), Corrections, *J. Geoph. Res.*, Vol.76, p.5002.

BSSC (1994), NEHRP Recommended Provisions for Seismic Regulations for New Buildings, Part 1- Provisions, FEMA; Federal Emergency Management Agency, 222A, 290p.

Building and Housing Research Center (1992), Accelerograms of the Manjil Iran Earthquake of 20 June 1990, Vol.2, Pub.No.143.

Building and Housing Research Center (1993), A Collection of the Accelerogram Network of the Islamic Republic of Iran, Pub. No.179, 173p.

Bullen K. E. and B. A. Bolt (1985), An Introduction to the Theory of Seismology, Cambridge Univ. Press, 4th Edi., 499 p.

Caillot V. (1992), Quantification Statistique et Etude Expérimentale des Mouvements Sismiques, Application à l'évaluation du Risque, Ph.D thesis, Observatoire de Grenoble, Université Joseph-Fourier, (published by 'études et recherches des laboratoire des points et chaussées, série géotechnique GT51, January 1993). 192p.

Campbell K.W. (1981), Near-Source Attenuation of Peak Horizontal Attenuation, *Bul. of Seismological Soc. of America*, Vol.71, No.6, pp.2039-2070.

Duval, A.M. (1994), Détermination de la réponse d'un site aux séisme à l'aide de bruit de fond: Evaluation expérimental, Thèse de Doctorat, Université Pierre et Marie Curie, Paris.

Duward J.A., D.M. Boore and W.B. Joyner (1996), The Amplitude Dependence of High Frequency Spectral Decay: Constraint on Soil Non-linearity, *Proc. Int. Workshop on Site Response*, Yokusoka Japan, pp.82,103.

Eslami A.A., and P. Mozaffari (1992), Qualitative and Quantitative Analysis of Rudbar Earthquake (Northern Part of Iran), in the Selected papers of the International Conf. on

- Continental Earthquakes, IASPEI Publication Series for the IDNDR, Vol.3, pp. 114-121.
- Eshghi S. et al. (1994), Ebrahimabad Earthquake of 20 June 1994, and a Review on the Southern Zagros Earthquakes of Charak and Dadenjan of 1992 and Mouk of 1994, IIEES Newsletter (Pajouheshnameh), Vol.3, No.3, special issue. (in Persian).
- Esteva L. (1970), Seismic Risk and Seismic Design Criteria for Nuclear Power Plants, The MIT Press (edited by J. Hansen), Cambridge, Massachusetts, pp. 142-182.
- Frankel A. (1991), High-Frequency Spectral Falloff of Earthquakes, Fractal dimension of Complex Rupture, b Values, and the Scaling of Strength on Faults, J. Geoph. Res., Vol.96, N.B4, pp.6291-6302.
- Fukushima Y. and T. Tanaka (1990), A New Attenuation Relation for Peak Horizontal Acceleration of Strong Earthquake Ground Motion in Japan, Bul. of Seismological Soc. of America, Vol.80, No.4, pp.757-783.
- Fukushima Y., J.-C. Gariel and R. Tanaka (1995), Site-Dependent Attenuation Relations of Seismic Motion Parameters at Depth Using Borehole Data, Bul. of Seismological Soc. of America, Vol.85, No.6, pp.1790-1804.
- Fukushima Y., T. Tanaka and S. Kataoka (1988), A New Attenuation Relationship for Peak Ground Accelerations derived from Strong Motion Accelerograms, Proc. 9th World Conf. on Earthquake Eng., Vol. pp.343-348.
- Gariel J.-C. and M. Campillo (1989), The Influence of the Source on the High-Frequency Behavior of the Near-Field Acceleration Spectrum: A Numerical Study, Geoph; Res. Let., Vol.16, No.4, pp.279-282.

- Hanks, T.C. (1979), b Value and  $\omega^\gamma$  seismic Source models: implications for Tectonic Stress Variations along Active Crustal Fault Zones, J. Geoph. Res., Vol.84, pp.2235-2242.
- Hanks T.C. (1982),  $f_{max}$ , Bull. Seismol Soc. of America, Vol.72, pp.1867-1880.
- Hanks T.C. and H. Kanamori (1979), A Moment Magnitude Scale, J. of Geoph. Res., Vol.84, No.B5, pp.2348-2350.
- Haskell N.A. (1964), Total Energy and Energy Spectral Density of Elastic Wave Radiation from Propagating Faults, Bull. Seismol Soc. of America, Vol.54, pp.1811-1841.
- Heydari M. and M. Zaré (1995), Seismotectonics of Recent Earthquakes in Western Fars Area; Southern Zagros Iran, Proc. 2nd Int Conf. on Seismology and Earthquake Engineering (SEE-2), Tehran, Vol.2, pp. 1279-1300.
- Husid R., H. Median and J. Rios (1969), Analysis de terremotos Norteamericanos y Japonesses, Revista del IDIEM 8, Chile.
- Jafari M.K., M. Kamalian and M. Chamanzad (1995), Microzonation of the Tehran Region, Proc. 2nd Int. Conf. On Seismology and Earthquake Engineering (SEE-2), Tehran, Vol.2, pp.1301-1311.
- Jafari M.K., M. Kamalian and M. Chamanzad (1996), Microzonation Study in the Tehran Region, Proc. 11th World Conf. on Earthquake Engineering (WCEE), Accopolco, paper no. 895.
- Jackson J. and D.P. McKenzie (1984), Active Tectonics of the Alpine Himalayan Belt between western Turkey and Pakistan, Geoph, J. R. Astron. Soc., Vol.77, pp. 185-264.

- Jackson J. and D.P. McKenzie (1988), The Relationship between the Plate Motions and Seismic Moment Tensors, and the Rates of the Active Deformation in the Mediterranean and Middle East, *Geoph. J. R. Astron. Soc.* Vol.93, pp.45-73.
- Japan Working Group for TC-4 Committee (1992), Seismic Zoning on Geotechnical Hazards, Draft, 114P.
- Jeong, G.D. and W.D. Iwan (1988), The Effect of Earthquake Duration on the Damage of Structures, *Earthq. Eng. Struct. Dyn.*, Vol.16, pp.1201-1211.
- Joyner W.B. and D. M. Boore (1981), Peak Horizontal Acceleration and Velocity from Strong Motion Records from the 1979 Imperial Valley, California, *Earthquake, Bul. of Seismological Soc. of America*, Vol.71, No.6, pp.2011-2038.
- Joyner W.B. and D. M. Boore (1993), Methods for Regression Analysis of Strong Motion Data, *Bul. of Seismological Soc. of America*, Vol.83, No.2, pp.469-487.
- Kadinsky-Cade K. and M. Barazanji (1982), Seismotectonics of Southern Iran, *Tectonics*, Vol.1, No.5, pp.389-412.
- Kanamori, H. (1977), The Energy Release in Great Earthquakes, *J. Geoph. Res.*, Vol.82, pp.2981-2987.
- Kanamori H., and D.L. Anderson (1975), Theoretical Basis of some Empirical Relations in Seismology, *Bull. Seismol Soc. of America*, Vol.65, pp1073-1095.
- Koliopoulos B.N, B.N. Margaris and N.S. Klimis (1998), Duration and Energy Characteristics of Greek Strong motion Records, *Journal of Earthquake Eng.*, Vol.2, No.3, pp.1-27.

- Konno K., and T. Ohmachi (1998), Ground Motion Characteristics Estimated from Spectral Ratio between Horizontal and Vertical Components of Microtremors, *Bull. of the Seismological society of America*, Vol. 88, No.1, pp. 228-241.
- Lachet C., Hatzfeld D., Bard P.-Y., Thodulidis N., Papaioannou C., and A. Savvaidis (1996), Site Effects and Microzonation in the City of Thessaloniki (Greece) Comparison of Different Approaches, *Bull. of the Seismological society of America*, Vol. 86, No.6, pp. 1692-1703.
- Lacave-Lachet C., P.Y. Bard, J.C. Gariel, and K. Irikura (1998), Straightforward Methods to Detect non-linear response of the Soil. Application to the Recordings of the Kobe Earthquake (Japan 1995), submitted to the *Journal of Seismology*, 25p.
- McCann Jr. M.W. and H. Shah (1979), Determining Strong Motion Duration of Earthquakes, *Bull. Seismol. Soc. of America*, Vol.69, No.4, pp.1253-1265.
- Moinfar A.A. and H. Adibnazari (1982), The Tabas Earthquake of September 16, 1978, Building and Housing Research Center, Technical Rep. No.47.
- Moinfar A.A. M. Eetemadi (1982), Accelerograms of the Golbaf-Sirch 1982 Earthquakes, Building and Housing Research Center, Internal Report., (in Persian).
- Moinfar A.A. and Shoja-Taheri J. (1988), Fathabad-Ghir, Iran Earthquake Study of the Strong Motions Records, Proc. 9th World Conf. on Earthquake Engineering, Tokyo-Kyoto, Vol.VIII, pp.149-154.
- Moinfar A.A. and A. Naderzadeh (1990), An Immediate and Preliminary Report on the Manjil Iran Earthquake of 20 June 1990, Building and Housing Research Center, Rep. No.119, 68p.

- Nabavi M.H. (1975), An introduction to the Geology of Iran, Geol. Sur. Iran.
- Ni J. and M. Barazangi (1986), Seismotectonics of the Zagros Continental Collision Zone and a Comparison with the Himalayas, *J. of Geoph. Res.*, Vol.91, No.B8, pp.8205-8218.
- Niazi M. (1986), Accelerograms of the 1978 Tabas, Iran, Earthquake, *Earthquake Spectra* . Vol.2, pp.635-651.
- Niazi M. and Y. Bozorgnia (1992), The 1990 Manjil, Iran Earthquake: Geology and Seismology Overview, PGA Attenuation, and Observed Damage, *Bulletin of the Seismological Society of America*, Vol.82, No.4, pp.774-799.
- Page R. A., D.M. Boore and J.H. Deitrich (1975), estimation of Bedrock motion at the Ground surface, Profess. Paper 941-A.
- Papageorgiou A.S. and K. Aki (1983), A specific Barrier model for the Quantitative Description of Inhomogeneous Faulting and the Prediction of the Strong Ground Motion. I. Description of the Model, *Bul. of the Seis. Soc. of America*, Vol.73, No.3, pp.693-722.
- Riepl, J., Bard P.-Y., Hatzfeld D., Papaioannou C. and S. Nechtschein (1998), Detailed Evaluation of Site Response Estimation Methods Across and Along the Sedimentary Valley of Volvi (EURO-SEISTEST), *Bull. of the Seismological society of America*, Vol. 88, No.2, pp. 488-502.
- Saikia C.K. (1994), Modeling of Strong Ground Motions from the 16 September 1978 Tabas, Iran, Earthquake, *Bulletin of the Seismological Society of America*, Vol.84, No.1, pp.31-46.
- Shoja-Taheri J. (1984), Accelerograms of the 1978 Tabas (Iran) Earthquake: The Generalized records and Correlations between the Strong Motion Parameters in Different Frequency

- Bands, Presented at Regional Assembly of IASPEI, Heyderabad, India.
- Shoja-Taheri J. and J. Anderson (1988), The 1978 Tabas, Iran, Earthquake: An Interpretation of the Strong Motion Records, *Bulletin of the Seismological Society of America*, Vol. 78, No.1, pp.142-171.
- Theodulidis, N. and P.-Y. Bard (1995), (H/V) Spectral ratio and geological conditions: an analysis of strong motion data from Greece and Taiwan (SMART-1), *Soil Dynamics and Earthquake Engineering*, 14: pp.177-197.
- Trifunac M.D. and A.G. Brady (1975), A Study on the Duration of the Strong Earthquake Ground Motions, *Bull. Seismol. Soc. of America*, Vol.65, No.3, pp.581-626.
- Uang C.M., and V.V. Bertero (1990), Evaluation of Seismic Energy in Structures, *Earthq. Eng. Struct. Dyn.*, Vol.19, pp.77-90.
- Udwadia F.E. and M.D.Trifunac (1974), Characterization of the Response Spectra through the Statistics of Oscillator Response, *Bull. Seismol Soc. of America*, Vol.64, No.1, pp.205-219.
- Vanmarcke E.H. and S.-S. P. Lai (1980), Strong Motion duration and RMS Amplitude of Earthquake Records, *Bull. Seismol Soc. of America*, Vol.70, No.4, pp.1293-1307.
- Zaré M. (1991), The Seismotectonic and Neotectonic Analysis of the Reconstruction Operation of the Sefid-Rud Dam, with the Special Reference to the Earthquake of 20th June 1990, NW Iran, *Proc. of the 5th Int. Conf. on Soil Dynamics and Earthquake Engineering*, vol.2, Karlsruhe, Computational Mechanics Pub. Southampton.
- Zaré M. (1993), Macrozonation of the Landslides for the Manjil Iran 1990 Earthquake, *Proc. 3rd Int. Conf. on Case-Histories in Geotechnical Eng.* Vol.1, Univ. of Missouri-Rola, St.



Louis.

Zaré M. (1994), The Study of Site Effects on the Strong Ground Motions during Earthquakes, a Case-Study on the Manjil 1990 Earthquake, M.Sc. Thesis, Engineering Geology Dept. Tarbiat-Modarres University, Tehran, 214p., (in Persian).

Zaré M. and A.A. Moinfar (1994), Comment on the 'Rudbar-Tarom Earthquake of 20 June 1990, in NW Persia : a Preliminary Field and Seismological Observations and its Tectonic Significance « by; Berberian et al 1992 », Bulletin of the Seismological Society of America, Vol.84, No.2, pp.484-485.

Zaré M. (1995), Site Dependent Attenuation of Strong Motions for Iran, Seismic Zonation, 5th Int. Con. Nice, Ouest Pub. Paris. Vol.2, pp.1227-1236.

Zaré M. (1996), Deux Exemple de Mouvements de Forts Séismes en Champ proche en Iran, 4ém Colloque National en Génie Parasismique, AFPS, Paris, Proc. Vol.1, pp.112-119.

Zaré M., P-Y. Bard, M.Ghafory-Ashtiany (1999a), Site Characterizations for the Iranian Strong Motion network, Journal of Soil Dynamics and Earthquake Engineering, Vol.18, no.2, pp.101-123.

Zaré M., P-Y. Bard, M.Ghafory-Ashtiany (1999b), Moment Magnitude for the Strong Motion Accelerograms in Iran, in preparation, 22 pages.

Zaré M., P-Y. Bard, M.Ghafory-Ashtiany (1999c), Duration and Energy Content of Strong Motions in Iran, submitted to the Journal of Earthquake Engineering, 42 pages.

Zaré M., P-Y. Bard, M.Ghafory-Ashtiany (1999d), Strong Motion Attenuation in Iran, submitted to the Bulletin of the Seismological Society of America.

## Chapitre 9

### Annexes





Annexe-3: Nombre des points utilisés, valeurs de Sigma, a, b, c1, c2, c3, c4 pour 146 fréquences indiquée dans l'Annexe-1, pour l'ensemble des données iraniennes (composante verticale), pour d=1.0 .

Table with 8 columns and 43 rows. Columns: Points, 3.005E+00, 4.005E+00, 4.005E+00, 4.005E+00, 6.900E+01, 6.900E+01, 7.100E+01, 1.500E+02. Rows include values for sigma, alpha, and other parameters.

Table with 8 columns and 43 rows. Columns: b, 3.784E-03, 5.087E-03, 5.975E-03, 4.481E-03, 6.457E-03, 5.985E-03, 5.500E-03, 6.662E-03. Rows include values for b, c1, and c2.

C3:	-4.290E+00	-1.297E+01	-1.301E+01	-1.315E+01	-5.262E+00	-5.310E+00	-5.506E+00	-5.230E+00
	-4.741E+00	-4.780E+00	-4.725E+00	-4.605E+00	-4.651E+00	-4.626E+00	-4.615E+00	-4.609E+00
	-4.632E+00	-4.843E+00	-4.838E+00	-4.869E+00	-4.849E+00	-4.647E+00	-4.614E+00	-4.602E+00
	-4.585E+00	-4.599E+00	-4.591E+00	-4.583E+00	-4.557E+00	-4.517E+00	-4.431E+00	-4.423E+00
	-4.387E+00	-4.290E+00	-4.284E+00	-4.243E+00	-4.233E+00	-4.184E+00	-4.134E+00	-4.102E+00
	-4.033E+00	-4.000E+00	-3.936E+00	-3.900E+00	-3.883E+00	-3.840E+00	-3.817E+00	-3.809E+00
	-3.773E+00	-3.751E+00	-3.731E+00	-3.677E+00	-3.666E+00	-3.620E+00	-3.569E+00	-3.538E+00
	-3.455E+00	-3.308E+00	-3.302E+00	-3.251E+00	-3.234E+00	-3.187E+00	-3.172E+00	-3.112E+00
	-3.093E+00	-3.018E+00	-2.932E+00	-2.909E+00	-2.858E+00	-2.807E+00	-2.792E+00	-2.725E+00
	-2.696E+00	-2.652E+00	-2.472E+00	-2.449E+00	-2.371E+00	-2.353E+00	-2.286E+00	-2.218E+00
	-2.205E+00	-2.127E+00	-2.104E+00	-1.998E+00	-1.908E+00	-1.894E+00	-1.826E+00	-1.796E+00
	-1.785E+00	-1.732E+00	-1.684E+00	-1.600E+00	-1.597E+00	-1.524E+00	-1.509E+00	-1.468E+00
	-1.440E+00	-1.407E+00	-1.351E+00	-1.295E+00	-1.250E+00	-1.227E+00	-1.200E+00	-1.182E+00
	-1.170E+00	-1.137E+00	-1.094E+00	-1.083E+00	-1.021E+00	-9.563E-01	-9.226E-01	-8.316E-01
	-8.187E-01	-7.730E-01	-7.401E-01	-7.324E-01	-7.299E-01	-7.292E-01	-7.185E-01	-7.117E-01
	-7.178E-01	-7.288E-01	-7.166E-01	-6.997E-01	-6.914E-01	-6.572E-01	-6.414E-01	-6.308E-01
	-6.512E-01	-6.440E-01	-6.422E-01	-6.009E-01	-5.961E-01	-5.891E-01	-5.593E-01	-5.978E-01
	-5.924E-01	-6.062E-01	-6.649E-01	-6.809E-01	-6.973E-01	-7.474E-01	-7.633E-01	-2.578E-01
	-3.916E-01	-9.180E+00						
C4:	-4.077E+00	-1.291E+01	-1.296E+01	-1.308E+01	-5.653E+00	-5.694E+00	-5.830E+00	-5.280E+00
	-4.745E+00	-4.707E+00	-4.658E+00	-4.460E+00	-4.518E+00	-4.497E+00	-4.484E+00	-4.455E+00
	-4.476E+00	-4.653E+00	-4.659E+00	-4.730E+00	-4.732E+00	-4.569E+00	-4.550E+00	-4.544E+00
	-4.522E+00	-4.531E+00	-4.526E+00	-4.526E+00	-4.496E+00	-4.451E+00	-4.411E+00	-4.407E+00
	-4.373E+00	-4.272E+00	-4.266E+00	-4.234E+00	-4.223E+00	-4.193E+00	-4.143E+00	-4.118E+00
	-4.048E+00	-4.010E+00	-3.937E+00	-3.896E+00	-3.875E+00	-3.802E+00	-3.779E+00	-3.772E+00
	-3.735E+00	-3.714E+00	-3.693E+00	-3.646E+00	-3.637E+00	-3.592E+00	-3.546E+00	-3.518E+00
	-3.438E+00	-3.265E+00	-3.258E+00	-3.211E+00	-3.194E+00	-3.153E+00	-3.140E+00	-3.088E+00
	-3.072E+00	-3.002E+00	-2.928E+00	-2.905E+00	-2.858E+00	-2.809E+00	-2.796E+00	-2.730E+00
	-2.701E+00	-2.654E+00	-2.506E+00	-2.481E+00	-2.387E+00	-2.368E+00	-2.305E+00	-2.243E+00
	-2.230E+00	-2.160E+00	-2.140E+00	-2.045E+00	-1.928E+00	-1.911E+00	-1.841E+00	-1.816E+00
	-1.806E+00	-1.749E+00	-1.687E+00	-1.587E+00	-1.583E+00	-1.500E+00	-1.484E+00	-1.441E+00
	-1.414E+00	-1.388E+00	-1.335E+00	-1.284E+00	-1.239E+00	-1.215E+00	-1.186E+00	-1.166E+00
	-1.155E+00	-1.124E+00	-1.082E+00	-1.069E+00	-1.012E+00	-9.487E-01	-9.166E-01	-8.247E-01
	-8.091E-01	-7.373E-01	-6.843E-01	-6.545E-01	-6.477E-01	-6.503E-01	-6.451E-01	-6.378E-01
	-6.416E-01	-6.368E-01	-6.046E-01	-5.772E-01	-5.655E-01	-5.338E-01	-5.182E-01	-5.067E-01
	-5.285E-01	-5.292E-01	-5.438E-01	-5.430E-01	-5.506E-01	-5.615E-01	-5.459E-01	-5.678E-01
	-5.506E-01	-5.944E-01	-6.868E-01	-7.142E-01	-7.068E-01	-7.629E-01	-7.763E-01	-1.959E-01
	-3.651E-01	-9.069E+00						

Annexe-4: Base des données de ce mémoire.





Table with 31 columns: No, Record, Station, Site, Date, Mw, R(km), Kh, Kv, Stress Drop (Bar), Fc Corner freq. Hz, fmax (H) Hz, fmax (V) Hz, Dur (H1) sec, Dur (V) sec, Dur (H2) sec, Arms (H1) m/s, Arms (V) m/s, Arms (H2) m/s, Ea (H1) m2/s3, Ea (V) m2/s3, Ea (H2) m2/s3, PGA (H1) m/sec2, PGA (V) m/sec2, PGA (H2) m/sec2, Vmax (H1) m/sec, Vmax (V) m/sec, Vmax (H2) m/sec, Dmax (H1) m, Dmax (V) m, Dmax (H2) m. Contains records 216-270.

Table with 31 columns: No, Record, Station, Site, Date, Mw, R(km), Kh, Kv, Stress Drop (Bar), Fc Corner freq. Hz, fmax (H) Hz, fmax (V) Hz, Dur (H1) sec, Dur (V) sec, Dur (H2) sec, Arms (H1) m/s, Arms (V) m/s, Arms (H2) m/s, Ea (H1) m2/s3, Ea (V) m2/s3, Ea (H2) m2/s3, PGA (H1) m/sec2, PGA (V) m/sec2, PGA (H2) m/sec2, Vmax (H1) m/sec, Vmax (V) m/sec, Vmax (H2) m/sec, Dmax (H1) m, Dmax (V) m, Dmax (H2) m. Contains records 271-323.







Thèse de Doctorat de l'Université Joseph Fourier  
Grenoble I

*Titre de l'ouvrage:*

**CONTRIBUTION À L'ÉTUDE DES MOUVEMENTS FORTS EN IRAN; DU CATALOGUE AUX LOIS D'ATTÉNUATION**

*Auteur:* Mehdi ZARÉ

*Etablissement:* Laboratoire de Géophysique Interne et Tectonophysique

*Résumé:*

Les études de risque sismique en Iran sont dans leur phase initiale. Ainsi, il n'existait jusqu'à présent aucun catalogue d'enregistrements accélérométriques en Iran, et aucune étude sur l'ensemble des données iraniennes n'avait été réalisée. Ce mémoire présente donc la première étude d'ensemble sur les mouvements forts en Iran. Un premier objectif a été d'établir un catalogue des mouvements forts d'Iran en faisant correspondre à chaque enregistrement de qualité suffisante, un événement sismique de localisation et magnitude connues, pour 279 enregistrements accélérométriques, analogues et digitaux. Cette correspondance a pu se faire sur la base des catalogues sismologiques internationaux (ISC, NEIC,... etc.) ou nationaux. Pour 189 autres enregistrements numériques, pour lesquelles aucune information télé-sismique ou locale n'était disponible, les distances hypocentrales et les moments sismiques ont été estimés sur la base des enregistrements eux-mêmes. Une attention particulière a été accordée aux effets de sites, en choisissant notamment 50 stations accélérométriques du réseau national où les enregistrements ont été nombreux. Une nouvelle classification pour les effets de sites est proposée - basée sur les rapports H/V - qui s'avère relativement simple dans son principe, et plus fiable que les classifications déjà utilisées. Finalement, les lois d'atténuation pour différents paramètres de mouvement fort (dont Arms, Intensité Arias, PGA, PGV, et PGD, énergie, durée et valeurs spectrales) sont obtenues et discutées sur la base d'un total de 468 enregistrements accélérométriques en 3 composantes.

*Mots Clés:* Sismologie de l'ingénieur, Iran, mouvements forts, effets de site, loi d'atténuation, moment sismique, chute de contrainte, source, accélérogrammes, catalogue, durée, énergie, Zagros, Alborz, Iran-central